

Departament de Matemàtica Aplicada I
Universitat Politècnica de Catalunya

**Local and global phenomena in
piecewise-defined systems: from big
bang bifurcations to splitting of
heteroclinic manifolds**

Albert Granados Corsellas

Supervisors: Tere Martínez-Seara Alonso
Michael Schanz

Barcelona, Juny 2012

Memòria presentada per aspirar el grau de Doctor en Matemàtiques per la
Univeristat Politècnica de Catalunya.
Programa de doctorat de Matemàtica Aplicada.

Als meus pares, pel seu recolzament, els seus ànims, l'empenta, els consells, la comprensió, la seva lluita i fidelitat als seus valors. Sense això res no hagués sortit bé.

Agraïments/ Acknowledgements

Acabar la tesi torna a ser per mi un d'aquells moments en què tinc la sensació d'haver creuat una nova meta, potser aquest cop una que, fins no fa tant, no pensava que acabaria creuant. És un d'aquell moments en que un fa una pausa per mirar la feina feta i sentir-se'n satisfet, malgrat això no s'hagi de dir. Però és sobretot moment de mirar enrere per tenir una perspectiva dels esdeveniments, casualitats i persones que m'han dut fins aquí i ho han fet possible. En fer-ho no puc més que sentir-me afortunat per haver viscut el que he viscut i per tenir i haver tingut al costat tanta gent que m'ha ajudat, de qui ho he après tot, que m'ha fet feliç i que, en definitiva, i ha fet possible que creués aquesta meta. És moment doncs d'estar agraït.

Voldria agrair a la Tere la paciència, dedicació, comprensió i confiança que ha tingut aquests anys que hem estat treballant plegats, tot el que m'ha ensenyat i tot el que d'ella he après, tant a nivell científic com humà, que ha estat moltíssim.

Ich möchte Michael Schanz und Viktor Avrutin bedanken, für alle seine Hilfe mit jedem Verlängerung Prozess des DAAD Stipendium und auch für alles, dass ich von ihnen gelernt habe.

Voldria agrair també a l'Enric Fossas els seus consells i la seva visió en molts dels aspectes que aquí presentem, especialment al capítol 4, però sobretot volia agrair-li la seva confiança introduint-me al món de la recerca i per donar-me l'empenta que he necessitat en molts moments per seguir endavant amb això.

I would like to thank John Hogan, for his advices and ideas in many of the contents of this work, specially in chapters 5 and 6, for inviting me to Bristol, for his hospitality and for visiting us to Stuttgart.

Voldria agrair també a en Lluís Alsedà i l'Alejandro Luque per les discussions a Sevilla i Dresden, il·luminant-me el camí dels mapes al cercle, ajudant-me així a escriure el capítol 3.

Molt sincerament voldria agrair els seus constants ànims i immens ajut al Marcel Guàrdia, tant aquests darrers anys durant la tesi com al llarg de la carrera, així com per la seva amistat.

A Gerard Olivar, Fabiola Angulo i en Gustavo Osorio, por invitarme a Colombia, por su ospitalidad y darme la oportunidad de conocer tantas aplicaciones de los sistemas no suaves.

M'agradaria també agrair a tot el grup del MA1 pel suport, interès, per tot el que he après de vosaltres, pel bon ambient que es respira al departament. En especial l'Amadeu per la seva capacitat de liderar el grup i motivar el jovent. Quisiera agradecer también especialmente a Abraham sus consejos y el estar siempre allí, dispuesto a tener una larga charla sobre cualquier cosa interesante y compartir conocimientos frente a nuestros cafés. Voldria agrair també a tots els que tant m'heu ajudat en les sempre complicadíssimes caramboles administratives (ich möchte auch bedanken alle ihr die mit den immer schwierigen Verwaltungsaufgaben, so viel mir geholfen habt), Ute Gräter, Ursula Habel, Carme Capdevila, Ester Pineda, Maika Sánchez i Hilda Rodón. Auch Ralf Aumüller für alle deine Hilfe mit den Linux und Netzwerke Aspekten. Similarment al Pau Roldán, pels seus consells i ajut en el càlcul en paral·lel.

D'altra banda voldria agrair a tots els que m'heu fet tant feliç durant aquests anys, i que us dec tant i tant: sense vosaltres això no hagués sortit. No voldria deixar-me a ningú:

A J.S. Bach, per la seva eterna obra que en tants moments m'ha acompanyat durant tots aquests anys. A Maria Salomé, per haver-me descobert i fet entendre millor el món de la música.

A Loulogio, la gent de l'APM, del Polònia, del Crackòvia i tots aquells anòmis/mes que constantment alimenteu el nostre sentit de l'humor.

Al Roberto, al Gurb, la Patufa, la Moffi, el Mofletito, el Wall-e i l'Eva, per estar sempre allà, vetllant per mi constantment.

A tots els meus amics i amigues, per premiar-me amb la vostra companyia i amistat, sense vosaltres no sóc. Molt especialment a la gent d'Stuttgart per la vostra companyia i simpatia, al Miquel, al Martí, a la Pilar, al Toni, a la Sara, a l'Eva, al Marco, a la Núria i al Marc. A la gent de la uni, Mauri, Agnès, Yuse, Mireia, Sergi, Isaac, Mikel, Joan, Dario, Mari Carmen, Pere, Laia, Meritxell, Aly,... Però sobretot sobretot, a aquest grup indestructible que som i que tant compartim, al Ferran, a la Gemma, a la Gemmita, al Pau, al Pabli, a la Carmen, al Dídac i al Sansa.

A vosaltres, Dani i Txesco, per tot el que hem viscut i viurem, per estar sempre allà.

A la meva àvia, per la seva preocupació constant i per estar sempre disposada a ajudar, a mi i a tothom. Sobretot pels seus ciris, sense els quals això segur que no hagués acabat en bon port.

Al Dani i l'Alba, per la seva complicitat i companyia durant tants anys, per tot el que m'heu donat i el que he après de vosaltres.

Als meus pares, pel seu suport constant en tants aspectes, pels seus consells i per haver estat el meu referent.

Finalment voldria agrair a la Goeske la seva infinita paciència i comprensió, per fer-me sempre costat i donar-me perspectiva, equilibri i calma, per fer-me millor persona, i per fer-me sentir tan estimat i tan feliç.

Contents

List of Figures	xiii
Abstract	1
1 Introduction	3
1.1 Big Bang bifurcations	3
1.1.1 General description	3
1.1.2 Period incrementing	6
1.1.3 Period adding, extension to 2D maps and applications	7
1.2 Melnikov methods in piecewise-defined systems	8
1.2.1 Extension of classical Melnikov methods	9
1.2.2 The scattering map in a two-degrees of freedom piecewise-defined Hamiltonian smooth system	11
I Big bang bifurcations and applications	13
2 Sufficient conditions for a period incrementing big bang bifurcation in one-dimensional maps	15
2.1 Introduction	15
2.2 Definitions, properties and statement of the results	16
2.3 Increasing-decreasing globally-contracting maps	19
2.4 Extension of the result	27
2.4.1 Increasing-decreasing locally-contracting maps	27
2.4.2 Border collision curves near the origin	28
2.4.3 Proof of Theorem 2.2.2	30
2.5 Examples	32
2.5.1 Example 1	32
2.5.2 Example 2	36
2.6 Conclusions	40

3	A rigorous approach to the period adding big bang bifurcation and the extension to 2-dimensional piecewise-defined maps	41
3.1	Introduction	41
3.2	Period adding big bang bifurcation	42
3.3	Big bang bifurcations in 2-dimensional maps	52
3.4	Conclusions	57
4	Occurrence of big bang bifurcations in discretized sliding-mode control systems	59
4.1	Introduction	59
4.2	A system with a relay based control	60
4.2.1	System description	60
4.2.2	General system dynamics	62
4.3	Big bang bifurcation of the period adding type	63
4.3.1	The one-dimensional case	63
4.3.2	A second order system	66
4.4	Conclusions	68
II	Melnikov methods and scattering map in piecewise-smooth systems	71
5	The Melnikov method and subharmonic orbits in a piecewise-smooth system	73
5.1	Introduction	73
5.2	System description	73
5.2.1	General system definition	73
5.2.2	Poincaré impact map	77
5.2.3	Coefficient of restitution	79
5.2.4	Some formal definitions and notation	81
5.3	Existence of subharmonic orbits	85
5.3.1	Conservative case, $r = 1$: Melnikov method for subharmonic orbits .	85
5.3.2	Dissipative case, $r < 1$	89
5.4	Intersection of the separatrices	91
5.5	Example: the rocking block	96
5.5.1	System equations	96
5.5.2	Existence of periodic orbits	98
5.5.3	Existence curves	102
5.6	Conclusions	103

6	The scattering map in two-coupled piecewise-smooth systems	107
6.1	Introduction	107
6.2	System description	107
6.2.1	Two uncoupled systems	107
6.2.2	The coupled system in the extended phase space	111
6.3	Some notation and properties	114
6.3.1	Impact map associated with $u = 0$	114
6.3.2	The domains of the maps	119
6.3.3	Impact sequence	121
6.3.4	Explicit expressions for the flows	122
6.3.5	Perturbative formulas	125
6.3.6	Invariant manifolds and their persistence	128
6.4	Scattering map	145
6.4.1	Transverse intersection of the stable and unstable manifolds	145
6.4.2	First order properties of the scattering map	154
6.5	Example: two linked rocking blocks	165
6.6	Conclusions	172
	Bibliography	175

List of Figures

2.1	Influence of the parameters c_ℓ, c_r on a map as defined in (2.3.1). a) $c_\ell, c_r < 0$, b) $c_\ell = c_r = 0$ and c) $c_\ell, c_r > 0$	17
2.2	“Trapped” orbit	20
2.3	Definition of the sequences $\{a_n\}$ and $\{b_n\}$. The dotted box corresponds to the absorbing interval.	22
2.4	Backward and forward iterates of $(0, c_\ell]$. $f_r((0, c_\ell])$ (dark segment) is smaller than $f_\ell^{-n}((0, c_\ell]) \forall n$. Therefore, at most one a_j can be reached by $f_r((0, c_\ell])$	23
2.5	The interval $f_r((0, c_\ell])$ is split when it returns to the right domain.	24
2.6	System function of Example 1 defined in Eq. (2.5.1)	32
2.7	(a): border collision bifurcation curves for Example 1. A blow up of the neighborhood of the point A is shown in Fig. 2.9(a). (b): numerical (black) and first order approximations of the analytical (gray) border collision bifurcation curves near the origin. (c): bifurcation diagram through the curve surrounding the origin in (b) parameterized by ϕ anti-clockwise. The gray regions indicate coexistence between two periodic orbits (d): periods of the detected orbits in (c).	33
2.8	Bifurcation structure around the period adding big bang bifurcation occurring at $(0, \pi)$ for Example 1. (a) Bifurcation diagram along the curve labeled in Fig. 2.7(a) and parameterized clockwise by ϕ . (b) Periods of the detected periodic orbits.	35
2.9	Bifurcation scenario near the point A (see Fig. 2.7(a)). (a): Blow up labeled in Fig. 2.7(a). The two dotted straight lines are the directions along which the right and left images of 0 by $f_3(x)$ remain (locally) constant. (b): one-dimensional bifurcation diagram along the segment labeled in (a): period incrementing scenario. (c): magnification of the coexistence (gray region) between the periodic orbits $\mathcal{RL}(\mathcal{RL}^2)^2$ and $\mathcal{RL}(\mathcal{RL}^2)^3$ shown in (b). (d): bifurcation diagram along the segment labeled (d) in Fig. 2.9(a); far enough from A , the period incrementing structure generated at A disappears.	37
2.10	(a): system function of Example 2 defined in Eq. (2.5.8). (b): border collision bifurcation curves of Example 2.	38

2.11	Bifurcation structure around the big bang bifurcation points at $(c_\ell, c_r) = (1, 0)$ ((a) and (b)) and $(c_\ell, c_r) = (p_2, 0)$ ((c) and (d)). (a) and (c) Bifurcation diagram along the curves labeled in Fig. 2.10(b). (b) and (d) periods of the periodic orbits. The gray regions indicate coexistence between two periodic orbits.	39
3.1	Simultaneous collision of two fixed points with positive associated eigenvalues with the boundary.	42
3.2	Border collision bifurcation curves in the parameter space $c_\ell \times c_r$ for the period adding big bang bifurcation. The fixed points x_ℓ^* and x_r^* are labeled in the regions where they exist.	44
3.3	Bifurcation scenario found along the curve plot in Fig. 3.2 and parametrized by the angle ϕ . (a) bifurcation diagram. (b) periods of the period orbits	45
3.4	Infinite tree formed by the concatenation of symbolic sequences of periodic orbits obtained in the adding structure.	46
3.5	Symbolic sequences and the Farey tree formed by their rotation numbers in the adding scheme for a quadratic map.	47
3.6	Different configurations for the circle map f . (a) continuous, (b) invertible and (c) non-invertible. (d) inverse of (b)	49
3.7	Devil's staircase: rotation numbers (ρ) of the periodic orbits obtained for the Arnol'd circle map when varying the parameter $\Omega' \in [0, 1]$. The set I correspond to the values of Ω' for which the map \hat{f}^{-1} is topological conjugated to the Arnol'd circle map (3.2.3).	52
3.8	$\mathcal{L}^7\mathcal{R}$ -periodic orbit (white points) for a two-dimensional piecewise-defined map undergoing a period incrementing big bang bifurcation. Two (virtual) fixed points are marked with crosses. As pointed lines their associated eigendirections. In thinner dashed lines are also plot the trajectories by f_ℓ converging to the (virtual) fixed point $z_\ell^* \in \mathcal{X}_r$	55
3.9	Coexistence of a $\mathcal{L}^7\mathcal{R}$ and a $\mathcal{L}^6\mathcal{R}$ periodic orbits (white points) for a two-dimensional piecewise-defined map undergoing a period incrementing big bang bifurcation. Two (virtual) fixed points are marked with crosses. As pointed lines their associated eigendirections. In thinner dashed lines are also plot the trajectories by f_ℓ converging to the (virtual) fixed point $z_\ell^* \in \mathcal{X}_r$	58
4.1	A linear control system by a relay.	60
4.2	(a) Big bang bifurcation in the (y_c, k) parameter space for $a_0 = -2$, $b = 1$ and $T = 0.1$. The fixed points z_i^* are labeled in the regions where they are feasible, and, as dashed lines, the border collision bifurcation curves where they become virtual are shown. The periods of the periodic orbits found along the pointed curve parametrized by σ are shown in (b).	66

4.3	Big bang bifurcation in the (y_c, k) parameter space for $a_0 = -2$, $a_1 = -5$, $b = 1$, $c_1 = 1.5$ and $T = 0.1$	68
5.1	Phase portrait for the unperturbed system (5.2.2).	76
5.2	Poincaré impact map (5.2.14) represented schematically.	78
5.3	Stable and unstable manifolds of system (5.2.2) for $r < 1$ and $\varepsilon = 0$	80
5.4	Impact map for $r < 1$ and $\varepsilon > 0$	81
5.5	Sequence of impacts for $r < 1$ and $\varepsilon > 0$	82
5.6	Section of the unperturbed and perturbed invariant manifolds for $t = t_0$	92
5.7	Rocking block	96
5.8	Periodic orbits for $n = 5$ and $m = 1$, $r = 1$, $\omega = 5$ and $\varepsilon = 1.6565 \cdot 10^{-2}$. Their initial conditions are ε -close to the points given in Eqs. (5.5.20) and (5.5.21).	100
5.9	$(5, 1)$ -periodic orbits for $\omega = 5$ and $\frac{\tilde{z}}{\varepsilon} = 0.07$. Following the obtained solution, the perturbation parameter δ has been increased up to its maximum value. Initial conditions close to (\bar{y}_0, \hat{t}_0^1) and (\bar{y}_0, \hat{t}_0^2) have been used in (a) and (b), respectively.	101
5.10	Existence curves of a $(5, 1)$ -periodic orbit for $\omega = 5$. Expression derived from Theorem 5.3.2 (black line), expression for ε_{\min} derived from [Hog89] (dotted line) and $1 - r = \rho\varepsilon$ (dashed line).	104
6.1	Invariant objects for the unperturbed coupled system.	111
6.2	Schematic representation of the manifolds Λ^+ and Λ^-	112
6.3	Schematic representation of the maps P_ε^- , P_ε^+ and P_ε	116
6.4	Scheme of the manifolds $\tilde{\Lambda}^\pm$, the tori $\tilde{\mathcal{T}}_c^\pm$ and their invariant manifolds.	129
6.5	Two rocking blocks linked by a spring.	166
6.6	Melnikov-like function given in (6.5.5) for $v = 0.7$. (a) $\tau = s = 0$ and (b) $\tau = 1.1$	169
6.7	Function ΔU_1 for $v = 0.7$ and $s = 0$. $\bar{\zeta}$ has been set to the first positive zero of the respective Melnikov function (6.5.5).	170
6.8	Heteroclinic trajectory with initial condition \tilde{z}_0^* given in (6.5.7) for $\varepsilon = 0.1$, integrating backwards and forwards in time. In (a) the $x - y$ coordinates, in (b) the $u - v$ ones.	172
6.9	$U(\phi(t; \tilde{z}_0^*; \varepsilon))$ with $\varepsilon = 0.1$. The vertical dashed lines approximately correspond to the times where the trajectory no longer rolls about the manifolds $\tilde{\Lambda}_\varepsilon^\pm$ and escapes.	173

Abstract

This thesis is divided in two parts.

In the first part, we formally study the phenomenon of the so-called big bang bifurcations, both for one and two-dimensional piecewise-smooth maps with a single switching boundary. These are a special type of organizing centers consisting on points in parameter space with co-dimension higher than one from which an infinite number of bifurcation curves emerge. These separate existence regions of periodic orbits with arbitrarily large periods. We show how a mechanism for their occurrence in piecewise-defined maps is the simultaneous collision of fixed (or periodic) points with the switching boundary. For the one-dimensional case, the sign of the eigenvalues associated with the colliding fixed points determines the possible bifurcation scenarios. When they are attracting, we show how the two typical bifurcation structures, so-called period incrementing and period adding, occur if they have different sign or both are positive, respectively. Providing rigorous arguments, we also conjecture sufficient conditions for their occurrence in two-dimensional piecewise-defined maps. In addition, we also apply these results to first and second order systems controlled with relays, systems in slide-mode control.

In the second part of this thesis, we discuss global aspects of piecewise-defined Hamiltonian systems. These are piecewise-defined systems such that, when restricted to each domain given in its definition, the system is Hamiltonian. We first extend classical Melnikov theory for the case of one degree of freedom under periodic non-autonomous perturbations. We hence provide sufficient conditions for the persistence of subharmonic orbits and for the existence of transversal heteroclinic/homoclinic intersections. The crucial tool to achieve this is the so-called impact map, a regular map for which classical theory of dynamical systems can be applied. We also extend these sufficient conditions to the case when the trajectories are forced to be discontinuous by means of restitution coefficient simulating a loss of energy at the impacts. As an example, we apply our results to a system modeling the dynamical behaviour of a rocking block. Finally, we also consider the coupling of two of the previous systems under a periodic perturbation: a two and a half degrees of freedom piecewise-defined Hamiltonian system. By means of a similar technique, we also provide sufficient conditions for the existence of transversal intersections between stable and unstable manifolds of certain invariant manifolds when the perturbation is considered. In terms of the rocking blocks, these are associated with

the mode of movement given by small amplitude rocking for one block while the other one follows large oscillations of small frequency. These heteroclinic intersections allow us to define the so-called scattering map, which links asymptotic dynamics in the invariant manifolds through heteroclinic connections. It is the essential tool in order to construct a heteroclinic skeleton which, when followed, can lead to the existence of Arnold diffusion: trajectories that, in large time scale destabilize the system by further accumulating energy.

Chapter 1

Introduction

1.1 Big Bang bifurcations

In the first part of this thesis we study in a general way which are the dynamical phenomena behind these bifurcations. This allows us to provide general conditions not only for the occurrence of the so-called *big bang* bifurcations but also to predict the involved bifurcation structures.

Chapter 2 is devoted to provide sufficient conditions for the occurrence of the bifurcation scenario referred as *period incrementing* for one-dimensional piecewise-defined maps. It results from a collaboration with Viktor Avrutin and of Michael Schanz, and has been published in [AGS11].

Chapter 3 is more a guideline of a proposal of future work in order to provide and prove similar conditions for the so-called *period adding* scenario (§3.2). We also provide a proposal on how these two previous results can be extended to two-dimensional piecewise-defined maps (§3.3).

In Chapter 4 we apply the previous results, for one and two-dimensional maps, to first and second order linear systems in sliding-mode control. In a very natural way, we derive from a general control scheme based on a relay systems for which the previous results hold. We show how to predict big bang bifurcations occurring in the parameter space formed by the relevant parameters from the control design point of view. This results from a joined work with Enric Fossas, and has been published in DEEDS, [FG12].

1.1.1 General description

In the context of piecewise-smooth dynamics, big bang bifurcations have been reported in the literature (see references below) as specific type of organizing centers in parameter space, where an infinite number of bifurcation curves issue from, separating existence regions of different periodic orbits with arbitrarily large periods. Typically, this codimension-two phenomenon has been detected in one-dimensional piecewise-smooth

maps when globally investigating two-dimensional parameter spaces ([AS06a, ASB06, ASB07]), although it is known that they occur also in higher-dimensional maps and flows.

The importance of these points lies on the fact that they organize the dynamics in the parameter space, as all the possible periodic orbits existing in a neighborhood of such a point are “created” there. In the cited works it was shown that there are several types of big bang bifurcations, which cause different bifurcation scenarios to occur in their neighborhood.

Usually, these detections have been performed numerically and supported by analytical calculations, as no systematic procedures to detect and describe them have been reported until now. As these bifurcations can be observed in many systems in several fields, the question arises how to predict their occurrence and how to determine their type.

Based on experience and observation, such a phenomenon seems to appear for piecewise-defined maps when, under certain conditions, two fixed points (or periodic orbits) collide simultaneously with the boundary. More precisely, consider an n -dimensional state space X split into two parts, X_ℓ and X_r , by a hypersurface Σ and two two-parameter diffeomorphisms $f_\ell(x; c_\ell, c_r), f_r(x; c_\ell, c_r) : X \rightarrow X$. Suppose that $f_i, i \in \{\ell, r\}$, possesses a unique¹ (stable) fixed point¹ x_i^* with real associated eigenvalues. Suppose also that for $c_\ell = c_r = 0$, both fixed points cross Σ transversally at the points $\tilde{x}_i^* \in \Sigma^2$. Suppose also that, near $c_\ell = c_r = 0$, the position of the fixed point x_i^* is locally controlled by c_i . Let us then consider the piecewise-defined map

$$f(x) = \begin{cases} f_\ell(x; c_\ell, c_r) & \text{if } x \in X_\ell \\ f_r(x; c_\ell, c_r) & \text{if } x \in X_r. \end{cases}$$

It is clear that, whenever one of these points crosses transversely the boundary, it undergoes a border collision bifurcation ([NOY94]) and the fixed point becomes virtual. Then, all initial values tend to the other fixed point or, eventually, to a two-periodic orbit with one iteration at each side of Σ . However, if both fixed points become virtual (increasing both parameters through $(c_\ell, c_r) = (0, 0)$) then, for values of (c_ℓ, c_r) arbitrarily close to $(0^+, 0^+)$ it is possible to have periodic orbits of arbitrary period, with periodic points on both sides of Σ . That is, there may exist a *big bang* bifurcation at the origin of the parameter space $c_\ell \times c_r$. If one then encodes the periodic orbits depending on which side of Σ the consecutive iterates belong to, it is easy to see that the possible symbolic sequences of the periodic orbits mainly depend on the sign of the eigenvalues of the fixed points associated with the eigendirections pointing to Σ . In the general n -dimensional case, an explicit description of which symbolic sequences are possible and which are not, for every

¹We consider it unique for simplicity. Obviously, everything in what follows remains the same if both fixed points can be isolated from other invariant sets in a certain neighborhood.

¹For simplicity, we assume them to be fixed points, considering an appropriate iterated function everything can be argued similarly also for periodic orbits.

²Note that, for $n > 1$, we do not assume that $\tilde{x}_\ell^* = \tilde{x}_r^*$. Therefore, in general, f would not necessary have to be continuous at the codimension-two bifurcation point.

case, remains an open problem.

In the first part of this thesis, we will first restrict ourselves, in Chapter 2, to one-dimensional maps f such that both colliding fixed points are stable (f_ℓ and f_r are contractive near $x = 0$ if c_ℓ and c_r are small). In that case, one has $X = \mathbb{R}$, $\Sigma = \{0\}$ (up to translation) and f becomes a map with a single discontinuity at $x = 0$. The distance between the fixed points and the boundary is controlled by the offsets c_ℓ and c_r at the origin, and the sign of the eigenvalues of the fixed points are, obviously, given by the slopes of f_ℓ and f_r near $x = 0$ for c_ℓ and c_r small.

Then, regarding these signs one can consider two different interesting cases: positive-positive (increasing-increasing) and positive-negative (increasing-decreasing)³ for which the bifurcation scenarios near the codimension-two bifurcation point are very different.

The bifurcation scenarios for these two cases were first studied using the offsets as a particular parameterization of a linear piecewise-defined map by Leonov in the late 50's ([Leo59], see also [Mir87]). There, using direct computations, both scenarios were described, and have been later called *period adding* (increasing-increasing) and *period incrementing* (increasing-decreasing) ([AS06a]).

Later, it was shown that similar maps were obtained as first return maps of n -dimensional flows ($n \geq 3$) near a double homoclinic bifurcation, as in the Lorenz case. In this context, this type of (contracting) maps have been intensively studied ([CGT84, GGT84, GGT88, GPTT86, GH94, Hom96, LPZ89, TS86, PTT87, Spa82]), both near the codimension-two bifurcation point and far away from it.

For the contractive case, a first study of the codimension-two bifurcation point in a two-dimensional parameter space was performed in [CGT84]. It was there mentioned in a footnote that going through a certain region in this space one could find an infinite number of periodic (and also aperiodic) orbits and that this region shrinks infinitely to the origin of the parameter space, the big bang bifurcation point. One month later, it was stated in [GGT84] a first relation between the possible symbolic sequences of the periodic orbits near the codimension-two bifurcation point, their rotation numbers and their connection to the Farey numbers. This point was called there *gluing bifurcation*, as the periodic orbits created there were obtained by “gluing” other periodic orbits. This was finally proved in [GGT88] for a contraction ratio less than $\frac{1}{2}$ and later in [GT88] for the pure contracting case.

However, in none of these works the sign of the eigenvalues were considered and, therefore, no distinction between the different bifurcation scenarios was taken into account. This in fact represents the main difference between a gluing bifurcation and the codimension-two bifurcation point that, following [AS06a], we refer here as big bang bifurcation. While

³Recall that we are dealing in this work with maps contractive on both sides. Then, the decreasing-increasing case is equivalent to the increasing-decreasing one. For the decreasing-decreasing one, only a two-periodic orbit or one or two fixed points are possible.

the last one is characterized by an infinite number of bifurcation curves issuing from the point thereby separating periodic orbits with arbitrarily large periods, the first one refers to the fact that two periodic orbits are glued, although maybe an infinite number of times through successive gluing. This implies, for example, that for the decreasing-decreasing case (see footnote 3) a gluing bifurcation occurs creating a two-cycle, but is not a big bang bifurcation as the two colliding fixed points and the two-periodic orbit are the unique invariant objects that one can find near the codimension-two bifurcation point.

A long time after Leonov, in the context of the double homoclinic bifurcation, the scenario for the increasing-increasing case (period adding) was first described for a quadratic piecewise-defined map at the same time in [GPTT86] and [TS86], and later studied in more detail in [LPZ89, PTT87] using direct computations for low periods and renormalization techniques. There, it was shown that the infinite number of periodic orbits emerging from the origin of the parameter space are created by “gluing” them and adding their periods. More recent studies ([AS06a, ASB06, ASB07]) have shown, using direct computations and numerical simulations, that this phenomenon seems to appear for other piecewise-defined maps.

On the other hand, very rigorous works ([AF03, AL89, ALMT89, Gle90, HS90, LM01, LM06]) also gave classification, properties and the sets of periods of the possible periodic orbits using kneading invariants. This was done for expansive increasing-increasing piecewise-defined maps (also called Lorenz-like maps) by focusing on them as continuous circle maps. In this case, an explicit list of the possible periodic orbits is still missing when a similar parameterization controlling the offsets is used.

1.1.2 Period incrementing

The periodic orbits emerging from the origin of the parameter space for the increasing-decreasing case were first described also in [Leo59] ([Mir87]) for a piecewise-linear map. The resulting bifurcation scenario was proven in [GH94] for a particular parameterization of a contractive quadratic piecewise-defined map. This was achieved by collapsing the three-dimensional flow undergoing the double homoclinic bifurcation to a 2-dimensional branched template and using theory of knots and templates. This bifurcation scenario was named in [AS06a] *period incrementing* scenario when analyzing a piecewise-linear map using the offsets as parameters, because the periods of the periodic orbits emerging at the origin of the parameter space are incremented by a constant value. This is precisely what we prove independent of the particular topology in Chapter 2, in collaboration with Michael Schanz and Viktor Avrutin, through the result shown in Corollary 2.4.1. Additionally we make it independent of particular parameterizations in Theorem 2.2.2. There we show for a general piecewise-smooth one-dimensional map that, whenever two (stable) fixed points simultaneously collide with the boundary in such a way that the signs of the associated eigenvalues are different, then a big bang bifurcation of the period

incrementing type takes place.

This scenario is also included in the gluing bifurcation considered in [GGT84], as successive periodic orbits are created by using always the same “gluing orbit”. However, this leads to a much simpler bifurcation structure near the codimension-two bifurcation point than for the increasing-increasing case, in the sense that the second scenario contains orbits that do not exist in the first one.

Also in [Hom96] one can find an accurate description of both scenarios together with the mechanisms that create the orbits. The objective there was to describe the bifurcation scenario for a homoclinic bifurcation of a flow with a single homoclinic orbit under the existence of what is called in [Hom96] a *generalized homoclinic orbit*. This leads the first return map near the saddle point studied in [Hom96] to be the one considered above, but with dependence only on a single parameter making these results valid only in a distance from the codimension-two bifurcation point. By understanding the flow as a small perturbation of one with two homoclinic orbits, it is argued in [Hom96] that this also holds near the codimension-two bifurcation point. However, in Chapter 2, by embedding the period incrementing scenario in its natural two-dimensional parameter space, we show this independently of the flow stating it in the context of non-smooth dynamics. Moreover, we also show that the situation described there occurs for periodic orbits with arbitrarily large periods. In addition, this allows to relax the global contracting condition required in [Hom96] to be locally fulfilled.

1.1.3 Period adding, extension to 2D maps and applications

The bifurcation scenario obtained for the increasing-increasing case (period adding) has to be treated more carefully. After the simultaneous collision of the two stable fixed points, when they are virtual, the one-dimensional map can be reduced to a discontinuous map onto the circle. This map is injective and turns out that its inverse can be extended to a continuous (expanding) circle map onto the circle. For this map, the bifurcation scenario under continuous variation of both parameters leads to the so-called *devil's staircase* when looking at the rotation numbers of the periodic orbits. This opens a bridge between phenomena proper from non-smooth dynamics and classical rotation theory for circle maps, for which there exists a large literature ([ALMS85, ALMT89, AL89, AM90] among others). This is what we provide in Chapter 3 (section 3.2) through the conjectured Lemma 3.2.1. In addition, several results from the 80's ([GIT84, GGT84, CGT84, GGT88]) may be used to relate the rotation numbers of the periodic orbits with the symbolic sequences appearing in the period adding structure.

Following the idea given by the simultaneous collision of fixed points with a boundary under the variation of two parameters, we extend in § 3.3 these results to two-dimensional piecewise-defined maps. Basically, the conditions regarding the signs of the eigenvalues associated with the colliding fixed points (the monotony properties of the one-dimensional map near the codimension-two bifurcation) are translated by topological properties for

the two-dimensional case. More precisely, these refer to intersection of certain sets with their images at the codimension-two bifurcation point.

In Chapter 4, done in collaboration with Enric Fossas, we apply these results to certain control systems. More precisely, to first and second order systems in sliding-mode control. These are systems given by first and second order differential equations whose input is regulated in order to achieve a certain desired output. This regulation is performed by forcing the system to slide along a certain switching surface where, when restricted to it, the system behaves as desired. In practice, this is usually implemented in digital; hence, we consider the discretized version of these systems. This yields to a one or two-dimensional piecewise-defined map of the form considered in Chapters 2 and 3. Then, we show that, under variation of parameters relevant from the control design point of view, the conditions for the occurrence of a big bang bifurcation are given; specially, the ones described in Chapter 3 and hence leading to the existence of big bang bifurcations of the period adding type for these one and two-dimensional piecewise-defined maps.

1.2 Melnikov methods and scattering map in piecewise-smooth systems

In the second part of this thesis we focus on global aspects of piecewise-defined “Hamiltonian” systems. With this we refer to piecewise-defined systems defined in domains where, when restricting to them, the resulting system is Hamiltonian. This provides a piecewise-defined function that, when continuous, provides a preserved quantity and hence we refer to it as piecewise-defined Hamiltonian of the system.

The most paradigmatic examples of such systems are mechanical systems with impacts and electrical systems with switchings. In this part of the thesis we focus on a special type of piecewise-defined Hamiltonian systems obtained as a generalization of the so-called *rocking block*. It consists of a rigid planar block which can rock about to of the ground corners (see Fig. 5.7). Each of these two modes of motion is modeled by a classical Hamiltonian behaving like an inverted pendulum. The transition between both modes, given by the impacts with the ground (crossings of the switching manifold), leads to a system whose equations of motion are provided by a piecewise-defined continuous Hamiltonian. The phase portrait of these systems is formed by two C^0 heteroclinic connections which surround a region fully covered by C^0 periodic orbits.

In the second part of this thesis we first focus, on Chapter 5, on the persistence of these objects when considering a small periodic forcing, simulating an small earthquake, and a small loss of energy at the impacts, hence rigorously extending the classical Melnikov methods to such class of systems. This work, done in collaboration with Tere Seara and John Hogan, has been accepted for publication in SIADS, [GHS12].

In Chapter 6, we consider the cross product of two of such systems, leading to a two-degrees of freedom piecewise-defined Hamiltonian system with two switching manifolds. We focus on the mode of motion given by the periodic orbits for one system and the heteroclinic connections for the other one. In terms of the rocking block model, this is translated on a fast rocking mode of motion for one block while the other one performs large and lower frequency oscillations. This leads to the existence of three-dimensional C^0 invariant manifolds and four-dimensional heteroclinic manifolds. We then rigorously prove their persistence when introducing a Hamiltonian periodic perturbation which depends also on all variables. Moreover, this allows us to define the so-called *scattering map* similarly as in [DdlLS06], which is an essential tool to prove the existence of Arnol'd diffusion by means of heteroclinic chains.

1.2.1 Extension of classical Melnikov methods

The Melnikov method provides tools to determine the persistence of periodic orbits and homoclinic/heteroclinic connections for planar regular systems under non-autonomous periodic perturbations [GH83]. This persistence is guaranteed by the existence of simple zeros of the subharmonic Melnikov function and the Melnikov function, respectively. In this work we extend these classical results to a class of piecewise-smooth differential equations, which generalize a mechanical impact model. In such systems, the perturbation typically models an external forcing and, hence, affects a second order differential equation. In this chapter, we allow for a general periodic Hamiltonian perturbation, potentially influencing both velocity and acceleration. Note that no symmetry is assumed in either the perturbed or unperturbed system.

The unperturbed system is defined in two domains separated by a switching manifold Σ , and possesses one hyperbolic critical point on either side of Σ . We distinguish between two different unperturbed systems. In the first case, which we call conservative, two heteroclinic trajectories connect both hyperbolic points, and surround a region completely covered by periodic orbits including the origin. In the second case, we introduce an energy dissipation, which is modeled by an algebraic condition that forces the solutions to undergo a discontinuity every time they cross the switching manifold. Then, the origin becomes a global attractor and non-trivial periodic orbits and homoclinic/heteroclinic connections can not exist for the unperturbed system.

In order to consider the persistence of periodic orbits for a smooth system, the classical Melnikov method looks for fixed (or periodic) points of the time T stroboscopic map, where T is the period of the perturbation. Since this map is as regular as the flow, one can study its periodic points using classical perturbation methods.

However, for our class of systems, the time T stroboscopic map becomes unwieldy to

use because one has to check the number of times that the flow crosses the switching manifold, which is a priori unknown and can even be arbitrarily large. Hence, the regularity properties of this map are not straightforward. Instead of the classical stroboscopic map, using the switching manifold as a Poincaré section and adding time as variable, we consider the first return Poincaré map, the so-called *impact map*. For the system under consideration, the unperturbed impact map is defined on the cylinder and, under generic hypothesis, is a twist map. Moreover, this map is smooth and hence we can use classical perturbation theory to rigorously prove sufficient conditions for the existence of periodic orbits by looking for periodic points of the perturbed impact map. In the conservative case, these conditions turn out to be analogous to the ones given by the classical Melnikov method, so extending it to a class of piecewise-smooth systems (Theorem 5.3.1). In addition, we rigorously prove that the simple zeros of the subharmonic adapted Melnikov function can guarantee the existence of periodic orbits when the trajectories are discontinuous (Theorem 5.3.2). These discontinuities model a loss of energy on the system and, hence, we also provide conditions for the persistence of these orbits even when the system is dissipative.

The impact map can also be used to prove the existence of invariant KAM tori in the system since it is a twist map in the unperturbed case. After writing the system in action-angle variables, these ideas were applied in [KKY97] to a different system to prove the existence of such tori.

The use of perturbation methods for the existence of periodic orbits of some specific linear systems can be found in [TA07, CFGF11]. Other works have also been applied in [DLZ08, LH10, DL12] to general autonomous systems for the persistence of periodic orbits. The existence of subharmonic orbits in a class of piecewise-smooth systems is shown in [Yag] by uniformly approximating the solutions of the piecewise-smooth system with solutions of a smooth one.

The proof of the persistence of heteroclinic/homoclinic connections for periodically perturbed smooth systems is well established by the classical Melnikov method [GH83]. The main idea is to take some point on the unperturbed homoclinic/heteroclinic connection and consider a section normal to the unperturbed vector field at this point. By the regularity properties of the stable and unstable manifolds of hyperbolic critical points in smooth systems, one can measure the distance between the perturbed manifolds. The Melnikov method derives a first order asymptotic formula for this distance given by the so-called Melnikov function, which is a periodic function whose zeros give, up to first order in the perturbation parameter, the perturbed homoclinic/heteroclinic points. By contrast, since the vector normal to the unperturbed vector field is not defined everywhere in the piecewise-defined system considered here, we proceed as in [BK91, Hog92] and look for the intersection between the stable and unstable manifolds with the switching manifold. Since this intersection depends smoothly on the perturbation parameter, we obtain an asymptotic formula for the distance between the manifolds in this section,

which turns out to be a Melnikov function modified for the piecewise-smooth case. The zeros of this Melnikov function give rise to the existence of heteroclinic connections for the perturbed system. Therefore, we rigorously extend the classical Melnikov method for heteroclinic connections to these class of piecewise-smooth systems.

We also consider the loss of energy at the crossing of the switching surface, modeled by an algebraic condition which makes the system dissipative and the trajectories discontinuous. Then, we also rigorously show that the zeros of the Melnikov function can be used to guarantee the existence of transversal heteroclinic intersections. Both results are given in Theorem 5.4.1.

Other works [Kun00, Kuk07, BF08, BF11] have considered the extension of the Melnikov method to piecewise-defined systems. In these papers, the stable and unstable manifolds of a hyperbolic point located on one side of the switching manifold intersect it at two points that are connected by a trajectory defined on the other side of the switching manifold, thus forming a homoclinic loop for the unperturbed system. Then persistence is related with the zeros of a modified Melnikov function by proving the existence of solutions of a boundary value problem. A Melnikov method for some classes of nonlinear impact oscillators is developed in [DZ05, XFR09].

1.2.2 The scattering map in a two-degrees of freedom piecewise-defined Hamiltonian smooth system

In Chapter 6 we study global phenomena for a piecewise-defined Hamiltonian system resulting from the coupling of two systems of the class of the studied in Chapter 5. That is, we consider the generalization of a model based on two coupled rocking blocks (by a spring for instance) under a non-autonomous periodic Hamiltonian perturbation. This perturbation actually introduces both the coupling and the periodic forcing, which are controlled through the same perturbation parameter. This leads to a 5-dimensional non-smooth system with two switching manifolds such that, when restricted to the domains of the piecewise-definition, the system is a Hamiltonian system with 4 and half degrees of freedom.

In this system we focus on the configuration given by large amplitude oscillations for one block while the other one oscillates with higher frequency and smaller amplitude. For the unperturbed case, this mode of movement is associated with the dynamics given by the existence of certain 3-dimensional invariant manifolds that are only continuous and have stable and unstable C^0 manifolds. To understand the dynamics of the system it is crucial to study their persistence when the perturbation is considered. Due to the lack of regularity of these manifolds, classical perturbation theory cannot be applied. Instead, we translate these invariant objects in terms of an extension of the impact map, introduced in Chapter 5, associated with one of the switching manifolds, leading to new invariant objects that are smooth enough to apply classical theory.

Once we obtain the persistence of the original objects, we also provide sufficient conditions for the existence of 3-dimensional transversal heteroclinic intersections. This allows us to define the *scattering map* following [DdLS06], which associates dynamics in the invariant manifolds through heteroclinic connections. Moreover, by studying the first order terms of this map we provide sufficient conditions for the accumulation of energy in one of the two coupled systems, the one of that oscillates with higher frequency.

In terms of the rocking blocks, this is translated by the fact that, at each oscillation of the large amplitude oscillating block, the other one increases its amplitude of oscillations. The scattering map provides the so-called *heteroclinic skeleton* for further concatenations that, when followed, leads to trajectories which destabilize the system by energy accumulation, hence giving the existence of Arnold diffusion in such a piecewise-defined system.

Part I

Big bang bifurcations and applications

Chapter 2

Sufficient conditions for a period incrementing big bang bifurcation in one-dimensional maps

2.1 Introduction

As mentioned in the Introduction of this part of the work, we provide here sufficient conditions for the occurrence of a big bang bifurcations of the period incrementing type.

This work is organized as follows. In §2.2 we state some notation and definitions and present our result. In §2.3 we prove this result for globally contracting maps for a concrete parameterization consisting of the offsets at the origin. After that, this result is extended in §2.4.1 (Corollary 2.4.1) to locally contracting ones near the boundary with the same parameterization. This can be proved directly but, for clarity reasons, we prefer to do this intermediate step. In order to give details on how the bifurcations occur, we obtain in §2.4.2 a first order approximation of the border collision bifurcation curves that emerge at the big bang bifurcation for this concrete parameterization. Finally, we prove Theorem 2.2.2 in §2.4.3 and we make the result independent of concrete parameterizations permitting the parameters not only to vary the position of the fixed points but also the topology of the map. As these two sections are mainly technical, we encourage the reader not interested in the proofs to skip them up to §2.5. There, by two examples, we verify the predictions. In addition, we also verify the increasing-increasing case, and we conjecture that, in those examples, the period adding big bifurcation is caused by an infinite tree of big bang bifurcations of the period incrementing type.

2.2 Definitions, properties and statement of the results

Before restricting ourselves to the class of maps we are interested in, let us start with some standard definitions and properties of the symbolic dynamics which we are going to use in this work.

Definition 2.2.1. *Given a map $f : \mathbb{R} \rightarrow \mathbb{R}$ and $x \in \mathbb{R}$, we define the symbolic representation of an orbit starting at x , also called the itinerary of x , as $I_f(x) \in \{\mathcal{L}, \mathcal{R}\}^{\mathbb{N}}$, where*

$$I_f(x)(i) = \begin{cases} \mathcal{L} & \text{if } f^i(x) \leq 0 \\ \mathcal{R} & \text{if } f^i(x) > 0 \end{cases}, \quad i \geq 0.$$

Definition 2.2.2. *If x belongs to a n -periodic orbit of a map f , then we will write $I_f(x) = \underline{\theta} := (\theta, \theta, \dots)$ for some finite sequence θ of length n consisting of symbols \mathcal{L} and \mathcal{R} .*

Definition 2.2.3. *Given the shift map σ defined as $\sigma(\alpha_1, \alpha_2, \alpha_3, \dots) = (\alpha_2, \alpha_3, \dots)$ where $\alpha_i \in \{\mathcal{L}, \mathcal{R}\}$, we will say that two n -periodic sequences, $\underline{\theta}_1$ and $\underline{\theta}_2$, are shift-equivalent (or just equivalent), $\underline{\theta}_1 \sim \underline{\theta}_2$, if, and only if, there exists $0 \leq m < n$ such that $\sigma^m(\underline{\theta}_1) = \underline{\theta}_2$.*

It is easy to see that the relation \sim defines an equivalence class in the set of symbolic sequences.

Definition 2.2.4. *We will say that a n -periodic orbit x_1, \dots, x_n of a map f is of type $\underline{\theta}$ if one has $I_f(x_i) \sim \underline{\theta}$, with $1 \leq i \leq n$ and θ a finite sequence of length n . We will also call it a θ -periodic orbit.*

Let us now consider a two-parametric map $f(x; c_\ell, c_r)$ of the form¹

$$f(x; c_\ell, c_r) = \begin{cases} c_\ell + g_\ell(x; c_\ell, c_r) & =: f_\ell(x; c_\ell, c_r) & \text{if } x \leq 0 \\ -c_r + g_r(x; c_\ell, c_r) & =: f_r(x; c_\ell, c_r) & \text{if } x > 0 \end{cases} \quad (2.2.1)$$

such that

C.1 g_ℓ and g_r are $C^\infty(\mathbb{R})$ functions such that for $i, j \in \{\ell, r\}$

$$g_i(0; c_\ell, c_r) = 0$$

and the limit

$$\lim_{x \rightarrow 0} \frac{g_i(x; c_\ell, c_r)}{g_i(x; 0, 0)}$$

exists,

¹We will also avoid writing the dependence on the parameters explicitly and we will refer to it just as $f(x)$ or f .

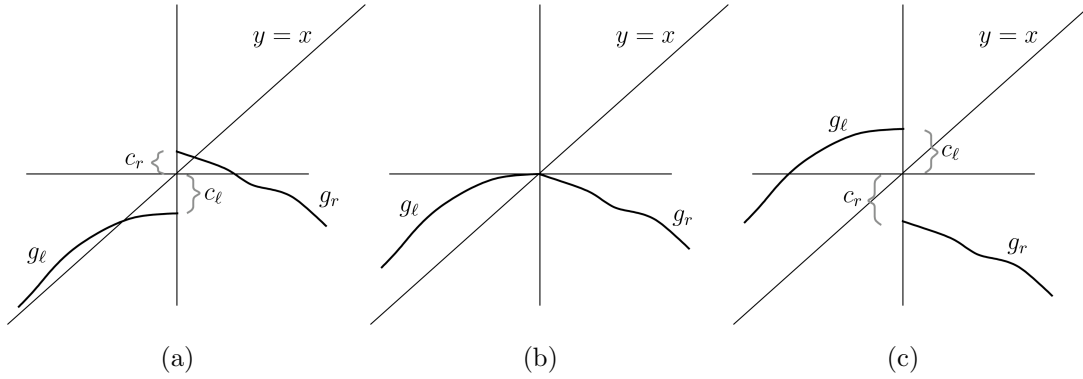


Figure 2.1: Influence of the parameters c_ℓ, c_r on a map as defined in (2.3.1). a) $c_\ell, c_r < 0$, b) $c_\ell = c_r = 0$ and c) $c_\ell, c_r > 0$.

C.2 there exists $\varepsilon_\ell > 0$ such that $0 < g'_\ell(x; c_\ell, c_r) < 1 \forall x \in (-\varepsilon_\ell, 0)$ if $0 \leq c_\ell, c_r \ll 1$,

C.3 there exists $\varepsilon_r > 0$ such that $-1 < g'_r(x; c_\ell, c_r) < 0 \forall x \in (0, \varepsilon_r)$ if $0 \leq c_\ell, c_r \ll 1$,

where

$$g'(x; c_\ell, c_r) = \frac{\partial g(x; c_\ell, c_r)}{\partial x}.$$

Note that conditions C.2 and C.3 allow $g_i(x; c_\ell, c_r)$ to have zero slope at $x = 0$.

Note also that if $-1 \ll c_\ell, c_r < 0$ then the map has two fixed points, one at every side of $x = 0$ (see Fig. 2.1). Due to C.2 and C.3, both fixed points are attracting and, therefore, all orbits with sufficiently small initial conditions will be attracted to one of them, depending on the sign of the initial condition. If one of the parameters c_ℓ, c_r becomes positive, the corresponding fixed point disappears (becomes virtual through a border collision bifurcation) and all those orbits will be attracted to the other fixed point. However, if both parameters are positive but small enough, both fixed points disappear (are virtual) and the orbits starting near the origin stay forever near the origin jumping from one side of $x = 0$ to the other one. The possible asymptotic behaviors of these orbits is precisely what our result describes, which is reflected in the next

Theorem 2.2.1. *Let f be a map of type (2.2.1) fulfilling conditions C.1–C.3. Then, there exists $\varepsilon_0 > 0$ such that, for every $n > 0$ and every $\varepsilon > \varepsilon_0$,*

a) *There exist two curves² in parameter space $c_\ell \times c_r$, $\xi_{\mathcal{RL}^{n-1}}^d(c_\ell)$ and $\xi_{\mathcal{RL}^{n+1}}^c(c_\ell)$, passing*

²The meaning of the upper indices d and c refer to “creation” and “destruction” of the corresponding periodic orbits. These terms of course depend on the point of view that one uses to observe the bifurcation scenario. We choose here to describe the bifurcation curves in the anticlockwise order.

through the origin, such that for every $0 < c_\ell < \varepsilon$ with $\xi_{\mathcal{RL}^{n-1}}^d(c_\ell) < c_r < \xi_{\mathcal{RL}^{n+1}}^c(c_\ell)$, there exists a unique periodic orbit, which is stable and of type $\underline{\mathcal{RL}^n}$.

- b) For every $0 < c_\ell < \varepsilon$, $\xi_{\mathcal{RL}^{n+1}}^c(c_\ell) < c_r < \xi_{\mathcal{RL}^n}^d(c_\ell)$, there coexist two periodic orbits, which are stable and of type $\underline{\mathcal{RL}^n}$ and $\underline{\mathcal{RL}^{n+1}}$.

Moreover, for $(c_\ell, c_r) = (0, 0)$ there exists an open set containing the origin where the unique invariant object is the stable fixed point $x = 0$.

This means that, when considering the parameter space $c_\ell \times c_r \simeq \mathbb{R}^2$, there exists an infinite number of border collision bifurcation curves, $\xi_{\mathcal{RL}^n}^{d,c}$, emerging from the origin, separating all the possible dynamics that one can find near $x = 0$. These curves are ordered anti-clockwise as follows (see also Fig 2.7(b) for a graphical explanation). Given $n \geq 1$, one first finds a curve where an $\underline{\mathcal{RL}^n}$ -periodic orbit is created through a border collision, $\xi_{\mathcal{RL}^n}^c$, and coexists with an other one of type $\underline{\mathcal{RL}^{n-1}}$ until one finds the curve $\xi_{\mathcal{RL}^{n-1}}^d$ where the $\underline{\mathcal{RL}^{n-1}}$ orbit is destroyed. After that, only the $\underline{\mathcal{RL}^n}$ -periodic orbit exists until the next border collision bifurcation occurs at the curve $\xi_{\mathcal{RL}^{n+1}}^c$ where a periodic orbit of type $\underline{\mathcal{RL}^{n+1}}$ is created. From there on, both orbits coexist until the $\underline{\mathcal{RL}^n}$ -periodic orbit is destroyed at $\xi_{\mathcal{RL}^n}^d$. This is repeated for all n ad infinitum starting with the curve $\xi_{\mathcal{RL}^1}^c$, which is located in the 4th quadrant, and followed by the curve $\xi_{\mathcal{R}}^d$, which is the (positive) horizontal axis. Note that, following this point of view, the curve $\xi_{\mathcal{R}}^c$ is in fact the negative horizontal axis. All other border collision bifurcation curves mentioned above are located in the first quadrant and accumulate at the vertical axis. Details on how these bifurcation curves are obtained will be given in §2.4.2 for the case that the functions g_ℓ and g_r do not depend on the parameters c_ℓ, c_r . As already stated in Theorem 2.2.1, all the dynamics described above disappear exactly at the origin of the parameter space, where only a stable fixed point exists.

Obviously, if one interchanges ℓ by r in conditions C.2 and C.3 (decreasing-increasing case) and \mathcal{L} by \mathcal{R} everything above holds. That is, periodic orbits of type $\underline{\mathcal{RL}^n}$ become periodic orbits of type $\underline{\mathcal{LR}^n}$.

Regarding what has been said in the introduction, we will refer to the point $(c_\ell, c_r) = (0, 0)$ as a *Big Bang* bifurcation. In particular, for the situation described above one has the following

Definition 2.2.5. *Let B be a point in a 2-dimensional parameter space such that the bifurcation scenario along the boundary of an arbitrary small neighborhood of B is equivalent to the one described in Theorem 2.2.1 for the origin. Then we will say that there exists a big bang bifurcation of period incrementing type in B .*

Then one can formulate Theorem 2.2.1 in a more compact form as

Theorem 2.2.2. *For a map of type (2.2.1) which satisfies the conditions C.1–C.3, the origin of the parameter space $c_r \times c_\ell$ represents a big bang bifurcation point of the period incrementing type.*

2.3 Increasing-decreasing globally-contracting maps

As already mentioned in the introduction, in this section we will prove Theorem 2.2.2 hardening the conditions C.1–C.3. On one hand, we will assume g_i to be globally contracting and not only near $x = 0$. In addition, we will omit the dependency of g_i on the parameters. Then, in §2.4.1 using a simple result (Lemma 2.4.1) we will see that Theorem 2.2.2 also holds under these assumptions (Corollary 2.4.1). Finally, using a perturbation argument, we will prove Theorem 2.2.2 for the conditions C.1–C.3.

Before going into details, let us state the strategy that we are going to follow. In order to show that only \mathcal{RL}^n -periodic orbits are possible for $c_\ell, c_r > 0$, we will show that other type of periodic orbits can not exist (Lemmas 2.3.1, 2.3.2 and 2.3.3). This permits us using the map $f_\ell^n(f_r)$ to show in Lemma 2.3.6 that only a periodic orbit of type \mathcal{RL}^n can exist for some n . After that, considering the sequence of preimages of 0 under the action of f_ℓ , we will see that \mathcal{RL}^n -periodic orbits exist for every n (Lemma 2.3.7), that they are created and destroyed via border collision bifurcations and that at most two of them can coexist (Lemma 2.3.5).

Let us consider a map as defined in (2.2.1) but relaxing the dependency on the parameters

$$f(x; c_\ell, c_r) = \begin{cases} c_\ell + g_\ell(x) & =: f_\ell(x; c_\ell) & \text{if } x \leq 0 \\ -c_r + g_r(x) & =: f_r(x; c_r) & \text{if } x > 0 \end{cases} \quad (2.3.1)$$

such that

C.1' $g_\ell(x)$ and $g_r(x)$ are $C^\infty(\mathbb{R})$ functions such that $g_r(0) = g_\ell(0) = 0$

C.2' $0 < g'_\ell(x) < 1$ if $x < 0$

C.3' $-1 < g'_r(x) < 0$ if $x > 0$

C.4' $\lim_{x \rightarrow \pm\infty} f(x; c_\ell, c_r) = -\infty$.

We start the proofs of these results with the following lemma.

Lemma 2.3.1. *Given $\theta = I_f(x)$ with f as defined in (2.3.1) fulfilling the conditions C.1'–C.4', if $I_f(x)(i) = \mathcal{R}$ and $c_r > 0$ then $I_f(x)(i+1) = \mathcal{L}$. That is, no consecutive \mathcal{R} 's are possible in θ .*

Proof. Obvious, as $(0, \infty)$ is mapped into $(-\infty, 0)$. □

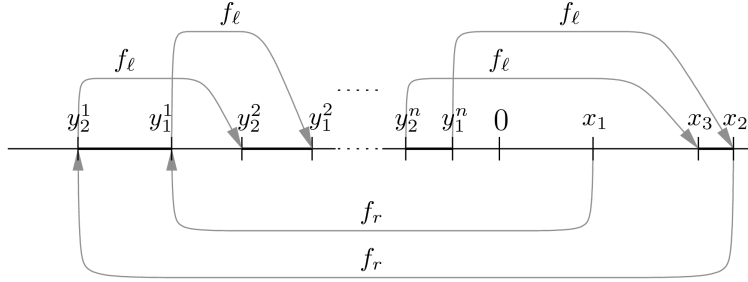


Figure 2.2: “Trapped” orbit

Remark 2.3.1. Note that the previous Lemma does not need $I_f(x)$ to be a periodic sequence.

Lemma 2.3.1 obviously prohibits \mathcal{R}^n -periodic orbits to exist. Although two consecutive \mathcal{L} 's are possible, \mathcal{L}^n -periodic orbits are not, as the next result shows.

Lemma 2.3.2. If x belongs to a periodic orbit of a map f as defined in (2.3.1) fulfilling the conditions C.1'–C.4', then, if $c_\ell > 0$ there exists an i such that $I_f(x)(i) = \mathcal{R}$.

Proof. If $x > 0$, then one has $I_f(x)(0) = \mathcal{R}$. Otherwise, as f_ℓ is monotonically increasing with slope less than one and $f_\ell(0) > 0$, further iterates of x under the action of f_ℓ will necessarily reach the positive domain. \square

As a next step we show now that the word $\mathcal{R}\mathcal{L}^n\mathcal{R}\mathcal{L}^n$ can not be contained in any periodic orbit. It is worth to emphasize that with such a word, we obviously refer here (and in the following) to the compact representation, that is, it has to be followed by an \mathcal{R} , because a successive \mathcal{L} would lead to the word $\mathcal{R}\mathcal{L}^n\mathcal{R}\mathcal{L}^{n+1}$. This result is shown in the next Lemma based on a similar one presented in [GH94]. It is stated there using geometrical arguments in the Lorenz template that similar orbits are not possible for a three-dimensional flow undergoing a homoclinic bifurcation of the single twisted butterfly type. By contrast, we will use here only the nature of the map to prove it.

Lemma 2.3.3. If f is of type (2.3.1) with $c_\ell, c_r > 0$, holding C.1'–C.4', and there exists x_1 such that $I_f(x_1) = \underline{\theta}$, then the word $\mathcal{R}\mathcal{L}^n\mathcal{R}\mathcal{L}^n$ can not be contained in θ .

Proof. Let us suppose that there exists x_1 such that $I_f(x_1) = \underline{\theta}$ with $\theta = \mathcal{R}\mathcal{L}^n\mathcal{R}\mathcal{L}^n\theta_2$ for some finite word θ_2 . Note that using the relation \sim one can consider that θ is given in this form. Let us write this periodic orbit as

$$\underbrace{x_1, y_1^1, y_1^2, \dots, y_1^n, x_2, y_2^1, y_2^2, \dots, y_2^n}_{\mathcal{R}\mathcal{L}^n\mathcal{R}\mathcal{L}^n}, \underbrace{x_3, \dots}_{\theta_2}, \underbrace{x_1, \dots, \dots}_{\mathcal{R}\mathcal{L}^n\mathcal{R}\mathcal{L}^n}, \dots,$$

where $x_i > 0$ and $y_i^j < 0$ (see Fig. 2.2). Let us also assume that $x_1 < x_2$ (otherwise the same argument can be performed with the points x_2 and x_3) and let us iterate the whole interval $[x_1, x_2]$. As f_r is decreasing and $c_r > 0$, $f_r([x_1, x_2]) = [y_2^1, y_1^1]$ with $f_r(x_2) = y_2^1 < f_r(x_1) = y_1^1 < 0$, the interval is twisted. Moreover, as f_r and f_ℓ are, respectively, decreasing and increasing contracting functions, we have

$$\mu([x_1, x_2]) > \mu([y_2^1, y_1^1]) > \mu([y_2^2, y_1^2]) > \cdots > \mu([y_2^n, y_1^n]) > \mu([x_3, x_2]),$$

where $\mu([a, b]) = |b - a|$ is the length of the interval $[a, b]$.

Now, as f_ℓ preserves orientation and the length of $[x_1, x_2]$ is decreased, $x_3 \in (x_1, x_2)$ and therefore $y_3^1 = f_r(x_3)$ needs also n iterations to return to the right side.

Repeating the same argument with $[x_3, x_2]$, one has that $f_\ell^n(y_3^1) = x_4 \in (x_3, x_2)$. Iterating the argument, the orbit of x_1 will be “trapped” in (x_3, x_2) and will never reach x_1 again, so it can not be periodic. \square

Remark 2.3.2. *Note that it is crucial in the last proof that both points x_1 and x_2 return to the right domain $(0, \infty)$ after exactly the same number n of iterations under the action of f_ℓ . That is, the interval $f^m([x_1, x_2])$ remains connected for all m .*

Before considering periodic sequences containing the word $\mathcal{RL}^n\mathcal{RL}^m$ with $n \neq m$, let us state some properties and definitions of maps of type (2.3.1) fulfilling the conditions C.1’–C.4’.

We first note that the left branch f_ℓ reaches its maximum value at $x = 0$ ($f_\ell(0) = c_\ell > 0$) and, therefore, when a point $y < 0$ is re-injected into the right domain by f_ℓ it has to be necessarily in $(0, c_\ell]$. On the other hand, as f_r is monotonically decreasing, every point $x \in (0, c_\ell]$ will be injected into the left domain in the interval $[\nu, 0]$, where $\nu = f_r(c_\ell) < 0$. Hence, the interval $[\nu, c_\ell]$ acts as an “absorbing” interval as all orbits starting at any point $x \in \mathbb{R}$ will reach it after some number of iterations and will never leave it. Therefore we have the following lemma.

Lemma 2.3.4. *Let $f(x)$ be a map of type (2.3.1) which fulfills the conditions C.1’–C.4’ and let $\nu = f_r(c_\ell)$. For every $x \in \mathbb{R}$ there exists an m_0 such that $f^m(x) \in [\nu, c_\ell] \forall m \geq m_0$. Therefore, the map f can be considered as a map on the interval $[\nu, c_\ell]$:*

$$f : [\nu, c_\ell] \rightarrow [\nu, c_\ell]$$

Remark 2.3.3. *Note that this global reduction is true as the functions g_ℓ/g_r are globally increasing/decreasing and contractive (C.1’–C.4’). In the next section, where the conditions C.1’–C.4’ are going to be relaxed, this reduction will be valid only locally.*

Let us now consider the sequences $\{a_n\}$ and $\{b_n\}$ formed, respectively, by the preimages of 0 by the left branch and by the preimages of these preimages by the right branch

$$a_0 = 0, \quad a_n = f_\ell^{-1}(a_{n-1}) \text{ with } n > 0, \quad (2.3.2)$$

$$b_n = f_r^{-1}(a_n) \text{ with } n \geq n_0, \quad (2.3.3)$$

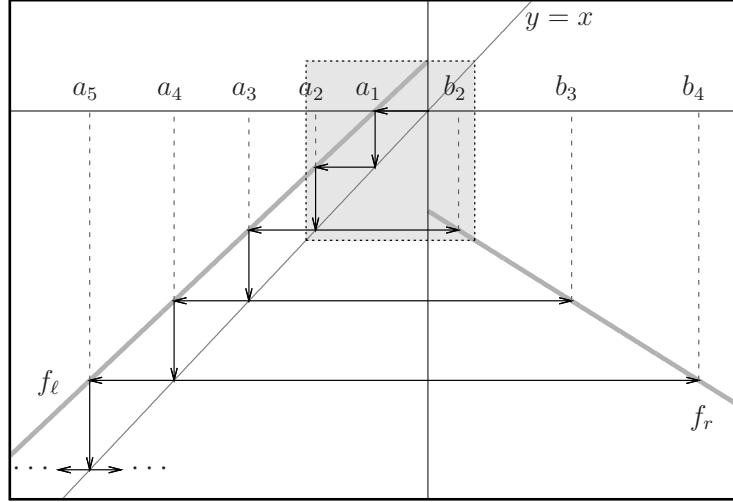


Figure 2.3: Definition of the sequences $\{a_n\}$ and $\{b_n\}$. The dotted box corresponds to the absorbing interval.

with some n_0 as explained below (see Fig. 2.3). Note that, as f_ℓ is a monotonically increasing function, if $c_\ell > 0$ the sequence $\{a_n\}$ verifies $a_{n+1} < a_n \leq 0 \forall n \geq 0^3$. Although the preimages of 0 by the left branch (a_n) exist $\forall n$, b_n is defined for $n \geq n_0$ where n_0 is such that $a_{n_0} \leq -c_r < a_{n_0-1}$.

Due to the contractiveness of both functions f_ℓ and f_r , the following inequalities hold

$$\frac{\mu([a_{n+1}, a_n])}{\mu([a_n, a_{n-1}])} > 1, \quad n > 0 \quad (2.3.4)$$

$$\frac{\mu([b_n, b_{n+1}])}{\mu([b_{n-1}, b_n])} > 1, \quad n > n_0.$$

The sequence $\{a_n\}$ defined in Eq. (2.3.2) splits the interval $(-\infty, 0]$ into sub-intervals of the form $(a_{n+1}, a_n]$ (see Fig. 2.3) such that $\forall y \in (a_{n+1}, a_n]$ the number of iterations needed for y to return to the right domain is exactly $n+1$. On the other hand, the intervals $(0, b_{n_0})$ and $[b_n, b_{n+1})$ with $n \geq n_0$, form a partition of $(0, \infty)$, such that $\forall x \in [b_n, b_{n+1})$ the point $f_r(x)$ needs exactly $n+1$ iterations by f_ℓ to return to the positive domain.

For a fixed value $(c_\ell, c_r) \in \mathbb{R}^+ \times \mathbb{R}^+$, the number of iterations that a periodic orbit can perform in the negative domain is determined by the number of elements of the sequence $\{b_n\}$ contained in the absorbing interval $[\nu, c_\ell]$. For example if b_2 and b_3 would be contained in the absorbing interval $[\nu, c_\ell]$, then the number of iterations of a periodic

³Note that $f^0(0) = 0$ as the function $f^0(x)$ is the identity.

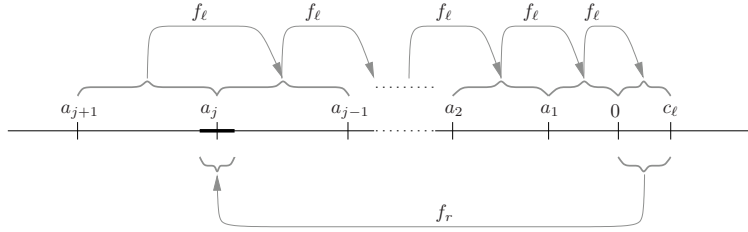


Figure 2.4: Backward and forward iterates of $(0, c_\ell]$. $f_r((0, c_\ell])$ (dark segment) is smaller than $f_\ell^{-n}((0, c_\ell]) \forall n$. Therefore, at most one a_j can be reached by $f_r((0, c_\ell])$.

orbit can be two, three or four. However, as the next result shows, at most one element of the sequence $\{b_n\}$ can be contained in the absorbing interval $[\nu, c_\ell]$.

Lemma 2.3.5. *If f is a map of type (2.3.1) fulfilling conditions C.1'–C.4', then there exists at most one a_j (equiv. b_j) such that $a_j \in f_r((0, c_\ell])$ (equiv. $b_j \in (0, c_\ell]$).*

Proof. Recalling that $c_\ell = f_\ell(0)$, one has (see Fig. 2.4)

$$\begin{aligned} [a_{n+1}, a_n] &= f_\ell^{-1}([a_n, a_{n-1}]) \\ [a_1, 0] &= f_\ell^{-1}([0, c_\ell]). \end{aligned}$$

Using the property shown in Eq. (2.3.4) one has

$$\mu([0, c_\ell]) < \mu([a_{n+1}, a_n]) \forall n,$$

and, since f_r is a contractive function one obtains

$$\mu(f_r((0, c_\ell]) < \mu([a_{n+1}, a_n]) \forall n.$$

Therefore, at most one a_n can be located in $f((0, c_\ell])$. □

For a fixed j , the uniqueness of such a b_j (in case of existence) in the last Lemma implies that the periodic sequences of a map under the considered conditions can be either $\underline{\mathcal{RL}}^j$, $\underline{\mathcal{RL}}^{j+1}$ or sequences containing these two words only. However, what we want to show is that the last case is not possible and in fact the only admissible periodic sequences are exactly $\underline{\mathcal{RL}}^j$ and $\underline{\mathcal{RL}}^{j+1}$. Therefore, let us consider the two only possible cases: for a certain j , either $(0, c_\ell] \subset (b_j, b_{j+1})$ (which means $b_j = 0$ or $b_j \notin [0, c_\ell]$) or $(0, c_\ell] = (0, b_j) \cup [b_j, c_\ell]$ (which means $b_j \in (0, c_\ell]$ ($c_\ell < b_{j+1}$), which is the case shown in Fig. 2.3.

In the first case, as the periodic orbits have to be contained in the interval $[\nu, c_\ell]$, they always need the same number of iterations on the negative domain and the result comes from Lemmas 2.3.1, 2.3.2 and 2.3.3.

In the second case, we have to show that if a periodic orbit reaches $(0, b_j)$ it can not reach $[b_j, c_\ell]$ and vice versa, that is, once an orbit enters the absorbing interval $[\nu, c_\ell]$, the number of iterations needed to return to the positive domain is preserved and is either j or $j + 1$. Both cases are included in the following lemma.

Lemma 2.3.6. *Let f be a map as defined in (2.3.1) fulfilling conditions C.1'–C.4'. If $x \in \mathbb{R}$ belongs to a periodic orbit of f then there exists $n > 0$ such that $I_f(x) = \underline{\mathcal{R}\mathcal{L}^n}$ up to shift-equivalence.*

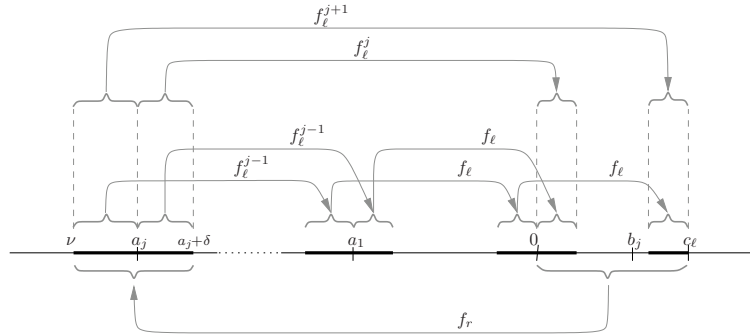


Figure 2.5: The interval $f_r((0, c_\ell])$ is split when it returns to the right domain.

Proof. If $\nexists a_j \in f_r((0, c_\ell])$, then $f_r((0, c_\ell]) \subset (a_n, a_{n-1})$ for some n and

$$f_\ell^n(f_r((0, c_\ell])) \subset (0, c_\ell].$$

Due to the contractiveness, the map $f_\ell^n f_r(x)$ has a fixed point and f an $\underline{\mathcal{L}^n \mathcal{R}}$ -periodic orbit. By Lemmas 2.3.1, 2.3.2 and 2.3.3, it is the unique one.

Now let us suppose that there exists $a_j \in f_r((0, c_\ell])$ which, by Lemma 2.3.5, must be unique. We also have a unique $b_j \in (0, c_\ell]$. As f_r is monotonously decreasing and thus the interval $(0, c_\ell]$ is inverted, we can write

$$f_r((0, c_\ell]) = [\nu, a_j + \delta)$$

for some $\delta > 0$.

As f_ℓ is continuous in $(-\infty, 0]$ and $f_\ell(a_n) = a_{n-1} \forall n > 1$, the interval $f_\ell^n([\nu, a_j + \delta))$ remains connected and contains a_{j-n} for $n = 1, \dots, j$ (see Fig. 2.5). For $n = j$, the interval contains 0 and therefore it contains positive and negative points. The positive ones are immediately mapped into $(a_j, a_j + \delta)$ by f_r in such a way that $f_r(0^+) = (a_j + \delta)^-$. Negative points need one more iteration by f_ℓ and will be mapped into $(b_j, c_\ell]$ with $f_\ell(0^-) = c_\ell^-$, so

the initial interval is split. After that, these points will be mapped into $[\nu, a_j]$ verifying that $f_r(c_\ell^-) = \nu^+$. Summarizing,

$$\begin{aligned} f_r((0, b_j)) &= (a_j, a_j + \delta) \\ f_r([b_j, c_\ell]) &= [\nu, a_j] \end{aligned}$$

and

$$\begin{aligned} f_\ell^{j+1}([\nu, a_j]) &\subset [b_j, c_\ell] \\ f_\ell^j((a_j, a_j + \delta)) &\subset (0, b_j), \end{aligned}$$

so

$$\begin{aligned} f_\ell^{j+1}(f_r([b_j, c_\ell])) &\subset [b_j, c_\ell] \\ f_\ell^j(f_r(0, b_j)) &\subset (0, b_j), \end{aligned}$$

and, for an orbit starting in $(0, c_\ell]$, the number of steps performed in the negative domain before being re-injected to the positive domain will remain constant and equal to j or $j+1$ depending on whether it starts in $(0, b_j)$ or $[b_j, c_\ell]$, respectively. Therefore, only symbolic sequences of the form $\mathcal{RL}^j\mathcal{RL}^j\dots$ or $\mathcal{RL}^{j+1}\mathcal{RL}^{j+1}\dots$ with starting points in $(0, c_\ell]$ are possible.

As it has been proven above, that the number of steps on the left side of a periodic orbit must be preserved, we can apply Lemma 2.3.3 to show that if x belongs to a periodic orbit of a map under the considered conditions, then necessarily $I_f(x) = \underline{\mathcal{RL}^n}$ for some $n > 0$. \square

Now we ask about the reciprocal of Lemma 2.3.6, that is, we want to show that periodic orbits of type $\underline{\mathcal{RL}^n}$ exist $\forall n > 0$.

Lemma 2.3.7. *Let f be of the form defined in (2.3.1) and fulfilling conditions C.1'-C.4'. Then, for every $n \geq 1$ and every $c_\ell > 0$, there exists $c_r > 0$ such that f possesses an orbit with the symbolic sequence $\underline{\mathcal{RL}^n}$.*

The proof of this Lemma is in fact an extension of the arguments presented in [Hom96] §3.3.

Proof. It is clear that for every $n \geq 2$ and every $c_\ell > 0$ there exists $c_r > 0$ such that

$$f_r((0, c_\ell]) \cap [a_n, a_{n-1}] \neq \emptyset,$$

which can be given due to one of the next three situations (see Figs. 2.4 and 2.5)

S.1 $a_{n-1} \in f_r((0, c_\ell])$

$$\text{S.2 } f_r((0, c_\ell]) \subset (a_n, a_{n-1})$$

$$\text{S.3 } a_n \in f_r((0, c_\ell])$$

If S.1 holds, $b_{n-1} \in (0, c_\ell]$ and

$$\begin{aligned} f_\ell^n f_r &: [b_{n-1}, c_\ell] \longrightarrow [b_{n-1}, c_\ell] \\ f_\ell^{n-1} f_r &: (0, b_{n-1}) \longrightarrow (0, b_{n-1}), \end{aligned}$$

are continuous contracting functions which must have a unique (stable) fixed point. Therefore, two stable periodic orbits $\underline{\mathcal{R}\mathcal{L}^n}$ and $\underline{\mathcal{R}\mathcal{L}^{n-1}}$ coexist. Note that for $n = 2$ this proves also the existence of a $\underline{\mathcal{R}\mathcal{L}}$ orbit.

In the second case (S.2), $b_{n-1} \notin (0, c_\ell]$ ($[0, c_\ell] \subset (b_{n-1}, b_n)$) and

$$f_\ell^n f_r : (0, c_\ell] \longrightarrow (0, c_\ell]$$

is a continuous contracting function which also must have a unique (stable) fixed point. In this case, there exists a unique periodic orbit of type $\underline{\mathcal{R}\mathcal{L}^n}$ which is the unique attractor in $(0, c_\ell]$.

Finally, if S.3 holds, replacing n by $n - 1$ and arguing as in S.1, one has that a stable periodic orbit of type $\underline{\mathcal{R}\mathcal{L}^n}$ coexists with a stable $\underline{\mathcal{R}\mathcal{L}^{n+1}}$ -periodic one. \square

Remark 2.3.4. *By contrast to all orbits $\underline{\mathcal{R}\mathcal{L}^n}$ with $n \geq 2$, the periodic orbit $\underline{\mathcal{R}\mathcal{L}}$ exists not only for $c_r > 0$ but also for $c_r \leq 0$. In that case, it coexists with the fixed point $\underline{\mathcal{R}}$ ($\underline{\mathcal{L}^0\mathcal{R}}$).*

Remark 2.3.5. *Note that the transitions between cases S.1, S.2 and S.3 are given by border collision bifurcations where the respective periodic orbits are created or destroyed when they collide with the boundary $x = 0$. This defines the curves ξ^c and ξ^d used in Theorem 2.2.1. See §2.4.2 for more details.*

Remark 2.3.6. *As it is known, invariant objects of piecewise-smooth systems do not necessarily have to be separated by another invariant object. In this case, the coexistence of stable periodic objects may also be separated by the discontinuity (and its preimages) (see [dBCK08] for an extensive overview about piecewise-smooth dynamics).*

Theorem 2.3.1. *For a map of type (2.3.1) which fulfills the conditions C.1'–C.4', the origin of the parameter space $c_\ell \times c_r$ represents a big bang bifurcation point of the period incrementing type.*

Proof. It is clear that for $(c_\ell, c_r) = (0, 0)$ the map f possesses a stable fixed point at $x = 0$. In a first step we have to show that an infinite number of bifurcation curves separating existence regions of different periodic orbits are issuing from the origin. In a second step we have to show that a smooth change of the parameters across the bifurcation curve

confining the regions of existence of a unique \mathcal{RL}^n orbit lead to the creation of (coexisting) \mathcal{RL}^{n+1} - or \mathcal{RL}^{n-1} -periodic orbits.

The key to show the first step is the fact that the sequence $\{a_n\}$ collapses to the origin as $c_\ell \rightarrow 0$, that is

$$\lim_{c_\ell \rightarrow 0} a_n = 0 \quad \forall n \geq 1.$$

This is due to the continuity of f_ℓ and the fact that it is a monotonically increasing function. As $[a_1, 0] = f_\ell^{-1}([0, c_\ell])$ (compare Fig. 2.4), it is clear that $a_1 \rightarrow 0$ as $c_\ell \rightarrow 0$. Now, iterating the argument and using that $a_n = f_\ell^{-1}(a_{n-1})$, it is clear that for every $\varepsilon > 0$, arbitrarily small, there exists $c_\ell(\varepsilon)$ small enough such that $-\varepsilon < a_n < 0$. By Lemma 2.3.7, there exists c_r such that $f_r([0, c_\ell])$ contains a_n and, therefore, a periodic orbit of type \mathcal{RL}^n exists.

On the other hand, it is clear that $c_r \rightarrow 0$ as $a_n \rightarrow 0$ and, therefore, a \mathcal{RL}^n -periodic orbit exists for every n for values of (c_ℓ, c_r) arbitrarily close to the origin. Finally, if $(c_\ell, c_r) = (0, 0)$, the map possesses a stable fixed point which absorbs all orbits and thus all periodic orbits disappear at that point. \square

2.4 Extension of the result

2.4.1 Increasing-decreasing locally-contracting maps

In this section we relax the global monotonically-contracting conditions C.1'–C.4' to be fulfilled near the origin and show that the results of the previous section are valid sufficiently close to the origin of the parameter space. Thus we restrict ourselves to maps of type (2.3.1) fulfilling

C.1'' g_ℓ and g_r are $C^\infty(\mathbb{R})$ functions such that $g_\ell(0) = g_r(0) = 0$

C.2'' There exists $\varepsilon_\ell > 0$ such that $0 < g'_\ell(x) < 1 \quad \forall x \in (-\varepsilon_\ell, 0)$

C.3'' There exists $\varepsilon_r > 0$ such that $-1 < g'_r(x) < 0 \quad \forall x \in (0, \varepsilon_r)$

Due to the smoothness of functions f_ℓ and f_r near the origin, there exists an open neighborhood of this point where both functions are contracting and which contains the absorbing interval $[\nu, c_\ell]$ if c_r and c_ℓ are small enough.

On the other hand, the values of c_r given by Lemma 2.3.7 tend to 0 as $c_\ell \rightarrow 0^+$, and therefore all results of the previous section hold under these conditions.

From the previous arguments one has the next result.

Lemma 2.4.1. *Let f be a map of type (2.3.1) keeping conditions C.1''–C.3''. Then there exist c_ℓ^0 and c_r^0 such that if $0 < c_\ell < c_\ell^0$ and $0 < c_r < c_r^0$ f is contracting in $[\nu, c_\ell]$. Moreover, for every $c_r < c_r^0$ and every n , there exists $0 < \varepsilon < c_\ell^0$ such that $a_j \in [\nu, 0] \quad \forall j \leq n$ if $c_\ell < \varepsilon$.*

Corollary 2.4.1. *Under conditions C.1''–C.3'', a map of type (2.3.1) undergoes a big bang bifurcation of the period incrementing type at the origin of the parameter space $c_\ell \times c_r$.*

Remark 2.4.1. *If one changes condition C.3' by g_r to be a constant function for $x \geq 0$, then all the results presented above are still valid except for one detail. In such a case, one has only to take into account that, as $f_r((0, c_\ell])$ would be a single point. Then, conditions S.1 and S.3 in the proof of Lemma 2.3.7 become $a_{n-1} = f_r((0, c_\ell])$ and $a_n = f_r((0, c_\ell])$, respectively, preventing the coexistence between two different orbits. Therefore, (b) in Theorem 2.2.1 no longer holds as $\xi_{\mathcal{RL}^{n-1}}^c = \xi_{\mathcal{RL}^n}^d$. Such a situation has been referred to in the literature ([AS06a]) as pure period incrementing scenario, and therefore the origin of the parameter space represents a pure period incrementing big bang bifurcation.*

Recalling Remark 2.3.5, the orbits given in Theorem 2.2.2 are created and destroyed at border collision bifurcation curves, which are mentioned in the first version of the same result, Theorem 2.2.1. In the next section, approximating them up to first order, we will give details on how they are obtained.

2.4.2 Border collision curves near the origin

Given $n > 0$ and $c_\ell > 0$ (which we will always assume to be small enough), we know (Lemma 2.3.7) that there exists $c_r > 0$ such that one of the next cases hold

$$\text{S.1 } a_{n-1} \in f_r((0, c_\ell])$$

$$\text{S.2 } f_r((0, c_\ell]) \subset (a_n, a_{n-1})$$

$$\text{S.3 } a_n \in f_r((0, c_\ell])$$

implying the existence of a \mathcal{RL}^n -periodic orbit. As has been shown in the proof of Lemma 2.3.7, every case above leads to different dynamics. Therefore, the limiting parameter values define a (border collision) bifurcation. Then for each of the cases above, for every c_ℓ we will find the extremal value of c_r and obtain the bifurcation curves, $\xi_{\mathcal{RL}^n}^{c,d}$ at which an \mathcal{RL}^n orbit is created or destroyed.

The smallest value of c_r which leads S.1 to be fulfilled is given by

$$f_r(c_\ell) = a_{n-1} \tag{2.4.1}$$

and corresponds to the creation of the periodic orbit \mathcal{RL}^n coexisting with the periodic orbit \mathcal{RL}^{n-1} . The transition between S.1 to S.2 is given by

$$f_r(0) = a_{n-1}$$

where the periodic orbit $\underline{\mathcal{R}\mathcal{L}^{n-1}}$ is destroyed leading the periodic orbit $\underline{\mathcal{R}\mathcal{L}^n}$ to be the unique attractor (near the origin).

Increasing c_r , one finds the value of this parameter which satisfies the condition

$$f_r(c_\ell) = a_n.$$

At this parameter value, representing the transition from S.2 to S.3, the periodic orbit $\underline{\mathcal{R}\mathcal{L}^{n+1}}$ is created and coexists with $\underline{\mathcal{R}\mathcal{L}^n}$.

Finally, the next bifurcation is given by

$$f_r(0) = a_n \tag{2.4.2}$$

where the periodic orbit $\underline{\mathcal{R}\mathcal{L}^n}$ is destroyed as S.3 no longer holds.

Summarizing, for every $c_\ell > 0$ and $n > 0$, Eqs. (2.4.1) and (2.4.2) give the value of c_r for the border collision bifurcations where, respectively, the $\underline{\mathcal{R}\mathcal{L}^n}$ -periodic orbit is created and destroyed. Therefore, in parameter space, the respective border collision bifurcation curves in a sufficiently small open set \mathcal{U} of the origin will be given by

$$\begin{aligned} \xi_{\mathcal{R}\mathcal{L}^n}^c &= \{(c_\ell, c_r) \in \mathcal{U}, c_\ell > 0 \mid f_r(c_\ell) = a_{n-1}\} \\ \xi_{\mathcal{R}\mathcal{L}^n}^d &= \{(c_\ell, c_r) \in \mathcal{U}, c_\ell > 0 \mid f_r(0) = a_n\} \end{aligned}$$

However, in order to obtain first order approximation of these curves, it is more convenient to consider the equations

$$F^c(c_\ell, c_r) := f_\ell^{n-1}(f_r(c_\ell)) = 0 \tag{2.4.3}$$

$$F^d(c_\ell, c_r) := f_\ell^n f_r(0) = 0 \tag{2.4.4}$$

which are equivalent to (2.4.1) and (2.4.2), respectively. In addition, as

$$\begin{aligned} \frac{\partial F^c}{\partial c_r}(0, 0) &= \begin{cases} -1 & \text{if } n = 1 \\ -g'_\ell(0)^{n-1} & \text{if } n > 1 \end{cases} \\ \frac{\partial F^d}{\partial c_r}(0, 0) &= -g'_\ell(0)^n, \end{aligned}$$

one can always write c_r as a function of c_ℓ if $g'_\ell(0) \neq 0$. Therefore, using

$$\frac{\partial F^c}{\partial c_\ell}(0, 0) = \begin{cases} g'_r(0) & \text{if } n = 1 \\ 1 + g'_\ell(0) + g'_\ell(0)^2 + \dots & \text{if } n > 1 \\ \dots + g'_\ell(0)^{n-1} g'_r(0) & \text{if } n > 1 \end{cases} \tag{2.4.5}$$

$$\frac{\partial F^d}{\partial c_\ell}(0, 0) = 1 + g'_\ell(0) + g'_\ell(0)^2 + \dots + g'_\ell(0)^{n-1} + g'_\ell(0)^n > 0 \tag{2.4.6}$$

and applying the Implicit Function Theorem, the first order approximation of the bifurcation curves are given by the expressions

$$\begin{aligned}
c_r &= \xi_{\mathcal{RL}^n}^c(c_\ell) = -\frac{\frac{\partial F^c}{\partial c_\ell}}{\frac{\partial F^c}{\partial c_r}} c_\ell + O(c_\ell^2) \\
&= \frac{1 + g'_\ell(0) + g'_\ell(0)^2 + \cdots + g'_\ell(0)^{n-1} g'_r(0)}{g'_\ell(0)^{n-1}} c_\ell + O(c_\ell^2) \tag{2.4.7}
\end{aligned}$$

$$\begin{aligned}
c_r &= \xi_{\mathcal{RL}^n}^d(c_\ell) = -\frac{\frac{\partial F^d}{\partial c_\ell}}{\frac{\partial F^d}{\partial c_r}} c_\ell + O(c_\ell^2) \\
&= \frac{1 + g'_\ell(0) + g'_\ell(0)^2 + \cdots + g'_\ell(0)^{n-1} + g'_\ell(0)^n}{g'_\ell(0)^n} c_\ell + O(c_\ell^2). \tag{2.4.8}
\end{aligned}$$

Remark 2.4.2. *In the case that $g'_\ell(0) = 0$, all the bifurcation curves $\xi_{\mathcal{RL}^n}^{c,d}$, with $n > 1$, are vertical at the origin and one can not proceed with this approach to obtain approximated expressions. However, one can always obtain c_ℓ as a function of c_r instead, although, in order to distinguish between the curves, a higher order analysis becomes necessary because all first order approximations lead to the vertical axis.*

Remark 2.4.3. *Recalling that $f_\ell^0 = Id$, for $n = 1$ one has that*

$$\begin{aligned}
\frac{\partial F^c}{\partial c_\ell}(0,0) &= g'_r(0) \\
\frac{\partial F^c}{\partial c_r}(0,0) &= -1.
\end{aligned}$$

Hence, the curve (2.4.7) becomes

$$\xi_{\mathcal{RL}^n}^c(c_\ell) = g'_r(0)c_\ell + O(c_\ell^2),$$

which, assuming $g'_r(0) \neq 0$, has negative slope. Thus, as mentioned in the discussion below Theorem 2.2.1, this bifurcation curve is located in the fourth quadrant.

Using $n = 0$ in Eq. (2.4.4), it clearly comes that the curve $\xi_{\mathcal{R}}^d$ is the horizontal axis, $c_r = 0$.

As one can see from Eqs. (2.4.7)-(2.4.8), all other bifurcation curves have positive slope and, hence, are located in the first quadrant.

2.4.3 Proof of Theorem 2.2.2

In order to prove Theorem 2.2.2 we first consider a map of the form (2.2.1) and obtain from it a new map

$$\tilde{f}(x) = \begin{cases} c_\ell + g_\ell(x; 0, 0) & =: \tilde{f}_\ell(x; c_\ell) & x < 0 \\ -c_r + g_r(x; 0, 0) & =: \tilde{f}_r(x; c_r) & x > 0 \end{cases} \tag{2.4.9}$$

which is of type (2.3.1) and fulfills conditions C.1''–C.3''. Note in particular that conditions C.2 and C.3 for a map of type (2.2.1) imply that (2.4.9) fulfills conditions C.2'' and C.3''. Therefore, Corollary 2.4.1 applies and the system (2.4.9) undergoes a big bang bifurcation of the period incrementing type at the origin of the parameter space $c_\ell \times c_r$. Then, one only needs to show that all the bifurcation curves issuing from the origin of the parameter space also exist for the system (2.2.1). For that purpose, let us consider for example the bifurcation curve defined by the equation

$$\tilde{f}_\ell^n(\tilde{f}_r(0; c_r); c_\ell) = 0. \quad (2.4.10)$$

which, for convenience, we solve isolating c_ℓ as a function of c_r . Thus, recalling Remarks 2.4.2 and 2.4.3, we know that (2.4.10) possesses a (unique) solution c_ℓ^* for every c_r arbitrarily small and for every $n \geq 1$, defining the border collision bifurcation curve $c_\ell = \tilde{\xi}_{\mathcal{RL}^n}^d(c_r)$. Now, we wonder whether the corresponding equation

$$f_\ell^n(f_r(0; c_\ell, c_r); c_\ell, c_r) = 0 \quad (2.4.11)$$

that defines the corresponding bifurcation curve for the original system can also be solved for c_ℓ for every c_r small. Note that the functions f_ℓ and f_r can be written as

$$\begin{aligned} f_\ell(x; c_\ell, c_r) &= \tilde{f}_\ell(x; c_\ell) + G_\ell(x; c_\ell, c_r) \\ f_r(x; c_\ell, c_r) &= \tilde{f}_r(x; c_r) + G_r(x; c_\ell, c_r), \end{aligned}$$

with $G_i(x; 0, 0) = 0$ and $\frac{\partial G_i}{\partial j}(0; 0, 0) = 0$, $i \in \{\ell, r\}$ $j \in \{x, c_\ell, c_r\}$. As a consequence of that, a straight forward calculation shows that equation (2.4.11) can be written as

$$F(c_\ell, c_r) := f_\ell^n(f_r(0; c_\ell, c_r); c_\ell, c_r) = \tilde{f}_\ell^n(\tilde{f}_r(0; c_r); c_\ell) + G(c_\ell, c_r) = 0$$

with G containing only higher order terms, that is, $G(0, 0) = 0$ and $\frac{\partial G}{\partial c_i}(0, 0) = 0$ $i \in \{\ell, r\}$. Now, as

$$F(0, 0) = 0, \quad \frac{\partial F}{\partial c_\ell}(0, 0) \neq 0,$$

one can apply the Implicit Function Theorem at $(c_\ell, c_r) = (0, 0)$ and show that Eq. (2.4.11) can be solved for c_ℓ . In addition, the fact that the limit

$$\lim_{x \rightarrow 0} \frac{g_\ell(x; c_\ell, c_r)}{g_\ell(x; 0, 0)}$$

exists, ensures us that this solution will be of the form

$$c_\ell = \xi_{\mathcal{RL}^n}^d(c_r) = \tilde{\xi}_{\mathcal{RL}^n}^d(c_r) + \Psi(c_r). \quad (2.4.12)$$

where $\Psi(c_r)$ is such that

$$\lim_{c_r \rightarrow 0} \frac{\Psi(c_r)}{\tilde{\xi}_{\mathcal{RL}^n}^d(c_r)} = 0,$$

that is, $\Psi(c_r)$ depends on c_r in higher order terms than $\tilde{\xi}_{\mathcal{R}\mathcal{L}^n}^d(c_r)$ does. Therefore, by considering c_r small enough, it is clear that both bifurcation curves are arbitrarily close to each other.

Finally, arguing similarly with the other bifurcation curves, it comes that the bifurcation scenarios of systems (2.2.1) and (2.3.1) near $(c_\ell, c_r) = (0, 0)$ are the same, which proves the result.

2.5 Examples

In this section we will illustrate the results obtained so far with two examples.

2.5.1 Example 1

Let us consider

$$f(x) = \begin{cases} c_\ell + \frac{9}{10} \sin(x) =: f_\ell(x) & \text{if } x \leq 0 \\ -c_r - \frac{1}{2} \sin(x) =: f_r(x) & \text{if } x > 0 \end{cases} \quad (2.5.1)$$

shown in Fig. 2.6, which fulfills the conditions C.1''–C.3'' and, in particular, C.1–C.3.

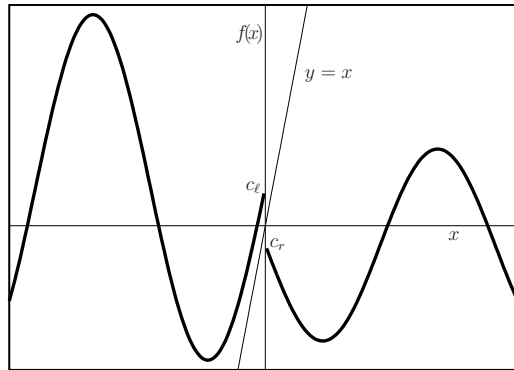


Figure 2.6: System function of Example 1 defined in Eq. (2.5.1)

As one can see in Fig. 2.7, there exists a big bang bifurcation of the period incrementing type at the origin of the parameter space $c_\ell \times c_r$, as predicted by Theorem 2.2.2 or Corollary 2.4.1, which also applies. A global overview of the bifurcation scenario is presented in Fig. 2.7(a), and a magnification near the origin of this space is shown in Fig. 2.7(b). There one can observe the expected infinite number of border collision bifurcation curves separating the regions of existence of the different periodic orbits. There it is also shown the first order approximation of the bifurcation curves reported in §2.4.2. As one can see in the one-dimensional bifurcation diagram presented in Fig. 2.7(c) along the curve parameterized by ϕ in Fig. 2.7(b), the periodic orbits that exist near the origin

are of type \mathcal{RL}^n . As labeled in the figures, there exist regions where only one periodic orbit of type \mathcal{RL}^n exists, and there exist other regions where two periodic orbits of type \mathcal{RL}^n and \mathcal{RL}^{n+1} coexist.

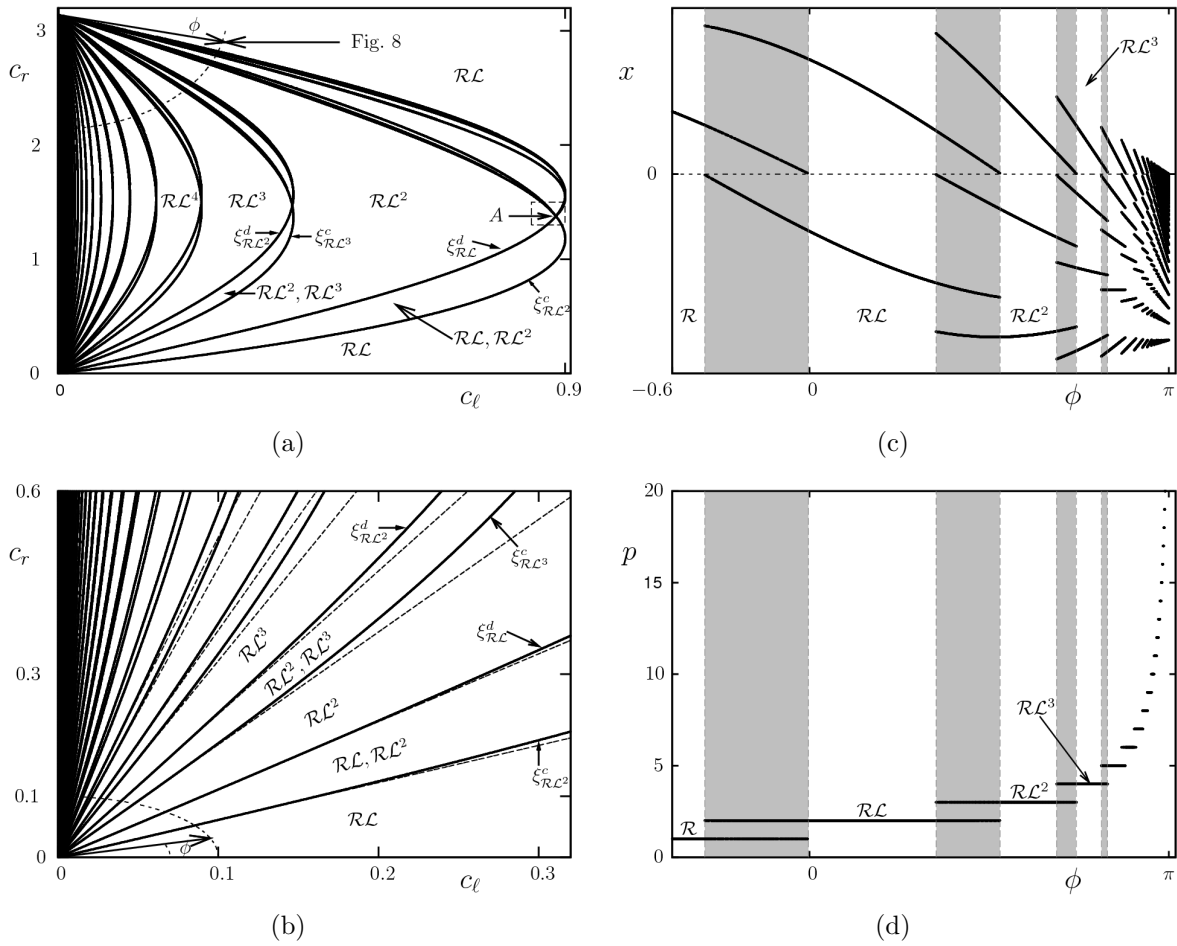


Figure 2.7: (a): border collision bifurcation curves for Example 1. A blow up of the neighborhood of the point A is shown in Fig. 2.9(a). (b): numerical (black) and first order approximations of the analytical (gray) border collision bifurcation curves near the origin. (c): bifurcation diagram through the curve surrounding the origin in (b) parameterized by ϕ anti-clockwise. The gray regions indicate coexistence between two periodic orbits (d): periods of the detected orbits in (c).

As one can see in Fig. 2.7(a), near $(0, \pi)$ there exists another point where an infinite number of bifurcation curves seem to emerge from.

In order to investigate this point in more detail and see whether the result presented above can be applied, let us first note that it is given by the intersection between the

border collision bifurcation curves $\xi_{\mathcal{R}}^d$ (the vertical axis) and $\xi_{\mathcal{RL}}^d$. This means that, at this point, a periodic orbit of type \mathcal{RL} collides with the boundary together with the fixed point \mathcal{L} . This is exactly what we have considered in this work, the simultaneous collision of two fixed points with the boundary. Let us therefore consider the following composite map

$$f_2(x) = \begin{cases} f_\ell(x) & \text{if } x \leq 0 \\ f_\ell f_r(x) & \text{if } x > 0 \end{cases} \quad (2.5.2)$$

which collapses the \mathcal{RL} -periodic orbit of (2.5.1) to the fixed point \mathcal{R} of (2.5.2). Easily, one sees that, for $(c_\ell, c_r) = (0^+, \pi^-)$, $f_\ell(0) = 0^+$, $f_\ell f_r(0) = 0^-$, $f'_\ell(0^-) = \frac{9}{10}$ and $(f_\ell f_r)'(0^+) = \frac{9}{20}$. This means that $f_2(x)$ possesses two stable fixed points which, when increasing c_ℓ and decreasing c_r through $(0, \pi)$, collide simultaneously with the boundary $x = 0$. However, $f_2(x)$ does not fulfill the conditions of Theorem 2.2.2 as the eigenvalues associated with both fixed points are both positive.

As mentioned in the introduction, this situation leads to the so-called period adding big bang bifurcation and the orbits are organized by a Farey-tree-like structure. That is, near the big bang bifurcation, there exist an infinite number of bifurcation curves separating existence regions of different periodic orbits in such a way that, in between two regions there exists another region locating a unique periodic orbit obtained by “gluing” them and thus having a period which results from the addition of the periods of those. This implies that between two different bifurcation curves there exist an infinite number of them (see for example [AS06a] for an extended explanation). This is shown in Fig. 2.8 by the one-dimensional bifurcation diagram along the curve shown in Fig. 2.7(a).

From the global overview of the bifurcation scenario shown in Fig. 2.7(a) it seems that all the bifurcation curves created at $(0, \pi)$ disappear at the intersection points of the curves $\xi_{\mathcal{RL}^n}^d$ and $\xi_{\mathcal{RL}^{n+1}}^c$. However, as we will immediately show, this can not be the case. Let us take a closer look for example at the point labeled with A in Fig. 2.7(a) whose surrounding is magnified in Fig. 2.9(a). As this point is given by the intersection of the curves $\xi_{\mathcal{RL}^2}^c$ and $\xi_{\mathcal{RL}}^d$, it represents the simultaneous collision of the periodic orbits \mathcal{RL}^2 and \mathcal{RL} with the boundary. Therefore, the composite map

$$f_3(x) = \begin{cases} f_\ell f_r f_\ell(x) & \text{if } x \leq 0 \\ f_\ell f_r(x) & \text{if } x > 0 \end{cases} \quad (2.5.3)$$

possesses two fixed points colliding with the boundary $x = 0$ at the point A . The coordinates of A can be calculated solving the equations

$$\begin{cases} f_\ell f_r f_\ell(0) = 0 \\ f_\ell f_r(0) = 0 \end{cases},$$

which leads to $A = (c_\ell^A, c_r^A) \simeq (0.88325, 1.37759)$.

One could also consider the iterated functions $f_r f_\ell f_\ell$ and $f_\ell f_\ell f_r$ for the left branch. However, one can see that the first option is the proper way of writing the corresponding

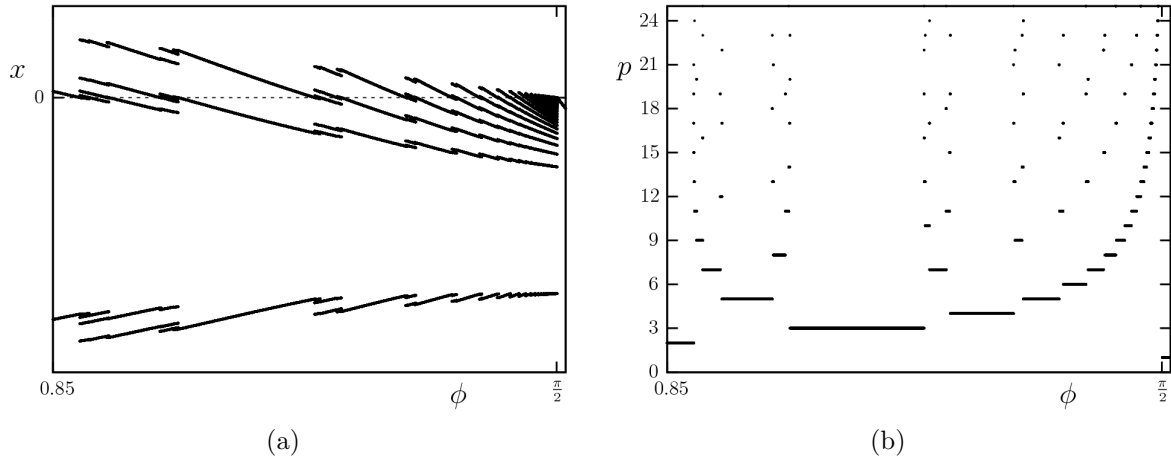


Figure 2.8: Bifurcation structure around the period adding big bang bifurcation occurring at $(0, \pi)$ for Example 1. (a) Bifurcation diagram along the curve labeled in Fig. 2.7(a) and parameterized clockwise by ϕ . (b) Periods of the detected periodic orbits.

iterate, as it collapses the corresponding periodic orbit of (2.5.1) to that fixed point of the third iterate which collides with the boundary $x = 0$ at the point A .

Expanding the gaps and the slopes of each branch of $f_3(x)$ at the discontinuity near A , one has

$$f_\ell f_r f_\ell(0)(\tilde{c}_\ell, \tilde{c}_r) \simeq 1.05483\tilde{c}_\ell + 0.17280\tilde{c}_r + O(\tilde{c}_\ell^2, \tilde{c}_r^2, \tilde{c}_\ell\tilde{c}_r) \quad (2.5.4)$$

$$(f_\ell f_r f_\ell)'(0)(\tilde{c}_\ell, \tilde{c}_r) \simeq 0.04935 + 0.01994\tilde{c}_\ell + 0.25224\tilde{c}_r + O(\tilde{c}_\ell^2, \tilde{c}_r^2, \tilde{c}_\ell\tilde{c}_r) \quad (2.5.5)$$

$$f_\ell f_r(0)(\tilde{c}_\ell, \tilde{c}_r) \simeq \tilde{c}_\ell - 0.17280\tilde{c}_r + O(\tilde{c}_r^2) \quad (2.5.6)$$

$$(f_\ell f_r)'(0)(\tilde{c}_\ell, \tilde{c}_r) \simeq -0.086401 + 0.44162\tilde{c}_r + O(\tilde{c}_r^2), \quad (2.5.7)$$

where $\tilde{c}_\ell = c_\ell - c_\ell^A$ and $\tilde{c}_r = c_r - c_r^A$. From Eqs. (2.5.4) and (2.5.6), it is clear that there exist two directions in the parameter space (presented in Fig. 2.9(a) as two dotted straight lines) along which the position of the fixed points with respect the boundary (the offsets at the origin) can be locally varied independently. This means that the re-parameterization

$$\begin{aligned} \hat{c}_\ell &:= f_\ell f_r f_\ell(0) = 1.05483\tilde{c}_\ell + 0.17280\tilde{c}_r + \text{h.o.t.} \\ \hat{c}_r &:= f_\ell f_r(0) = \tilde{c}_\ell - 0.17280\tilde{c}_r + \text{h.o.t.} \end{aligned}$$

writes f_3 in the form of Eq. (2.2.1) fulfilling C.1. In addition, it comes from equations (2.5.5) and (2.5.7) that the conditions C.2 and C.3 are also fulfilled: the colliding fixed points of (2.5.3) are stable and have associated eigenvalues of different sign. As a consequence, Theorem 2.2.2 applies to f_3 and, therefore, the point A represents a big bang

bifurcation of the incrementing type for the original map (2.5.1).

As the colliding fixed points of (2.5.3) with positive associated eigenvalue is \mathcal{L} , the periodic orbits undergoing the incrementing scenario for f_3 are of the form \mathcal{RL}^n . This implies that the periodic orbits for the original map (2.5.1) emerging at the point A are of type $\mathcal{RL}(\mathcal{RL}^2)^n$, which are shift-equivalent to $\mathcal{LR}(\mathcal{LR})^n$ (see Definition 2.2.3). This is shown in Fig. 2.9(b) where a one-dimensional bifurcation diagram is performed along the corresponding segment labeled in Fig. 2.9(a). As the coexistence regions between the periodic orbits of type $\mathcal{RL}(\mathcal{RL}^2)^n$ and $\mathcal{RL}(\mathcal{RL}^2)^{n+1}$ can not be observed there, a magnification for the case $n = 2$ is shown in Fig. 2.9(c).

However, the question arises, where do all other border collision bifurcation curves created at $(0, \pi)$ end? As shown in Fig. 2.9(d), when moving away from A , there exists a point between the two segments labeled in Fig. 2.9(a) where the coexistence shown in Fig. 2.9(c) disappears. This point is given by the intersection of the corresponding curves $\xi_{\mathcal{RL}(\mathcal{RL}^2)^3}^c$ and $\xi_{\mathcal{RL}(\mathcal{RL}^2)^2}^d$ exactly as happened at the point A with the curves $\xi_{\mathcal{RL}^2}^c$ and $\xi_{\mathcal{RL}}^d$. Such a point would be the analogous to the one given by the intersection of the curves $\xi_{\mathcal{RL}(\mathcal{RL}^2)}^c$ and $\xi_{\mathcal{RL}}^d$ labeled with B in Fig. 2.9(a). This self similarity suggests that this process takes place for every border collision curve, so forming an infinite tree of big bang bifurcations of period incrementing type whose mother node is the point $(0, 0)$, generating the complete period adding structure absorbed by the point $(0, \pi)$.

2.5.2 Example 2

Let us now consider a second example fulfilling conditions C.1''–C.3'' (and C.1–C.3)

$$f(x) = \begin{cases} c_\ell + \frac{2}{5}x(x+2) =: f_\ell(x) & \text{if } x \leq 0 \\ -c_r + \frac{1}{2}x(x-1) =: f_r(x) & \text{if } x > 0 \end{cases} \quad (2.5.8)$$

which is shown in Fig. 2.10(a).

As expected, the origin of the parameter space $c_\ell \times c_r$, presented in Fig. 2.10(b), is a big bang bifurcation point of the period incrementing type. Moreover, arguing exactly as before, one can show that the situation between the points $(0, 2)$ and $(0, 0)$ is the same as in the previous example between $(0, \pi)$ and $(0, 0)$. This has been validated with numerical simulations which we do not show as they are equivalent to the ones presented in Figs. 2.7(b), 2.7(c), 2.7(d) and 2.8. Therefore we omit further comments in that direction.

However, there exists in the c_ℓ axis of Fig. 2.10(b) several points that deserve special interest. For example, let us consider the point $(1, 0)$. As one can see in Fig. 2.10(b), this point is given by the collision of the bifurcation curves $\xi_{\mathcal{R}}^d$ (the horizontal axis) and $\xi_{\mathcal{RL}}^c$, where the fixed point \mathcal{R} and the periodic orbit \mathcal{RL} simultaneously collide with the boundary. Therefore, after re-parameterization along proper directions in the parameter

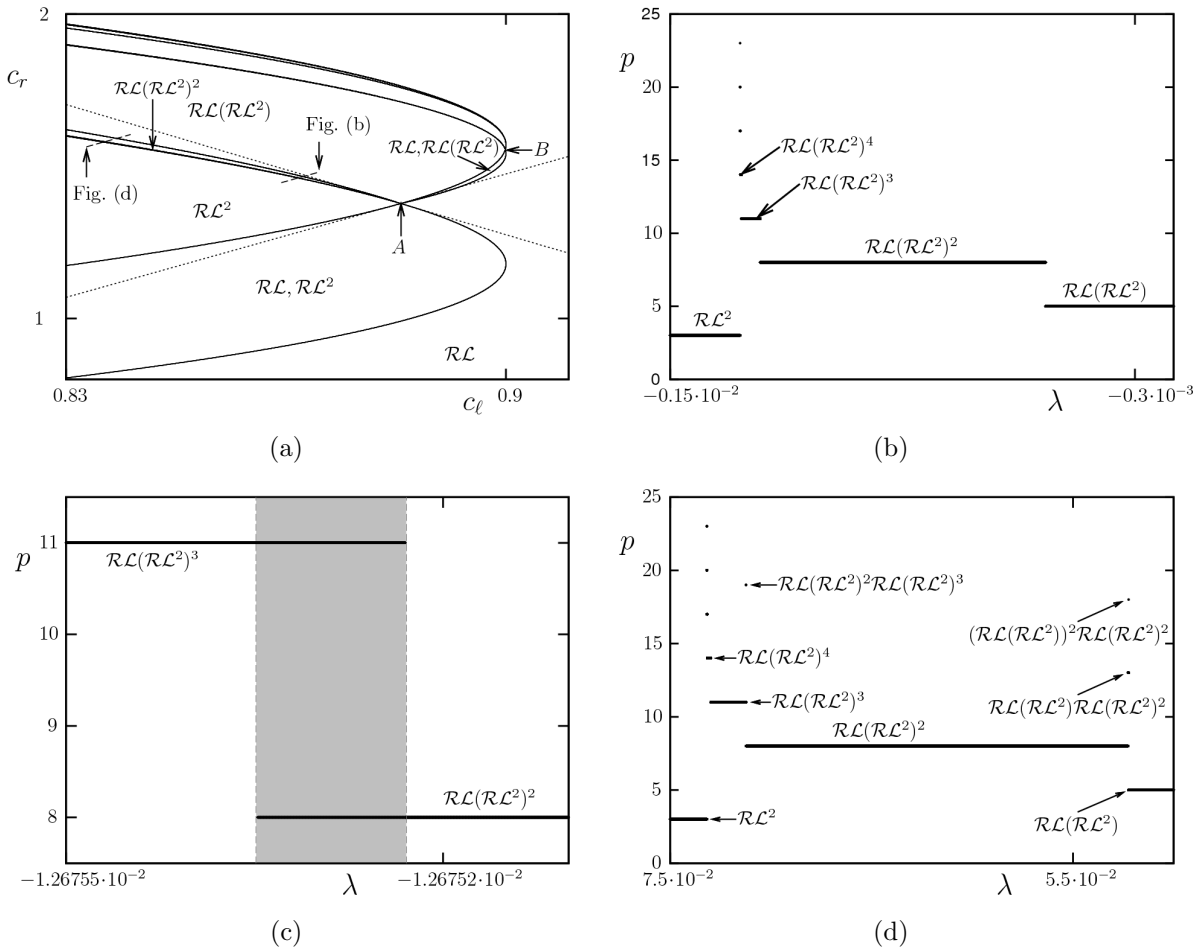


Figure 2.9: Bifurcation scenario near the point A (see Fig. 2.7(a)). (a): Blow up labeled in Fig. 2.7(a). The two dotted straight lines are the directions along which the right and left images of 0 by $f_3(x)$ remain (locally) constant. (b): one-dimensional bifurcation diagram along the segment labeled in (a): period incrementing scenario. (c): magnification of the coexistence (gray region) between the periodic orbits $\mathcal{R}\mathcal{L}(\mathcal{R}\mathcal{L}^2)^2$ and $\mathcal{R}\mathcal{L}(\mathcal{R}\mathcal{L}^2)^3$ shown in (b). (d): bifurcation diagram along the segment labeled (d) in Fig. 2.9(a); far enough from A , the period incrementing structure generated at A disappears.

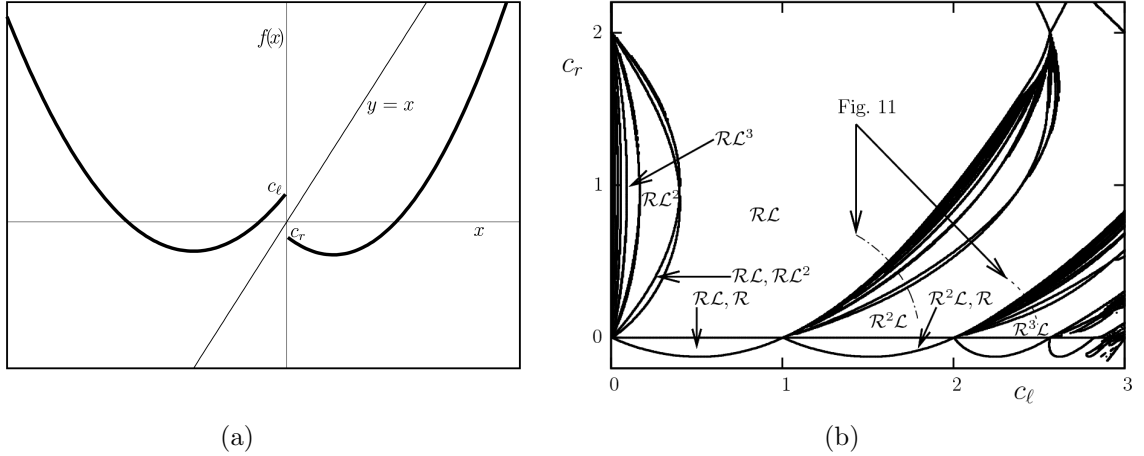


Figure 2.10: (a): system function of Example 2 defined in Eq. (2.5.8). (b): border collision bifurcation curves of Example 2.

space⁴, the map

$$f_2(x) = \begin{cases} f_r f_\ell(x) & \text{if } x \leq 0 \\ f_r(x) & \text{if } x > 0 \end{cases} \quad (2.5.9)$$

can be written as in (2.2.1) fulfilling C.1. As before, as the colliding periodic orbits are stable and their associated eigenvalues have the proper signs, conditions C.2 and C.3 are also fulfilled. Therefore, Theorem 2.2.2 applies and the point $(1, 0)$ represents a big bang bifurcation of period incrementing type. As the periodic orbit with positive associated eigenvalue is \mathcal{RL} , the periodic orbits of the original map, (2.5.8), emerging at $(1, 0)$ are of type $\mathcal{R}(\mathcal{RL})^n$. This is shown in Figs. 2.11(a) and 2.11(b) through the one-dimensional bifurcation diagram along the curve labeled in Fig. 2.10(b).

One can proceed analogously and show that the situation is repeated for the other points, $(p_n, 0)$, also located at the horizontal axis of Fig. 2.10(b).

In order to show that, let us consider the equation

$$f_r^n f_\ell(0) = f_r(0), \quad c_r = 0 \quad (2.5.10)$$

and let p_n be the root of the Eq. (2.5.10) which is not a root of the same equation using

⁴We skip the details as one has just to proceed as in Example 1.

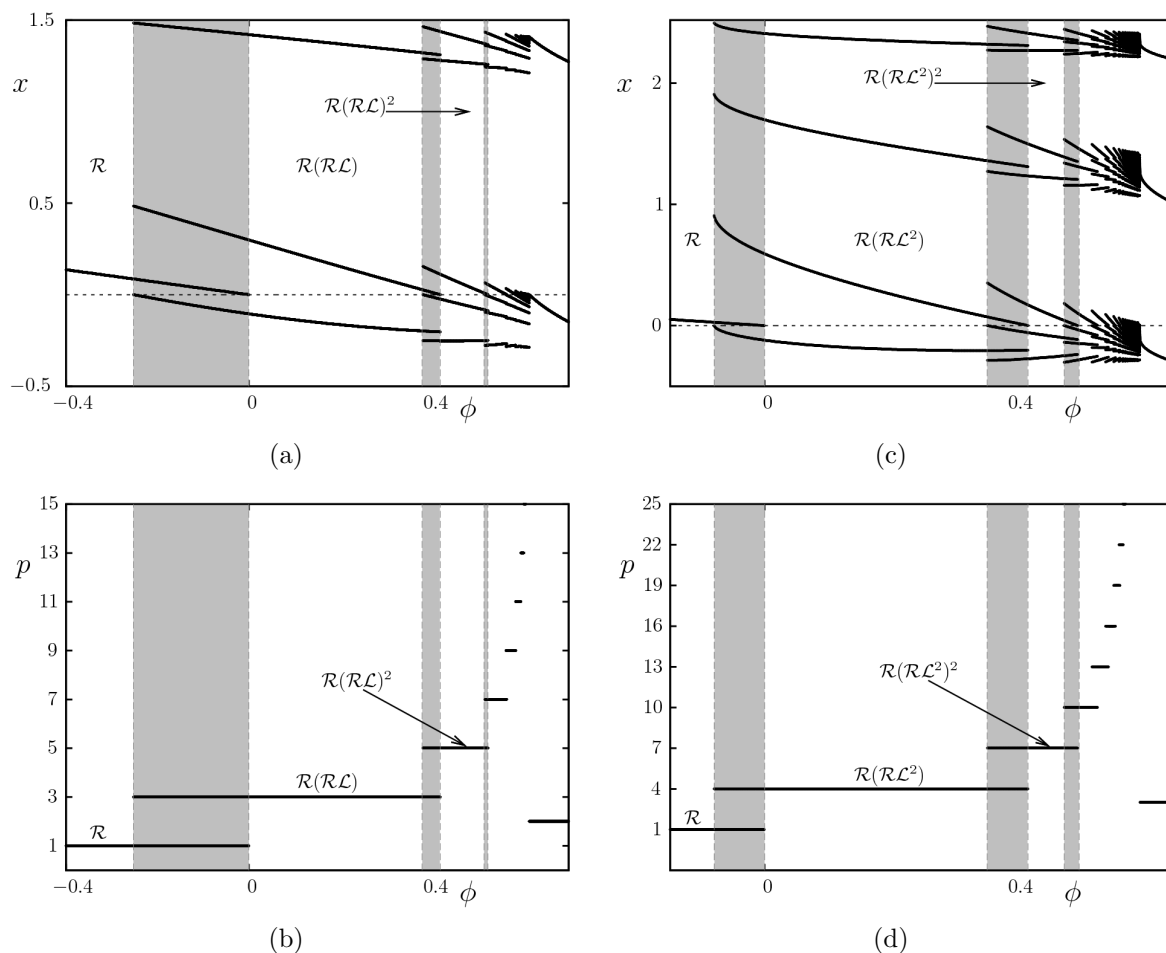


Figure 2.11: Bifurcation structure around the big bang bifurcation points at $(c_\ell, c_r) = (1, 0)$ ((a) and (b)) and $(c_\ell, c_r) = (p_2, 0)$ ((c) and (d)). (a) and (c) Bifurcation diagram along the curves labeled in Fig. 2.10(b). (b) and (d) periods of the periodic orbits. The gray regions indicate coexistence between two periodic orbits.

$n - 1$ instead of n . Then, one can easily see that the map

$$f_n(x) = \begin{cases} f_r^n f_\ell(x) & \text{if } x \leq 0 \\ f_r(x) & \text{if } x > 0 \end{cases} \quad (2.5.11)$$

possesses two colliding fixed points (is continuous at $(c_\ell, c_r) = (p_n, 0)$). Again, under proper re-parameterization, it can be written in the form of (2.2.1) and the conditions C.1–C.3 hold at $(c_\ell, c_r) = (p_n, 0)$. Therefore, for every $(p_n, 0)$ there exists an arbitrarily small open set containing that point such that only periodic orbits of type $\mathcal{R}(\mathcal{R}^n \mathcal{L})^m$ exist for all $m \geq 0$. Moreover, there exist regions in that open set where two $\overline{\mathcal{R}(\mathcal{R}^n \mathcal{L})^m}$ and $\mathcal{R}(\mathcal{R}^n \mathcal{L})^{m+1}$ orbits coexist $\forall m \geq 0$.

2.6 Conclusions

In this chapter we have shown that big bang bifurcations occur in low-dimensional piecewise-smooth systems typically whenever two fixed points cross simultaneously the boundary and become virtual. This is given by a transverse intersection between two border collision bifurcation curves when the considered parameters control the distance between the boundary and the fixed points.

So far we have presented this situation for the one-dimensional case for which the boundary is represented by a single point ($x = 0$) where the map has a jump discontinuity. By Theorem 2.2.2, we have explicitly and rigorously characterized the infinite number of periodic orbits that appear after the collision of two fixed points with the boundary when they are attracting (the map is locally contractive) and have associated eigenvalues of opposite sign: a big bang bifurcation of periodic incrementing type occurs. As mentioned in Remark 2.4.1, in the case that the branch corresponding to the fixed point with negative associated eigenvalue is replaced by a constant function in an open set containing $x = 0$, the bifurcation scenario remains the same except that the coexistence regions disappear, and a big bang of the so-called pure incrementing type occurs.

We have also given examples showing that one can consider a proper renormalization of the map in order to study other big bang bifurcations in the parameter space. In the same examples we have also checked the result conjectured in the introduction; that is, when both eigenvalues of the colliding fixed points are positive, then the so-called period adding big bang bifurcation takes place. A proof of that is left for future work, but in Chapter 3 we present a sketch of it. Using also renormalization arguments we have suggested that the bifurcation curves issuing from the detected period adding big bang bifurcation are “collected” by an infinite cascade of period incrementing big bang bifurcations. A rigorous and more detailed study of this situation will be reported elsewhere.

Chapter 3

A rigorous approach to the period adding big bang bifurcation and the extension to 2-dimensional piecewise-defined maps

3.1 Introduction

In this chapter we discuss several aspects for further research on the topics related with big bang bifurcations.

In §3.2 we first provide a rigorous proposal for further research in order to extend the results given in Chapter 2 to the increasing-increasing case, which, as announced in the Introduction of this thesis, leads to the *period adding* big bang bifurcation. This type of bifurcation was introduced in [AS06a] when numerically simulating a discontinuous linear map. In our approach we propose to study a topological conjugacy between the piecewise-defined map and a classical Arnol'd circle map, for which the bifurcation scenario is well known. Hence, we profit in this approach from the classical theory developed so far to provide generic condition of the occurrence of big bang bifurcation of the period adding type in one-dimensional maps.

As it was already noted in these mentioned chapters, big bang bifurcation are basically given by the simultaneous collision of two invariant objects with a boundary. When these are fixed points, this necessary reflects a loss of continuity of the map at this intersection for one-dimensional maps. However, this is not the case when considering higher dimensions, where it turns out that continuity at the simultaneous collision is not necessary to undergo big bang bifurcations.

In §3.3, we propose an extension of the results so far understood about big bang bifurcations for one-dimensional piecewise-defined maps to the two-dimensional case.

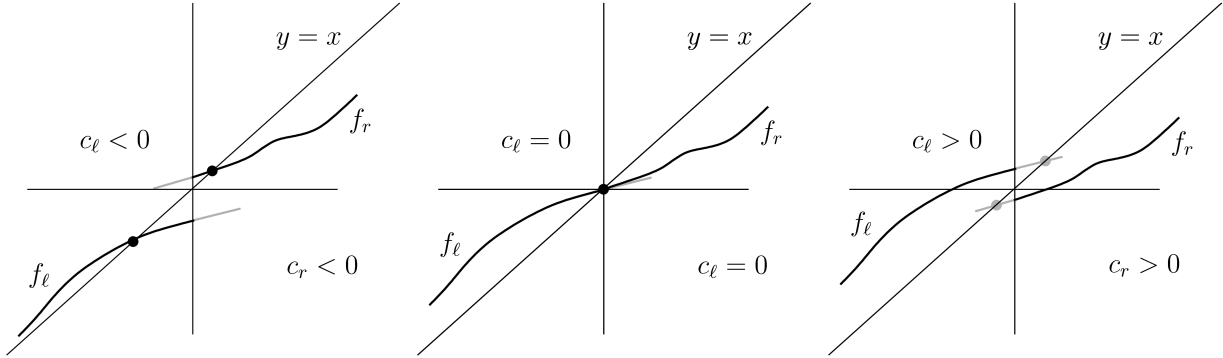


Figure 3.1: Simultaneous collision of two fixed points with positive associated eigenvalues with the boundary.

3.2 Period adding big bang bifurcation

As announced in the Introduction of this thesis, the so-called *period adding* big bang bifurcation exhibits a much more complicated structure as the *period incrementing* one reported in Chapter 2. In this section we first introduce a generic map which depends on two parameters and we conjecture that, under certain conditions, this map undergoes a period adding big bang bifurcation. After describing this bifurcation, we provide rigorous arguments which form a guide to proof this result. A complete extension of it is left as future work.

As in the case of the period incrementing big bang bifurcation (see Chapter 2), we consider a piecewise-defined one-dimensional map of the form

$$f(x; c_\ell, c_r) = \begin{cases} c_\ell + g_\ell(x) =: f_\ell(x; c_\ell) & \text{if } x \leq 0 \\ -c_r + g_r(x) =: f_r(x; c_r) & \text{if } x > 0 \end{cases} \quad (3.2.1)$$

which reproduces the simultaneous collision of two (attracting) fixed points with the boundary (see Fig. 3.1). As for the period incrementing case we assume that both fixed points are attracting, but in this case both have positive associated eigenvalues. Hence, we assume that the map (3.2.1) fulfills

D.1 g_ℓ and g_r are smooth functions at $x = 0$ s.t. $g_\ell(0) = g_r(0) = 0$

D.2 There exists $\varepsilon_\ell > 0$ such that $0 \leq g'_\ell(x) < 1 \forall x \in (-\varepsilon_\ell, 0]$

D.3 There exists $\varepsilon_r > 0$ such that $0 \leq g'_r(x) < 1 \forall x \in [0, \varepsilon_r)$

Then, the origin of the parameter space $c_\ell \times c_r$ consists on a co-dimension two big bang bifurcation point of the period adding type. This means that the bifurcation scenario

around this points is as described below.

Arguing as in §2.4.3, one can show using the implicit function theorem that the map (3.2.1) is in fact the normal form for the period adding big bang bifurcation. That is, all the arguments that we provide here for the map (3.2.1) fulfilling conditions D.1–D.3 also hold for the more general map

$$f(x; c_\ell, c_r) = \begin{cases} c_\ell + g_\ell(x; c_\ell, c_r) & =: f_\ell(x; c_\ell, c_r) & \text{if } x \leq 0 \\ -c_r + g_r(x; c_\ell, c_r) & =: f_r(x; c_\ell, c_r) & \text{if } x > 0 \end{cases} \quad (3.2.2)$$

satisfying

D'.1 g_ℓ and g_r are $C^\infty(\mathbb{R})$ functions such that for $i, j \in \{\ell, r\}$

$$g_i(0; c_\ell, c_r) = 0$$

and the limit

$$\lim_{x \rightarrow 0} \frac{g_i(x; c_\ell, c_r)}{g_i(x; 0, 0)}$$

exists,

D'.2 there exists $\varepsilon_\ell > 0$ such that $0 < g'_\ell(x; c_\ell, c_r) < 1 \forall x \in (-\varepsilon_\ell, 0)$ if $0 \leq c_\ell, c_r \ll 1$,

D'.3 there exists $\varepsilon_r > 0$ such that $0 < g'_r(x; c_\ell, c_r) < 1 \forall x \in (0, \varepsilon_r)$ if $0 \leq c_\ell, c_r \ll 1$,

where

$$g'(x; c_\ell, c_r) = \frac{\partial g(x; c_\ell, c_r)}{\partial x}.$$

We hence proceed arguing for the map (3.2.1) under conditions D.1–D.3.

Similarly as for the period incrementing case, when considering the parameter space $c_\ell \times c_r$ one distinguishes 4 different possible scenarios given by the signs of the parameters c_ℓ and c_r (see Fig. 3.3). When both are negative, two fixed points, $x_\ell^* < 0$ and $x_r^* > 0$, coexist, and their domains of attraction are split by the boundary $x = 0$. When they have opposite signs, only one them remains while the other one becomes virtual. Finally, when both are positive, both fixed points becomes virtual and an infinite number of different periodic orbits exist in the vicinity of the point $(c_\ell, c_r) = (0, 0)$. These are separated by an infinite number of border collision bifurcation curves, equivalently as in Fig. 3.2.

In Fig. 3.3 we show the bifurcation scenario obtained while varying the parameters c_ℓ and c_r along the curve. The periodic orbits that appear along this curve are equivalent to the bifurcation diagram shown in Fig. 3.3(a) whose periods are given in Fig. 3.3(b). There one can see that between two regions of existence of two periodic orbits with periods n and m one can find a region where a periodic orbit with period $n + m$ exists. This occurs

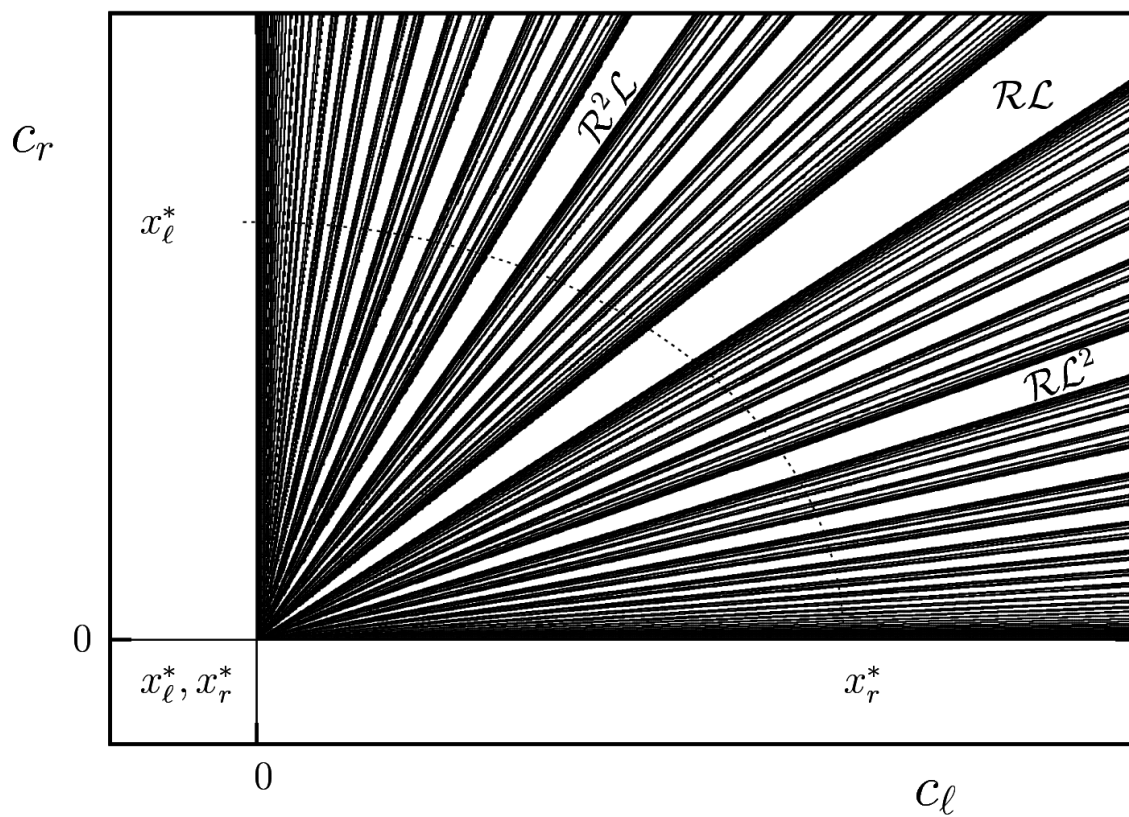


Figure 3.2: Border collision bifurcation curves in the parameter space $c_l \times c_r$ for the period adding big bang bifurcation. The fixed points x_l^* and x_r^* are labeled in the regions where they exist.

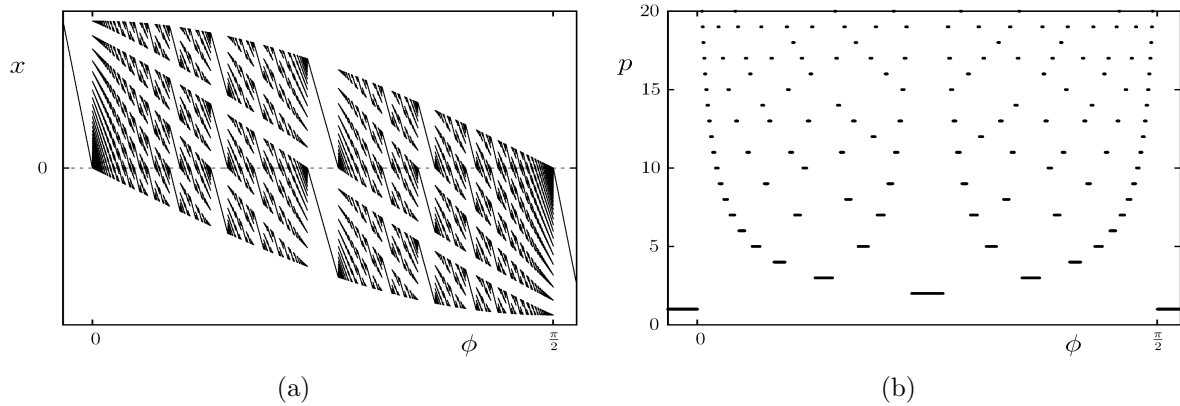


Figure 3.3: Bifurcation scenario found along the curve plot in Fig. 3.2 and parametrized by the angle ϕ . (a) bifurcation diagram. (b) periods of the period orbits

ad-infinitum forming the so-called adding scenario.

In terms of the symbolic dynamics introduced in section 2.2, this addition of periods is in fact a consequence of the concatenation of the symbolic sequences of periodic orbits. That is, given two regions of existence in the parameter space $c_\ell \times c_r$ of two periodic orbits with symbolic sequences Ψ and Φ , there exist a region in between where one finds a periodic orbit with symbolic sequence $\Psi\Phi$ (the concatenation). This forms the infinite tree schemed in Fig. 3.4.

Moreover, the rotation number of these orbits form a Farey tree. It can be seen ([GIT84, Vee86, Vee87]) that given a periodic orbit with a certain symbolic sequence, its rotation number is given by the number of times that the symbol \mathcal{R} appears in the sequence divided by the length of the sequence (the period of the periodic orbit). To show an example, in Fig.3.5 we provide a blow up of the nested regions between the existence regions where the periodic orbits with symbolic sequences $\mathcal{L}\mathcal{R}$ and $\mathcal{L}^2\mathcal{R}$ exist.

Let us show that, if $c_\ell, c_r > 0$ are small enough, such a map is a map onto the interval $[-c_r, c_\ell]$.

For c_ℓ and c_r positive and small enough, f_ℓ and f_r are increasing functions when restricted to $[f_r(0), 0] = [-c_r, 0]$ and $[0, f_\ell(0)] = [0, c_\ell]$, respectively. This guaranties that, in this case, the minimum of f_ℓ and the maximum of f_r in $[-c_r, c_\ell]$ occur at $x = -c_r$ and $x = c_\ell$, respectively (see Fig. 3.6). As f_ℓ and f_r are contractive near the origin, it comes that, if

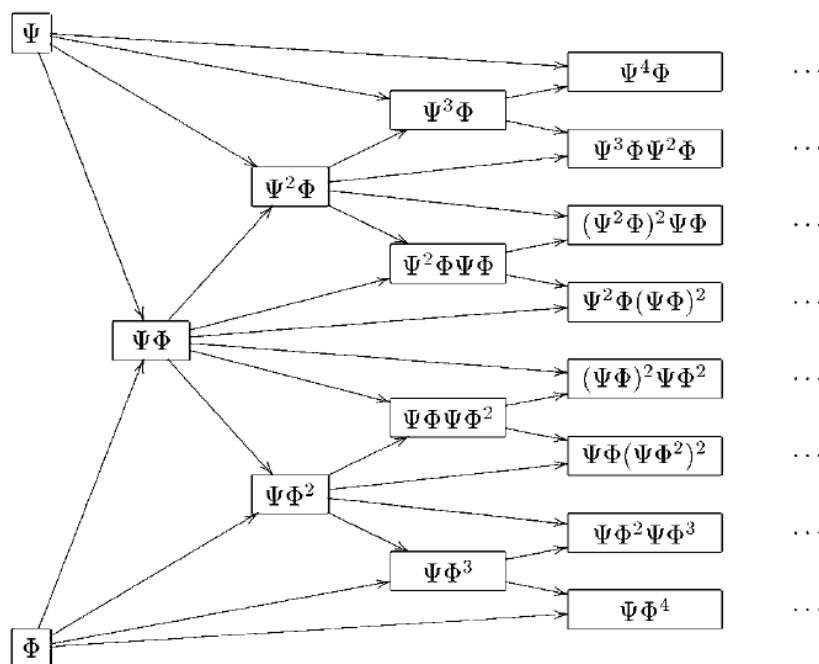


Figure 3.4: Infinite tree formed by the concatenation of symbolic sequences of periodic orbits obtained in the adding structure.

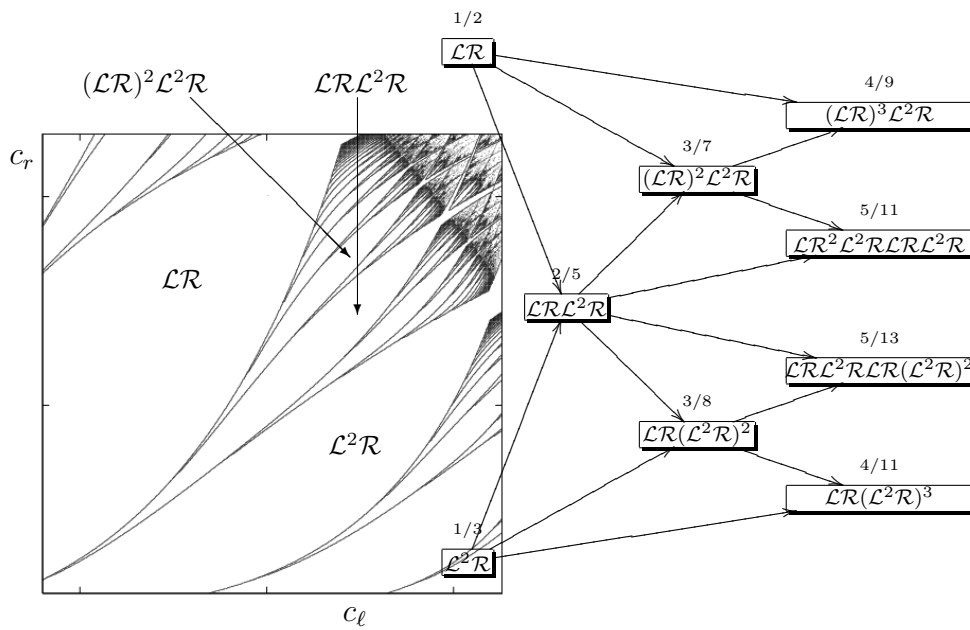


Figure 3.5: Symbolic sequences and the Farey tree formed by their rotation numbers in the adding scheme for a quadratic map.

$c_\ell, c_r > 0$ are small enough, then

$$\begin{aligned} -c_r &= f_r(0) \leq f_\ell(-c_r), \\ f_r(c_\ell) &\leq f_\ell(0) = c_\ell. \end{aligned}$$

Identifying $-c_r \sim c_\ell$, this allows us to think on the map f as a circle map,

$$f : \mathbb{T}_{c_\ell, c_r} \longrightarrow \mathbb{T}_{c_\ell, c_r},$$

where \mathbb{T}_{c_ℓ, c_r} is the circle given by $\mathbb{T}_{c_\ell, c_r} = \mathbb{R} \setminus [-c_r, c_\ell]$.

Let us now wonder about the invertibility of f . Using D.2 and D.3, it comes that, if $c_\ell, c_r > 0$ are small enough,

$$\begin{aligned} |g_\ell(-c_r)| &< c_r \\ |g_r(c_\ell)| &< c_\ell. \end{aligned}$$

Hence,

$$\begin{aligned} g_r(c_\ell) - g_\ell(-c_r) &\leq |g_r(c_\ell)| + |g_\ell(-c_r)| \\ &\leq c_r + c_\ell. \end{aligned}$$

In other words, $-c_r + g_r(c_\ell) \leq c_\ell + g_\ell(-c_r)$, and hence

$$f_r(c_\ell) \leq f_\ell(-c_r),$$

and f has the form shown in Figs. 3.6(a) and 3.6(b).

This, together with the monotonicity of the functions g_ℓ and g_r near the origin, makes f to be injective and thus invertible in $f(\mathbb{T}_{c_\ell, c_r})$ if $c_\ell, c_r > 0$ are small enough.

Note that if $c_\ell, c_r > 0$ are large enough, the map f loses its invertibility when $f_r(c_\ell) > f_\ell(-c_r)$ (see Fig. 3.6(c)).

We then distinguish between the two possibilities shown in Figs. 3.6(a) and 3.6(b).

If

$$f_\ell(-c_r) = f_r(c_\ell),$$

(Fig. 3.6(a)) f is then an homeomorphism on the circle \mathbb{T}_{c_ℓ, c_r} .

On the other hand, if

$$f_\ell(-c_r) > f_r(c_\ell),$$

(see Fig. 3.6(b)) then f is discontinuous at $x = -c_r \sim c_\ell$. However, it is an injective map and thus invertible in $f(\mathbb{T}_{c_\ell, c_r})$.

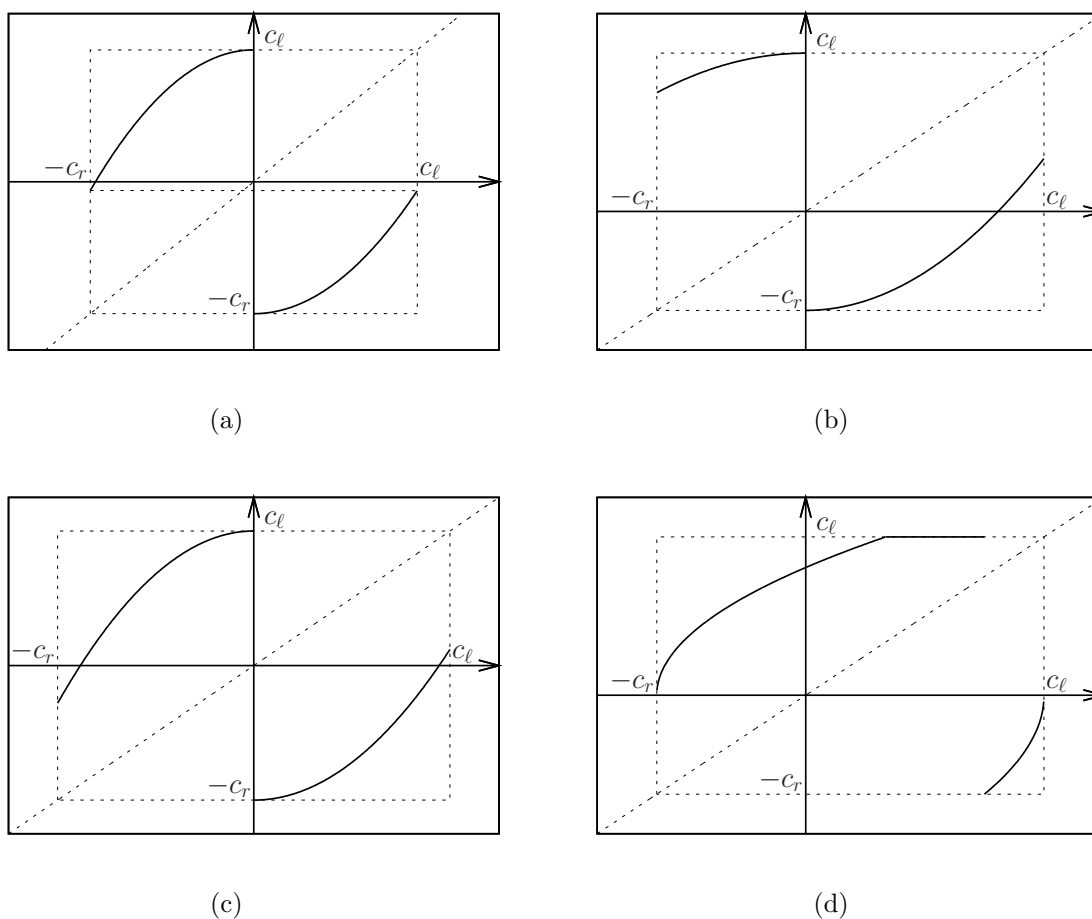


Figure 3.6: Different configurations for the circle map f . (a) continuous, (b) invertible and (c) non-invertible. (d) inverse of (b)

Let us consider

$$f^{-1} : \mathbb{T}_{c_\ell, c_r} \longrightarrow \mathbb{T}_{c_\ell, c_r},$$

given by

$$f^{-1} = \begin{cases} f_r^{-1}(x) & \text{if } -c_r \leq x \leq f_r(c_\ell) \\ f_\ell^{-1}(x) & \text{if } f_\ell(c_\ell) \leq x \leq c_\ell \end{cases}$$

and is schematically shown in Fig. 3.6(d).

Note that, if $f_r(c_\ell) \neq f_\ell(-c_r)$ ($f_r(c_\ell) < f_\ell(-c_r)$), due to the discontinuity at $x = c_\ell \sim -c_r$ the inverse map f^{-1} is not defined at $[f_r(c_\ell), f_\ell(-c_r)]$ and it is therefore neither continuous. However, we are interested on invariant objects (periodic orbits) of f , which are also invariant for f^{-1} , which, if they exist, they are located outside the interval $[f_r(c_\ell), f_\ell(-c_r)]$. Hence, we can argue as in [PTT87] and fill this interval with a constant the value c_ℓ (see Fig. 3.6(d)). Thus, the map

$$f^{-1} = \begin{cases} f_r^{-1}(x) & \text{if } -c_r \leq x \leq f_r(c_\ell) \\ c_\ell & \text{if } f_r(c_\ell) \leq x \leq f_\ell(-c_r) \\ f_\ell^{-1}(x) & \text{if } f_\ell(c_\ell) \leq x \leq c_\ell \end{cases}$$

is a continuous circle map which captures the invariant objects of f , and hence their (local) dynamics.

We now want to make use of results for circle maps obtained so far in the literature in order to study the periodic orbits of f^{-1} . To this end, we first obtain an equivalent map defined in a set independent of the parameters c_ℓ and c_r . We consider a diffeomorphism

$$\phi(x; c_r, c_\ell) : \mathbb{T}_{c_\ell, c_r} \longrightarrow \mathbb{T},$$

fulfilling $\phi(-c_r; c_r, c_\ell) = 0$ and $\phi(c_\ell; c_r, c_\ell) = 1$, and $\mathbb{T} = \mathbb{R} \setminus \mathbb{Z}$ is the usual circle. This diffeomorphism provides us a map \hat{f}^{-1}

$$\hat{f}^{-1} : \mathbb{T} \longrightarrow \mathbb{T}$$

defined as

$$\hat{f}^{-1} = \begin{cases} \phi \circ f_r^{-1} \circ \phi^{-1}(x) & \text{if } 0 \leq x \leq \phi(f_r(c_\ell)) \\ 1 & \text{if } \phi(f_r(c_\ell)) \leq x \leq \phi(f_\ell(-c_r)) \\ \phi \circ f_\ell^{-1} \circ \phi^{-1}(x) & \text{if } \phi(f_\ell(-c_r)) \leq x \leq 1, \end{cases}$$

which is continuous map onto \mathbb{T} and topologically conjugated to f^{-1} .

As are interested on the bifurcation scenario along a curve surrounding the origin of the parameter space $c_\ell \times c_r$ for $c_\ell, c_r > 0$, we perform the reparametrization

$$\begin{aligned} c_r &= \varepsilon \sin \Omega \\ c_\ell &= \varepsilon \cos \Omega, \end{aligned}$$

with $\varepsilon > 0$ and $\Omega \in (0, \frac{\pi}{2})$. For every $\varepsilon > 0$ we obtain hence a one-parameter family of maps $\hat{f}^{-1}(x; \Omega)$. It is our goal now to show that, if $\varepsilon > 0$ is small enough, this map undergoes the period-adding bifurcation scenario described above when Ω is varied. The key step to see this is the following result, for which we do not provide a proof and hence we conjecture. Its proof is left as future work.

Lemma 3.2.1. *There exist a diffeomorphism*

$$h : \mathbb{T} \longrightarrow \mathbb{T}$$

and a monotonously increasing diffeomorphism

$$\varphi : \begin{array}{ccc} (0, 1) \supset I & \longrightarrow & [0, \frac{\pi}{2}] \\ & \Omega' \longmapsto & \Omega \end{array}$$

with $\phi(I) = [0, \frac{\pi}{2}]$, such that

$$h \circ \hat{f}^{-1}(h^{-1}(x); \varphi(\Omega')) = \Theta(x),$$

where

$$\Theta(x) = x + \Omega' + \frac{1}{2\pi} \sin 2\pi x \tag{3.2.3}$$

is the Arnol'd circle map. Moreover, the set of rotation numbers of the periodic orbits of $\Theta(x)$ obtained when varying $\Omega \in I$ is $[0, 1] \cap \mathbb{Q}$.

This result provides topological conjugacy between the Arnol'd circle map for all the parameter values of $\Omega' \in I$ for which $\Theta(x)$ exhibits complicated dynamics. The rotation number, which is defined as

$$\rho(\Omega') = \lim_{n \rightarrow \infty} \frac{\Theta^n(x) - x}{n},$$

that one obtains when varying $\Omega' \in I$ form the so-called *devil's staircase*, as shown in Fig. 3.7. This means that the rotation numbers take only rational values and the resulting function, $\rho(\Omega')$, is flat almost everywhere (for all values of $\Omega' \in [0, 1]$ except in a Cantor set). This implies that, for almost all $\Omega' \in [0, 1]$, $\Theta(x)$ is mode-locked and hence only a periodic orbit with rotation number $\rho(\Omega')$ exists.

In terms of the Lemma 3.2.1, the set $I = [a, b]$ is such that

$$\begin{aligned} a &= \sup(\Omega'), \rho(\Omega') = 0 \\ b &= \inf(\Omega'), \rho(\Omega') = 1, \end{aligned}$$

(see Fig. 3.7).

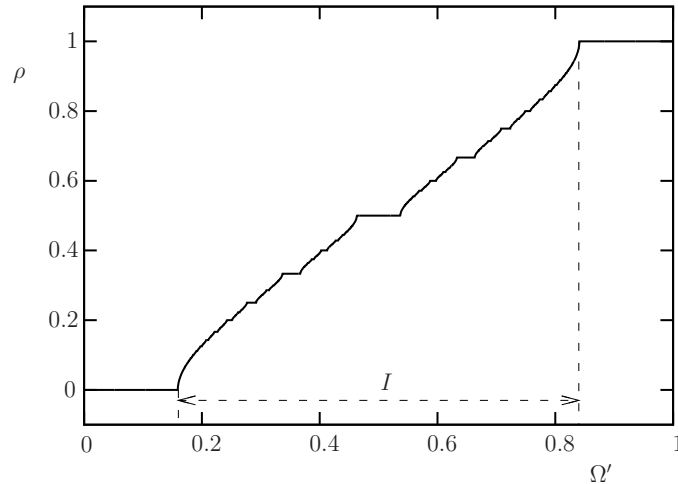


Figure 3.7: Devil's staircase: rotation numbers (ρ) of the periodic orbits obtained for the Arnol'd circle map when varying the parameter $\Omega' \in [0, 1]$. The set I correspond to the values of Ω' for which the map \hat{f}^{-1} is topological conjugated to the Arnol'd circle map (3.2.3).

As the rotation number is invariant under topological conjugacy, the map \hat{f}^{-1} (and hence the original map f in (3.2.1)) possess periodic orbits whose rotation numbers form a devil's staircase when varying $\Omega = \varphi(\Omega') \in [0, \frac{\pi}{2}] = \varphi(I)$.

As it is well known, the rotation numbers obtained along the devil's staircase form the Farey tree. It only remains then to show that the symbolic sequences of the periodic orbits obtained when varying Ω form the adding structure. This can be done uniquely relating the rotation numbers with symbolic sequences by using results reported in the literature ([GIT84, GGT84, CGT84, GGT88]). This is left for future work.

3.3 Big bang bifurcations in 2-dimensional maps

In this section we propose an extension to two-dimensional maps of the results so far presented for big bang bifurcations for one-dimensional maps. As in the previous section, we give this in terms of a first approach or a guideline for future work to obtain and proof results regarding big bang bifurcations for two-dimensional piecewise-defined maps.

For the case of the period incrementing big bang bifurcation, we also provide a partial adaptation of some of the arguments given in Chapter 2. However, we only conjecture sufficient conditions for the period adding case; a proof of them is totally left for future work. As it will be shown in Chapter 4, this result, regarding the adding case, turns out

to be of practical interest, as it can be applied to predict and explain bifurcation scenarios obtained in discretized sliding-mode control systems.

Let Σ be a curve splitting \mathbb{R}^2 in two connected components, \mathcal{X}_ℓ and \mathcal{X}_r . We then adapt the general maps given in (2.3.1) and (3.2.1) undergoing a simultaneous collision of fixed points to \mathbb{R}^2 . Consider a piecewise-defined map

$$f : \mathbb{R}^2 \longrightarrow \mathbb{R}^2$$

of the form

$$f(z) := \begin{cases} f_\ell(z; c_\ell), & \text{if } z \in \mathcal{X}_\ell \\ f_r(z; c_r), & \text{if } z \in \mathcal{X}_r, \end{cases} \quad (3.3.1)$$

with $z = (x, y)$.

Let us assume that, for $|c_\ell|$ and $|c_r|$ small enough, the maps f_ℓ and f_r possess two isolated attracting fixed points z_ℓ^*, z_r^* , respectively, with real associated eigenvalues. Let us also assume that they satisfy that

$$f_\ell(z_\ell^*; c_\ell) = z_\ell^* \in \begin{cases} \mathcal{X}_\ell & \text{if } c_\ell < 0 \\ \Sigma & \text{if } c_\ell = 0 \\ \mathcal{X}_r & \text{if } c_\ell > 0 \end{cases}$$

and

$$f_r(z_r^*; c_r) = z_r^* \in \begin{cases} \mathcal{X}_r & \text{if } c_r < 0 \\ \Sigma & \text{if } c_r = 0 \\ \mathcal{X}_\ell & \text{if } c_r > 0 \end{cases}$$

That is, for $c_\ell = c_r = 0$ both fixed points transversally cross the boundary Σ and f simultaneously undergoes two border collision bifurcations. In other words, two border collision bifurcation curves transversally cross each other in the two-dimensional parameter space $c_\ell \times c_r$.

Note that we do not assume that $f_\ell(z_\ell^*; 0) = f_r(z_r^*; 0) \in \Sigma$ and hence we do not require the map to be continuous when both fixed points collide with the boundary, for $c_\ell = c_r = 0$.

Let us assume that there exist two open sets $\mathcal{U}_\ell, \mathcal{U}_r \subset \mathbb{R}^2$ such that

$$f_\ell(z_\ell^*; 0) = z_\ell^* \in \Sigma \cap (\mathcal{U}_\ell \cap \mathcal{U}_r) \quad (3.3.2)$$

$$f_r(z_r^*; 0) = z_r^* \in \Sigma \cap (\mathcal{U}_\ell \cap \mathcal{U}_r) \quad (3.3.3)$$

$$f_\ell(\mathcal{U}_\ell \cap \mathcal{X}_\ell; 0) \subset \mathcal{X}_\ell. \quad (3.3.4)$$

Then, the result that we conjecture states that

- i)* if $f_r(\mathcal{U}_r \cap \mathcal{X}_r; 0) \subset \mathcal{X}_\ell$ the origin of the parameter space $c_\ell \times c_r$ represents a big bang bifurcation of the period incrementing type

ii) if $f_r(\mathcal{U}_r \cap \mathcal{X}_r; 0) \subset \mathcal{X}_r$ the origin of the parameter space $c_\ell \times c_r$ represents a big bang bifurcation of the period adding type.

Note that, as we have required the eigenvalues associated with the attracting fixed points z_ℓ^* and z_r^* to be real for $|c_\ell|$ and $|c_r|$ small enough, both situations will basically occur depending on the sign of the eigenvalues of the fixed points z_r^* and the relative position of their eigendirections with respect to Σ .

A precise study of *i)* is considered beyond the scope of this thesis and hence left for future work. It is used, however, in Chapter 4 to predict the occurrence of a big bang bifurcation in a second order sliding-mode control discretized system. There we also give numerical evidence of this fact.

We now give some details on how the methodology presented in Chapter 2 could be adapted to prove *ii)*.

In order to argue that, for $c_\ell, c_r > 0$ small enough, only periodic orbits with symbolic sequences of the form $\mathcal{L}^n \mathcal{R}$ exist, with arbitrarily large n , we start with some definitions. Assuming $c_\ell > 0$ small enough, let us consider the sequence

$$\mathcal{A}_n := f_\ell^{-n}(\Sigma), \quad n \geq -1 \quad (3.3.5)$$

with $\mathcal{A}_0 = \Sigma$. For simplicity we are assuming that f_ℓ is invertible in the whole curve Σ if $c_\ell > 0$ is small enough. If not, one should restrict f_ℓ to a proper domain containing \mathcal{U}_ℓ where the preimages of Σ by f_ℓ exist. One can always find such a domain if $c_\ell > 0$ is small enough because of the existence of the attracting fixed point.

Conditions stated in Eqs. (3.3.2) and (3.3.4) ensure us that the segments \mathcal{A}_n exist for all $n > 0$ if $c_\ell > 0$ is small enough, and are located at \mathcal{X}_ℓ . More over, by making $c_\ell > 0$ small enough and choosing \mathcal{U}_ℓ also small enough, the set $\mathcal{U}_\ell \cap \mathcal{X}_\ell$ is split in different sets bounded by consecutive segments \mathcal{A}_n . These sets are given by the intersection between the sets

$$L_n = \{z \in \mathcal{X}_\ell \mid f_\ell^i(z) \in \mathcal{X}_\ell, \quad i < n, \quad f_\ell^n(z) \in X_r\}, \quad (3.3.6)$$

and \mathcal{U}_ℓ . These are characterized by the fact that they are mapped into \mathcal{X}_r after exactly n iterations and satisfy that $L_{n+1} = f_\ell^{-1}(L_n)$. We also define the set

$$L_0 = f_\ell(L_1) \subset \mathcal{X}_r. \quad (3.3.7)$$

Let us then consider the sequence of sets given by the inverses of L_n by the map f_r ,

$$R_n := f_r^{-1}(L_n), \quad n \geq 0.$$

In Fig. 3.8 we show an example on how all these definitions look like for a map with $\Sigma = \{x = 0\}$.

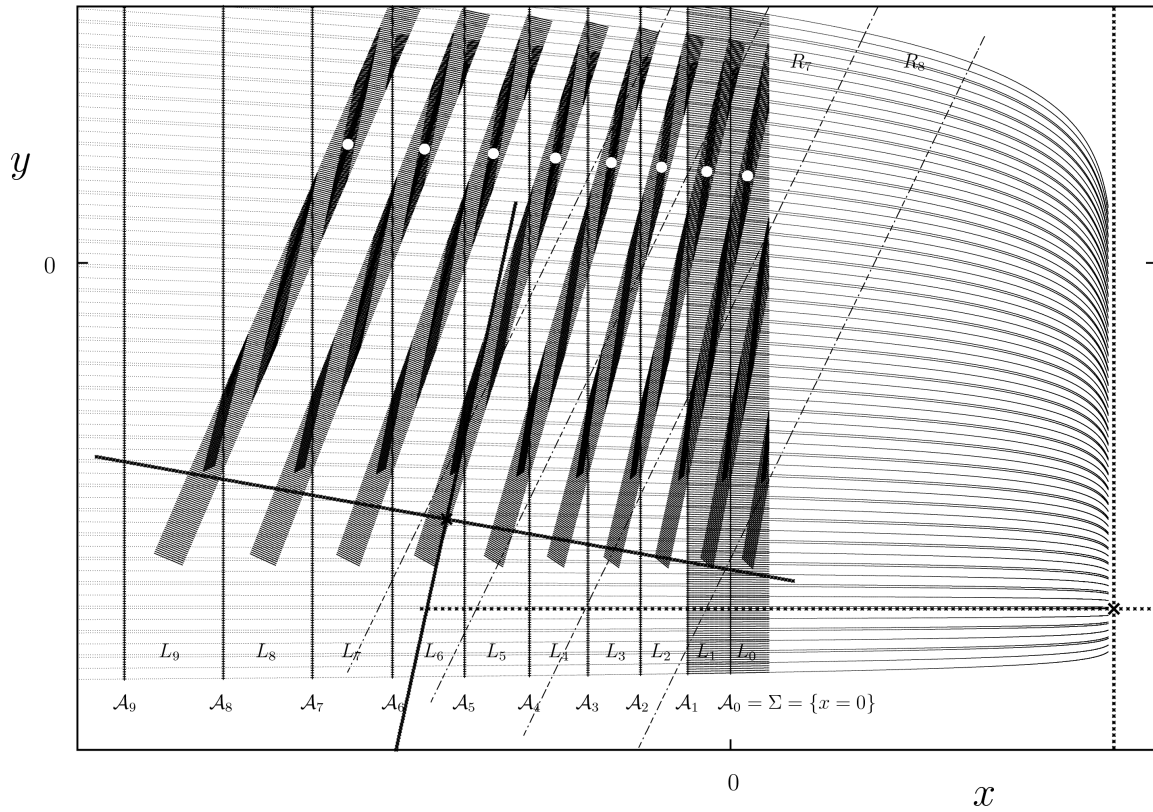


Figure 3.8: $\mathcal{L}^7 \mathcal{R}$ -periodic orbit (white points) for a two-dimensional piecewise-defined map undergoing a period incrementing big bang bifurcation. Two (virtual) fixed points are marked with crosses. As pointed lines their associated eigendirections. In thinner dashed lines are also plot the trajectories by f_ℓ converging to the (virtual) fixed point $z_\ell^* \in \mathcal{X}_r$.

Under the assumptions stated above, it comes that, for every $n > 0$ and every $c_r > 0$ small enough there exist $c_\ell > 0$, such

$$R_n \cap L_0 \neq \emptyset.$$

In other words, for every n we can find c_ℓ and c_r arbitrarily smalls such that

$$f_r(L_0) \cap L_n \neq \emptyset.$$

This defines a partition of L_0 in sets of the form $R_n \cap L_0$, allowing us to construct a map

$$F : L_0 \longrightarrow L_0,$$

given by

$$F(x; c_\ell, c_r) = f_\ell^n \circ f_r(x; c_r) \text{ if } x \in R_n \cap L_0.$$

Due to the contractiveness of the maps f_ℓ and f_r when $c_\ell, c_r >$ are small enough, the map F is also contractive in L_0 .

At its return to L_0 , it may occur that the image of a set $R_n \cap L_0$ intersects $R_i \cap L_0$,

$$F(R_n \cap L_0) \cap (R_i \cap L_0) \neq \emptyset.$$

In this case, due to the contractiveness of F , it comes that for every $x \in R_n \cap L_0$ there exists j such that $F^j(x) \notin R_n \cap L_0$ and all points escape from $R_n \cap L_0$.

This can be observed in Fig. 3.8, where

$$F(R_8 \cap L_0) = f_\ell^8(f_r(R_8 \cap L_0; c_\ell), c_r) \cap (R_7 \cap L_0) \neq \emptyset \quad (3.3.8)$$

and all points in $R_8 \cap L_0$ are finally mapped into $R_7 \cap L_0$ and escape from $R_8 \cap L_0$.

Due to the contractiveness of F , this can not occur for all sets $R_i \cap L_0$ forming the partition of L_0 , and hence there must exist some n such that

$$F(R_n \cap L_0) = f_\ell^n(f_r(R_n \cap L_0; c_\ell), c_r) \subset R_n \cap L_0.$$

As the map $f_\ell^n \circ f_r$ is smooth, this implies that this map must have fixed point. Thus, there exists an attracting periodic orbit for the map f in (3.3.1), which has the symbolic sequence $\mathcal{L}^n \mathcal{R}$.

When continuously varying one of the parameters c_ℓ or c_r , this periodic orbit undergoes a border collision and

$$f_\ell^n(f_r(R_n \cap L_0; c_r), c_\ell) \cap (R_i \cap L_0) \neq \emptyset,$$

with $i = n + 1$ or $i = n - 1$. This gives rise to a period orbit of the form $\mathcal{L}^{n+1} \mathcal{R}$ or $\mathcal{L}^{n-1} \mathcal{R}$, respectively.

It may also occur that there exist two sets $R_i \cap L_0$ and $R_j \cap L_0$ such that

$$\begin{aligned} F(R_i \cap L_0) &= f_\ell^i(f_r(R_i \cap L_0; c_r); c_\ell) \subset R_i \cap L_0 \\ F(R_j \cap L_0) &= f_\ell^j(f_r(R_j \cap L_0; c_r); c_\ell) \subset R_j \cap L_0 \end{aligned}$$

leading to the coexistence of two periodic orbits with symbolic sequences $\mathcal{L}^i\mathcal{R}$ and $\mathcal{L}^j\mathcal{R}$, respectively. This is shown for example mentioned above in Fig. 3.9. As their domains of attraction are split in L_0 by preimages of \mathcal{A}_k by f_r , at most two of such periodic orbits can coexist because there exists only one boundary, Σ , whose preimages by f_ℓ are \mathcal{A}_k . Moreover, if such sets exist, they have to be adjoin (see Fig. 3.9), and hence the coexisting periodic orbits have symbolic sequences of the form $\mathcal{L}^n\mathcal{R}$ and $\mathcal{L}^{n+1}\mathcal{R}$. Otherwise, as the map f is only defined with one boundary, Σ , the non-invariant sets located in between should be expanded, which is not possible due to the contractiveness of F .

Further details and more precise and rigorous statement of the arguments provided above are left for future work.

3.4 Conclusions

In this chapter we have proposed a detailed future work direction in order to extend the result presented in Theorem 2.2.2 to the increasing-increasing case. Instead of explicit calculations of the bifurcations curves, we propose to obtain a topological equivalent map defined in the circle and to which one can apply well known classical theory. The value of this approach remains on the relation of particular phenomena of piecewise-smooth systems with well known results of theory of circle maps, hence avoiding the need of a new theory.

In addition, we extend the results regarding big bang bifurcations to two-dimensional piecewise-defined maps. For the case of the period incrementing we have been able to adapt some of the arguments and techniques used for the one-dimensional case in Chapter 2.

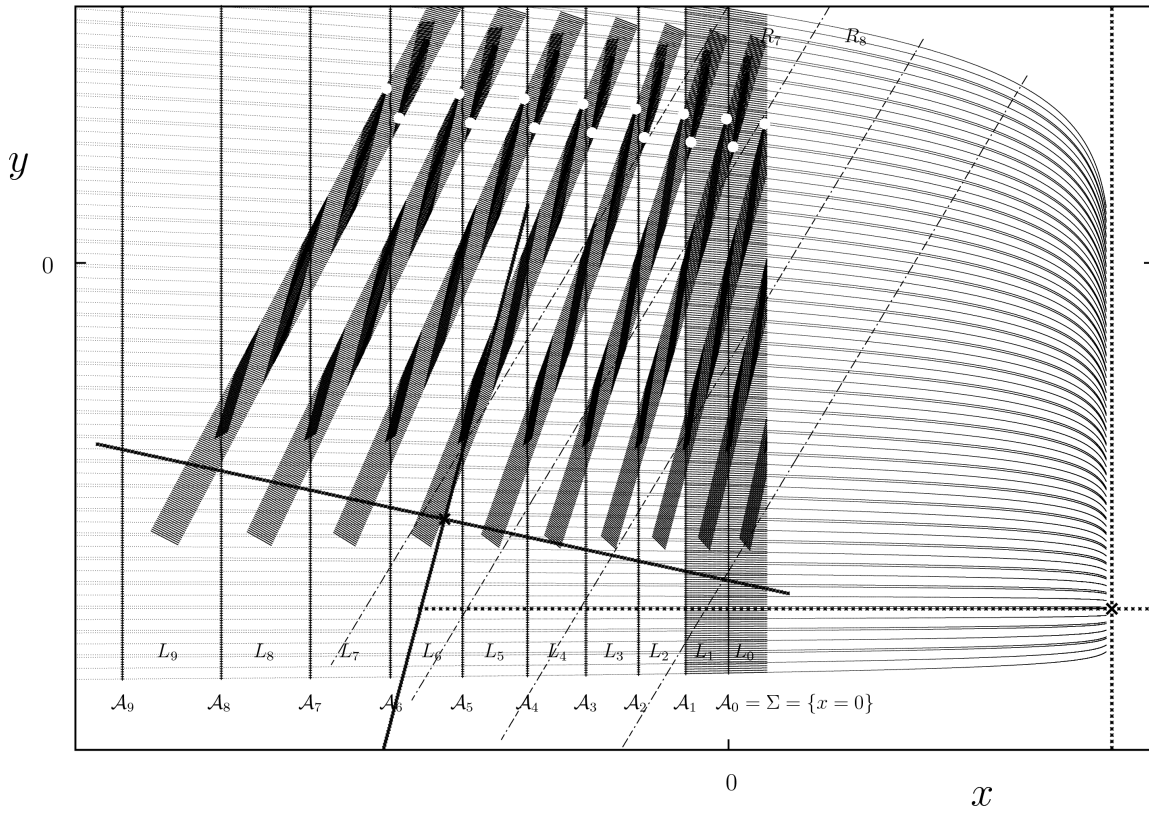


Figure 3.9: Coexistence of a $\mathcal{L}^7\mathcal{R}$ and a $\mathcal{L}^6\mathcal{R}$ periodic orbits (white points) for a two-dimensional piecewise-defined map undergoing a period incrementing big bang bifurcation. Two (virtual) fixed points are marked with crosses. As pointed lines their associated eigendirections. In thinner dashed lines are also plot the trajectories by f_ℓ converging to the (virtual) fixed point $z_\ell^* \in \mathcal{X}_r$.

Chapter 4

Occurrence of big bang bifurcations in discretized sliding-mode control systems

4.1 Introduction

There exist many methods in order to force a system to exhibit a certain desired behaviour. If its output is required to be near a certain value, one common strategy consists on implementing a control system such that two different actions are applied depending on the sign of a certain switching function which depends on the actual state and its derivatives. In general, this leads to a non-smooth system which, among other phenomena can exhibit sliding.

As, in practice, the states are sampled at particular values of time, one considers a discretization of such a construction through a zero order holder, keeping the sampled value constant until the next sampling. Instead of a differential equation, the system is then usually modeled by a map, whose dynamics may differ completely from the time continuous system where a “continuous sampling” of the states (infinite sampling frequency) is assumed. This especially occurs when the states are close to the switching manifold, as this map does not coincide with the stroboscopic Poincaré map of the time-continuous system. In particular, new bifurcation phenomena may be introduced.

Because of the nowadays hegemony of digital implementations, this has become a relevant topic in the control literature. In ([YC03, GY08, WYL08, Gal10, GY11]) the discretization effects of a sliding mode controller in a planar system is studied. Specifically, the discontinuous control results from the addition of the equivalent control plus a sign function, properly weighted. Then, a zero-order holder device is applied. As it is proven in [GY11], the resulting dynamics show an infinite number of periodic orbits with arbitrarily large periods near a certain point in a two-dimensional space. Similar phenomena

were also shown in [KST04] for one-dimensional systems derived from power converters.

Such points in parameter space assemble the so-called *big bang* bifurcations, first introduced in [AS06b] when simulating a one-dimensional piecewise-linear system, better understood and generalized later in [AGS11]. Unfortunately, the theory derived so far only considers one-dimensional maps and, hence, it can't be applied to the above mentioned planar systems in sliding-mode control.

It is worth mentioning here that, when controllers are implemented through switches, as in the case of power electronics, the resulting sliding-mode control actions reduce to the discontinuous term; *i.e.* $\varepsilon \text{sign}(\sigma)$. Then, the digitized dynamics matches perfectly with the maps that yield to *big bang* bifurcations. On the contrary, when the continuous term (the equivalent control) is included, the derived map is not longer contractive, which is highly required in the theoretical results obtained so far.

In this work, we use recent results for big bang bifurcations to explain the behaviour of a class of digitized sliding mode controlled first order systems. Specifically, in terms of [AS06b], a big bang bifurcation of the period adding type is shown to happen in that systems when the on-off control is digitized. Moreover, big bang bifurcations are shown to happen in on-off sliding mode controlled planar systems. Since the theory is not complete in this case, sufficient conditions for such a bifurcation to occur in two-dimensional piecewise maps are conjectured and corroborated by simulation.

4.2 A system with a relay based control

4.2.1 System description

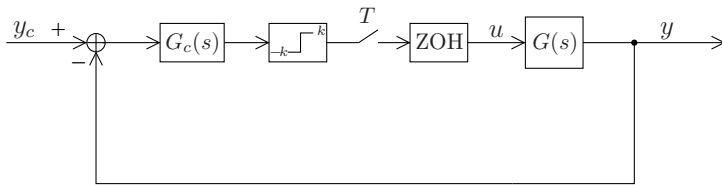


Figure 4.1: A linear control system by a relay.

Let us consider a n th-order system given by its Laplace transform

$$G_s(s) = \frac{b}{U(s)},$$

where $U(s)$ is a polynomial of the form

$$U(s) = s^n + a_{n-1}s^{n-1} + \dots + a_0, \quad (4.2.1)$$

which we assume to have only negative real roots.

Equivalently, one can also consider that the system is modeled by the differential equation

$$y^{(n)} + a_{n-1}y^{(n-1)} + \dots + a_0y = bu,$$

where $y^{(i)} = d^i y/dt^i$ and u is the input of the system.

Let us suppose that we wish to control the system and make its output, y , close to a certain desired value y_c . Although there exist many ways to achieve this, we consider the closed loop control scheme shown in Fig. 4.1.

On one hand, a certain control law is implemented by the block $G_c(s)$, which is assumed to be of the form

$$G_c(s) = 1 + c_1s + \dots + c_{n-1}s^{n-1},$$

with $c_{n-1} \neq 0$. This is to let the system have relative degree 1 and allow sliding motion on σ (see below).

Its output is then sent to a relay of gain k , hence providing a sliding-mode control with a sliding surface (also called switching surface) given by the controller G_c ,

$$\sigma := y - y_c + c_1(y^1 - y_c^1) + \dots + c_{n-1}(y^{n-1} - y_c^{n-1}) = 0. \quad (4.2.2)$$

In this work we consider $y_c \in \mathbb{R}$ constant, and thus $y_c^{(i)} = 0$ for $i \geq 1$.

Depending on the sign of the signal given by the controller G_c , the relay outputs the value k or $-k$, which yield sliding motions on σ provided that the sign and the absolute value of k are properly chosen.

Finally, the control output is digitized through a zero-order holder device, as in a real implementation. This is represented in Fig. 4.1 by a switch that samples the output of the relay at time-multiples of the sampling-period T and a zero order holder (ZOH), which keeps the sampled value constant until the next sampling. Close to the sliding surface (4.2.2), the dynamics of the discretized system differs from the time continuous one, although they tend to be the same as $T \rightarrow 0$. It is our goal to study the dynamics of the discretized system.

After performing a proper change of variables to decrease the order of the system by increasing its dimension, $y_i = y^{(i)}$, the closed loop dynamics can be written as

$$\dot{\bar{y}} = A\bar{y} + \bar{b}u \quad (4.2.3)$$

with $\bar{y} = (y_0, \dots, y_{n-1})^T \in \mathbb{R}^n$ and

$$A = \begin{pmatrix} 0 & 1 & 0 & \dots & & 0 \\ 0 & 0 & 1 & & & 0 \\ \vdots & \vdots & & \ddots & & \\ 0 & 0 & \dots & 0 & 1 & 0 \\ -a_0 & -a_1 & \dots & & -a_{n-2} & -a_{n-1} \end{pmatrix}, \bar{b} = \begin{pmatrix} 0 \\ \vdots \\ 0 \\ b \end{pmatrix}.$$

for $t \in [iT, (i+1)T)$, the input u is a constant equal to

$$u = \begin{cases} -k & \text{if } \sigma(\bar{y}) < 0 \\ k & \text{if } \sigma(\bar{y}) > 0 \end{cases} \quad (4.2.4)$$

where σ is the sliding surface given by the controller $G_c(s)$ in Equation (4.2.2).

Sliding modes occur if the vector fields $F^\pm = Ax \pm bk$ obtained by replacing $u = \pm k$, point both to the surface σ . Since F^\pm are smooth everywhere, this can be checked through

$$(L_{F^+}\sigma)(L_{F^-}\sigma) < 0. \quad (4.2.5)$$

Let us define $u_{eq} = -\frac{(\nabla\sigma)A\bar{y}}{c_{n-1}b}$, then the previous inequality mets on the subset of σ defined by

$$-|k| < u_{eq} < |k| \quad (4.2.6)$$

(see [Utk77] for details). In turn, this result can be read as *for k properly selected (both in sign and in absolute value), there is sliding motion on σ .*

Equivalently, the dynamics of the system are given by the discrete model

$$\bar{y}_{i+1} = P(\bar{y}_i),$$

where P_l (resp. P_r) is the piecewise defined stroboscopic map associated with F^+ , (resp. F^-) which is linear and can be explicitly integrated. We obtain

$$P(\bar{y}) = \begin{cases} P_l(\bar{y}) := \bar{\rho}\bar{y} + \bar{\mu}_\ell & \text{if } \sigma(\bar{y}) < 0 \\ P_r(\bar{y}) := \bar{\rho}\bar{y} + \bar{\mu}_r & \text{if } \sigma(\bar{y}) > 0, \end{cases} \quad (4.2.7)$$

with

$$\bar{\rho} = e^{AT}, \quad \bar{\mu}_r = k(\bar{\rho} - Id)(A^{-1}\bar{b}), \quad \bar{\mu}_\ell = -k(\bar{\rho} - Id)(A^{-1}\bar{b}).$$

4.2.2 General system dynamics

Each branch of the map (4.3.1), P_r and P_ℓ , has a fixed point

$$\bar{y}_r^* = -(\bar{\rho} - Id)^{-1}\bar{\mu}_r, \quad \bar{y}_\ell^* = -(\bar{\rho} - Id)^{-1}\bar{\mu}_\ell, \quad (4.2.8)$$

which may be *feasible* or *virtual* depending on whether it belongs to the domain of their respective map or not.

Regarding the possible dynamics, we distinguish between three situations. If both fixed points are feasible ($\sigma(\bar{y}_r^*) > 0$ and $\sigma(\bar{y}_\ell^*) < 0$) they also become fixed points of the map (4.3.1). Hence, if all eigenvalues of $\bar{\rho}$ have modulus less than 1, both are locally asymptotically stable. If only one of both fixed points is feasible ($\sigma(\bar{y}_r^*) < 0$ and $\sigma(\bar{y}_\ell^*) < 0$ or vice-versa) and the same condition for $\bar{\rho}$ holds, then it becomes the unique

fixed point of the map (4.3.1). For the same reason, all trajectories tend towards it, and now its domain of attraction becomes \mathbb{R}^n .

Note that, in these two previous cases, the control specification is not fulfilled as σ is not flow invariant by the piecewise vector field F .

The third situation occurs when both fixed points are virtual ($\sigma(\bar{y}_r^*) < 0$ and $\sigma(\bar{y}_\ell^*) > 0$). If all the eigenvalues of $\bar{\rho}$ have modulus less than 1 and are real (hence positive) then there are sliding motions in the original continuous-time system. In this case, and at least for linear and planar systems, the dynamics of the digitized map consists on periodic orbits which may possess arbitrarily large periods and whose iterates jump on both sides of the sliding surface $\sigma = 0$. Properly tuning the parameters, the amplitude of all these orbits can be chosen arbitrarily small. Additionally, the design conditions are satisfied in this case, as the asymptotic dynamics are close to $\sigma = 0$. A precise description of all the possible periodic orbits is the main scope of this work, and results from the existence of a *bing bang* bifurcation. This is discussed in the next section for first and second order systems.

4.3 Big bang bifurcation of the period adding type

4.3.1 The one-dimensional case

Let us first study the one-dimensional case ($n = 1$ and $G_c(s) = 1$) when (4.2.3) is a scalar equation, which was reported in [FG11]. After applying the change of variable $z = y - y_c$ to the original system, the sliding surface is given by $z = 0$, and the map (4.2.7) becomes

$$\tilde{P}(z) = \begin{cases} \tilde{P}_\ell(z) := \rho z + \mu_\ell & \text{if } z < 0 \\ \tilde{P}_r(z) := \rho z + \mu_r & \text{if } z > 0 \end{cases} \quad (4.3.1)$$

with

$$\rho = e^{a_0 T} < 1, \quad \mu_r = (\rho - 1)(y_c - \frac{bk}{a_0}) \in \mathbb{R} \text{ and } \mu_\ell = (\rho - 1)(y_c + \frac{bk}{a_0}) \in \mathbb{R}, \quad (4.3.2)$$

and the fixed points

$$z_r^* = -\frac{\mu_r}{\rho - 1} \in \mathbb{R}, \quad z_\ell^* = -\frac{\mu_\ell}{\rho - 1} \in \mathbb{R}. \quad (4.3.3)$$

In order to describe the dynamics of the map (4.3.1) when both fixed points of its branches are virtual, $\mu_r < 0$ and $\mu_\ell > 0$, we first focus on the bifurcations that occur in their transition from virtual to feasible or vice versa. To this end, we first restrict ourselves to a suitable two-dimensional parameter space, in terms of (4.3.3), where the position of z_r^* and z_ℓ^* with respect to the boundary $z = 0$ can be independently represented. More precisely, we are interested on the existence of two curves such that a variation of the

parameters along them, affects only the position of one fixed point. We proceed arguing with the parameters ρ , μ_r and μ_ℓ in (4.3.1), although we will later translate our discussion to the original parameters a , T , b , k and y_c .

We remark that we benefit from the linearity of the system in order to perform explicit calculations, although the same argumentations below hold also for a non-linear system.

As these transitions occur when one of the fixed points collides with the boundary $z = 0$, these are given by border collision bifurcations. Although the parameter ρ influences on the position of both fixed points, as we are restricted to $0 < \rho < 1$, its variation does not lead to such type of bifurcations. Hence, we focus on the $\mu_\ell \times \mu_r$ parameter space.

There, the vertical and horizontal axis represent border collision bifurcation curves that the fixed points, μ_ℓ^* and μ_r^* , undergo. Of particular interest is the origin of this parameter space, which is a co-dimension two bifurcation point, as both fixed points simultaneously collide with the boundary. Depending on the sign of the eigenvalues associated with the colliding fixed points, such a point may become a *big bang* bifurcation point, where an infinite number of (border collision) bifurcation curves emanate from. If this occurs, these bifurcation curves separate existence regions of periodic orbits located at the region in the parameter space $\mu_\ell \times \mu_r$ where both fixed points are virtual.

This basically depends on the sign of the eigenvalues of the colliding fixed points, which, for the one-dimensional case, are the slopes of the map near the discontinuity. The possible bifurcation scenarios for a one-dimensional contracting linear map with one discontinuity were described in [AS06b] through numerical observations, and were generalized in [AGS11] (see also the bibliography reported there). With independence of the particular nature of the map, it was proven there that when the sign of the eigenvalues associated with the colliding fixed points are different (also known as increasing-decreasing/decreasing-increasing case), then a big bang bifurcation of the *period incrementing* type occurs. It was also suggested that, when both are positive (increasing-increasing case), a *period adding* big bang bifurcation (described below) occurs. Although this result was conjectured, the resulting bifurcation scenario has been highly reported in the literature ([Leo59, CGT84, GGT84, GGT88, GPTT86, GH94, Hom96, TS86, PTT87]), and hence it is a well accepted result.

In our case, as the eigenvalues associated with the colliding fixed points are positive, $0 < \rho < 1$, a big bang of the period adding type occurs at the origin of the parameter space $\mu_\ell \times \mu_r$.

This implies that the region located near the origin of the parameter space where both fixed points are virtual is fully covered by an infinite number of regions where a unique periodic orbit exists. All these regions collapse at the origin and, hence, all the possible periodic orbits exist for any arbitrarily small neighbourhood containing the origin of the parameter space.

To understand how these periodic orbits are organized, let us introduce the following symbolic codification (see [AS06b] for a more extended explanation). Let (z_1, \dots, z_n) be the sequence of points forming a periodic orbit of period n , then we consider the symbolic sequence obtained by replacing each of these points by \mathcal{L} if $z_i < 0$ and \mathbb{R} if $z_i > 0$. Then, the symbolic sequences of the periodic orbits are obtained by a gluing process between periodic orbits. More precisely, in-between the regions of existence of two periodic orbits of periods n and m with symbolic sequences α and β one finds a region where the $(n + m)$ -periodic orbit with symbolic sequence $\alpha\beta$ (their concatenation) exists. As the symbolic sequences are glued, the periods are added, and hence this scenario was referred in [AS06b] as period adding. This process starts with the fixed points $z_\ell^* \rightarrow \mathcal{L}$ and $z_r^* \rightarrow \mathbb{R}$, which are “glued” to form the 2-periodic orbit $\mathcal{L}\mathbb{R}$, and is repeated add infinitum. Thus, in any arbitrarily small neighbourhood of the origin of the parameter space one can find an infinite number of periodic orbits with arbitrarily large periods.

Let us adapt the situation described before in terms of the parameters involved in the original system (4.2.3)-(4.2.4) for $n = 1$. Let us first focus on their influence on the dynamics of the map (4.3.1).

As it comes from the relations shown in (4.3.2), the most relevant parameters regarding the influence on the location of the fixed points z_ℓ^* and z_r^* are y_c , k and b . We proceed arguing with the pair (y_c, k) , as they are the parameters to be tuned and, hence, are of more interest from the control design point of view. However, the following discussion can be easily extended to the pair (y_c, b) .

In this parameter space, the lines

$$k = -a_0/by_c \text{ and } k = a_0/by_c \quad (4.3.4)$$

represent border collision bifurcation curves for z_ℓ^* and z_r^* , respectively. Hence, as both are attracting with positive associated eigenvalues ($0 < \rho < 1$), a big bang bifurcation of the period adding type occurs at the intersection of these lines, $(y_c, k) = (0, 0)$, where two border collision bifurcation simultaneously occur.

Note that, although the parameter a_0 also influences on the position of the fixed points, it comes that a big bang bifurcation may occur for $a_0 = 0$. However, for such a value the fixed points are no longer attractive and, hence, the results obtained so far on big bang bifurcation can not be applied.

To demonstrate this, we show in Fig. 4.2(a) the bifurcation scenario in the $y_c \times k$ parameter space, where one can observe the infinite number of bifurcation curves emanating from the origin. The adding scenario is presented in Fig. 4.2(b), where the periods of the periodic orbits found along the curve marked in Fig. 4.2(a) are shown.

It comes from the adding procedure described above that all the periodic orbits step at both sides of the boundary $z = 0$. Hence, each of these n -periodic orbits correspond in the original 1-dimensional continuous model (4.2.3)-(4.2.4) to a continuous nT -periodic

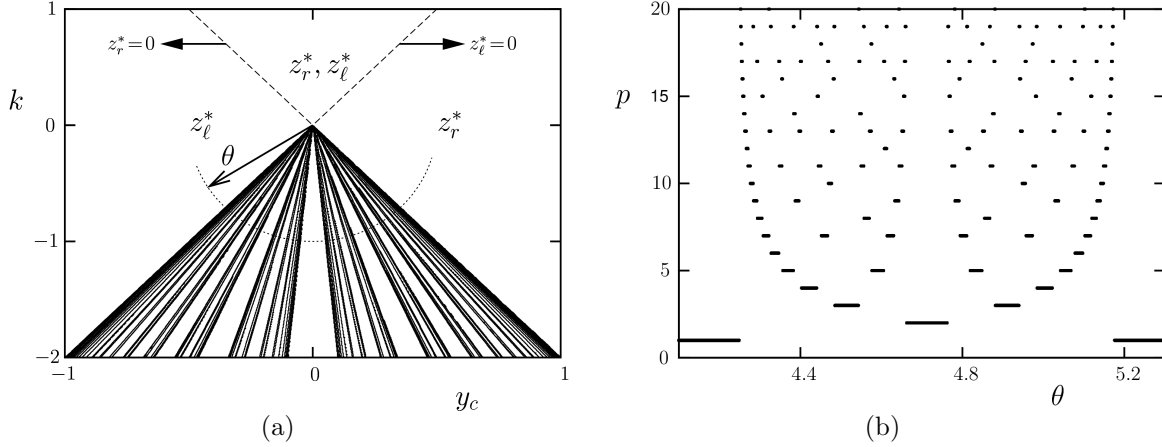


Figure 4.2: (a) Big bang bifurcation in the (y_c, k) parameter space for $a_0 = -2$, $b = 1$ and $T = 0.1$. The fixed points z_i^* are labeled in the regions where they are feasible, and, as dashed lines, the border collision bifurcation curves where they become virtual are shown. The periods of the periodic orbits found along the pointed curve parametrized by σ are shown in (b).

orbit which oscillates around $y = y_c$. In addition, the amplitude of all these orbits tend to zero as the parameters y_c and k get close to the big bang bifurcation.

4.3.2 A second order system

We now extend the results shown in the previous section to a second order system. In this case, we have

$$A = \begin{pmatrix} 0 & 1 \\ -a_0 & -a_1 \end{pmatrix}, \bar{b} = \begin{pmatrix} 0 \\ b \end{pmatrix}, \sigma = y_1 - y_c + c_1 y_2,$$

where a_0 and a_1 are such that the eigenvalues of the matrix A have real negative eigenvalues.

For commodity, in order to easily proceed as before and argue with the relative position of the fixed points \bar{z}_l^* and \bar{z}_r^* with respect the boundary, we introduce new coordinates $\bar{z} = (z_1, z_2)$ given by

$$\bar{z} = \underbrace{\begin{pmatrix} 1 & c_1 \\ a_0 c_1 - a_1 & 1 \end{pmatrix}}_{\phi} - \begin{pmatrix} y_c \\ 0 \end{pmatrix}.$$

Note that one can always perform such a change of variables as long as the vector $(1, c_1)^T$ is not an eigenvector of the matrix A .

In these new variables, the map (4.2.7) becomes

$$\tilde{P}(\bar{z}) = \begin{cases} \tilde{P}_\ell(\bar{z}) := \tilde{\rho}\bar{z} + \bar{\mu}_\ell & \text{if } z_1 < 0 \\ \tilde{P}_r(\bar{z}) := \tilde{\rho}\bar{z} + \bar{\mu}_r & z_1 > 0, \end{cases} \quad (4.3.5)$$

where

$$\begin{aligned} \tilde{\rho} &= e^{\tilde{A}T}, \quad \tilde{A} = \begin{pmatrix} -a_1 & -1 \\ a_0 & 0 \end{pmatrix} \\ \bar{\mu}_\ell &= (\tilde{\rho} - Id)\tilde{A}^{-1} \left(-\phi \begin{pmatrix} 0 \\ kb \end{pmatrix} + \tilde{A} \begin{pmatrix} y_c \\ 0 \end{pmatrix} \right) \\ \bar{\mu}_r &= (\tilde{\rho} - Id)\tilde{A}^{-1} \left(\phi \begin{pmatrix} 0 \\ kb \end{pmatrix} + \tilde{A} \begin{pmatrix} y_c \\ 0 \end{pmatrix} \right). \end{aligned}$$

The main advantage of this change of variables consists on the fact that the boundary becomes $z_1 = 0$, independently of the parameters, while the matrix $\tilde{\rho}$ remains only dependent on the parameters a_i . Hence, the relevant parameters for the study of the border collision bifurcations only influence the position of the fixed points, which become

$$\begin{aligned} \bar{z}_\ell^* &= \begin{pmatrix} -y_c - \frac{kb}{a_0} \\ -\frac{kb}{a_0}(a_0c_1 - a_1) \end{pmatrix} \\ \bar{z}_r^* &= \begin{pmatrix} -y_c + \frac{kb}{a_0} \\ \frac{kb}{a_0}(a_0c_1 - a_1) \end{pmatrix} \end{aligned}$$

The border collision bifurcation curves that the fixed points undergo become the same expressions as in the one-dimensional case, given in (4.3.4). Hence, arguing again in the $y_c \times k$ parameter space, for $y_c = k = 0$ both fixed points simultaneously collide with the boundary $z_1 = 0$ and become virtual.

We now conjecture an extension to 2-dimensional maps of the result used above for the one-dimensional maps. In the considered situation regarding the simultaneously collision of attracting fixed points with the boundary, there exist a big bang bifurcation of the period adding type if there exist an open neighbourhood \mathcal{U} such that, at the simultaneous collision,

$$\begin{aligned} \bar{z}_\ell^*, \bar{z}_r^* &\in \mathcal{U} \\ \tilde{P}_i(\mathcal{U} \cap \mathcal{X}_i) &\subset \mathcal{U} \cap \mathcal{X}_i, \quad i \in \{\ell, r\}, \end{aligned}$$

where \mathcal{X}_ℓ and \mathcal{X}_r are the left and right part of \mathbb{R}^2 separated by the boundary.

In our case, these conditions coincide with the sliding conditions given in (4.2.5). This

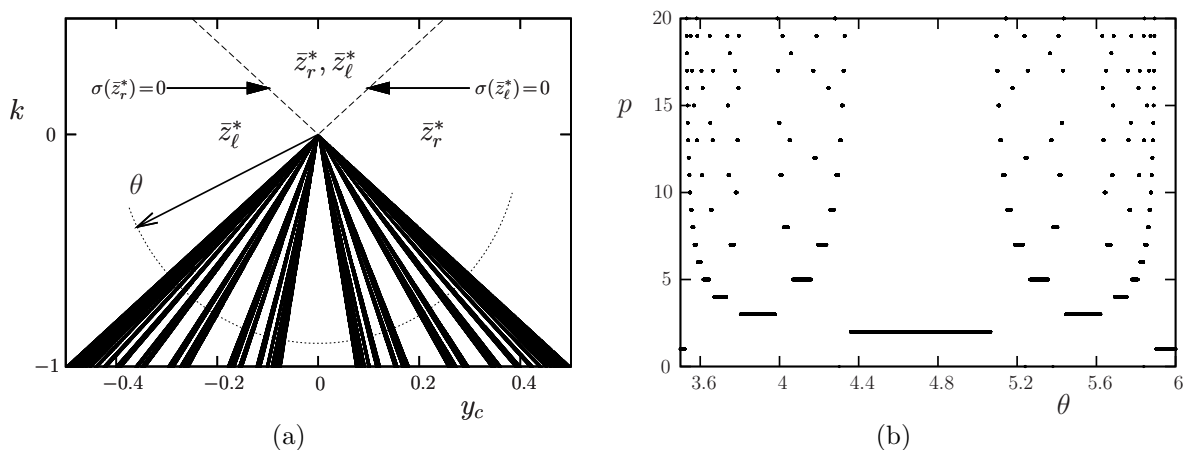


Figure 4.3: Big bang bifurcation in the (y_c, k) parameter space for $a_0 = -2$, $a_1 = -5$, $b = 1$, $c_1 = 1.5$ and $T = 0.1$.

is because, at the big bang bifurcation point, $k = y_c = 0$, both fixed points collide with origin of the state space, $\bar{z}_i^*(0, 0)^T$. Hence, near the bifurcation point, $|u_{eq}| \ll 1$ and thus condition (4.2.6) is fulfilled if

$$c_1 \neq 0.$$

Note that, although the map (4.3.5) is continuous at $\bar{z} = (0, 0)^T$ at the big bang bifurcation point because both fixed points coincide at $\bar{z} = (0, 0)^T$, continuity is not assumed in the conditions mentioned above.

The simulations shown in Fig. 4.3 show how a big bang bifurcation of the period adding type occurs for $y_c = k = 0$ if $c_1 \neq 0$.

4.4 Conclusions

In this chapter we have applied the results and methodology presented in Chapters 2 and 3 to an application example consisting of a general system controlled by relays in sliding-mode operation. We have hence shown the existence of a co-dimension-2 big bang bifurcation in a two-dimensional parameter space relevant from the control design point of view.

When discretized, the original system becomes a piecewise-defined system with a single boundary. The discretization is obtained through a stroboscopic map of flows with at-

tracting critical points, which become critical points of the piecewise-defined maps with positive associated eigenvalues. Hence, as suggested in Chapter 3, this big bang bifurcation is of the period adding type.

In addition, we also consider a second order system which leads a two-dimensional piecewise-defined for which the results conjectured in §3.3 hold, hence exhibiting also a big bang bifurcation of the period adding type. We also provide numerical simulations in order to confirm the predicted behaviour.

Although the first and second order systems that we have used as example were linear, all the arguments that we have presented in this chapter can be applied to systems with nonlinear transfer function under the same control-mode.

Part II

Melnikov methods and scattering map in piecewise-smooth systems

Chapter 5

The Melnikov method and subharmonic orbits in a piecewise-smooth system

5.1 Introduction

As explained in the introduction of this thesis, this chapter is devoted to extend classical Melnikov methods to a class of piecewise-smooth “Hamiltonian” systems. It is organized as follows.

In §5.2 we describe the class of system that we consider and introduce some notation and tools needed for this work. In §5.3, we prove the existence of periodic orbits distinguishing between the conservative and dissipative cases. §5.4 is devoted to heteroclinic connections. Finally, in §5.5, we use the example of the rocking block to illustrate the results obtained regarding the periodic orbits, and compare with the work of [Hog89].

5.2 System description

5.2.1 General system definition

We divide the plane into two sets (see Figs. 5.1-5.2),

$$\begin{aligned} S^+ &= \{(x, y) \in \mathbb{R}^2 \mid x > 0\} \\ S^- &= \{(x, y) \in \mathbb{R}^2 \mid x < 0\} \end{aligned}$$

separated by the switching manifold

$$\Sigma = \Sigma^+ \cup \Sigma^- \cup (0, 0) \tag{5.2.1}$$

where

$$\begin{aligned}\Sigma^+ &= \{(x, y) \in \mathbb{R}^2 \mid x = 0, y > 0\} \\ \Sigma^- &= \{(x, y) \in \mathbb{R}^2 \mid x = 0, y < 0\}.\end{aligned}$$

We consider the piecewise-smooth system

$$\begin{pmatrix} \dot{x} \\ \dot{y} \end{pmatrix} = \begin{cases} \mathcal{X}_0^+(x, y) + \varepsilon \mathcal{X}_1^+(x, y, t) & \text{if } (x, y) \in S^+ \\ \mathcal{X}_0^-(x, y) + \varepsilon \mathcal{X}_1^-(x, y, t) & \text{if } (x, y) \in S^- \end{cases} \quad (5.2.2)$$

We assume $\mathcal{X}_0^\pm \in C^\infty(\mathbb{R}^2)$ and $\mathcal{X}_1^\pm(x, y, t) \in C^\infty(\mathbb{R}^3)$, although this can be relaxed to less regularity in S^\pm and $S^\pm \times \mathbb{R}$, respectively.

System (5.2.2) is a Hamiltonian system associated with a C^0 piecewise-smooth Hamiltonian of the form

$$H_\varepsilon(x, y, t) = H_0(x, y) + \varepsilon H_1(x, y, t). \quad (5.2.3)$$

The unperturbed $C^0(\mathbb{R}^2)$ Hamiltonian H_0 is a classical Hamiltonian given by

$$H_0(x, y) := \frac{y^2}{2} + V(x) := \begin{cases} H_0^+(x, y) := \frac{y^2}{2} + V^+(x) & \text{if } (x, y) \in S^+ \cup \Sigma \\ H_0^-(x, y) := \frac{y^2}{2} + V^-(x) & \text{if } (x, y) \in S^- \end{cases} \quad (5.2.4)$$

with $V^\pm \in C^\infty(\mathbb{R})$ satisfying $V^+(0) = V^-(0)$.

Similarly, the non-autonomous T -periodic $C^0(\mathbb{R}^3)$ perturbation, εH_1 , is given by

$$H_1(x, y, t) := \begin{cases} H_1^+(x, y, t) & \text{if } (x, y) \in S^+ \cup \Sigma^+ \\ H_1^-(x, y, t) & \text{if } (x, y) \in S^- \cup \Sigma^- \end{cases}$$

satisfying $H_1^+(0, y, t) = H_1^-(0, y, t) \forall (y, t) \in \mathbb{R}^2$.

Then, the relation between (5.2.2) and (5.2.3) is given by

$$\begin{aligned}\mathcal{X}_0^+ + \varepsilon \mathcal{X}_1^+ &= J \nabla (H_0^+ + \varepsilon H_1^+) \\ \mathcal{X}_0^- + \varepsilon \mathcal{X}_1^- &= J \nabla (H_0^- + \varepsilon H_1^-),\end{aligned} \quad (5.2.5)$$

where J is the usual symplectic matrix

$$J = \begin{pmatrix} 0 & 1 \\ -1 & 0 \end{pmatrix}.$$

We assume that the phase portrait of the unperturbed system (5.2.2) ($\varepsilon = 0$) is topologically equivalent to the one shown in Fig. 5.1, which we make precise in the following hypotheses.

C.1 There exist two hyperbolic critical points $z^+ \equiv (x^+, y^+) \in S^+$ and $z^- \equiv (x^-, y^-) \in S^-$ of saddle type belonging to the energy level

$$\{(x, y) \mid H_0(x, y) = c_1 > 0\}. \quad (5.2.6)$$

C.2 The form of the Hamiltonian H_0 in Eq. (5.2.4), ensures that \mathcal{X}_0^\pm are both tangent to Σ at $(0, 0) \in \Sigma$. We require that V^\pm satisfy

$$(V^+)'(0) > 0; (V^-)'(0) < 0,$$

and so $(0, 0)$ is an invisible quadratic tangency for both vector fields. Following [GST11], we call the point $(0, 0)$ an invisible fold-fold.

C.3 There exist two heteroclinic orbits given by $W^u(z^-) = W^s(z^+)$ and $W^u(z^+) = W^s(z^-)$ surrounding the origin and contained in the energy level (5.2.6).

C.4 The region between both heteroclinic orbits is fully covered by periodic orbits surrounding the origin given by

$$\Lambda_c = \{(x, y) \in \mathbb{R}^2 \mid H_0(x, y) = c\} \quad (5.2.7)$$

with $0 < c < c_1$, and Λ_c intersects Σ transversally exactly twice.

C.5 The period of Λ_c is a regular function of c with strictly positive derivative for $0 < c < c_1$.

Note that, as the unperturbed Hamiltonian H_0 is C^∞ in S^+ and S^- , the fact that the heteroclinic orbits are in the energy level $H_0(x, y) = c_1$ follows automatically from hypothesis C.1. However, we include it explicitly for clarity.

We wish to determine which of these objects and characteristics persist and which are destroyed when the small non-autonomous T -periodic perturbation εH_1 is considered. The splitting of the separatrices and the persistence of periodic orbits is of interest. In the smooth case, these answers are given completely by the classical Melnikov method [GH83]. Hence, it is natural to check whether these classical tools are still valid for the piecewise-smooth system presented above and if any changes to the method are necessary. Another interesting question that can be addressed with a similar approach is the existence of 2-dimensional invariant tori of system (5.2.2) (see [KKY97, Kun00]).

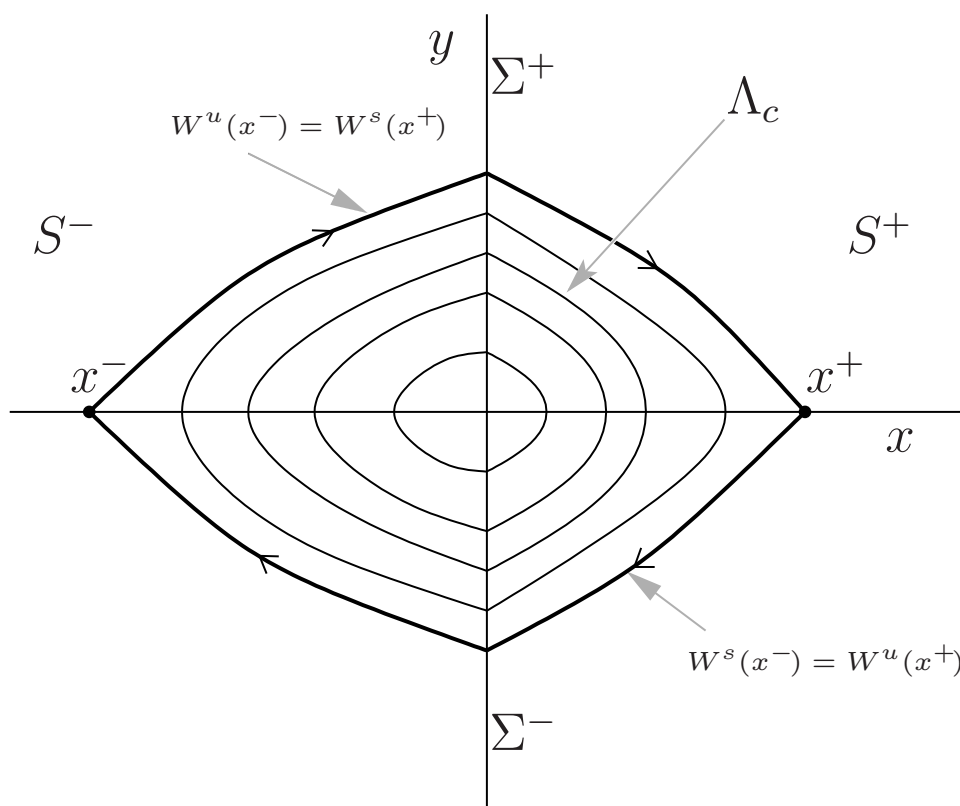


Figure 5.1: Phase portrait for the unperturbed system (5.2.2).

5.2.2 Poincaré impact map

To study system (5.2.2) we will proceed as in [Hog89] using the Poincaré impact map. We consider the extended phase space $\mathbb{R}^2 \times \mathbb{R}$ adding time as a system variable and equation $\dot{t} = 1$ to Eq. (5.2.2). As the perturbation is periodic, this time variable is usually defined in $\mathbb{T} = \mathbb{R}/T$; however, it will be more useful for us to consider \mathbb{R} instead. We want to study the motion in the region surrounded by the heteroclinic orbit, so we consider in this extended phase-space the Poincaré section

$$\tilde{\Sigma}^+ = \{(0, y, t) \in \mathbb{R}^2 \times \mathbb{R} \mid 0 < y < \sqrt{2c_1}\}. \quad (5.2.8)$$

To simplify the notation, as the first coordinate in $\tilde{\Sigma}^+$ is always 0, we will omit its repetition whenever this does not lead to confusion. The domain of the Poincaré map is not $\tilde{\Sigma}^+$ but a suitable open set U , that depends on ε and, for $\varepsilon = 0$, does not contain the heteroclinic connection.

We now define the Poincaré impact map

$$P_\varepsilon : U \subset \tilde{\Sigma}^+ \longrightarrow \tilde{\Sigma}^+,$$

as follows (see Fig. 5.2). First, using the section

$$\tilde{\Sigma}^- = \{(0, y, t) \in \mathbb{R}^2 \times \mathbb{R} \mid -\sqrt{2c_1} < y < 0\}, \quad (5.2.9)$$

with $(0, y_0, t_0) \in U^+ \subset \tilde{\Sigma}^+$, we define the map

$$P_\varepsilon^+ : U^+ \subset \tilde{\Sigma}^+ \longrightarrow \tilde{\Sigma}^-,$$

as

$$P_\varepsilon^+(y_0, t_0) = (\Pi_y(\phi^+(t_1; t_0, 0, y_0, \varepsilon)), t_1) \quad (5.2.10)$$

where $\phi^+(t; t_0, x, y, \varepsilon)$ is the flow associated with system (5.2.2) restricted to S^+ , and $t_1 > t_0$ is the smallest value of t satisfying the condition

$$\Pi_x(\phi^+(t_1; t_0, 0, y_0, \varepsilon)) = 0. \quad (5.2.11)$$

where Π_x, Π_y are projections onto the x and y axes, respectively. Similarly, we consider

$$P_\varepsilon^- : U^- \subset \tilde{\Sigma}^- \longrightarrow \tilde{\Sigma}^+$$

for $(0, y_1, t_1) \in U^- \subset \tilde{\Sigma}^-$ defined by

$$P_\varepsilon^-(y_1, t_1) = (\Pi_y(\phi^-(t_2; t_1, 0, y_1, \varepsilon)), t_2) \quad (5.2.12)$$

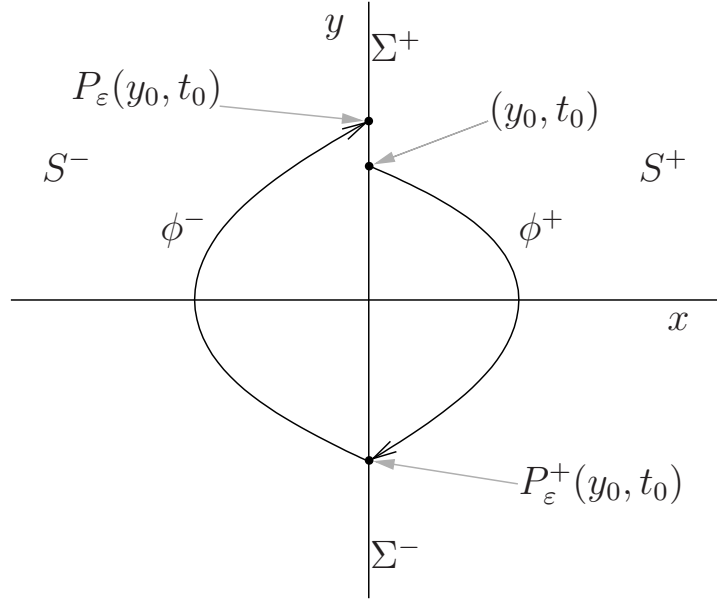


Figure 5.2: Poincaré impact map (5.2.14) represented schematically.

where $\phi^-(t; t_1, x, y, \varepsilon)$ is the flow associated with (5.2.2) restricted to S^- , and $t_2 > t_1$ is the smallest value of t satisfying the condition

$$\Pi_x(\phi^-(t_2; t_1, 0, y_1, \varepsilon)) = 0. \quad (5.2.13)$$

Then the Poincaré impact map is defined as the composition

$$P_\varepsilon : U \subset \tilde{\Sigma}^+ \longrightarrow \tilde{\Sigma}^+ \\ (y_0, t_0) \longmapsto P_\varepsilon^- \circ P_\varepsilon^+(y_0, t_0) \quad (5.2.14)$$

Notice that, as assumed in C.4, for the unperturbed flow all initial conditions in Σ^+ lead to periodic orbits surrounding the origin. Hence, we can give a closed expression for P_0 , the Poincaré impact map when $\varepsilon = 0$. Let

$$\alpha^\pm(\pm y) = \pm 2 \int_0^{(V^\pm)^{-1}(h)} \frac{1}{\sqrt{2(h - V^\pm(x))}} dx, \quad h = H_0(0, \pm y) = \frac{y^2}{2} \quad (5.2.15)$$

be the time needed by an orbit of the unperturbed system with initial condition $(0, \pm y) \in \Sigma^\pm$ to reach Σ^\mp . In the unperturbed case, the orbit with initial condition $(0, y) \in \Sigma^+$ has period

$$\alpha(y) = \alpha^+(y) + \alpha^-(-y). \quad (5.2.16)$$

Then the Poincaré impact map when $\varepsilon = 0$ is defined in the whole $\tilde{\Sigma}^+$, and can be written as

$$P_0(y_0, t_0) = (y_0, t_0 + \alpha(y_0)). \quad (5.2.17)$$

Thus, if ε is small enough, the perturbed trajectories starting at $\tilde{\Sigma}^+$ cross $\tilde{\Sigma}^+$ again. The Poincaré impact map is well defined, and is as smooth as the flow restricted to S^+ and S^- .

Note that in the symmetric case, $V^+(x) = V^-(-x)$, $\alpha^+(y) = \alpha^-(-y)$ is half the period of the unperturbed periodic orbit with initial condition $(0, y) \in \Sigma^+$.

5.2.3 Coefficient of restitution

As the name of the previous map suggests, it is typically used to deal with systems with impacts, as is the case of the mechanical example of section 5.5. In order to include the loss of energy at the impact, one considers a coefficient of restitution, $r \in (0, 1]$, that reduces the velocity, y , at every impact. More precisely, if a trajectory crosses Σ transversally at some point $(0, y_B)$ at $t = t_B$, then the state is replaced by $(0, ry_B)$ at a later time t_A to proceed with the evolution of the system. In other words, the system slides along Σ from $(0, y_B)$ to $(0, ry_B)$ during time $t_A - t_B$ and

$$y(t_A) = ry(t_B). \quad (5.2.18)$$

For the rest of this article we will assume that the loss of energy is produced instantaneously and hence $t_A = t_B$. Thus, there is no sliding along Σ and the trajectory jumps from $(0, y_B)$ to $(0, ry_B)$.

Clearly, when such a condition is introduced to a system of the type (5.2.2), the unperturbed system ($\varepsilon = 0$) is no longer conservative, the origin becomes a global attractor and none of the conditions C.1–C.5 hold. In particular, the orbits with initial conditions on the unstable manifolds $W^u(z^-)$ and $W^u(z^+)$ tend to the origin and can not intersect the stable manifolds $W^s(z^+)$ and $W^s(z^-)$, respectively (see Fig. 5.3).

Although periodic orbits surrounding the origin are not possible for the unperturbed case if $r < 1$, they may exist if $\varepsilon > 0$. However, roughly speaking, as these orbits will have to overcome the loss of energy, the magnitude of the forcing can not be arbitrarily small. We will make a precise statement of this fact in §5.3.2 (see also [Hog89]).

To study the existence of periodic orbits we will use again the impact map, which can also be defined for $r < 1$ as (see Fig. 5.4)

$$\tilde{P}_{\varepsilon, r}(y_0, t_0) := R_r \circ P_\varepsilon^- \circ R_r \circ P_\varepsilon^+(y_0, t_0) \quad (5.2.19)$$

where

$$R_r(y_0, t_0) = (ry_0, t_0).$$

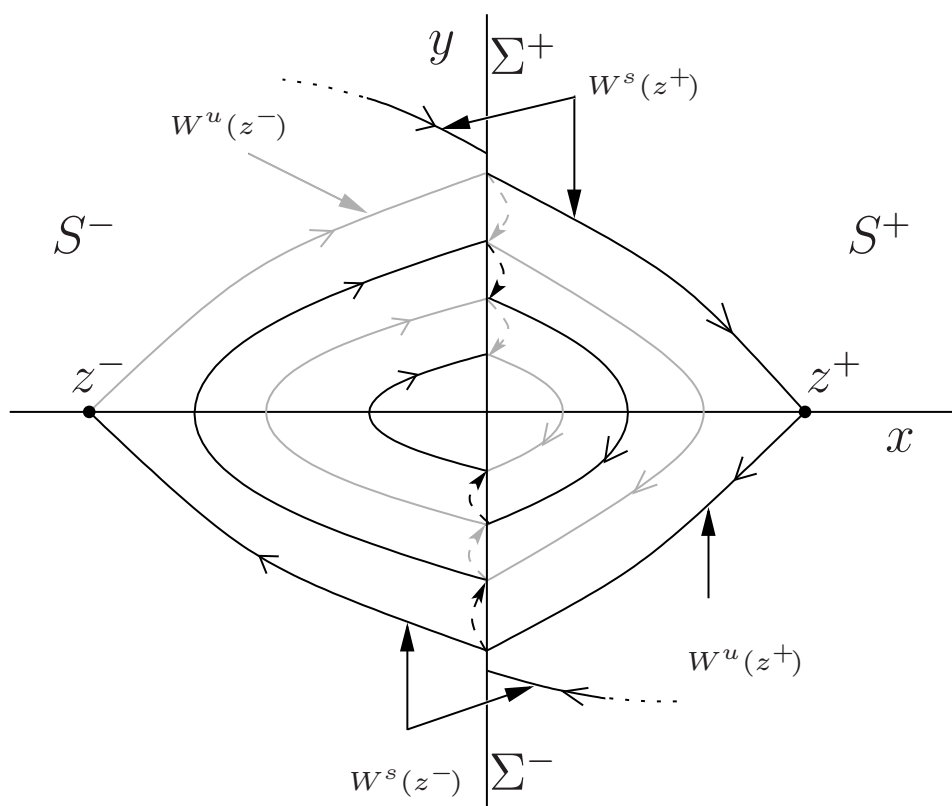


Figure 5.3: Stable and unstable manifolds of system (5.2.2) for $r < 1$ and $\varepsilon = 0$.

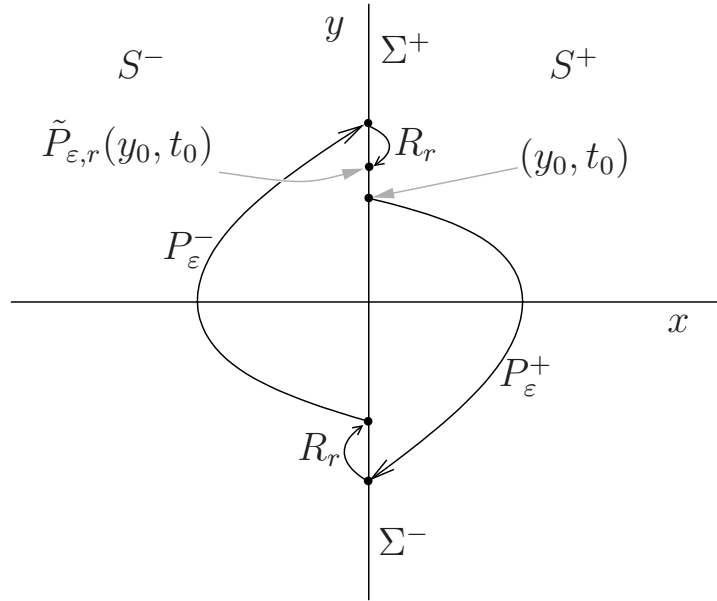


Figure 5.4: Impact map for $r < 1$ and $\varepsilon > 0$.

Note that $\tilde{P}_{\varepsilon,r}$ is as smooth as the flow restricted to S^\pm , since it is the composition of smooth maps.

Using Eqs. (5.2.15) and (5.2.16), the impact map, $\tilde{P}_{\varepsilon,r}$, for $\varepsilon = 0$ and $r < 1$ can be written as

$$\tilde{P}_{0,r}(y_0, t_0) = (r^2 y_0, t_0 + \alpha^+(y_0) + \alpha^-(-r y_0)). \quad (5.2.20)$$

Note that, for any $\varepsilon > 0$,

$$\tilde{P}_{\varepsilon,1}(y_0, t_0) = P_\varepsilon(y_0, t_0).$$

5.2.4 Some formal definitions and notation

Up to now, we have considered separately the solutions of system (5.2.2) in S^+ and S^- until they reach the switching manifold Σ . Given an initial condition (x_0, y_0, t_0) , one can extend the definition of a solution, $\phi(t; t_0, x_0, y_0, \varepsilon, r)$, of system (5.2.2), (5.2.18) for all $t \geq t_0$ by properly concatenating ϕ^+ or ϕ^- whenever the flow crosses Σ transversally. Depending on the sign of x_0 , one applies either $\phi^+(t; t_0, x_0, y_0, \varepsilon)$ or $\phi^-(t; t_0, x_0, y_0, \varepsilon)$ until the trajectory reaches Σ , and then one applies (5.2.18). If $x_0 = 0$, one proceeds similarly depending on the sign of y_0 . This is because $\dot{x} = y + O(\varepsilon)$ is always an equation of the flow and the orbits twist clockwise.

In this work, we will mainly use solutions with initial conditions $(0, y_0, t_0) \in \tilde{\Sigma}^+$. In

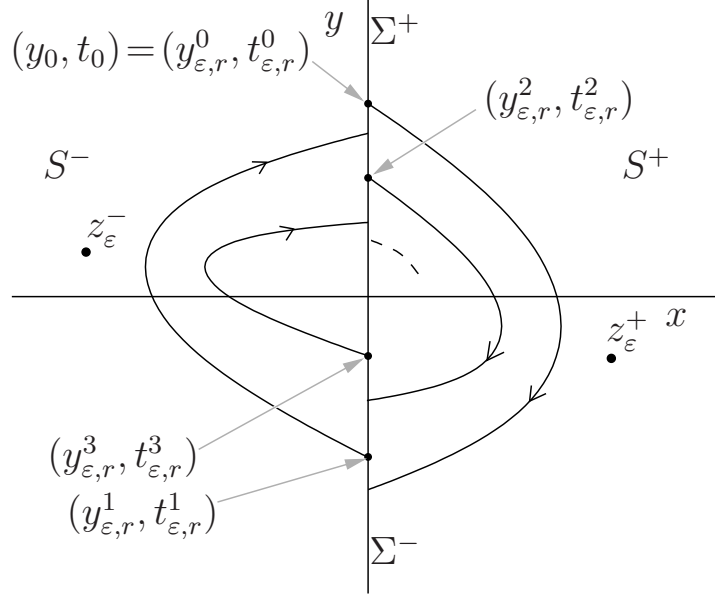


Figure 5.5: Sequence of impacts for $r < 1$ and $\varepsilon > 0$.

that case, we define the sequence of impacts $(0, y_{\varepsilon,r}^i, t_{\varepsilon,r}^i)$ (see Fig. 5.5), if they exist, as

$$(y_{\varepsilon,r}^i, t_{\varepsilon,r}^i) = \begin{cases} R_r \circ P_{\varepsilon}^{-}(y_{\varepsilon,r}^{i-1}, t_{\varepsilon,r}^{i-1}) & \text{if } y_{\varepsilon,r}^{i-1} < 0 \\ R_r \circ P_{\varepsilon}^{+}(y_{\varepsilon,r}^{i-1}, t_{\varepsilon,r}^{i-1}) & \text{if } y_{\varepsilon,r}^{i-1} > 0 \end{cases}, \quad (5.2.21)$$

with $(y_{\varepsilon,r}^0, t_{\varepsilon,r}^0) = (y_0, t_0)$ and P_{ε}^{\pm} defined in (5.2.10) and (5.2.12). Notice that the sequence (5.2.21) will be finite if the flow reaches Σ a finite number of times only.

For the unperturbed case, for any point $(0, y_0, t_0) \in \tilde{\Sigma}^+$, the sequence (5.2.21) becomes

$$(y_{0,r}^i, t_{0,r}^i) := \begin{cases} (r^i y_0, t_{0,r}^{i-1} + \alpha^{-}(-r^{i-1} y_0)) & \text{if } i \geq 2 \text{ even} \\ (-r^i y_0, t_{0,r}^{i-1} + \alpha^{+}(r^{i-1} y_0)) & \text{if } i \geq 1 \text{ odd} \end{cases}, \quad (5.2.22)$$

where α^{\pm} are defined in Eq. (5.2.15).

Once the impacts $(y_{\varepsilon,r}^i, t_{\varepsilon,r}^i)$ are defined, the solution of the non-autonomous system (5.2.2),(5.2.18) with initial condition $(0, y_0, t_0) \in \tilde{\Sigma}^+$ is given by

$$\phi(t; t_0, 0, y_0, \varepsilon, r) := \begin{cases} \phi^{+}(t; t_{\varepsilon,r}^{2i}, 0, y_{\varepsilon,r}^{2i}, \varepsilon) & \text{if } t_{\varepsilon,r}^{2i} \leq t < t_{\varepsilon,r}^{2i+1} \\ \phi^{-}(t; t_{\varepsilon,r}^{2i+1}, 0, y_{\varepsilon,r}^{2i+1}, \varepsilon) & \text{if } t_{\varepsilon,r}^{2i+1} \leq t < t_{\varepsilon,r}^{2i+2} \end{cases}, \quad i \geq 0. \quad (5.2.23)$$

Note that in the case when the number of impacts is finite, we take the last interval of time to be infinitely long.

In the rest of the chapter we will generally distinguish between the conservative ($r = 1$) and dissipative ($r < 1$) cases. We will omit the parameter r in the flow ϕ whenever we refer to $r = 1$.

Note that we have only defined the solution of the system for an initial condition $(0, y_0, t_0) \in \tilde{\Sigma}^+$. Given $(0, y_0, t_0) \in \tilde{\Sigma}^-$, one defines similarly this solution by just properly shifting the subscripts of t_ε^i in (5.2.23). In addition, it is possible to extend precisely this definition to an arbitrarily initial condition (x_0, y_0, t_0) .

As is usual when dealing with Hamiltonian systems, we will use the unperturbed Hamiltonian to measure the distance between states. In addition, as we are dealing with a perturbation problem, we will frequently use expansions in powers of ε . In this case, the integral of the Poisson brackets of the Hamiltonians H_1 and H_0 typically provides a compact expression for the linear terms in ε . Given $m \geq 1$, $(0, y_0, t_0) \in \tilde{\Sigma}^+$ and its impact sequence $(0, y_{\varepsilon,r}^i, t_{\varepsilon,r}^i)$, $0 \leq i \leq 2m$, for the piecewise-smooth system (5.2.2),(5.2.18) when $r \leq 1$, we introduce

$$\begin{aligned} & \int_{t_0}^{t_{\varepsilon,r}^{2m}} \{H_0, H_1\} (\phi(t; t_0, 0, y_0, \varepsilon, r), t) dt \\ & := \sum_{i=0}^{m-1} \left(\int_{t_{\varepsilon,r}^{2i}}^{t_{\varepsilon,r}^{2i+1}} \{H_0^+, H_1^+\} (\phi^+(t; t_{\varepsilon,r}^{2i}, 0, y_{\varepsilon,r}^{2i}, \varepsilon), t) dt \right. \\ & \quad \left. + \int_{t_{\varepsilon,r}^{2i+1}}^{t_{\varepsilon,r}^{2i+2}} \{H_0^-, H_1^-\} (\phi^-(t; t_{\varepsilon,r}^{2i+1}, 0, y_{\varepsilon,r}^{2i+1}, \varepsilon), t) dt \right) \end{aligned} \quad (5.2.24)$$

where $\{Q(x, y), R(x, y)\} = \frac{\partial Q}{\partial x} \frac{\partial R}{\partial y} - \frac{\partial Q}{\partial y} \frac{\partial R}{\partial x}$ is the canonical Poisson bracket of the Hamiltonians Q and R .

The next Lemma provides an expression for $H_0(\phi(t_{\varepsilon,r}^{2m}; t_0, 0, y_0, \varepsilon, r))$, which we will use below.

Lemma 5.2.1. *Let $m \geq 1$ and $(0, y_0, t_0) \in \tilde{\Sigma}^+$, and let $(0, y_{\varepsilon,r}^i, t_{\varepsilon,r}^i)$, $i = 0, \dots, 2m$, be its associated impact sequence as defined in (5.2.21). Then,*

$$\begin{aligned} H_0(0, y_{\varepsilon,r}^{2m}) - H_0(0, y_0) &= r^2 \left[\varepsilon \int_{t_0}^{t_{\varepsilon,r}^{2m}} \{H_0, H_1\} (\phi(t; t_0, 0, y_0, \varepsilon, r), t) dt \right. \\ & \quad \left. + \sum_{i=0}^{2m-1} \left(H_0(0, y_{\varepsilon,r}^i) - H_0\left(0, \frac{y_{\varepsilon,r}^i}{r}\right) \right) \right]. \end{aligned} \quad (5.2.25)$$

Proof. The proof of this Lemma comes from a straightforward application of the fundamental theorem of calculus to the smooth functions $H_0^\pm(\phi^\pm(t; t_0, 0, \pm y_0, \varepsilon))$, using the

fact that

$$\begin{aligned} H_0(0, y_{\varepsilon, r}^{2m}) &= H_0(r\phi(t_{\varepsilon, r}^{2m}; t_0, 0, y_0, \varepsilon, r)) \\ &= r^2 H_0(\phi(t_{\varepsilon, r}^{2m}; t_0, 0, y_0, \varepsilon, r)), \end{aligned}$$

taking into account the intermediate gaps induced by the impact condition (5.2.18) and that

$$\frac{d}{dt} H_0^\pm(\phi^\pm(t; t^*, x^*, y^*, \varepsilon)) = \varepsilon \{H_0^\pm, H_1^\pm\}(\phi^\pm(t; t^*, x^*, y^*, \varepsilon))$$

for any $(x^*, y^*) \in S^\pm \cup \Sigma^\pm$ and $t \geq t^*$ such that $\phi^\pm(t; t^*, x^*, y^*, \varepsilon) \in S^\pm$. \square

The following Lemma gives us an expression for the expansion in powers of ε of $H_0(0, y_{\varepsilon, r}^{2m}) - H_0(0, y_0)$, which we will use in §5.3.

Lemma 5.2.2. *Let $m \geq 1$ and $(0, y_0, t_0) \in \tilde{\Sigma}^+$, and let $(0, y_{\varepsilon, r}^i, t_{\varepsilon, r}^i)$, $i = 0, \dots, 2m$, be its associated impact sequence as defined in (5.2.21). Then, if $\varepsilon \simeq 0$, the Taylor expansion of expression (5.2.25) becomes*

$$\begin{aligned} H_0(0, y_{\varepsilon, r}^{2m}) - H_0(0, y_0) &= \frac{y_0^2}{2}(r^{4m} - 1) + \varepsilon G^m(y_0, t_0) \\ &\quad + O(\varepsilon^2) + O(\varepsilon(r - 1)) \end{aligned} \quad (5.2.26)$$

where

$$G^m(y_0, t_0) = \int_0^{m\alpha(y_0)} \{H_0, H_1\}(\phi(t; 0, 0, y_0, 0), t + t_0) dt \quad (5.2.27)$$

and $\alpha(y_0)$ is given in (5.2.16).

Proof. The zero order term in ε of the expansion is found by noting that, if $\varepsilon = 0$, from expression (5.2.22), one has $H_0(0, y_{0, r}^i) = H_0(0, \frac{y_0^{i+1}}{r})$. Hence all the terms in the sum of Eq. (5.2.25) cancel each other except for the first and the last one. This, in combination with the fact that $H_0(0, y) = \frac{y^2}{2}$, gives the first term in Eq. (5.2.26). For the linear term in ε , one first obtains

$$\begin{aligned} &r^2 \left[\int_{t_0}^{t_{\varepsilon, r}^{2m}} \{H_0, H_1\}(\phi(t; t_0, 0, y_0, 0, r), t) dt \right. \\ &\quad \left. + (r^2 - 1) \sum_{i=1}^{2m-1} \left(\frac{d}{d\varepsilon} (H_0((y_{\varepsilon, r}^i, t_{\varepsilon, r}^i))) \Big|_{\varepsilon=0} \right) \right]. \end{aligned}$$

Then, by applying Eq. (5.2.20) m times, one has that $t_{\varepsilon, 1}^{2m} = t_0 + m\alpha(y_0) + O(\varepsilon)$. Thus, by expanding this for r near 1 and ε near 0 and noting that the unperturbed flow is autonomous and hence $\phi(t; t_0, 0, y_0, 0) = \phi(t - t_0; 0, 0, y_0, 0)$, one gets expression (5.2.27). \square

Remark 5.2.1. *If in Eq. (5.2.27) we take $\alpha(y_0) = \frac{nT}{m}$, then we recover the classical Melnikov function for the subharmonic orbits [GH83] with the modified integral (5.2.24).*

5.3 Existence of subharmonic orbits

5.3.1 Conservative case, $r = 1$: Melnikov method for subharmonic orbits

Let us consider system (5.2.2) neglecting the loss of energy at impact ($r = 1$ in Eq. (5.2.18)). According to C.1–C.5, for $\varepsilon = 0$, this system possesses a continuum of periodic orbits, Λ_c in Eq. (5.2.7), surrounding the origin. Our main goal in this section is to investigate the persistence of these orbits when the (periodic) non-autonomous perturbation is considered ($\varepsilon > 0$). The classical Melnikov method for subharmonic orbits, which here, in principle, does not apply, provides sufficient conditions for the persistence of periodic orbits for a smooth system with an equivalent, smooth, unperturbed phase portrait.

The period of the orbits Λ_c tends to infinity as they approach the heteroclinic orbit. More precisely, if $q_c(t)$ is the periodic orbit satisfying $q_c(0) = (0, y_0)$ with $H_0(0, y_0) = c$, its period $\alpha(y_0)$ tends to infinity as $c \rightarrow c_1$ (see formula (5.2.16)). As we are interested in finding periodic orbits for $0 < \varepsilon \ll 1$, we will use the unperturbed periodic solutions as ε -close approximations to them. In general, such perturbation results are valid only for finite time and therefore, from now on, we will restrict ourselves to a set of the form

$$\tilde{\Sigma}_{\tilde{c}}^+ = \left\{ (0, y, t) \in \tilde{\Sigma}^+ \mid 0 \leq y \leq \tilde{c} \right\}, \quad (5.3.1)$$

for a fixed \tilde{c} satisfying $0 \leq \tilde{c} < \sqrt{2c_1}$. Note that, if $(0, y_0, t_0) \in \tilde{\Sigma}_{\tilde{c}}^+$ then $\alpha(y_0)$ is uniformly bounded ($\alpha(y_0) < \alpha(\tilde{c})$). However, following [GH83], it is also possible to extend the method for all the periodic orbits up to the heteroclinic connection.

To look for periodic orbits we will use the impact map defined in (5.2.14). In terms of this map, a point in $U \subset \tilde{\Sigma}^+$ will lead to a periodic orbit of period nT if it is a solution of the equation

$$P_\varepsilon^m(y_0, t_0) = (y_0, t_0 + nT), \quad (5.3.2)$$

for some m . We take m to be the smallest integer such that (5.3.2) is satisfied. In that case, $\phi(t; t_0, 0, y_0, \varepsilon)$ will be a periodic orbit of period nT , which crosses the switching manifold Σ exactly $2m$ times. We will call this an (n, m) -periodic orbit. Then for (n, m) -periodic orbits with $\varepsilon > 0$ we have the following result analogous to the smooth case

Theorem 5.3.1. *Consider a system as defined in (5.2.2) satisfying C.1–C.5, and let $\alpha(y_0)$ be the function defined in (5.2.15)–(5.2.16). Assume that the point $(0, \bar{y}_0, \bar{t}_0) \in \tilde{\Sigma}_{\tilde{c}}^+$ satisfies*

H.1 $\alpha(\bar{y}_0) = \frac{n}{m}T$, with $n, m \in \mathbb{Z}$ relatively prime

H.2 $\bar{t}_0 \in [0, T]$ is a simple zero of

$$M^{n,m}(t_0) = \int_0^{nT} \{H_0, H_1\}(q_c(t), t + t_0) dt, \quad c = H_0(0, \bar{y}_0), \quad (5.3.3)$$

where $q_c(t) = \phi(t; 0, 0, \bar{y}_0)$ is the periodic orbit such that $\alpha(\bar{y}_0) = \frac{nT}{m}$.

Then, there exists ε_0 such that, for every $0 < \varepsilon < \varepsilon_0$, one can find y_0^* and t_0^* such that $\phi(t; t_0^*, 0, y_0^*, \varepsilon)$ is an (n, m) -periodic orbit.

Proof. The proof of the result comes from a straightforward application of the implicit function theorem to equation (5.3.2). Let us fix n and m relatively prime. We replace equation (5.3.2) by

$$\begin{pmatrix} H_0(0, \Pi_{y_0}(P_\varepsilon^m(y_0, t_0))) \\ \Pi_{t_0}(P_\varepsilon^m(y_0, t_0)) \end{pmatrix} - \begin{pmatrix} H_0(0, y_0) \\ t_0 + nT \end{pmatrix} = \begin{pmatrix} 0 \\ 0 \end{pmatrix}. \quad (5.3.4)$$

That is, we use the Hamiltonian H_0 to measure the distance between the points $(0, \Pi_{y_0}(P_\varepsilon^m(y_0, t_0)))$ and $(0, y_0)$.

Using the second equation in (5.3.4) we have

$$\begin{aligned} \Pi_{y_0}(P_\varepsilon^m(y_0, t_0)) &= \Pi_y(\phi(t_0 + nT; t_0, 0, y_0, \varepsilon)) \\ 0 &= \Pi_x(\phi(t_0 + nT; t_0, 0, y_0, \varepsilon)). \end{aligned}$$

This allows us to rewrite Eq. (5.3.4) as

$$\begin{pmatrix} H_0(\phi(t_0 + nT; t_0, 0, y_0, \varepsilon)) - H_0(0, y_0) \\ \Pi_{t_0}(P_\varepsilon^m(y_0, t_0)) - nT - t_0 \end{pmatrix} = \begin{pmatrix} 0 \\ 0 \end{pmatrix}. \quad (5.3.5)$$

We expand Eq. (5.3.5) in powers of ε . Using Eq. (5.2.17), the second component of (5.3.5) becomes

$$\Pi_{t_0}(P_\varepsilon^m(y_0, t_0)) - t_0 - nT = m\alpha(y_0) - nT + O(\varepsilon) = 0, \quad (5.3.6)$$

where $\alpha(y_0)$ is the period of the periodic orbit $q_c(t)$, $c = H_0(0, y_0)$, given in Eq. (5.2.16). On the other hand, using Lemma 5.2.2 and noting that

$$\Pi_{y_0}(P_\varepsilon^m(y_0, t_0)) = y_{\varepsilon,1}^{2m},$$

the first equation in (5.3.5) can be written as

$$\begin{aligned} &H_0(0, \Pi_{y_0}(P_\varepsilon^m(y_0, t_0))) - H_0(0, y_0) \\ &= \varepsilon \int_0^{m\alpha(y_0)} \{H_0, H_1\}(\phi(t; 0, 0, y_0, 0), t + t_0) dt + O(\varepsilon^2) \\ &= \varepsilon G^m(y_0, t_0) + O(\varepsilon^2). \end{aligned}$$

where $G^m(y_0, t_0)$ is given in (5.2.27). Hence, Eq. (5.3.5) finally becomes

$$F_{n,m}(y_0, t_0, \varepsilon) := \begin{pmatrix} G^m(y_0, t_0) + O(\varepsilon) \\ m\alpha(y_0) - nT + O(\varepsilon) \end{pmatrix} = \begin{pmatrix} 0 \\ 0 \end{pmatrix}, \quad (5.3.7)$$

where the order in ε of the first component has been reduced and, thus, the implicit function theorem can be applied to Eq. (5.3.7). Therefore, one needs

$$\text{S.1 } F_{n,m}(\bar{y}_0, \bar{t}_0, 0) = (0, 0)^T$$

$$\text{S.2 } \det(D_{y_0, t_0} F(\bar{y}_0, \bar{t}_0, 0)) \neq 0, \text{ where } D_{y_0, t_0} \equiv D \text{ is the Jacobian with respect to the variables } y_0 \text{ and } t_0.$$

The first condition is satisfied by noting in Eq. (5.3.7) that \bar{y}_0 has to be such that $\alpha(\bar{y}_0) = \frac{nT}{m}$ and \bar{t}_0 a zero of the subharmonic Melnikov function

$$M^{n,m}(t_0) := G^m(\bar{y}_0, t_0) = \int_0^{nT} \{H_0, H_1\}(q_c(t), t + t_0) dt,$$

where $q_c(t)$, $c = H_0(0, \bar{y}_0)$, is the unperturbed periodic orbit of period $\frac{nT}{m}$ such that $q_c(0) = (0, y_0)$, and therefore $q_c(t) = \phi(t; 0, 0, \bar{y}_0, 0)$.

In addition, for $\varepsilon = 0$, $DF_{n,m}$ is given by

$$DF_{n,m}(y_0, t_0, 0) = \begin{pmatrix} \frac{\partial G^m}{\partial y_0} & \frac{\partial G^m}{\partial t_0} \\ m\alpha'(y_0) & 0 \end{pmatrix}.$$

By C.5, $\alpha'(y_0) \neq 0$, and the second condition is satisfied if \bar{t}_0 is a simple zero of the subharmonic Melnikov function, $M^{n,m}(t_0)$, which completes hypothesis *H.2*.

Finally, applying the implicit function theorem to (5.3.7) at $(y_0, t_0, \varepsilon) = (\bar{y}_0, \bar{t}_0, 0)$, there exists $\varepsilon_0 > 0$ such that, if $0 < \varepsilon < \varepsilon_0$, then there exist unique $y_0^*(\varepsilon)$ and $t_0^*(\varepsilon)$ solutions of the equation (5.3.4), which have the form

$$\begin{aligned} y_0^* &= \bar{y}_0 + O(\varepsilon) \\ t_0^* &= \bar{t}_0 + O(\varepsilon). \end{aligned}$$

Hence, the orbit $\phi(t; t_0^*, 0, y_0^*, \varepsilon)$ is an (n, m) -periodic orbit, as it has period nT and impacts $2m$ times with the switching manifold Σ in every period. \square

Remark 5.3.1. *The upper bound ε_0 given in the theorem depends on n and m . However, for every fixed m , it is possible to obtain $\varepsilon_0(m)$, such that for $\varepsilon < \varepsilon_0(m)$, we can apply the theorem for all n such that $\alpha^{-1}(\frac{nT}{m}) \in \tilde{\Sigma}_\varepsilon^+$. This is because the approximation of the perturbed flow by the unperturbed periodic orbit is performed m times beyond the period of the unperturbed periodic orbit.*

Remark 5.3.2. *The proof of the result provides us with a constructive method to find the initial condition for nT -periodic orbits for $\varepsilon > 0$.*

S.1 Given n and m , find \bar{y}_0 such that $\alpha(\bar{y}_0) = \frac{n}{m}T$ using Eq. (5.2.16).

S.2 Find \bar{t}_0 such that $M^{n,m}(t_0)$ has a simple zero at $t_0 = \bar{t}_0$.

S.3 Use (\bar{y}_0, \bar{t}_0) as seed to solve Eq. (5.3.4) numerically.

Lemma 5.3.1. *The subharmonic Melnikov function (5.3.3) is either identically zero or generically possesses at least one simple zero.*

Proof. The proof comes from the fact that $M^{n,m}(t_0)$ has average

$$\langle M^{n,m}(t_0) \rangle = \frac{1}{T} \int_0^T M^{n,m}(t_0) dt_0$$

equal to zero.

$$\begin{aligned} \langle M^{n,m}(t_0) \rangle &= \frac{1}{T} \int_0^T \int_0^{nT} \{H_0, H_1\}(q_c(t), t + t_0) dt dt_0 \\ &= \frac{1}{T} \int_0^{nT} \int_0^T \{H_0, H_1\}(q_c(t), t + t_0) dt_0 dt \\ &= \int_0^{nT} \{H_0, \langle H_1 \rangle\}(q_c(t)) dt. \end{aligned}$$

Recalling that $\alpha(y_0) = \frac{nT}{m}$ (see (5.2.15)-(5.2.16)) and letting

$$\begin{aligned} q_c^+(t) &= \phi^+(t; 0, 0, y_0, 0) \\ q_c^-(t) &= \phi^-(t; \alpha^+(y_0), 0, -y_0, 0), \end{aligned}$$

$\langle M^{n,m}(t_0) \rangle$ can be written as

$$\begin{aligned} & m \left(\int_0^{\alpha^+(y_0)} \{H_0^+, \langle H_1^+ \rangle\}(q_c^+(t)) dt + \int_{\alpha^+(y_0)}^{\frac{nT}{m}} \{H_0^-, \langle H_1^- \rangle\}(q_c^-(t)) dt \right) \\ &= -m \left(\int_0^{\alpha^+(y_0)} \frac{d}{dt} (\langle H_1^+ \rangle(q_c^+(t))) dt + \int_{\alpha^+(y_0)}^{\frac{nT}{m}} \frac{d}{dt} (\langle H_1^- \rangle(q_c^-(t))) dt \right) \\ &= -m \left(\langle H_1^+ \rangle(q_c^+(\alpha^+(y_0))) - \langle H_1^+ \rangle(q_c^+(0)) \right. \\ &\quad \left. + \langle H_1^- \rangle(q_c^-(\frac{nT}{m})) - \langle H_1^- \rangle(q_c^-(\alpha^+(y_0))) \right) = 0. \end{aligned}$$

□

Note that, if $M^{n,m}(t_0) \equiv 0$ then a second order analysis is required to study the existence of periodic orbits.

5.3.2 Dissipative case, $r < 1$

We now focus on the situation when the coefficient of restitution r introduced in §5.2.3 is considered. As already mentioned, for $\varepsilon = 0$ the origin is a global attractor and hence none of the periodic orbits studied in the previous section exists if the amplitude of the perturbation is small enough. However, as was shown in [Hog89] for the rocking block model, for ε large enough an infinite number periodic orbits surrounding the origin can exist. This was studied analytically and numerically for the rocking block model under symmetry assumptions for the particular case $m = 1$. Here, our goal is to relate the periodic orbits existing for the dissipative case to those which exist for $r = 1$ in the general system (5.2.2),(5.2.18). As will be shown below, all the periodic orbits given by Theorem 5.3.1 can also exist for the dissipative case, when $r < 1$ is small enough compared with $\varepsilon > 0$. In other words, we generalise in this section the result presented for the conservative case.

As in §5.3.1, in order to obtain the initial conditions of a (n, m) -periodic orbit for $r < 1$, one has to solve the equation

$$\tilde{P}_{\varepsilon, r}^m(y_0, t_0) = (y_0, t_0 + nT), \quad (5.3.8)$$

where $\tilde{P}_{\varepsilon, r}$, is defined in Eq. (5.2.19). The next result states that, under certain conditions regarding r and ε , Eq. (5.3.8) can be solved.

Theorem 5.3.2. *Consider system (5.2.2),(5.2.18). Let $(0, \bar{y}_0, \bar{t}_0) \in \tilde{\Sigma}^+$ be such that $\alpha(\bar{y}_0) = \frac{nT}{m}$, with n and m relatively prime, and \bar{t}_0 a simple zero of the subharmonic Melnikov function (5.3.3). There exists ρ such that, given $\tilde{\varepsilon}, \tilde{r} > 0$ satisfying $0 < \frac{\tilde{r}}{\tilde{\varepsilon}} < \rho$, there exists δ_0 such that, if $\varepsilon = \tilde{\varepsilon}\delta$ and $r = 1 - \tilde{r}\delta$, then $\forall 0 < \delta < \delta_0$ there exists (y_0^*, t_0^*) which is a solution of Eq. (5.3.8). Moreover, $y_0^* = \bar{y}_0 + O(\delta)$, $t_0^* = \bar{t}_0 + O(\delta) + O(\tilde{r}/\tilde{\varepsilon})$ and the solution (y_0^*, t_0^*) tends to the one given in Theorem 5.3.1 as $r \rightarrow 1^-$.*

Proof. As in the conservative case, we use the unperturbed Hamiltonian to measure the distance between points in Σ . Then, Eq. (5.3.8) can be rewritten as

$$\begin{pmatrix} H_0\left(0, \Pi_{y_0}(\tilde{P}_{\varepsilon}^m(y_0, t_0))\right) \\ \Pi_{t_0}(\tilde{P}_{\varepsilon}^m(y_0, t_0)) \end{pmatrix} - \begin{pmatrix} H_0(0, y_0) \\ t_0 + nT \end{pmatrix} = \begin{pmatrix} 0 \\ 0 \end{pmatrix}. \quad (5.3.9)$$

As in Theorem 5.3.1, we proceed by expanding this equation in powers of ε and $r - 1$ using (5.2.26) and (5.2.27) obtaining

$$\begin{pmatrix} \frac{y_0^2}{2}(r^{4m} - 1) + \varepsilon G^m(y_0, t_0) + O(\varepsilon^2) + O(\varepsilon(r - 1)) \\ \sum_{i=0}^{m-1} \alpha^+(r^{2i} y_0) + \sum_{i=0}^{m-1} \alpha^-(-r^{2i+1} y_0) + O(\varepsilon) - nT \end{pmatrix} = \begin{pmatrix} 0 \\ 0 \end{pmatrix}. \quad (5.3.10)$$

Note that, for $r = 1$, Eq. (5.3.10) becomes Eq. (5.3.5).

We are interested in studying Eq. (5.3.10) when $1 - r$ and ε are both small. Therefore, for $\tilde{\varepsilon} > 0$ and $\tilde{r} > 0$ we set

$$\varepsilon = \tilde{\varepsilon}\delta, \quad r = 1 - \tilde{r}\delta, \quad (5.3.11)$$

where $\delta > 0$ is a small parameter. Then Eq. (5.3.10) becomes

$$\begin{aligned} \tilde{F}_{n,m}(y_0, t_0, \delta) := \\ \begin{pmatrix} -2m\tilde{r}y_0^2 + \tilde{\varepsilon}G^m(y_0, t_0) + O(\delta) \\ m\alpha(y_0) + O(\delta) - nT \end{pmatrix} = \begin{pmatrix} 0 \\ 0 \end{pmatrix}. \end{aligned} \quad (5.3.12)$$

We now need to apply the implicit function theorem to (5.3.12).

The first step is to solve Eq. (5.3.12) for $\delta = 0$. The second equation gives $\alpha(\bar{y}_0) = \frac{nT}{m}$, as in Theorem 5.3.1. To solve the first equation, we define

$$f^{n,m}(t_0) = -2m\tilde{r}\bar{y}_0^2 + \tilde{\varepsilon}M^{n,m}(t_0), \quad (5.3.13)$$

and \hat{t}_0 will be given by a zero of $f^{n,m}(t_0)$. Assume now that \bar{t}_0 is a simple zero of $M^{n,m}(t_0)$. As $M^{n,m}(t_0)$ is a smooth periodic function, it possesses at least one local maximum. Let t_M be the closest value to \bar{t}_0 where $M^{n,m}(t_0)$ possesses a local maximum, and assume $(M^{n,m})'(t_0) \neq 0$ for all t_0 between \bar{t}_0 and t_M . If $(M^{n,m})'(t_0)$ vanishes between \bar{t}_0 and t_M , we then take t_M to be the closest value to \bar{t}_0 such that $(M^{n,m})'(t_0) = 0$ to ensure that $(M^{n,m})'(t_0) \neq 0$ between \bar{t}_0 and t_M . We then define $\rho := \frac{M^{n,m}(t_M)}{2m\bar{y}_0^2}$. Then, if

$$0 < \frac{\tilde{r}}{\tilde{\varepsilon}} < \rho, \quad (5.3.14)$$

there exists \hat{t}_0 $\frac{\tilde{r}}{\tilde{\varepsilon}}$ -close to \bar{t}_0 where $f^{n,m}(t_0)$ has a simple zero. Since $\alpha'(\bar{y}_0) > 0$, a similar calculation to the one in Theorem 5.3.1 shows that

$$\det \left(D\tilde{F}_{y_0, t_0}(\bar{y}_0, \hat{t}_0, 0) \right) \neq 0,$$

and hence we can apply the implicit function theorem near $(y_0, t_0, \delta) = (\bar{y}_0, \hat{t}_0, 0)$ to show that there exists δ_0 such that, if $0 < \delta < \delta_0$, then there exists

$$(y_0^*, t_0^*) = (\bar{y}_0, \hat{t}_0) + O(\delta) = (\bar{y}_0, \bar{t}_0) + O(\delta) + O(\tilde{r}/\tilde{\varepsilon})$$

which is a solution of Eq. (5.3.8).

This solution tends to the one given by Theorem 5.3.1 when $\tilde{r} \rightarrow 0^+$. This is a natural consequence of the fact that $\tilde{P}_{\varepsilon, r}^m$ uniformly tends to P_ε^m as $r \rightarrow 1^-$. \square

Remark 5.3.3. *In order to determine ρ in (5.3.14), we have imposed t_M to be the local maximum of the Melnikov function closest to its simple zero, \bar{t}_0 . Instead, one could also use the absolute maximum so increasing the range given in Eq. (5.3.14). However, in this case, the values where $(M_1^{n,m})'(t_0) = 0$ have to be avoided to ensure that the desired zero of $f^{n,m}(t_0)$ is simple.*

Remark 5.3.4. *Arguing as in Remark 5.3.1, for every m fixed, the constant $\delta_0(m)$ can be taken such that if $\delta < \delta_0(m)$, there exist periodic orbits for all n such that $\alpha(\frac{nT}{m})^{-1} \in \tilde{\Sigma}$.*

5.4 Intersection of the separatrices

We now focus our attention on the invariant manifolds of the saddle points of system (5.2.2),(5.2.18) when $\varepsilon > 0$. As explained in §5.2, for $\varepsilon = 0$, there exist two heteroclinic orbits connecting the critical points z^\pm if $r = 1$ (see Fig. 5.1) whereas, if $r < 1$, the unstable manifolds $W^u(z^\pm)$ spiral discontinuously from z^\pm to the origin and $W^s(z^\pm)$ becomes unbounded (see Fig. 5.3). As we will show, in both cases, heteroclinic orbits may exist for the perturbed system.

For a smooth system with Hamiltonian $K_0(x, y) + \varepsilon K_1(x, y, t)$, the persistence of homoclinic or heteroclinic connections is achieved by the well known Melnikov method which states that if the Melnikov function

$$M(t_0) = \int_{-\infty}^{+\infty} \{K_0, K_1\}(\phi(t; t_0, z_0, 0), t + t_0) dt,$$

with $z_0 = (x_0, y_0) \in W^u(z^-) = W^s(z^+)$, has a simple zero, then the stable and unstable manifolds intersect for $\varepsilon > 0$ small enough (see [GH83]).

In this section we will modify the classical Melnikov method and we will rigorously prove that it is still valid for a piecewise-smooth system of the form (5.2.2), even if $r \leq 1$.

There exist in the literature several works where this tool has been used in particular piecewise-smooth examples, [Hog92, BK91]. Theorem 5.4.1 generalises the result stated in [BK91] where the Melnikov method is shown to work, although the proof there is not complete.

The homoclinic version of a piecewise-defined system with a different topology was studied in [Kun00, Kuk07, BF08, DZ05, XFR09]. However, as noted in the Introduction, the tools developed there do not apply for a system of the type (5.2.2).

We begin by discussing the persistence of objects for $\varepsilon > 0$ and $r \leq 1$. It is clear that by separately extending the systems $\mathcal{X}_0^\pm + \varepsilon \mathcal{X}_1^\pm$ to $\mathbb{R}^2 \times \mathbb{T}$, where $\mathbb{T} = \mathbb{R}/T$, we get two smooth systems for which the classical perturbation theory holds. It follows then that, as z^\pm are hyperbolic fixed points, for $\varepsilon > 0$ small enough there exist two hyperbolic T -periodic orbits, $\Lambda_\varepsilon^\pm \equiv \{z_\varepsilon^\pm(\tau); \tau \in [0, T]\}$, with two-dimensional stable and unstable manifolds $W^{s,u}(\Lambda_\varepsilon^\pm)$.

As the system is non-autonomous, we fix the Poincaré section

$$\Theta_{t_0} = \{(x, y, t_0), (x, y) \in \mathbb{R}^2\},$$

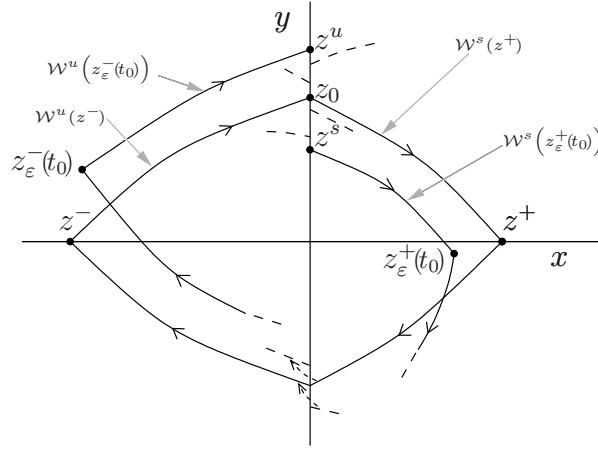


Figure 5.6: Section of the unperturbed and perturbed invariant manifolds for $t = t_0$.

and consider the time T stroboscopic map

$$\Pi_{t_0} : \Theta_{t_0} \longrightarrow \Theta_{t_0+T},$$

where

$$\Pi_{t_0}(z) = \phi(t_0 + T; t_0, z, \varepsilon, r)$$

and ϕ is defined §5.2.4.

This map has $z_\varepsilon^\pm(t_0)$ as hyperbolic fixed points with one dimensional stable and unstable manifolds (curves) $W^{s,u}(z_\varepsilon^\pm(t_0))$ (see Fig. 5.3). Proceeding as in [BK91], we fix the section Σ defined in (5.2.1) and study its intersection with the stable and unstable manifolds $W^u(z_\varepsilon^-(t_0))$ and $W^s(z_\varepsilon^+(t_0))$. In the unperturbed conservative case ($\varepsilon = 0$ and $r = 1$), $W^u(z^-)$ and $W^s(z^+)$ intersect transversally Σ in a point z_0 . The perturbed manifolds, $W^u(z_\varepsilon^-(t_0))$ and $W^s(z_\varepsilon^+(t_0))$, intersect Σ at points $z^u(t_0)$ and $z^s(t_0)$ respectively, ε -close to z_0 (see Fig. 5.6). Recalling the effect of the coefficient of restitution (5.2.18) explained in §5.2.3, both invariant manifolds will intersect if, for some t_0 , one has $rz^u(t_0) = z^s(t_0)$, $r \leq 1$. As in [BK91] and [Hog92], we use the unperturbed Hamiltonian $H_0(x, y)$ to measure the distance $\Delta(t_0, \varepsilon, r)$ between z^u and z^s

$$\Delta(t_0, \varepsilon, r) = H_0(rz^u(t_0)) - H_0(z^s(t_0)) = r^2 H_0(z^u(t_0)) - H_0(z^s(t_0)). \quad (5.4.1)$$

We then have the following result.

Theorem 5.4.1. *Consider system (5.2.2), (5.2.18), and let $z_0 = W^s(z^+) \cap \Sigma$. Define the Melnikov function*

$$M(t_0) = \int_{-\infty}^{+\infty} \{H_0, H_1\}(\phi(t; t_0, z_0, 0), t) dt, \quad (5.4.2)$$

where

$$\phi(t; t_0, z_0, 0) = \begin{cases} \phi^-(t; t_0, z_0, 0) & \text{if } t \leq t_0 \\ \phi^+(t; t_0, z_0, 0) & \text{if } t > t_0 \end{cases} \quad (5.4.3)$$

is the piecewise-smooth heteroclinic orbit that exists for $r = 1$ and $\varepsilon = 0$. Assume that $M(t_0)$ possesses a simple zero at \bar{t}_0 . Then the following holds.

- a) If $r = 1$, there exists $\varepsilon_0 > 0$ such that, for every $0 < \varepsilon < \varepsilon_0$, one can find a simple zero $t_0^* = \bar{t}_0 + O(\varepsilon)$ of the function $\Delta(t_0, \varepsilon, 1)$. Hence, the curves $W^u(z_\varepsilon^-(t_0^*))$ and $W^s(z_\varepsilon^+(t_0^*))$ intersect transversally at some point, $z_h \in \Sigma$, ε -close to $z_0 \in \Sigma$, and

$$\{\phi(t; t_0^*, z_h, \varepsilon), t \in \mathbb{R}\}$$

is a heteroclinic orbit between the periodic orbits Λ_ε^- and Λ_ε^+ .

- b) If $r < 1$, there exists ρ such that, given $\tilde{\varepsilon}, \tilde{r} > 0$ satisfying $0 < \frac{\tilde{r}}{\tilde{\varepsilon}} < \rho$, one can find δ_0 such that, if $\varepsilon = \tilde{\varepsilon}\delta$ and $r = 1 - \tilde{r}\delta$, then, for $0 < \delta < \delta_0$, there exists a simple zero of the function $\Delta(t_0, \tilde{\varepsilon}\delta, 1 - \tilde{r}\delta)$ of the form $t_0^* = \bar{t}_0 + O(\frac{\tilde{r}}{\tilde{\varepsilon}}) + O(\delta)$. Hence, the curves $W^u(z_\varepsilon^-(t_0^*))$ and $W^s(z_\varepsilon^+(t_0^*))$ intersect Σ transversally at two points, $z_h^\pm \in \Sigma$, satisfying $z_h^+ = z_0 + O(\delta)$ and $z_h^- = z_h^+/r$, such that

$$\{\phi(t; t_0^*, z_h^\pm, \tilde{\varepsilon}\delta, 1 - \tilde{r}\delta), t \in \mathbb{R}\}$$

is a heteroclinic orbit between the periodic orbits Λ_ε^- and Λ_ε^+ .

Remark 5.4.1. Note that, for $r = 1$, we recover the classical result given by the Melnikov method for heteroclinic orbits extended to the piecewise-smooth system (5.2.2).

Proof. Applying the fundamental theorem of calculus to the functions

$$s \longmapsto H_0^{+/-}(\phi^{+/-}(s; t_0, z^{s/u}, \varepsilon)),$$

we obtain

$$H_0^{+/-}(z^{s/u}) = H_0^\pm(\phi(T^{s/u}; t_0, z^{s/u}, \varepsilon) + \int_{T^{s/u}}^{t_0} \frac{d}{ds} H_0^{+/-}(\phi^{+/-}(s; t_0, z^{s/u}, \varepsilon) ds),$$

and then make $T^{s/u} = +/-\infty$. However, the limits

$$\lim_{t \rightarrow +/-\infty} \phi^{+/-}(t; t_0, z^{s/u}, \varepsilon)$$

do not exist because the flow at the respective stable/unstable manifolds tends to the periodic orbit Λ_ε^\pm . To avoid this limit, we proceed as follows.

Given t_0 , we define

$$\begin{aligned} f_-(s) &= H_0^-(\phi^-(s; t_0, z^u, \varepsilon)) - H_0^-(\phi^-(s; t_0, z_\varepsilon^-(t_0), \varepsilon)), \quad s \leq t_0 \\ f_+(s) &= H_0^+(\phi^+(s; t_0, z^s, \varepsilon)) - H_0^+(\phi^+(s; t_0, z_\varepsilon^+(t_0), \varepsilon)), \quad s \geq t_0, \end{aligned} \quad (5.4.4)$$

which are well defined smooth functions because the flow is restricted to the stable and unstable invariant manifolds or to the hyperbolic periodic orbit and never crosses the switching manifold Σ .

Then, we write Eq. (5.4.1) as

$$\Delta(t_0, \varepsilon, r) = r^2 f_-(t_0) - f_+(t_0) + r^2 H_0^-(z_\varepsilon^-(t_0)) - H_0^+(z_\varepsilon^+(t_0)). \quad (5.4.5)$$

Noting that

$$H_0^\pm(z_\varepsilon^\pm(t_0)) = \underbrace{H_0^\pm(z^\pm)}_{c_1} + \varepsilon \underbrace{DH_0^\pm(z^\pm)}_0 \frac{\partial z_\varepsilon^\pm(t_0)}{\partial \varepsilon} \Big|_{\varepsilon=0} + O(\varepsilon^2), \quad (5.4.6)$$

Eq. (5.4.5) becomes

$$\Delta(t_0, \varepsilon, r) = r^2 f_-(t_0) - f_+(t_0) + (r^2 - 1)c_1 + O(\varepsilon^2) \quad (5.4.7)$$

We apply the fundamental theorem of calculus to the functions (5.4.4) to compute

$$\begin{aligned} f_-(t_0) &= f_-(T^u) + \int_{T^u}^{t_0} f'_-(s) ds = \\ &= f_-(T^u) + \varepsilon \int_{T^u}^{t_0} \left(\{H_0^-, H_1^-\}(\phi^-(s; t_0, z^u, \varepsilon), s) \right. \\ &\quad \left. - \{H_0^-, H_1^-\}(\phi^-(s; t_0, z_\varepsilon^-(t_0), \varepsilon), s) \right) ds \\ f_+(t_0) &= f_+(T^s) - \int_{t_0}^{T^s} f'_+(s) ds = \\ &= f_+(T^s) - \varepsilon \int_{t_0}^{T^s} \left(\{H_0^+, H_1^+\}(\phi^+(s; t_0, z^s, \varepsilon), s) \right. \\ &\quad \left. - \{H_0^+, H_1^+\}(\phi^+(s; t_0, z_\varepsilon^+(t_0), \varepsilon), s) \right) ds. \end{aligned} \quad (5.4.8)$$

Due to the hyperbolicity of the periodic orbits Λ_ε^\pm , the flow on $W^{s/u}(\Lambda_\varepsilon^{+/-})$ converges exponentially to them (forwards or backwards in time). That is, there exist positive constants C , λ and s_0 such that

$$\left| \phi^+(s; t_0, z^s, \varepsilon) - \phi^+(s; t_0, z_\varepsilon^+(t_0), \varepsilon) \right| < C e^{-\lambda s}, \quad \forall s > s_0,$$

and similarly for ϕ^- . This allows one to make $T^{s/u} \rightarrow +/-\infty$ in Eqs. (5.4.8), since

$$\lim_{s \rightarrow \pm\infty} f_\pm(s) = 0$$

and, moreover, the improper integrals converge in the limit. Now, expanding the expressions in (5.4.8) in powers of ε , we find

$$\begin{aligned} f_-(t_0) &= \varepsilon \int_{-\infty}^{t_0} \{H_0^-, H_1^-\} (\phi^-(s; t_0, z_0, 0), s) ds + O(\varepsilon^2) \\ f_+(t_0) &= -\varepsilon \int_{t_0}^{\infty} \{H_0^+, H_1^+\} (\phi^+(s; t_0, z_0, 0), s) ds + O(\varepsilon^2), \end{aligned} \quad (5.4.9)$$

where we have used property (5.4.6) to include the second terms in the integrals into the higher order terms. Finally, substituting Eq. (5.4.9) into Eq. (5.4.7), we obtain

$$\Delta(t_0, \varepsilon, r) = (r^2 - 1)c_1 + \varepsilon M(t_0) + O(\varepsilon^2) + O(\varepsilon(r - 1)), \quad (5.4.10)$$

where $M(t_0)$ is defined in Eq. (5.4.2).

We now distinguish between the cases $r = 1$ and $r < 1$. If $r = 1$, we recover the classical expression for the distance between the perturbed invariant manifolds. By applying the implicit function theorem, it is easy to show that, if $M(t_0)$ has a simple zero at \bar{t}_0 , then $\Delta(t_0, \varepsilon, 1)$ has a simple zero at $t_0^* = \bar{t}_0 + O(\varepsilon)$. Thus, the curves $W^u(z_\varepsilon^-(t_0^*))$ and $W^s(z_\varepsilon^+(t_0^*))$ intersect Σ transversally at some point, $z_h = z^u(t_0^*) = z^s(t_0^*) \in \Sigma$, ε -close to $z_0 \in \Sigma$. Therefore,

$$\{\phi(t; t_0^*, z_h, \varepsilon), t \in \mathbb{R}\},$$

is a heteroclinic orbit between the periodic orbits Λ_ε^- and Λ_ε^+ .

If $r < 1$, we define $\varepsilon = \tilde{\varepsilon}\delta$ and $r = 1 - \tilde{r}\delta$, and Eq. (5.4.10) becomes

$$\frac{\Delta(t_0, \tilde{\varepsilon}\delta, 1 - \tilde{r}\delta)}{\delta} = -2\tilde{r}c_1 + \tilde{\varepsilon}M(t_0) + O(\delta). \quad (5.4.11)$$

Then we argue as in Theorem 5.3.2. As $M(t_0)$ is a smooth periodic function, it possesses at least one local maximum. Let t_M be the closest value to \bar{t}_0 where $M(t_0)$ possesses a local maximum, and assume $M'(t_0) \neq 0$ for all t_0 between \bar{t}_0 and t_M . If $M'(t_0)$ vanishes between \bar{t}_0 and t_M , we then take t_M to be the closest value to \bar{t}_0 such that $M'(t_0) = 0$ to ensure that $M'(t_0) \neq 0$ between \bar{t}_0 and t_M . We then define $\rho := \frac{M(t_M)}{2c_1}$. Then, if

$$0 < \frac{\tilde{r}}{\tilde{\varepsilon}} < \rho,$$

there exists \hat{t}_0 $\frac{\tilde{r}}{\tilde{\varepsilon}}$ -close to \bar{t}_0 such that

$$-2\tilde{r}c_1 + M(\hat{t}_0) = 0$$

and $M'(\hat{t}_0) \neq 0$. Hence, we can apply the implicit function theorem to Eq. (5.4.11) near the point $(t_0, \delta) = (\hat{t}_0, 0)$ to conclude that there exists δ_0 such that, if $0 < \delta < \delta_0$, then one can find

$$t_0^* = \hat{t}_0 + O(\delta) = \bar{t}_0 + O(\delta) + O(\tilde{r}/\tilde{\varepsilon})$$

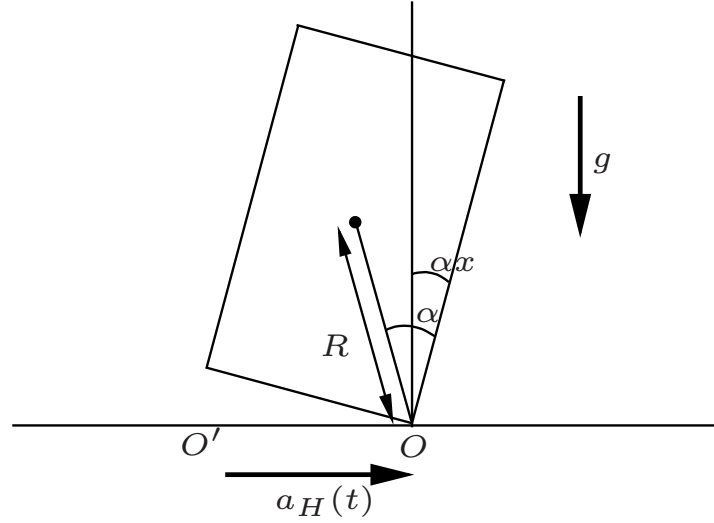


Figure 5.7: Rocking block

which is a simple solution of Eq. (5.4.11).

Hence, arguing similarly as for $r = 1$, there exist two points $z_h^+ = z^s(t_0^*) = z_0 + O(\delta)$ and $z_h^- = z^u(t_0^*) = z_0/r + O(\delta)r$ such that $z_h^+ = rz_h^-$ and

$$\{\phi(t; t_0^*, z_h^+, \tilde{\varepsilon}\delta, 1 - \tilde{r}\delta), t \in \mathbb{R}\}$$

where

$$\phi(t; t_0^*, z_h^+, \varepsilon, r) = \begin{cases} \phi^-(t; t_0, t_0^*, z_h^+/r, \varepsilon) & \text{if } t \leq t_0^* \\ \phi^+(t; t_0, t_0^*, z_h^+, \varepsilon) & \text{if } t \geq t_0^* \end{cases}$$

is a heteroclinic orbit between the periodic orbits Λ_ε^- and Λ_ε^+ . \square

5.5 Example: the rocking block

5.5.1 System equations

In order to illustrate our results, we consider the mechanical system shown in Fig. 5.7, which consists of a rocking block under a horizontal periodic forcing given by

$$a_H(t) = \varepsilon\alpha g \cos(\Omega t + \theta). \quad (5.5.1)$$

This system was first studied in [Hou63]. The fixed angle between one side of the block and the diagonal through the mass centre is denoted by α . When there is rotation, the

angular displacement from the vertical is given by αx . Then, the equations that govern the motion of the block, after a time scaling, are given by

$$\alpha \ddot{x} + \text{sign}(x) \sin(\alpha(1 - \text{sign}(x)x)) = -\alpha \varepsilon \cos(\alpha(1 - \text{sign}(x)x)) \cos(\omega t) \quad (5.5.2)$$

$$\dot{x}(t_A^+) = r \dot{x}(t_A^-) \quad (x = 0) \quad (5.5.3)$$

where $\omega = \sqrt{\frac{4R}{3g}} \Omega$ (see for example [YCP80, SK84, Hog89] for details).

The last equation, (5.5.3), simulates the loss of energy of the block at every impact with the ground, as described in §5.2.3 and the function

$$\text{sign}(x) = \begin{cases} 1 & \text{if } x > 0 \\ -1 & \text{if } x < 0 \end{cases} \quad (5.5.4)$$

distinguishes between the two modes of movement: rocking about the point O when $x > 0$ or rocking about O' when $x < 0$. Hence equations (5.5.2)–(5.5.4) are piecewise-smooth, conditions C.1–C.5 are satisfied and so results from previous sections can be applied. However, as our purpose is to compare with [Hog89], we will consider the terms linear in α of Eq. (5.5.2) instead, which will permit us to perform explicit analytical computations. This linearization is equivalent to the assumption that the block is slender [Hog89]. Thus, the system that we will consider, written in the form of Eq. (5.2.2), is

$$\left. \begin{aligned} \dot{x} &= y \\ \dot{y} &= x - 1 - \varepsilon \cos(\omega t) \end{aligned} \right\} \text{if } x > 0 \quad (5.5.5)$$

$$\left. \begin{aligned} \dot{x} &= y \\ \dot{y} &= x + 1 - \varepsilon \cos(\omega t) \end{aligned} \right\} \text{if } x < 0 \quad (5.5.6)$$

$$y(t_A^+) = r y(t_A^-) \quad (x = 0), \quad (5.5.7)$$

where the perturbation becomes a smooth function due to the linearization.

If $r = 1$, system (5.5.5)–(5.5.6) can be written in the form (5.2.5) using the Hamiltonian function

$$H_\varepsilon(x, y, t) = H_0(x, y) + \varepsilon H_1(x, t), \quad (5.5.8)$$

where

$$H_0(x, y) = \begin{cases} \frac{y^2}{2} - \frac{x^2}{2} + x, & \text{if } x > 0 \\ \frac{y^2}{2} - \frac{x^2}{2} - x, & \text{if } x < 0 \end{cases} \quad (5.5.9)$$

and

$$H_1(x, t) = x \cos(\omega t) \quad (5.5.10)$$

is a C^∞ and T -periodic function, with $T = 2\pi/\omega$.

In addition, when $\varepsilon = 0$, conditions C.1–C.5 are fulfilled, and the phase portrait for the system (5.5.5)–(5.5.6) is equivalent to the one shown in Fig. 5.1. That is, it possesses an invisible fold-fold of centre type at the origin and two saddle points at $(1, 0)$ and $(-1, 0)$ connected by two heteroclinic orbits.

Furthermore, the origin is surrounded by a continuum of periodic orbits whose periods monotonically increase as they approach to the heteroclinic connections. This can be shown as follows. Using Eqs. (5.2.15) and (5.2.16), the symmetries of the Hamiltonian (5.5.9) and assuming $y_0 > 0$, these periods are given by

$$\begin{aligned} \alpha(y_0) &= 4 \int_0^{1-\sqrt{1-y_0^2}} \frac{1}{\sqrt{y_0^2 + x^2 - 2x}} dx = \\ &= 2 \ln \left(\frac{1+y_0}{1-y_0} \right), \end{aligned} \quad (5.5.11)$$

and hence $\alpha'(y_0) > 0$.

5.5.2 Existence of periodic orbits

We first study the persistence of (n, m) -periodic orbits for $r = 1$ in Eq. (5.5.7) by applying Theorem 5.3.1. The subharmonic Melnikov function (5.3.3) becomes

$$M^{n,m}(t_0) = - \int_0^{nT} \Pi_y(q_c(t)) \cos(\omega(t + t_0)) dt, \quad (5.5.12)$$

where $q_c(t)$ is the periodic orbit of the unperturbed version of system (5.5.5)–(5.5.6) with energy level $c = \frac{y_0^2}{2}$ satisfying $q_c(0) = (0, \bar{y}_0)$ and

$$\bar{y}_0 = \alpha^{-1} \left(\frac{nT}{m} \right) = \frac{e^{\frac{nT}{2m}} - 1}{e^{\frac{nT}{2m}} + 1}. \quad (5.5.13)$$

We now want to obtain an explicit expression for Eq. (5.5.12). Thus we first note that the solution of system (5.5.5)–(5.5.6) with initial condition (x_0, y_0) at $t = t_0$ is given by

$$x^\pm(t) = C_1^\pm e^t + C_2^\pm e^{-t} \pm 1 \quad (5.5.14)$$

$$y^\pm(t) = C_1^\pm e^t - C_2^\pm e^{-t}, \quad (5.5.15)$$

where

$$C_1^\pm = \frac{x_0 + y_0 \mp 1}{2} e^{-t_0}, \quad C_2^\pm = \frac{x_0 - y_0 \mp 1}{2} e^{t_0}. \quad (5.5.16)$$

As explained in §5.2.4, the superscript $+$ is applied if $x_0 > 0$ or $x_0 = 0$ and $y_0 > 0$, and the superscript $-$ otherwise.

Assuming $x_0 = 0$ and $y_0 = \bar{y}_0 > 0$, it can be shown that

$$\Pi_y(q_c(t)) = \begin{cases} C_1 e^t - C_2 e^{-t}, & \text{if } 0 \leq t \leq \frac{nT}{2m} \\ -C_1 e^{t-\frac{nT}{2m}} + C_2 e^{-t+\frac{nT}{2m}}, & \text{if } \frac{nT}{2m} \leq t \leq \frac{nT}{m}, \end{cases} \quad (5.5.17)$$

where

$$C_1 = \frac{\bar{y}_0 - 1}{2}, \quad C_2 = \frac{-\bar{y}_0 - 1}{2}. \quad (5.5.18)$$

Thus, Eq. (5.5.12) becomes

$$\begin{aligned} M^{n,m}(t_0) = & - \sum_{j=0}^{m-1} \left(\int_0^{\frac{nT}{2m}} (C_1 e^t - C_2 e^{-t}) \cos \left(\omega \left(t + t_0 + j \frac{nT}{m} \right) \right) dt \right. \\ & \left. + \int_{\frac{nT}{2m}}^{\frac{nT}{m}} \left(-C_1 e^{t-\frac{nT}{2m}} + C_2 e^{-t+\frac{nT}{2m}} \right) \cos \left(\omega \left(t + t_0 + j \frac{nT}{m} \right) \right) dt \right) \end{aligned}$$

and, after some computations, we have

$$M^{n,m}(t_0) = \begin{cases} -\frac{4}{\omega^2 + 1} \cos(\omega t_0), & \text{if } m = 1 \\ 0, & \text{if } m > 1. \end{cases} \quad (5.5.19)$$

As $M^{n,1}(t_0)$ has two simple zeros, $\bar{t}_0^1 = \frac{T}{4}$ and $\bar{t}_0^2 = \frac{3T}{4}$, by Theorem 5.3.1, if $\varepsilon > 0$ is small enough, the non-autonomous system (5.5.5)-(5.5.6) possesses two subharmonic $(n, 1)$ -periodic orbits. In addition, the initial conditions of these periodic orbits are ε -close to

$$(0, \bar{y}_0, \bar{t}_0^1) = \left(0, \frac{e^{\frac{nT}{2}} - 1}{e^{\frac{nT}{2}} + 1}, \frac{T}{4} \right) \quad (5.5.20)$$

and

$$(0, \bar{y}_0, \bar{t}_0^2) = \left(0, \frac{e^{\frac{nT}{2}} - 1}{e^{\frac{nT}{2}} + 1}, \frac{3T}{4} \right), \quad (5.5.21)$$

respectively.

Proceeding as in Remark 5.3.2, one can solve Eq. (5.3.2) numerically with $m = 1$ and find the initial conditions for such a periodic orbit. In Fig. 5.8 we show the results for $n = 5$. Both periodic orbits are obtained by using the points given in Eqs. (5.5.20) and (5.5.21) to initiate Newton's method. Then, following the solution, ε was increased up to $\varepsilon = 1.6565 \cdot 10^{-2}$.

Since the subharmonic Melnikov function is identically zero, nothing can be said about

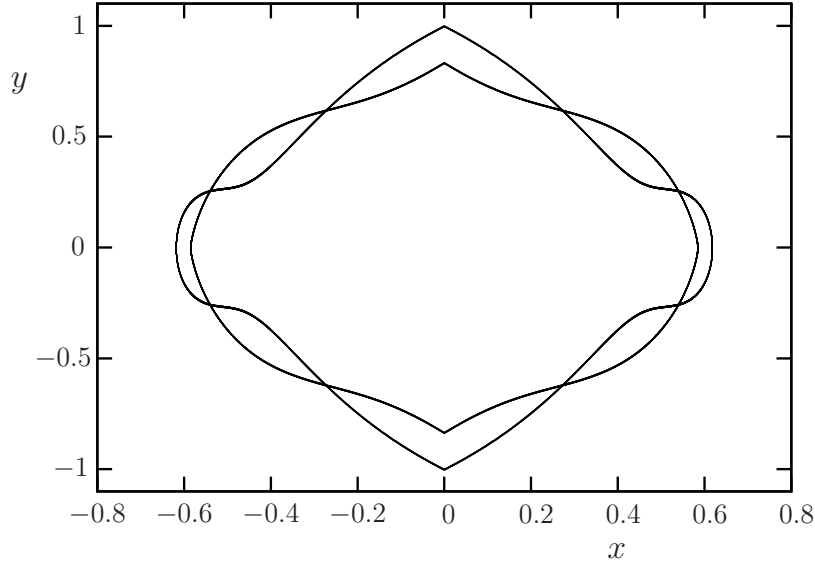


Figure 5.8: Periodic orbits for $n = 5$ and $m = 1$, $r = 1$, $\omega = 5$ and $\varepsilon = 1.6565 \cdot 10^{-2}$. Their initial conditions are ε -close to the points given in Eqs. (5.5.20) and (5.5.21).

the existence of (n, m) -periodic orbits with $m > 1$ (ultrasubharmonic orbits), using the first order analysis given in this work.

However, if instead of (5.5.10) one considers the perturbation

$$H_1(x, t) = x (\cos(\omega t) + \cos(k\omega t)),$$

then, it can be seen that the corresponding Melnikov function possesses simple zeros for $m = k$ and n relatively prime odd integers. Thus, periodic orbits impacting $m > 1$ times with the switching manifold can exist if higher harmonics of the perturbation are considered.

Let us now introduce the energy dissipation described in §5.3.2 and consider the whole system (5.5.5)-(5.5.7) with $r < 1$ using the Hamiltonian perturbation (5.5.8). From Theorem 5.3.2, simple zeros of the Melnikov function (5.5.19) also guarantee the existence of $(n, 1)$ -periodic orbits when $1 - r$ is small enough compared to ε . More precisely, taking

$$\varepsilon = \tilde{\varepsilon}\delta, \quad r = 1 - \tilde{r}\delta, \tag{5.5.22}$$

condition (5.3.14) becomes

$$0 < \frac{\tilde{r}}{\tilde{\varepsilon}} < \frac{1}{2} \left(\frac{e^{\frac{nT}{2}} + 1}{e^{\frac{nT}{2}} - 1} \right)^2 M^{n,1}(t_M) := \rho, \tag{5.5.23}$$

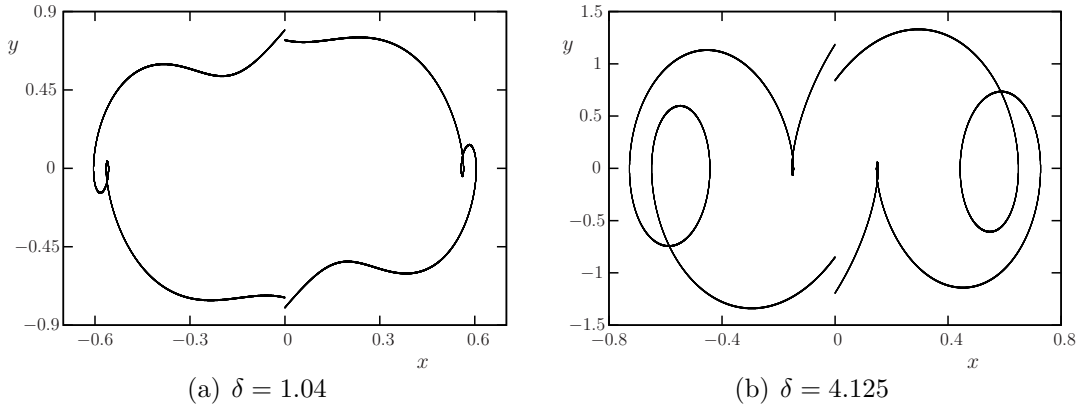


Figure 5.9: $(5, 1)$ -periodic orbits for $\omega = 5$ and $\frac{\tilde{r}}{\tilde{\varepsilon}} = 0.07$. Following the obtained solution, the perturbation parameter δ has been increased up to its maximum value. Initial conditions close to (\bar{y}_0, \hat{t}_0^1) and (\bar{y}_0, \hat{t}_0^2) have been used in (a) and (b), respectively.

where $M^{n,1}(t_M) = M^{n,1}(\frac{T}{2}) = \frac{4}{\omega^2+1}$ is the maximum value of the Melnikov function (5.5.19). Then, according to Theorem 5.3.2, there exists an $(n, 1)$ -periodic orbit if $\delta > 0$ is small enough. The initial condition of the periodic orbit is located in a δ -neighbourhood of the point $(x_0, y_0, t_0) = (0, \bar{y}_0, \hat{t}_0)$, where \bar{y}_0 is defined in Eq. (5.5.13), such that

$$\alpha(\bar{y}_0) = nT$$

and \hat{t}_0 is given by the simple zeros of Eq. (5.3.13), which becomes

$$-2\tilde{r}\bar{y}_0^2 + \tilde{\varepsilon}M^{n,1}(t_0) = 0. \quad (5.5.24)$$

Hence we find

$$\hat{t}_0^i = \frac{1}{\omega} \arccos \left(-\frac{\omega^2 + 1}{2} \left(\frac{e^{\frac{nT}{2}} - 1}{e^{\frac{nT}{2}} + 1} \right)^2 \frac{\tilde{r}}{\tilde{\varepsilon}} \right) + (i - 1)\frac{T}{2}, \quad i = 1, 2. \quad (5.5.25)$$

As before, if we set $n = 5$ and $\omega = 5$, then expression (5.5.23) becomes

$$0 < \frac{\tilde{r}}{\tilde{\varepsilon}} < 0.0914. \quad (5.5.26)$$

Hence, for any fixed ratio $\frac{\tilde{r}}{\tilde{\varepsilon}}$ satisfying (5.5.26) there exist two points, (\bar{y}_0, \hat{t}_0^i) , $i = 1, 2$, such that, if δ is small enough, Eq. (5.3.10) possesses a solution δ -close to them. Such a solution is an initial condition for an $(n, 1)$ -periodic orbit of system (5.5.5)-(5.5.7), with $r = 1 - \tilde{r}\delta$ and $\varepsilon = \tilde{\varepsilon}\delta$.

In Fig. 5.9 some of these orbits are shown for one value of the ratio $\frac{\tilde{r}}{\tilde{\varepsilon}}$ satisfying (5.5.26). Two different periodic orbits are shown, whose initial conditions are δ -close to (\bar{y}_0, \hat{t}_0^1) and

(\bar{y}_0, \hat{t}_0^2) . In both cases, δ tracks the solution, up to values where solutions of Eq. (5.3.9) can no longer be found. These values are used in the simulations shown in Fig. 5.9. Note that, above the limiting value of the ratio given in (5.5.26), no $(5, 1)$ -periodic orbits were found for $\omega = 5$ for any value of δ .

5.5.3 Existence curves

We now derive existence curves for the $(n, 1)$ -periodic orbits (n odd) and compare them with results obtained in [Hog89].

By integrating the linearized system and imposing symmetry conditions on the orbit, an explicit expression for the existence of $(n, 1)$ -periodic orbits in the r - ε plane was obtained in [Hog89], namely

$$\varepsilon_{\min}(R) = \frac{(1 + \omega^2) R (1 - \cosh(\frac{nT}{2}))}{\sqrt{\omega^2 \sinh^2(\frac{nT}{2}) R^2 + (2 - R)^2 (1 + \cosh(\frac{nT}{2}))^2}}, \quad (5.5.27)$$

where $R = 1 - r$. This exact global formula provides, for every n and r , the minimum value of the amplitude of the perturbation ε_{\min} such that a $(n, 1)$ -periodic orbit exists.

Unlike in [Hog89], we obtain similar curves in the r - ε plane by applying Theorem 5.3.2. As the existence of such orbits in Theorem 5.3.2 is proven using the implicit function theorem, the existence of these orbits is valid only locally. Hence, such existence curves are obtained by numerical continuation of the local periodic orbits. However, our method is more general; it does not depend on the details of the system, the type of perturbation or any symmetry assumptions. Moreover, it can also be applied when considering ultrasubharmonic periodic orbits ($m > 1$) as long as the hypothesis of Theorem 5.3.2 are fulfilled.

The limiting condition provided by Theorem 5.3.2 is given in Eq. (5.5.23). Thus, for a given r close to 1 (that is, $\tilde{r}\delta$ close to 0), it is natural to fix \tilde{r} and minimize ε by maximizing the ratio in (5.5.23), setting $\frac{1-r}{\varepsilon} = \frac{\tilde{r}\delta}{\tilde{\varepsilon}\delta} = \frac{\tilde{r}}{\tilde{\varepsilon}} = \rho$. As can be seen in Fig. 5.10 this curve, which is the straight line

$$1 - r = \rho\varepsilon,$$

is very close to the one obtained in [Hog89], given by (5.5.27).

One might think that these two curves should be identical due to the fact that the system appears to be linear in ε and piecewise-linear in x . Nevertheless, it is important to emphasize that the system solutions are in fact nonlinear in ε , since it is necessary to solve a nonlinear equation for the time when the solution crosses the switching manifold. Therefore, the curve $\frac{\tilde{r}}{\tilde{\varepsilon}} = \rho$, obtained using Melnikov theory, is not identical to the one obtained in [Hog89], but both curves are very close when ε is small (see Fig. 5.10).

As our method applies to general systems, the existence of periodic orbits given by Theorem 5.3.2 is only valid for $\delta < \delta_0 = \delta_0(\frac{\tilde{r}}{\varepsilon})$. Moreover, δ_0 tends to zero as $\frac{\tilde{r}}{\varepsilon} \rightarrow \rho$, as it is derived from the implicit function theorem. This is because, as $\frac{\tilde{r}}{\varepsilon} \rightarrow \rho$, the solution \hat{t}_0 which solves Eq. (5.5.24), tends to t_M , where t_M is a maximum of $M^{n,1}$ and hence $(M^{n,1})'(t_M) = 0$. Therefore, as \hat{t}_0 approaches t_M , the domain of validity provided by the implicit function theorem tends to zero, and thus so does δ_0 ($\delta_0 = O((M^{n,1})'(\hat{t}_0))$). As a consequence, it is not possible to find $\delta^* = \delta_0(\rho) > 0$ such that for any $\delta < \delta^*$ we could apply Theorem 5.3.2 to obtain periodic orbits. Hence, the condition $\frac{\tilde{r}}{\varepsilon} = \rho$ can not be used to derive a limiting relation between r and ε if we use a first order perturbation theory as in the Melnikov approach. Instead, we proceed as follows.

We first fix n odd and $\omega > 0$. Then, for every ratio $0 < \frac{\tilde{r}}{\varepsilon} < \rho$, we increase δ from 0 to δ_0 by numerically following the solution obtained using as initial condition one of the values provided in Eq. (5.5.20) or (5.5.21). This results in a curve in the r - ε plane parametrized by the ratio $\frac{\tilde{r}}{\varepsilon}$.

As our result is only locally valid, in order to compare it with [Hog89] we have to check whether both curves are tangent at the origin. From (5.5.27) we easily obtain

$$\varepsilon'_{\min}(0) = -\frac{1 + \omega^2}{2} \left(\frac{e^{\frac{nT}{2}} - 1}{e^{\frac{nT}{2}} + 1} \right)^2 = -\frac{1}{\rho},$$

which, by the inverse function theorem, tells us that both curves are tangent at the origin.

In Fig. 5.10, we show an example for $n = 5$ and $\omega = 5$ using initial conditions near (5.5.20). As can be seen, the expression derived from Theorem 5.3.2 (black line) provides, for every value of r , both the maximum and minimum values of ε for which a (5, 1)-periodic orbit exists, according to our method. The lower boundary derived in [Hog89], $(\varepsilon_{\min}(\cdot))^{-1}(\varepsilon)$ is also shown (dotted line). As demonstrated above, both curves are tangent at the origin, with slope equal to ρ . Note, however, that the minimum value does not coincide with the line $1 - r = \rho\varepsilon$, although their difference tends to zero as $r \rightarrow 1$. This confirms that one can not derive the minimum value of ε from condition (5.5.23) for every fixed r .

5.6 Conclusions

In this chapter we have extended the classical Melnikov methods, for subharmonic orbits and homoclinic/heteroclinic connections, to piecewise-defined Hamiltonian systems with a piecewise-defined periodic Hamiltonian perturbation. We rigorously prove that, when the unperturbed system has a piecewise-continuous Hamiltonian, the classical method also holds. In this case, simple zeros of the modified classical and subharmonic Melnikov functions guarantee the existence of subharmonic orbits and heteroclinic connections, respectively, in the perturbed system. We have also considered the case when the solution

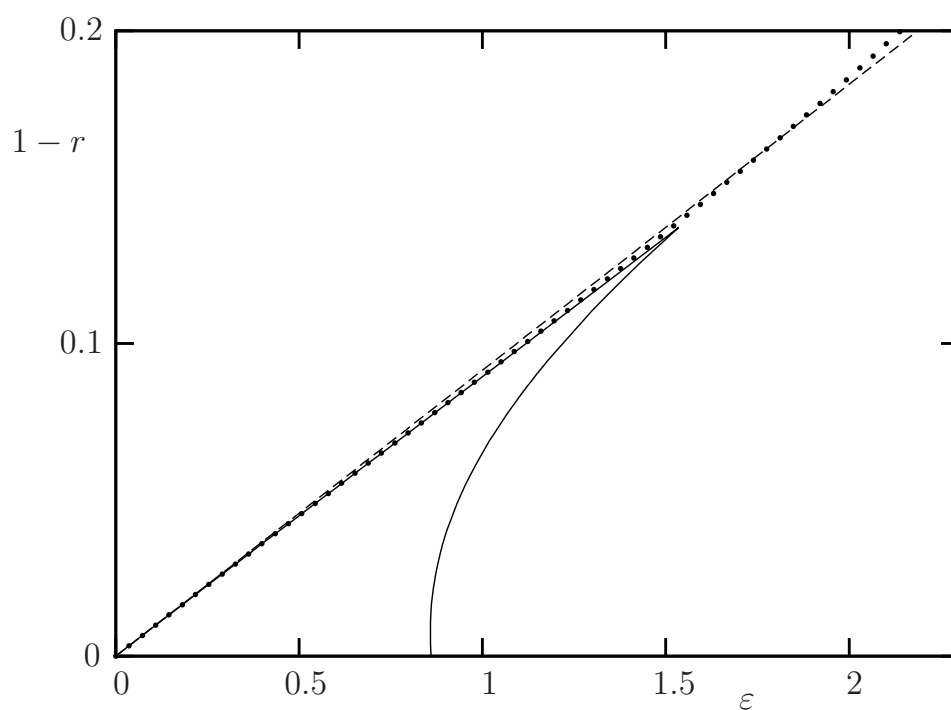


Figure 5.10: Existence curves of a $(5, 1)$ -periodic orbit for $\omega = 5$. Expression derived from Theorem 5.3.2 (black line), expression for ε_{\min} derived from [Hog89] (dotted line) and $1 - r = \rho\varepsilon$ (dashed line).

trajectories are discontinuous at the switching manifold, as in the case of an impacting system with energy loss represented by a coefficient of restitution. In this case, the unperturbed system has the origin as a global attractor. We have shown that the same results hold when this restitution coefficient is small enough with respect to the amplitude of the periodic perturbation.

In addition, our method provides a constructive way to find initial conditions for subharmonic orbits. In this way, we have found periodic orbits in the rocking block problem [Hog89]. We have also numerically obtained existence curves for these periodic orbits, and we have compared them with those given in [Hog89].

Future work should consider an extension of the method to quasi-periodic or almost-periodic perturbations. In [MS89] the authors present a generalization of the Melnikov method for this class of perturbation to smooth systems to show that the perturbed system has homoclinic trajectories. The Poincaré stroboscopic map is not a suitable tool for the systems treated in [MS89], as is the case for the periodic perturbations for piecewise-smooth systems that we have considered here. Hence, we believe that the results presented here can also be extended to quasi-periodic perturbations by the use of the impact map.

Chapter 6

The scattering map in two-coupled piecewise-smooth systems

6.1 Introduction

As explained in the introduction of this thesis, in this chapter we study the persistence of invariant manifolds for a system given by the cross product of two of the systems studied in chapter 5 when considering a small Hamiltonian perturbation which couples both systems and introduces a periodic forcing. This chapter is organized as follows.

In section 6.2 we introduce and describe the system and its invariant objects before the perturbation. In section 6.3 we introduce the essential tools, formulas and technical results which will allow us to rigorously prove the persistence of invariant manifolds (section 6.3.6), the existence of heteroclinic transversal intersections (section 6.4.1) and to define and provide first properties of the *scattering map* (section 6.4.2).

6.2 System description

6.2.1 Two uncoupled systems

In this work we consider a non-autonomous dynamical system formed by coupling two piecewise-defined systems in \mathbb{R}^2 through a non-autonomous periodic perturbation. We first define these two systems.

Let us split \mathbb{R}^2 in the two sets,

$$\begin{aligned} S^+ &= \{(q, p) \in \mathbb{R}^2 \mid q > 0\} \\ S^- &= \{(q, p) \in \mathbb{R}^2 \mid q < 0\} \end{aligned}$$

separated by a switching manifold

$$\Sigma = \Sigma^+ \cup \Sigma^- \cup \{(0, 0)\} \tag{6.2.1}$$

where

$$\begin{aligned}\Sigma^+ &= \{(0, p) \in \mathbb{R}^2 \mid p > 0\} \\ \Sigma^- &= \{(0, p) \in \mathbb{R}^2 \mid p < 0\}.\end{aligned}\tag{6.2.2}$$

Let us consider the piecewise-defined systems defined in $\mathbb{R}^2 \setminus \Sigma$

$$\begin{pmatrix} \dot{x} \\ \dot{y} \end{pmatrix} := \mathcal{X}(x, y) := \begin{cases} \mathcal{X}^+(x, y) & \text{if } (x, y) \in S^+ \\ \mathcal{X}^-(x, y) & \text{if } (x, y) \in S^- \end{cases}\tag{6.2.3}$$

$$\begin{pmatrix} \dot{u} \\ \dot{v} \end{pmatrix} := \mathcal{U}(u, v) := \begin{cases} \mathcal{U}^+(u, v) & \text{if } (u, v) \in S^+ \\ \mathcal{U}^-(u, v) & \text{if } (u, v) \in S^- \end{cases}\tag{6.2.4}$$

with $\mathcal{X}^\pm(x, y), \mathcal{U}^\pm(u, v) \in C^\infty(\mathbb{R}^2)$.

Let us assume that (6.2.3) and (6.2.4) are Hamiltonian systems associated, respectively, with the $C^0(\mathbb{R}^2)$ piecewise-defined Hamiltonians of the form

$$\begin{aligned}X(x, y) &:= \frac{y^2}{2} + Y(x) \\ &:= \begin{cases} X^+(x, y) := \frac{y^2}{2} + Y^+(x) & \text{if } (x, y) \in S^+ \\ X^-(x, y) := \frac{y^2}{2} + Y^-(x) & \text{if } (x, y) \in S^- \end{cases}\end{aligned}\tag{6.2.5}$$

$$\begin{aligned}U(u, v) &:= \frac{v^2}{2} + V(u) \\ &:= \begin{cases} U^+(u, v) := \frac{v^2}{2} + V^+(u) & \text{if } (u, v) \in S^+ \\ U^-(u, v) := \frac{v^2}{2} + V^-(u) & \text{if } (u, v) \in S^-, \end{cases}\end{aligned}\tag{6.2.6}$$

with $Y^\pm, V^\pm \in C^\infty(\mathbb{R}^2)$ fulfilling $Y^+(0) = Y^-(0) = 0$ and $V^+(0) = V^-(0) = 0$. Then, we have the following relations between systems (6.2.3) and (6.2.4) and the piecewise defined Hamiltonians (6.2.5) and (6.2.6), respectively,

$$\begin{aligned}\mathcal{X}^\pm &= J\nabla X^\pm \\ \mathcal{U}^\pm &= J\nabla U^\pm\end{aligned}\tag{6.2.7}$$

where J is the Symplectic matrix

$$J = \begin{pmatrix} 0 & 1 \\ -1 & 0 \end{pmatrix}.$$

From the form of the Hamiltonians (6.2.5) and (6.2.6), it becomes natural to extend the definition of the flow of \mathcal{X}^+ and \mathcal{U}^+ to $S^+ \cap \Sigma^+$ and the flows \mathcal{X}^- and \mathcal{U}^- to $S^- \cap \Sigma^-$. Hence, the Hamiltonians (6.2.5) and (6.2.6) become naturally extended to \mathbb{R}^2 as

$$X(x, y) = \begin{cases} X^+(x, y) & \text{if } (x, y) \in S^+ \cup \Sigma^+ \cup \{(0, 0)\} \\ X^-(x, y) & \text{if } (x, y) \in S^- \cup \Sigma^-, \end{cases}$$

and similarly for $U(u, v)$.

Note that the vector fields \mathcal{X}^+ and \mathcal{X}^- are tangent to Σ at $(0, 0)$ (resp. \mathcal{U}^+ and \mathcal{U}^-). To define the flow associated with system (6.2.3), we proceed as usual in non-smooth systems. Given an initial condition (x_0, y_0) , we apply $\phi_{\mathcal{X}^+}$ or $\phi_{\mathcal{X}^-}$ if $(x_0, y_0) \in S^\pm$, which are the flows associated to the smooth systems \mathcal{X}^\pm , until the switching manifold Σ is crossed at some point. Then, using this point as new initial condition one proceeds evolving with the flow associated with the new domain. Similarly for system (6.2.4). Note that, as no sliding across the switching manifold is possible, the definition of the flows becomes very straightforward.

This permits us to consider the flows

$$\phi_{\mathcal{X}}(t; x_0, y_0) \text{ and } \phi_{\mathcal{U}}(t; u_0, v_0) \tag{6.2.8}$$

associated to systems (6.2.3) and (6.2.4), respectively, that are C^0 functions piecewise-defined in t fulfilling

$$\begin{aligned} \phi_{\mathcal{X}}(0; x_0, y_0) &= (x_0, y_0) \\ \phi_{\mathcal{U}}(0; u_0, v_0) &= (u_0, v_0). \end{aligned}$$

Let us assume that the following conditions are fulfilled

- C.1 System (6.2.3) possesses two hyperbolic critical points $Q^+ \in S^+$ and $Q^- \in S^-$ of saddle type and belonging to the energy level $X(Q^\pm) = \bar{d}$.
- C.2 There exist two heteroclinic orbits given by $W^u(Q^-) = W^s(Q^+)$ and $W^u(Q^+) = W^s(Q^-)$, also located in the level of energy $X(x, y) = \bar{d}$.
- C.3 The Hamiltonians U^\pm in (6.2.6) fulfill

$$(V^+)'(0) > 0, \quad (V^-)'(0) < 0,$$

and so $(0, 0)$ is an invisible quadratic tangency for both vector fields \mathcal{U}^\pm in (6.2.4). Following [Kuz04, GST11], we call the point $(0, 0)$ an invisible fold-fold.

C.4 System (6.2.4) possesses a continuum of (piecewise-defined) periodic orbits surrounding the origin. These can be parametrized by the Hamiltonian U and have the form

$$\Lambda_c = \{(u, v) \in \mathbb{R}^2 \mid U(u, v) = c\}, \quad 0 < c \leq \bar{c}. \quad (6.2.9)$$

The main purpose of this chapter is to study the dynamics around one of the heteroclinic orbits. Hence, we focus from now on one of them, the upper one

$$\gamma^{\text{up}} := W^u(Q^-) \cap W^s(Q^+) = \{(x, y) \in \mathbb{R}^2 \mid X(x, y) = \bar{d}, y \geq 0\}.$$

There we consider the following parametrization

$$\gamma^{\text{up}} = \{\sigma^{\text{up}}(t), t \in \mathbb{R}\} \quad (6.2.10)$$

where $\sigma^{\text{up}}(t)$ is the solution of system (6.2.3) fulfilling

$$\begin{aligned} \sigma^{\text{up}}(0) &= (0, y_h) \in \Sigma^+ \\ \lim_{t \rightarrow \pm\infty} \sigma^{\text{up}}(t) &= Q^\pm, \end{aligned} \quad (6.2.11)$$

where $(0, y_h)$, $y_h = \sqrt{\bar{d}}$, is given by

$$(0, y_h) = W^u(Q^-) \cap \Sigma = W^s(Q^+) \cap \Sigma.$$

Equivalently, we could consider the lower heteroclinic connection,

$$\gamma^{\text{down}} = \{\sigma^{\text{down}}(t), t \in \mathbb{R}\} = W^u(Q^+) = W^s(Q^-),$$

and proceed similarly in the rest of this chapter with γ^{down} .

Before introducing the non-autonomous perturbation which will couple both systems described above, we roughly describe the invariant objects of the cross product of both systems (see Fig. 6.1), which is a ‘‘Hamiltonian’’ system with (piecewise-defined) Hamiltonian

$$H_0(u, v, x, s) = U(u, v) + X(x, y). \quad (6.2.12)$$

On one hand, the cross product of the periodic orbits Λ_c with the critical points Q^\pm gives rise to periodic orbits, $\Lambda_c \times Q^\pm$, which are hyperbolic when restricting the system to the level of energy $U(u, v) + X(x, y) = c + \bar{d}$. Although they are non-regular manifolds due to the non-smoothness of Λ_c , as it will be detailed later on §6.3.6 in the extended phase space, they have stable and unstable (non-regular) manifolds. Moreover, the stable/unstable manifolds of each periodic orbit of the form $\Lambda_c \times Q^+$ coincides with the unstable/stable manifolds of the periodic orbit $\Lambda_c \times Q^-$, respectively, and hence there exist (non-regular) heteroclinic manifolds connecting these periodic orbits.

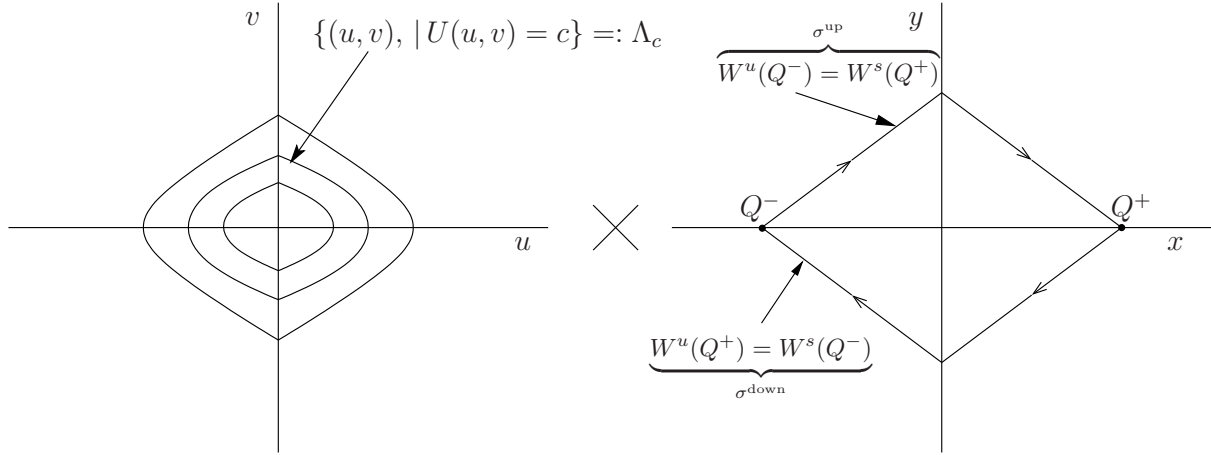


Figure 6.1: Invariant objects for the unperturbed coupled system.

Also of relevant interest in this work will be the manifold given by the cross product of the critical points Q^\pm with the union of all periodic orbits

$$\begin{aligned} \Lambda^+ &= \bigcup_{c \in [c_1, c_2]} \Lambda_c \times Q^+ \\ &= \{ (u, v, Q^+) \mid U(u, v) = c, c_1 \leq c \leq c_2, \} \\ \Lambda^- &= \bigcup_{c \in [c_1, c_2]} \Lambda_c \times Q^- \\ &= \{ (u, v, Q^-) \mid U(u, v) = c, c_1 \leq c \leq c_2, \} \end{aligned}$$

for some $0 < c_1, c_2 < \bar{c}$. In Fig. 6.2 schematically show these two manifolds.

As it will be shown in §6.3.6, these manifolds will lead to normally hyperbolic invariant manifolds for the impact map, introduced in §6.3.1.

6.2.2 The coupled system in the extended phase space

As announced above, we will focus our attention on the system given by coupling systems (6.2.3) and (6.2.4) through a non-autonomous T -periodic Hamiltonian perturbation, $\varepsilon h(u, v, x, y, s) \in C^\infty(\mathbb{R}^5)$ satisfying

$$h(u, v, x, y, s) = h(u, v, x, y, s + T), \quad \forall (u, v, x, y, s) \in \mathbb{R}^5.$$

Using this property, we will from now on consider the coupled system in the extended state space $\mathbb{R}^4 \times \mathbb{T}_T$, where $\mathbb{T}_T = \mathbb{R} \setminus T$. Let us remark that consider here \mathbb{T}_T not as the usual circle (modulus 1) but modulus T , because T is a relevant parameter from the

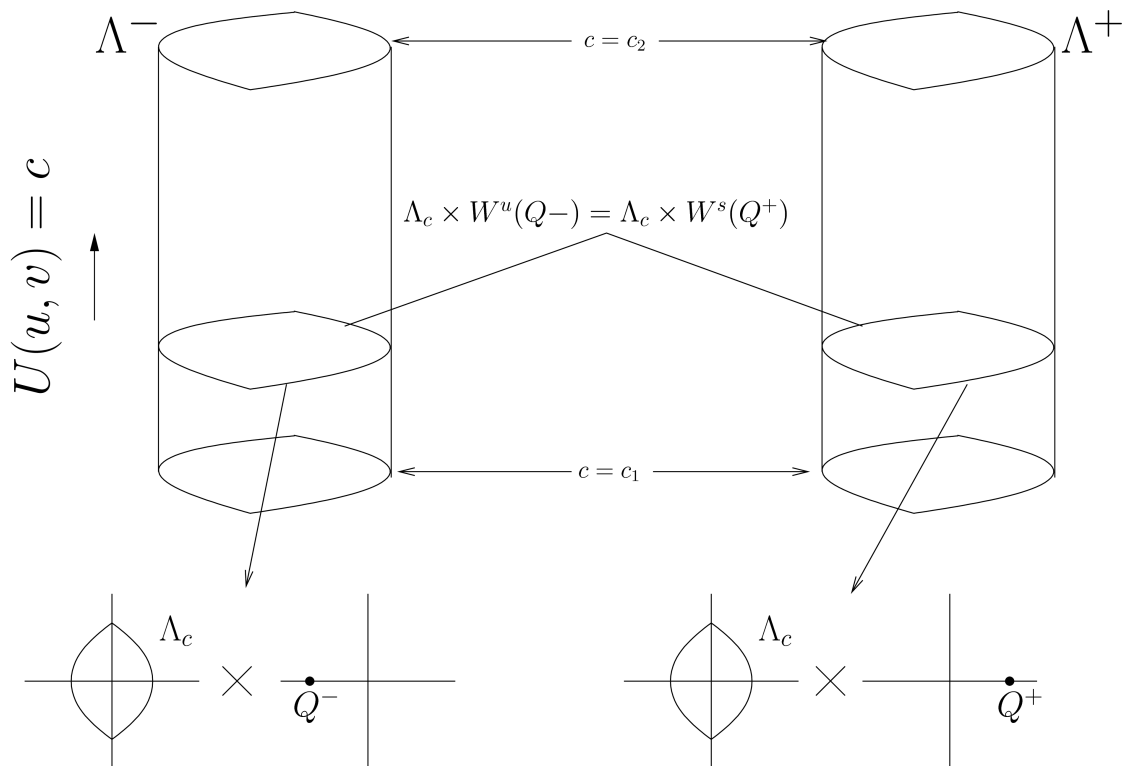


Figure 6.2: Schematic representation of the manifolds Λ^+ and Λ^- .

application point of view and hence we prefer to keep it.

We now add the variable $A \in \mathbb{R}$ to the variables of the extended state space and assume that the coupled system is, for $z = (u, v, x, y)$, the autonomous system associated with the C^0 Hamiltonian

$$\tilde{H}_\varepsilon(\tilde{z}, A) := A + H_\varepsilon(\tilde{z})$$

where

$$H_\varepsilon(\tilde{z}) := U(u, v) + X(x, y) + \varepsilon h(\tilde{z}), \quad \varepsilon > 0, \quad (6.2.13)$$

with $\tilde{z} = (z, s)$, $s \in \mathbb{T}_T$.

The addition of the variable $A \in \mathbb{R}$, the symplectic conjugate of s , is a standard formality to keep a Hamiltonian structure for the perturbed system, which is equivalent to adding the equations

$$\dot{s} = 1, \quad \dot{A} = -\frac{\partial}{\partial s} H_\varepsilon(u, v, x, y, s)$$

plus the terms coming from the perturbation, to the systems (6.2.3)-(6.2.4). Note that the variable A does not have any influence on the dynamics, as it does not appear in any differential equation. Thus, we only study the dynamics of the coupled system in the variables (u, v, x, y, s) , and refer to it as a system of two and a half degrees of freedom associated with the Hamiltonian $H_\varepsilon(u, v, x, y, s)$. Recalling that unperturbed systems (6.2.3) and (6.2.4) are piecewise-defined, these differential equations will be defined in four partitions in $\mathbb{R}^4 \times \mathbb{T}_T$ as follows

$$\begin{aligned} \begin{pmatrix} \dot{u} \\ \dot{v} \\ \dot{x} \\ \dot{y} \end{pmatrix} &= \begin{cases} J_4 \nabla (U^+ + X^+ + \varepsilon h) (\tilde{z}) & \text{if } \tilde{z} \in S^+ \cup \Sigma^+ \times S^+ \cup \Sigma^+ \times \mathbb{T}_T \\ J_4 \nabla (U^- + X^+ + \varepsilon h) (\tilde{z}) & \text{if } \tilde{z} \in S^- \cup \Sigma^+ \times S^+ \cup \Sigma^- \times \mathbb{T}_T \\ J_4 \nabla (U^- + X^- + \varepsilon h) (\tilde{z}) & \text{if } \tilde{z} \in S^- \cup \Sigma^- \times S^- \cup \Sigma^- \times \mathbb{T}_T \\ J_4 \nabla (U^- + X^+ + \varepsilon h) (\tilde{z}) & \text{if } \tilde{z} \in S^- \cup \Sigma^- \times S^+ \cup \Sigma^+ \times \mathbb{T}_T \end{cases} \\ \dot{s} &= 1, \end{aligned} \quad (6.2.14)$$

where

$$J_4 = \begin{pmatrix} 0 & 1 & 0 & 0 \\ -1 & 0 & 0 & 0 \\ 0 & 0 & 0 & 1 \\ 0 & 0 & -1 & 0 \end{pmatrix}.$$

These differential equations define four different autonomous flows in the extended phase space, $\tilde{\varphi}^{\pm\pm}(t; \tilde{z}_0; \varepsilon)$. Letting $\varphi^{\pm\pm}(t; t_0, z_0)$ be the correspondent non-autonomous flows

such that $\varphi^{\pm\pm}(t_0; t_0, z_0) = z_0$, we write $\tilde{\phi}^{\pm\pm}(t; \tilde{z}_0)$ fulfilling $\tilde{\phi}^{\pm\pm}(0; \tilde{z}_0) = \tilde{z}_0$ as

$$\tilde{\phi}^{\pm\pm}(t; \tilde{z}_0) = (\phi^{\pm\pm}(t; \tilde{z}_0), s_0 + t),$$

where $\phi^{\pm\pm}(t; \tilde{z}_0)$ are such that

$$\varphi^{\pm\pm}(t; t_0, z_0) = \phi^{\pm\pm}(t - t_0; \tilde{z}_0).$$

Proceeding similarly as we did for the systems \mathcal{U} and \mathcal{X} , by properly concatenating the flows $\tilde{\phi}^{+\pm}$ and $\tilde{\phi}^{-\pm}$ when the 3-dimensional switching manifold $u = 0$ is crossed, and $\tilde{\phi}^{++}$ and $\tilde{\phi}^{--}$ when $x = 0$ is crossed, we can define the solution, $\tilde{\phi}(t; \tilde{z}_0; \varepsilon)$, of the coupled system (6.2.14) fulfilling $\tilde{\phi}(0; \tilde{z}_0; \varepsilon) = \tilde{z}_0$. We will give explicit expressions for $\tilde{\phi}$ in §6.3.4. Note that $\tilde{\phi}$ is not differentiable at those times corresponding to the crossings with the switching manifolds, although it is as smooth as the flows $\phi^{\pm\pm}$ when restricted to the open domains given in the respective branches.

Note that, for $\varepsilon = 0$, the invariant objects described in §6.2.1 for the cross product of the systems (6.2.3) and (6.2.4) possess now one dimension more due to the addition of time as a variable. Hence, the periodic orbits $\Lambda_c \times Q^\pm$, which were homeomorphic to the circle, become now the tori $\Lambda_c \times Q^\pm \times \mathbb{T}_T$. Similarly for the 2-dimensional “invariant manifolds” Λ^\pm , which become the 3-dimensional “invariant manifolds” $\Lambda^\pm \times \mathbb{T}_T$. This will be explained in more detail in §6.3.6 after introducing the *impact* map in the next sections.

6.3 Some notation and properties

6.3.1 Impact map associated with $u = 0$

Let us define in $\mathbb{R}^4 \times \mathbb{T}_T$ the section

$$\tilde{\Sigma} = \Sigma \times \mathbb{R}^2 \times \mathbb{T}_T = \{(0, v, x, y, s)\} \quad (6.3.1)$$

where

$$\tilde{\Sigma}^+ = \Sigma^+ \times \mathbb{R}^2 \times \mathbb{T}_T = \{(0, v, x, y, s) \mid v > 0\} \quad (6.3.2)$$

$$\tilde{\Sigma}^- = \Sigma^- \times \mathbb{R}^2 \times \mathbb{T}_T = \{(0, v, x, y, s) \mid v < 0\} \quad (6.3.3)$$

and Σ and Σ^\pm are defined in (6.2.2).

Let us observe that $\tilde{\Sigma}$ is one of the switching manifolds of system (6.2.14) in the extended phase space, and will play an important role in our constructions. This is the section crossed by the “normally hyperbolic manifolds” $\Lambda_c \times Q^\pm \times \mathbb{T}_T$, and hence these objects are not regular but just continuous.

It is now our goal to define the impact map associated with $\tilde{\Sigma}$, which will be a map from section $\tilde{\Sigma}$ to itself. Basically, this map regularizes system (6.2.14) in some open domains, and will allow us to apply classical results for perturbation theory for smooth systems in order to rigorously proof incoming results such as persistence of invariant manifolds and their stable and unstable manifolds.

Before introducing this impact map, we first define four intermediate maps involving the sections $\tilde{\Sigma}$ and $\tilde{\Sigma}^\pm$ given in (6.3.1)–(6.3.3).

Let us first consider the projection onto the section $\tilde{\Sigma}$ by the flow $\tilde{\phi}$

$$\kappa_\varepsilon : \mathbb{R}^4 \times \mathbb{T}_T \longrightarrow \tilde{\Sigma}.$$

That is, given a point $\tilde{z} \in \mathbb{R}^4 \times \mathbb{T}_T$, one evolves, for positive values of time, using the flow associated with (6.2.14) and described in §6.2.2 until the switching manifold $\tilde{\Sigma}$ is reached. Although such a construction is well defined, we are interested on avoiding the concatenation of flows due to the crossing with the switching manifold given by $x = 0$. Hence, we restrict κ_ε to a suitable domain

$$\tilde{\mathcal{O}}_{\kappa_\varepsilon} \subset \mathbb{R}^4 \times \mathbb{T}_T \tag{6.3.4}$$

given by the points whose trajectory by $\tilde{\phi}$ first impacts the switching manifold given by $u = 0$ ($\tilde{\Sigma}$) than the one given by $x = 0$.

We will provide a more precise description of this set in §6.3.2. However, for a better understanding of the involving geometry, we note that $\tilde{\mathcal{O}}_{\kappa_\varepsilon}$ depends on ε and is formed by two connected components separated by the section $x = 0$. In addition, these components are not empty for $\varepsilon > 0$ small enough, as one can always find points (u, v, x, y, s) with (x, y) close enough to the critical points Q^\pm and (u, v) close enough to the origin of the $u - v$ plane, whose trajectory first impacts with the switching surface $u = 0$ rather than $x = 0$.

With this restriction, the map

$$\kappa_\varepsilon : \tilde{\mathcal{O}}_{\kappa_\varepsilon} \subset \mathbb{R}^4 \times \mathbb{T}_T \longrightarrow \tilde{\Sigma} \tag{6.3.5}$$

becomes

$$\kappa_\varepsilon(\tilde{z}) = \begin{cases} \tilde{\phi}^{++}(t_{\tilde{\Sigma}}; \tilde{z}; \varepsilon) & \text{if } \tilde{z} \in S^+ \times (S^+ \cup \Sigma^+) \times \mathbb{T}_T \\ \tilde{\phi}^{-+}(t_{\tilde{\Sigma}}; \tilde{z}; \varepsilon) & \text{if } \tilde{z} \in S^- \times (S^+ \cup \Sigma^+) \times \mathbb{T}_T \\ \tilde{\phi}^{+-}(t_{\tilde{\Sigma}}; \tilde{z}; \varepsilon) & \text{if } \tilde{z} \in S^+ \times (S^- \cup \Sigma^-) \times \mathbb{T}_T \\ \tilde{\phi}^{--}(t_{\tilde{\Sigma}}; \tilde{z}; \varepsilon) & \text{if } \tilde{z} \in S^- \times (S^- \cup \Sigma^-) \times \mathbb{T}_T \end{cases}$$

where $t_{\tilde{\Sigma}}$ is the smallest value of $t \geq 0$ such that $\tilde{\phi}^{\pm\pm}(t; \tilde{z}; \varepsilon) \in \tilde{\Sigma}$. We can hence precisely define the set

$$\tilde{\mathcal{O}}_{\kappa_\varepsilon} = \left\{ \tilde{z} \in \mathbb{R}^4 \times \mathbb{T}_T \mid \Pi_x \left(\tilde{\phi}(t; \tilde{z}; \varepsilon) \right) \neq 0 \forall t \in [0, t_{\tilde{\Sigma}}] \right\},$$

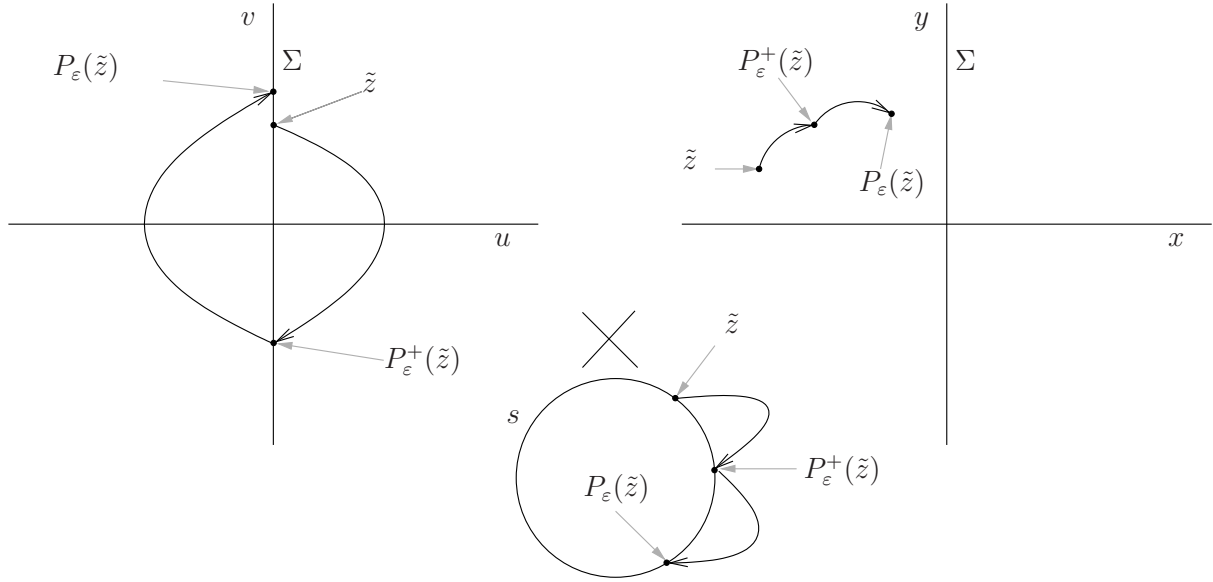


Figure 6.3: Schematic representation of the maps P_ε^- , P_ε^+ and P_ε .

where Π_x is the projection onto the x axis and $\tilde{\phi}(t; \tilde{z}; \varepsilon)$ is the flow associated with system (6.2.14), which, for $t \in [0, t_{\tilde{\Sigma}}]$, coincides with one of the flows $\tilde{\phi}^{\pm\pm}(t; \tilde{z}; \varepsilon)$ and hence is well defined and smooth.

Similarly, we consider an open set $\tilde{\mathcal{O}}_{\bar{\kappa}_\varepsilon}$ and define the map

$$\bar{\kappa}_\varepsilon : \tilde{\mathcal{O}}_{\bar{\kappa}_\varepsilon} \subset \mathbb{R}^4 \times \mathbb{T}_T \longrightarrow \tilde{\Sigma} \quad (6.3.6)$$

projecting to $\tilde{\Sigma}$ backwards in time. That is, considering $t_{\tilde{\Sigma}} \leq 0$. Hence $\tilde{\mathcal{O}}_{\bar{\kappa}_\varepsilon}$ becomes

$$\tilde{\mathcal{O}}_{\bar{\kappa}_\varepsilon} = \left\{ \tilde{z} \in \mathbb{R}^4 \times \mathbb{T}_T \mid \Pi_x \left(\tilde{\phi}(t; \tilde{z}; \varepsilon) \right) \neq 0 \forall t \in [t_{\tilde{\Sigma}}, 0] \right\}.$$

Remark 6.3.1. *The maps κ_ε and $\bar{\kappa}_\varepsilon$ are continuous in $(\mathbb{R}^2 \times \mathbb{R}^2 \times \mathbb{T}_T) \setminus \tilde{\Sigma}$. For $\tilde{z} \in \tilde{\Sigma}$, we have that $t_{\tilde{\Sigma}} = 0$ and therefore $\kappa_\varepsilon|_{\tilde{\Sigma}} = Id$. In fact, for $\tilde{z} \in \tilde{\Sigma}$, κ_ε is continuous on the left but not on the right, and viceversa for $\bar{\kappa}_\varepsilon$.*

We provide in Fig.6.3 a schematic representation of the definitions that follow.

We also consider two sets $\tilde{\mathcal{O}}_{P_\varepsilon^+} \subset \tilde{\Sigma}^+$ and $\tilde{\mathcal{O}}_{P_\varepsilon^-} \subset \tilde{\Sigma}^-$ with the same characteristics described for $\tilde{\mathcal{O}}_{\kappa_\varepsilon}$. That is, these are the set of points in $\tilde{\Sigma}^+$ and $\tilde{\Sigma}^-$ whose trajectories first hit the switching manifold given by $u = 0$, $\tilde{\Sigma}$, rather than the one given by $x = 0$. Then we define two maps

$$P_\varepsilon^+ : \tilde{\mathcal{O}}_{P_\varepsilon^+} \subset \tilde{\Sigma}^+ \longrightarrow \tilde{\Sigma}^- \quad (6.3.7)$$

$$P_\varepsilon^- : \tilde{\mathcal{O}}_{P_\varepsilon^-} \subset \tilde{\Sigma}^- \longrightarrow \tilde{\Sigma}^+ \quad (6.3.8)$$

as follows.

If $\tilde{z} = (0, v, x, y, s) \in \tilde{\mathcal{O}}_{P_\varepsilon^+} \subset \tilde{\Sigma}^+$ ($v > 0$), then

$$P_\varepsilon^+(\tilde{z}) = \begin{cases} \tilde{\phi}^{++}(t_{\tilde{\Sigma}^-}; \tilde{z}; \varepsilon) & \text{if } \tilde{z} \in \Sigma^+ \times (S^+ \cup \Sigma^+) \times \mathbb{T}_T \\ \tilde{\phi}^{+-}(t_{\tilde{\Sigma}^-}; \tilde{z}; \varepsilon) & \text{if } \tilde{z} \in \Sigma^+ \times (S^- \cup \Sigma^-) \times \mathbb{T}_T \end{cases}$$

where $t_{\tilde{\Sigma}^-}$ is the smallest value of $t > 0$ such that $\tilde{\phi}^{\pm\pm}(t; \tilde{z}; \varepsilon) \in \tilde{\Sigma}^-$. The set $\tilde{\mathcal{O}}_{P_\varepsilon^+}$ becomes then

$$\tilde{\mathcal{O}}_{P_\varepsilon^+} = \left\{ \tilde{z} \in \underbrace{\Sigma^+ \times \mathbb{R}^2 \times \mathbb{T}_T}_{\tilde{\Sigma}^+} \mid \Pi_x(\tilde{\phi}(t; \tilde{z}; \varepsilon)) \neq 0 \forall t \in [0, t_{\tilde{\Sigma}^-}] \right\}, \quad (6.3.9)$$

and, as $\tilde{\mathcal{O}}_{\kappa_\varepsilon}$, has two connected components in $\Sigma^+ \times (S^+ \cup \Sigma^+) \times \mathbb{T}_T$ and $\Sigma^+ \times (S^- \cup \Sigma^-) \times \mathbb{T}_T$.

If $\varepsilon = 0$, we can provide an explicit expression for P_0^+ as follows.

Let us recall that the flows $\tilde{\phi}^{\pm\pm}$ consist on the uncoupled flows $\phi_{\mathcal{U}}$ and $\phi_{\mathcal{X}}$ described in (6.2.8) but extended by adding the time s as state variable. Regarding conditions C.1–C4, the phase portrait of system \mathcal{U} is formed by the continuum of periodic orbits, Λ_c , which, due to the expression of the Hamiltonian U , are symmetric with respect to $v = 0$. Hence, the map P_0^+ can be written as

$$P_0^+(0, v, x, y, s) = (0, -v, \phi_{\mathcal{X}}(\alpha^+(v); x, y), s + \alpha^+(v)),$$

where

$$\alpha^+(v) = 2 \int_0^{(V^+)^{-1}(c)} \frac{1}{\sqrt{2(c - V^+(x))}} dx, \quad c = U(0, v) = \frac{v^2}{2} \quad (6.3.10)$$

is the time taken by the flow $\phi_{\mathcal{U}}(t; 0, v)$, with $v > 0$, to reach Σ^- . In the case that the Hamiltonian U is symmetric with respect to $u = 0$, this is half of the period of the periodic orbit Λ_c .

We will give a detailed description of $\tilde{\mathcal{O}}_{P_0^+}$ in §6.3.2.

Finally, if $\tilde{z} = (0, v, x, y, s) \in \tilde{\mathcal{O}}_{P_\varepsilon^-} \subset \tilde{\Sigma}^-$ ($v < 0$), then we similarly define

$$P_\varepsilon^-(\tilde{z}) = \begin{cases} \tilde{\phi}^{-+}(t_{\tilde{\Sigma}^+}; \tilde{z}; \varepsilon) & \text{if } \tilde{z} \in \Sigma^- \times (S^+ \cup \Sigma^+) \times \mathbb{T}_T \\ \tilde{\phi}^{--}(t_{\tilde{\Sigma}^+}; \tilde{z}; \varepsilon) & \text{if } \tilde{z} \in \Sigma^- \times (S^- \cup \Sigma^-) \times \mathbb{T}_T, \end{cases}$$

where $t_{\tilde{\Sigma}^+}$ is the smallest value of $t > 0$ such that $\tilde{\phi}^{-\pm}(t; \tilde{z}; \varepsilon) \in \tilde{\Sigma}^+$.

Hence, the set $\tilde{\mathcal{O}}_{P_\varepsilon^-}$ becomes

$$\tilde{\mathcal{O}}_{P_\varepsilon^-} = \left\{ \tilde{z} \in \underbrace{\Sigma^- \times \mathbb{R}^2 \times \mathbb{T}_T}_{\tilde{\Sigma}^-} \mid \Pi_x(\tilde{\phi}(t; \tilde{z}; \varepsilon)) \neq 0 \forall t \in [0, t_{\tilde{\Sigma}^+}] \right\}.$$

If $\varepsilon = 0$, the map P_0^- becomes

$$P_0^-(0, v, x, y, s) = (0, -v, \phi_{\mathcal{X}}(\alpha^-(v); x, y), s + \alpha^-(v)),$$

where

$$\alpha^-(v) = -2 \int_0^{(V^-)^{-1}(c)} \frac{1}{\sqrt{2(c - V^-(x))}} dx, \quad c = U(0, v) = \frac{v^2}{2} \quad (6.3.11)$$

is the time taken by the flow $\phi_{\mathcal{U}}(t; 0, v)$, with $v < 0$, to reach Σ^+ .

Finally, as it is usual when dealing with piecewise-defined systems, we construct the impact map as the composition of the maps P_ε^\pm . Let us consider an open set,

$$\tilde{\mathcal{O}}_{P_\varepsilon} \subset \tilde{\mathcal{O}}_{P_\varepsilon^+} \cup \tilde{\mathcal{O}}_{P_\varepsilon^-} \subset \tilde{\Sigma}, \quad (6.3.12)$$

and we define the Poincaré impact map

$$P_\varepsilon : \tilde{\mathcal{O}}_{P_\varepsilon} \subset \tilde{\Sigma} \longrightarrow \tilde{\Sigma}$$

as

$$P_\varepsilon(0, v, x, y, s) = \begin{cases} P_\varepsilon^+ \circ P_\varepsilon^-(0, v, x, y, s) & \text{if } (0, v, x, y, s) \in \tilde{\mathcal{O}}_{P_\varepsilon^-} \subset \tilde{\Sigma}^- \\ P_\varepsilon^- \circ P_\varepsilon^+(0, v, x, y, s) & \text{if } (0, v, x, y, s) \in \tilde{\mathcal{O}}_{P_\varepsilon^+} \subset \tilde{\Sigma}^+ \end{cases}$$

From now on, we will eventually omit the repetition of the coordinate $u = 0$, identifying $\tilde{\Sigma} \simeq \mathbb{R}^3 \times \mathbb{T}_T$. Moreover, we will use the following notation. When considering points $(0, v, x, y, s) \in \tilde{\Sigma} \subset \mathbb{R}^4 \times \mathbb{T}_T$, we will refer to them as $\tilde{\omega} = (v, x, y, s)$. We will include these points again back in $\mathbb{R}^4 \times \mathbb{T}_T$, writing $\tilde{z} = (0, \tilde{\omega})$.

Hence, the new variable of the impact map will be $\tilde{\omega}$. To avoid further complication on the notation, we will consider the set $\tilde{\mathcal{O}}_{P_\varepsilon}$ in $\mathbb{R}^3 \times \mathbb{T}_T$ and write the impact map

$$P_\varepsilon : \tilde{\mathcal{O}}_{P_\varepsilon} \longrightarrow \mathbb{R}^3 \times \mathbb{T}_T \quad (6.3.13)$$

as

$$P_\varepsilon(\tilde{\omega}) = \begin{cases} P_\varepsilon^+ \circ P_\varepsilon^-(\tilde{\omega}) & \text{if } \tilde{\omega} \in \tilde{\mathcal{O}}_{P_\varepsilon^-} \\ P_\varepsilon^- \circ P_\varepsilon^+(\tilde{\omega}) & \text{if } \tilde{\omega} \in \tilde{\mathcal{O}}_{P_\varepsilon^+} \end{cases} \quad (6.3.14)$$

The domain $\tilde{\mathcal{O}}_{P_\varepsilon}$ is defined as

$$\tilde{\mathcal{O}}_{P_\varepsilon} = \left\{ \tilde{\omega} = (v, x, y, s) \in ([-v_2, -v_1] \cup [v_1, v_2]) \times \mathbb{R}^2 \times \mathbb{T}_T \mid \Pi_x \left(\tilde{\phi}(t; (0, \tilde{\omega}); \varepsilon) \right) \neq 0 \forall t \in [0, \Pi_s(P_\varepsilon(\tilde{\omega})) - s] \right\}$$

and is formed by four connected subsets located in $[v_1, v_2] \times \mathbb{R}^2 \times \mathbb{T}_T$ and $[-v_2, -v_1] \times \mathbb{R}^2 \times \mathbb{T}_T$ which will be more precisely described in §6.3.2.

As we did for the maps P_0^\pm , if $\varepsilon = 0$ we can also obtain a closed expression for the map P_0 ,

$$P_0(v, x, y, s) = (v, \phi_{\mathcal{X}}(\alpha(v); x, y), s + \alpha(v)),$$

where

$$\alpha(v) = \tilde{\alpha}^+(|v|) + \alpha^-(-|v|) \quad (6.3.15)$$

is the period of the periodic orbit Λ_c , with $c = U(0, v)$, that system (6.2.4) possesses, and $\phi_{\mathcal{X}}(t; x, y)$ is $\phi_{\mathcal{X}}^+(t; x, y)$ if $(x, y) \in \Sigma^+ \cup S^+$ and $\phi_{\mathcal{X}}^-(t; x, y)$ if $(x, y) \in \Sigma^- \cup S^-$.

Note that the map P_ε is invertible in $\tilde{\mathcal{O}}_{P_\varepsilon^{-1}} := P_\varepsilon(\tilde{\mathcal{O}}_{P_\varepsilon})$ and hence it has sense to consider

$$P_\varepsilon^{-1} : \tilde{\mathcal{O}}_{P_\varepsilon^{-1}} \subset \mathbb{R}^3 \times \mathbb{T}_T \longrightarrow \mathbb{R}^3 \times \mathbb{T}_T. \quad (6.3.16)$$

Remark 6.3.2. *The maps P_ε^+ , P_ε^- , P_ε and P_ε^{-1} are regular maps in their respective domains, and are as smooth as the flows $\tilde{\phi}^{\pm\pm}(t; \tilde{z}; \varepsilon)$ restricted to $S^\pm \times S^\pm \times \mathbb{T}_T$, respectively. However, the maps κ_ε , $\bar{\kappa}_\varepsilon$ are also regular but when restricted to $\tilde{\mathcal{O}}_{\kappa_\varepsilon} \setminus \tilde{\Sigma}$ and $\tilde{\mathcal{O}}_{\bar{\kappa}_\varepsilon} \setminus \tilde{\Sigma}$.*

Remark 6.3.3. *The formulas provided for the definition of the maps κ_ε , $\bar{\kappa}_\varepsilon$ and P_ε^\pm can be applied beyond the domains $\tilde{\mathcal{O}}_{\kappa_\varepsilon}$, $\tilde{\mathcal{O}}_{\bar{\kappa}_\varepsilon}$ and $\tilde{\mathcal{O}}_{P_\varepsilon^\pm}$. However, the relation with the real dynamics of the system is lost, as the respective flows $\tilde{\phi}^{\pm\pm}$ are applied outside the domains given in (6.2.14), where they are used as flows of system (6.2.14).*

6.3.2 The domains of the maps

We now describe with a little more detail the sets $\tilde{\mathcal{O}}_{\kappa_\varepsilon}$, $\tilde{\mathcal{O}}_{\bar{\kappa}_\varepsilon}$, $\tilde{\mathcal{O}}_{P_\varepsilon^\pm}$ and $\tilde{\mathcal{O}}_{P_\varepsilon}$ where we have defined the maps κ_ε , $\bar{\kappa}_\varepsilon$, P_ε^\pm and P_ε , respectively.

As described in the previous section, these are given by points whose trajectories first impact with the switching surface given by $u = 0$ ($\tilde{\Sigma}$) rather than the one given by $x = 0$. In general, this implies that such points have to be isolated enough from the switching manifold $\mathbb{R}^2 \times \Sigma \times \mathbb{T}_T$.

Due to the form of the Hamiltonian X given in (6.2.5), for $\varepsilon \geq 0$ small enough the flow crosses the switching manifold $x = 0$ increasing x when $y > 0$ and decreasing x for $y < 0$. Hence, the points in $\tilde{\mathcal{O}}_{P_\varepsilon^+}$, $\tilde{\mathcal{O}}_{P_\varepsilon^-}$ and $\tilde{\mathcal{O}}_{\kappa_\varepsilon}$ can be arbitrarily close to $x = 0$ when $xy \geq 0$ (first and third quadrants of the $x - y$ plane), even containing some part of the segment $x = 0$, but not when $xy < 0$. Due to the backwards integration of the flow used in the map $\bar{\kappa}_\varepsilon$, this is precisely the contrary for the set $\tilde{\mathcal{O}}_{\bar{\kappa}_\varepsilon}$.

In any case, this implies that all sets $\tilde{\mathcal{O}}_{P_\varepsilon^+}$, $\tilde{\mathcal{O}}_{P_\varepsilon^-}$, $\tilde{\mathcal{O}}_{\kappa_\varepsilon}$ and $\tilde{\mathcal{O}}_{\bar{\kappa}_\varepsilon}$ consist on two connected components separated by the switching manifold given by $x = 0$, $\mathbb{R}^2 \times \Sigma \times \mathbb{T}_T$.

How these sets are separated from $x = 0$ depends on the time required to reach the switching manifold $u = 0$. For $\varepsilon = 0$ the Hamiltonian H_0 does not depend on s and systems \mathcal{U} and \mathcal{X} are uncoupled. Hence this time, denoted as $\alpha^\pm(v)$ in (6.3.10)-(6.3.11), depends exclusively on the projection to the $u - v$ plane of the initial condition and a geometric description of the sets becomes much easier. We then look at these sets as

ε -perturbations of the ones for $\varepsilon = 0$, which we describe below.

We first focus on $\tilde{\mathcal{O}}_{P_0^+}$ ($\varepsilon = 0$), whose precise definition is given in (6.3.9).

Let $(v, x, y, s) \in \tilde{\mathcal{O}}_{P_0^+}$ with $s \in \mathbb{T}_T$ a free coordinate and v is such that $0 < \frac{v^2}{2} \leq \bar{c}$. This guarantees that the flow crosses the surface $\tilde{\Sigma}^-$ and hence the image of (x, y, v, s) by the map P_0^+ exists. Let $\alpha^+(v)$ be the time taken by the flow $\phi_{\mathcal{U}}^+(t; 0, v)$ to reach the section Σ^- , given in (6.3.10), and assume that it is an increasing function of $v > 0$. Hence, $v = \sqrt{2\bar{c}}$ leads to the largest time, $t_c^+ := \alpha^+(\sqrt{2\bar{c}})$, required to reach the section $\tilde{\Sigma}^-$ and thus represents the most restrictive situation to describe the projection to the plane $x - y$ of the set $\tilde{\mathcal{O}}_{P_0^+}$.

Consider any open neighbourhood \mathcal{V}^+ containing Q^+ such that

$$\phi_{\mathcal{X}}^+(t_c^+; \mathcal{V}^+) \subset S^+.$$

Note that this set is not empty, as points arbitrarily close to Q^+ take arbitrarily large time by the flow $\phi_{\mathcal{X}}$ to reach $x = 0$.

Then, the set

$$\Sigma^+ \times \mathcal{V}^+ \times \mathbb{T}_T$$

which does not intersect with $x = 0$, is contained in $\tilde{\mathcal{O}}_{P_0^+} \cap (\Sigma^+ \times S^+ \times \mathbb{T}_T)$.

Also $\tilde{\mathcal{O}}_{P_0^+} \cap (\Sigma^+ \times S^+ \times \mathbb{T}_T)$ contains the set

$$\Sigma^+ \times \left(\bigcup_{t \leq 0} \phi_{\mathcal{X}}^+(t; \mathcal{V}^+) \cap S^+ \right) \times \mathbb{T}_T,$$

which reaches $x = 0$ and contains $\Sigma^+ \times (W^s(Q^+) \cap S^+) \times \mathbb{T}_T$.

Similarly, one can construct a tubular neighbourhood containing $\Sigma^+ \times Q^- \times \mathbb{T}_T$, $\Sigma^+ \times W^s(Q^-) \times \mathbb{T}_T$ and a piece of $\Sigma^+ \times W^u(Q^-) \times \mathbb{T}_T$ which is contained in $\tilde{\mathcal{O}}_{P_0^+} \cap (\Sigma^+ \times S^- \times \mathbb{T}_T)$.

This gives us a sketch of the two connected components that compound $\tilde{\mathcal{O}}_{P_0^+}$.

As mentioned above, we have considered the most restrictive situation given by $v = \sqrt{2\bar{c}}$. This means that, as long as $v > 0$ is decreased, the time needed to reach $u = 0$ decreases and the tubular sets described above become thicker and larger.

A very similar description applies to $\tilde{\mathcal{O}}_{P_0^-}$ but arguing with $\alpha^-(-\sqrt{2\bar{c}})$, where $\alpha^-(-v)$ is the time needed by the flow $\phi_{\mathcal{U}}^-(t; 0, -v)$ to reach the section Σ^+ , and is given in (6.3.11).

Taking into account expression (6.3.13), set $\tilde{\mathcal{O}}_{P_0}$ is given by the union of two smaller sets contained in $\tilde{\mathcal{O}}_{P_0^+}$ and $\tilde{\mathcal{O}}_{P_0^-}$. Therefore, $\tilde{\mathcal{O}}_{P_0}$ has four connected components located in

$$\begin{aligned} & \Sigma^+ \times S^+ \times \mathbb{T}_T \\ & \Sigma^+ \times S^- \times \mathbb{T}_T \\ & \Sigma^- \times S^+ \times \mathbb{T}_T \\ & \Sigma^- \times S^- \times \mathbb{T}_T. \end{aligned}$$

Regarding $\tilde{\mathcal{O}}_{\kappa_0}$, it has a similar shape in the (x, y) coordinates as the one described above. However, as we have defined κ_0 to be the identity in $\tilde{\Sigma}$, the description given above of the projection onto the $x - y$ plane applies for $\tilde{\mathcal{O}}_{\kappa_0}$ for points outside $\tilde{\Sigma}$ ($u \neq 0$). For points in $\tilde{\Sigma}$, the projection of $\tilde{\mathcal{O}}_{\kappa_0}$ onto the $x - y$ plane becomes \mathbb{R}^2 .

6.3.3 Impact sequence

Let $(v, x, y, s) \in \tilde{\mathcal{O}}_{P_\varepsilon}$ and $\varepsilon \geq 0$ small enough. Proceeding similarly as in [Hog89, GHS12], we define the direct sequence of impacts associated with the section $\tilde{\Sigma}$, $(v_\varepsilon^i, x_\varepsilon^i, y_\varepsilon^i, s_\varepsilon^i)$, as

$$(v_\varepsilon^i, x_\varepsilon^i, y_\varepsilon^i, s_\varepsilon^i) = \begin{cases} P_\varepsilon^+ (v_\varepsilon^{i-1}, x_\varepsilon^{i-1}, y_\varepsilon^{i-1}, s_\varepsilon^{i-1}) & \text{if } (v_\varepsilon^{i-1}, x_\varepsilon^{i-1}, y_\varepsilon^{i-1}, s_\varepsilon^{i-1}) \in \tilde{\mathcal{O}}_{P_\varepsilon^+} \\ P_\varepsilon^- (v_\varepsilon^{i-1}, x_\varepsilon^{i-1}, y_\varepsilon^{i-1}, s_\varepsilon^{i-1}) & \text{if } (v_\varepsilon^{i-1}, x_\varepsilon^{i-1}, y_\varepsilon^{i-1}, s_\varepsilon^{i-1}) \in \tilde{\mathcal{O}}_{P_\varepsilon^-}, \end{cases} \quad (6.3.17)$$

with $i \geq 0$ and $(v_\varepsilon^0, x_\varepsilon^0, y_\varepsilon^0, s_\varepsilon^0) = (v, x, y, s)$.

We also define the inverse sequence of impacts, if they exist, as

$$(v_\varepsilon^i, x_\varepsilon^i, y_\varepsilon^i, s_\varepsilon^i) = \begin{cases} (P_\varepsilon^+)^{-1} (v_\varepsilon^{i+1}, x_\varepsilon^{i+1}, y_\varepsilon^{i+1}, s_\varepsilon^{i+1}) & \text{if } (v_\varepsilon^{i+1}, x_\varepsilon^{i+1}, y_\varepsilon^{i+1}, s_\varepsilon^{i+1}) \in P_\varepsilon^+(\tilde{\mathcal{O}}_{P_\varepsilon^+}) \\ (P_\varepsilon^-)^{-1} (v_\varepsilon^{i+1}, x_\varepsilon^{i+1}, y_\varepsilon^{i+1}, s_\varepsilon^{i+1}) & \text{if } (v_\varepsilon^{i+1}, x_\varepsilon^{i+1}, y_\varepsilon^{i+1}, s_\varepsilon^{i+1}) \in P_\varepsilon^-(\tilde{\mathcal{O}}_{P_\varepsilon^-}), \end{cases} \quad (6.3.18)$$

with $i < 0$.

In general, this is a finite sequence, and is defined up to the n th iterate such that

$$\begin{aligned} (v_\varepsilon^n, x_\varepsilon^n, y_\varepsilon^n, s_\varepsilon^n) &\notin \tilde{\mathcal{O}}_{P_\varepsilon^+} \cup \tilde{\mathcal{O}}_{P_\varepsilon^-}, \quad n > 0 \\ (v_\varepsilon^n, x_\varepsilon^n, y_\varepsilon^n, s_\varepsilon^n) &\notin P_\varepsilon^-(\tilde{\mathcal{O}}_{P_\varepsilon^-}) \cup P_\varepsilon^+(\tilde{\mathcal{O}}_{P_\varepsilon^+}), \quad n < 0 \end{aligned}$$

That is, we consider all the impacts with the switching surface given by $u = 0$ of the trajectory associated with system (6.2.14) with initial condition $(0, v, x, y, s)$ that are previous to the first impact with the surface $x = 0$, both forwards and backwards in time. When this occurs, then it is possible to extend the sequence by properly concatenating the flow $\tilde{\phi}$ after such crossing. However, if we allowed the switching manifold $x = 0$ to be crossed between two elements of the impact sequence associated with $u = 0$, then the elements $(v_\varepsilon^i, x_\varepsilon^i, y_\varepsilon^i, s_\varepsilon^i)$ wouldn't be given by the smooth maps P_ε^\pm . Moreover, as the number of times that the switching manifold $x = 0$ would be crossed between the impacts $(v_\varepsilon^i, x_\varepsilon^i, y_\varepsilon^i, s_\varepsilon^i)$ and $(v_\varepsilon^{i+1}, x_\varepsilon^{i+1}, y_\varepsilon^{i+1}, s_\varepsilon^{i+1})$ is unknown and may arbitrarily large, such transition wouldn't be smooth, which is a property from we will later profit.

When $\varepsilon = 0$, of special interest will be the impact sequence associated with a point of the type

$$(v, 0, y_h, s) \in \tilde{\mathcal{O}}_{P_\varepsilon}$$

fulfilling

$$U(0, v) = c, \quad 0 < c < \bar{c},$$

and where $(0, y_h) = \sigma^{\text{up}}(0)$ is the intersection of the heteroclinic orbit of system \mathcal{X} , defined in (6.2.10)-(6.2.11), with the switching curve Σ . Hence, recalling that for the unperturbed case system (6.2.14) consists on the two uncoupled systems (6.2.3) and (6.2.4) plus the time variable s , the impact sequence of such a point is defined for all $i \in \mathbb{Z}$, because, as $(0, y_h) \in W^s(Q^+) \cap W^u(Q^-)$, the switching manifold $x = 0$ is never crossed again by the orbit of $(0, v, 0, y_h, s)$, neither forwards nor backwards in time. Moreover, assuming $v > 0$, and recalling that $(v_0^i, x_0^i, y_0^i, s_0^i) = (v, 0, y_h, s)$, it has the following expression,

$$(v_0^i, x_0^i, y_0^i, s_0^i) = \begin{cases} (-v, \sigma^{\text{up}}(s_0^{i-1} - s + \alpha^+(v)), s_0^{i-1} + \alpha^+(v)) & \text{for } i \text{ odd} \\ (v, \sigma^{\text{up}}(s_0^{i-1} - s + \alpha^-(-v)), s_0^{i-1} + \alpha^-(-v)) & \text{for } i \text{ even} \end{cases} \quad (6.3.19)$$

if $i > 0$, and

$$(v_0^i, x_0^i, y_0^i, s_0^i) = \begin{cases} (-v, \sigma^{\text{up}}(s_0^{i+1} - s - \alpha^-(-v)), s_0^{i+1} - \alpha^-(-v)) & \text{for } i \text{ odd} \\ (v, \sigma^{\text{up}}(s_0^{i+1} - s - \alpha^+(v)), s_0^{i+1} - \alpha^+(v)) & \text{for } i \text{ even} \end{cases} \quad (6.3.20)$$

if $i < 0$, where $\sigma^{\text{up}}(t)$ parametrizes the upper heteroclinic connection given in (6.2.10)-(6.2.11), and $\alpha^\pm(\pm v)$ are defined in (6.3.10) and (6.3.11).

Remark 6.3.4. *If $v < 0$, then one just have to replace α^\pm by α^\mp in expressions (6.3.19) and (6.3.20).*

6.3.4 Explicit expressions for the flows

Although the general solution of system (6.2.14) was already described in §6.2, the impact sequence defined in §6.3.3 permits us to provide explicit expressions for ϕ as long as the switching manifold $x = 0$ is not crossed. In this case, one has only to take into account the crossings with the switching surface given by $u = 0$, $\tilde{\Sigma}$, which are determined by the impact sequence.

For $\varepsilon > 0$ small enough, we first consider an initial condition $\tilde{z}_0 = (0, \tilde{\omega}_0)$, $\tilde{\omega}_0 \in \tilde{\mathcal{O}}_{P_\varepsilon}$, and the (direct and inverse) impact sequence $(v_\varepsilon^i, x_\varepsilon^i, y_\varepsilon^i, s_\varepsilon^i)$ associated with $\tilde{\omega}_0$. As mentioned above, this is in general a finite sequence. This is due to the fact that the flow eventually crosses the switching manifold given by $x = 0$. In addition, it may also happen that the flow does not cross $u = 0$ again; this would also make the impact sequence to be finite.

Hence, we assume that there exist natural numbers $-n_2, n_1 \in \mathbb{N}$ restricting the length of

the impact sequence, $-n_2 \leq i \leq n_1$. If this switching manifold is not crossed forwards or backwards in time, then we consider $n_2 = \infty$ or $n_1 = \infty$, respectively. For instance, assuming that $\tilde{z}_0 \in \Sigma^+ \times S^+ \times \mathbb{T}_T$, the flow $\tilde{\phi}(t; \tilde{z}_0; \varepsilon)$ such that $\tilde{\phi}(0; \tilde{z}_0; \varepsilon) = \tilde{z}_0$ becomes

$$\tilde{\phi}(t; \tilde{z}_0; \varepsilon) = \begin{cases} \tilde{\phi}^{++}(t + s_0 - s_\varepsilon^{2i}; 0, v_\varepsilon^{2i}, x_\varepsilon^{2i}, y_\varepsilon^{2i}, s_\varepsilon^{2i}; \varepsilon) & \text{if } s_\varepsilon^{2i} \leq t + s_0 < s_\varepsilon^{2i+1} \\ \tilde{\phi}^{-+}(t + s_0 - s_\varepsilon^{2i+1}; 0, v_\varepsilon^{2i+1}, x_\varepsilon^{2i+1}, y_\varepsilon^{2i+1}, s_\varepsilon^{2i+1}; \varepsilon) & \text{if } s_\varepsilon^{2i+1} \leq t + s_0 < s_\varepsilon^{2i+2}, \end{cases} \quad (6.3.21)$$

with

$$-n_2 \leq 2i, 2i + 1 \leq n_1.$$

Remark 6.3.5. *In general, $\tilde{\omega}_0$ can belong to any of the four connected components of $\tilde{\mathcal{O}}_{P_\varepsilon}$ described in §6.3.2. Hence, there exist in fact four different expressions for the flow given in (6.3.21). Assuming in general that $\tilde{z}_0 = (0, \tilde{\omega}_0) \in \Sigma^\pm \times S^\pm \times \mathbb{T}_T$, these are obtained by replacing the flow in the first branch of (6.3.21) by $\phi^{\pm\pm}$, and the one in the second one by $\phi^{\mp\pm}$.*

If the initial condition \tilde{z}_0 does not belong to the switching manifold $\tilde{\Sigma}$, we can make use of the maps κ_ε and $\bar{\kappa}_\varepsilon$ in order to provide an explicit expression for the flow $\phi(t; \tilde{z}_0; \varepsilon)$ through the impact sequences of the points $\kappa_\varepsilon(\tilde{z}_0)$ and/or $\bar{\kappa}_\varepsilon(\tilde{z}_0)$ as follows.

Let $\varepsilon > 0$ be small enough and let us assume that $\tilde{z}_0 \in \tilde{\mathcal{O}}_{\kappa_\varepsilon} \cap \tilde{\mathcal{O}}_{\bar{\kappa}_\varepsilon}$ and that the points

$$\tilde{\omega}_1 := \kappa_\varepsilon(\tilde{z}_0) \quad (6.3.22)$$

$$\tilde{\omega}_2 := \bar{\kappa}_\varepsilon(\tilde{z}_0) \quad (6.3.23)$$

fulfill

$$\tilde{\omega}_1 \in \tilde{\mathcal{O}}_{P_\varepsilon} \quad (6.3.24)$$

$$\tilde{\omega}_2 \in \tilde{\mathcal{O}}_{P_\varepsilon^{-1}}. \quad (6.3.25)$$

We now use the impact sequences of the points $\tilde{\omega}_1$ and $\tilde{\omega}_2$ in order to give an explicit expression of $\tilde{\phi}(t; \tilde{z}_0; \varepsilon)$ for $t \geq 0$ and $t < 0$, respectively. Using that

$$\tilde{z}_1 = \phi(\Pi_s(\tilde{\omega}_1) - \Pi_s(\tilde{\omega}_2); \tilde{z}_2; \varepsilon),$$

where

$$\begin{aligned} \tilde{z}_1 &= (0, \tilde{\omega}_1) \\ \tilde{z}_2 &= (0, \tilde{\omega}_2), \end{aligned}$$

the impact sequences $(v_\varepsilon^{i,j}, x_\varepsilon^{i,j}, y_\varepsilon^{i,j}, s_\varepsilon^{i,j})$ associated with $\tilde{\omega}_j$, $j = 1, 2$, are related by

$$(v_\varepsilon^{i,1}, x_\varepsilon^{i,1}, y_\varepsilon^{i,1}, s_\varepsilon^{i,1}) = (v_\varepsilon^{i+1,2}, x_\varepsilon^{i+1,2}, y_\varepsilon^{i+1,2}, s_\varepsilon^{i+1,2}).$$

Hence, it is possible to proceed with the direct and inverse sequence associated with only one point. However, as we will have to use a similar trick in §6.4.1, we prefer to use here the direct and inverse impact sequences of $\tilde{\omega}_1$ and $\tilde{\omega}_2$, defined in (6.3.17) and (6.3.18), respectively. Note that conditions (6.3.24) and (6.3.25) ensure us that these are not empty.

Let $(v_\varepsilon^{i,1}, x_\varepsilon^{i,1}, y_\varepsilon^{i,1}, s_\varepsilon^{i,1})$, $0 \leq i < n_1$ be the impact sequence associated with \tilde{z}_1 , where $n_1 > 0$ is given by the last element of the sequence before the section $x = 0$ is crossed. If it does not occur, then we consider $n_1 = \infty$.

Let also $(v_\varepsilon^{i,2}, x_\varepsilon^{i,2}, y_\varepsilon^{i,2}, s_\varepsilon^{i,2})$, $n_2 < i \leq 0$, be the impact sequence associated with \tilde{z}_2 , where $n_2 < 0$ is given by the last element of the sequence (backwards in time) before the section $x = 0$ is crossed. If it does not exist, we then consider $n_2 = -\infty$.

As an example, let us suppose that $\tilde{z}_0 \in S^+ \times S^+ \times \mathbb{T}_T$ and therefore $\tilde{z}_1 \in \Sigma^- \times S^+ \times \mathbb{T}_T$ and $\tilde{z}_2 \in \Sigma^+ \times S^+ \times \mathbb{T}_T$. Then, for $t \in [s_\varepsilon^{n_2,2} - s_0, s_\varepsilon^{n_1,1} - s_0)$, we can write the flow $\tilde{\phi}(t; \tilde{z}_0; \varepsilon)$, fulfilling $\tilde{\phi}(0; \tilde{z}_0; \varepsilon) = \tilde{z}_0$, as

$$\tilde{\phi}(t; \tilde{z}_0; \varepsilon) = \begin{cases} \tilde{\phi}(t + s_0 - s_\varepsilon^{0,2}; \tilde{z}_2; \varepsilon) & \text{if } s_\varepsilon^{n_2,2} \leq t + s_0 < s_\varepsilon^{0,2} \\ \tilde{\phi}^{++}(t; \tilde{z}_0; \varepsilon) & \text{if } s_\varepsilon^{0,2} \leq t + s_0 < s_\varepsilon^{0,1} \\ \tilde{\phi}(t + s_0 - s_\varepsilon^{0,1}; \tilde{z}_1; \varepsilon) & \text{if } s_\varepsilon^{0,1} \leq t + s_0 < s_\varepsilon^{n_1,1}, \end{cases} \quad (6.3.26)$$

where $\tilde{\phi}^{++}$ is the smooth flow associated with the respective domain in Eq. (6.2.14) and $\tilde{\phi}(t; \tilde{z}_i; \varepsilon)$ is given in (6.3.21).

Similarly, if $\tilde{z}_0 \in S^\pm \times S^\pm \times \mathbb{T}_T$, the explicit expression for $\tilde{\phi}(t; \tilde{z}_0; \varepsilon)$ becomes the same as in (6.3.26) but replacing $\tilde{\phi}^{++}$ with $\tilde{\phi}^{\pm\pm}$.

Note that this definition of $\tilde{\phi}$ is defined only as long as the impact manifold given by $x = 0$ is not crossed. We now extend it for initial conditions at $x = 0$. Hence, let us consider initial conditions of the form

$$\tilde{z}_0 = (u_0, v_0, 0, y_0, s_0), U(u_0, v_0) < \bar{c}, y_0 > 0. \quad (6.3.27)$$

Such a type of initial conditions will play an important role in §6.4.

In this case, as \tilde{z}_0 belongs to the switching manifold given by $x = 0$, by using the impact sequences associated with the points \tilde{z}_i given in (6.3.22)-(6.3.23), expression (6.3.26) provides us an explicit expression for the flow $\phi(t; \tilde{z}_0; \varepsilon)$ allowing it to cross the switching

manifold given by $x = 0$. For instance, assuming $\tilde{z}_0 \in S^+ \times \Sigma^- \times \mathbb{T}_T$ ($u_0 > 0$), it becomes

$$\tilde{\phi}(t; \tilde{z}; \varepsilon) = \begin{cases} \tilde{\phi}(t + s_0 - s_\varepsilon^{0,2}; \tilde{z}_2; \varepsilon) & \text{if } s_\varepsilon^{n_2,2} \leq t + s_0 < s_\varepsilon^{0,2} \\ \tilde{\phi}^{+-}(t; \tilde{z}_0; \varepsilon) & \text{if } s_\varepsilon^{0,2} \leq t + s_0 < s_0 \\ \tilde{\phi}^{++}(t; \tilde{z}_0; \varepsilon) & \text{if } s_0 \leq t + s_0 < s_\varepsilon^{0,1} \\ \tilde{\phi}(t + s_0 - s_\varepsilon^{0,1}; \tilde{z}_1; \varepsilon) & \text{if } s_\varepsilon^{0,1} \leq t + s_0 < s_\varepsilon^{n_1,1}. \end{cases} \quad (6.3.28)$$

As before, depending on the signs of u_0 and y_0 , $\tilde{z}_0 \in S^\pm \times \Sigma^\pm \times \mathbb{T}_T$ and the respective expression is obtained by replacing in (6.3.28) $\tilde{\phi}^{++}$ by $\tilde{\phi}^{\pm\pm}$ and $\tilde{\phi}^{+-}$ by $\tilde{\phi}^{\pm\mp}$.

In general, the impact sequences associated with the points \tilde{z}_1 and \tilde{z}_2 will be finite sequences ($n_1 < \infty$ and $n_2 > -\infty$).

For $\varepsilon = 0$, the unique points for which the expression of the flow given in (6.3.28) is valid for any $t \in \mathbb{R}$ are the heteroclinic points $\tilde{z}_0 = (u_0, v_0, 0, y_h, s_0)$, with $U(u_0, v_0) < \bar{c}$ and $s_0 \in \mathbb{T}_T$. Then $\tilde{z}_1 \in \mathbb{R}^2 \times W^s(Q^+) \times \mathbb{T}_T$ and $\tilde{z}_2 \in \mathbb{R}^2 \times W^u(Q^-) \times \mathbb{T}_T$ and the iterates of their associated impact sequences are all defined, forwards and backwards in time, respectively.

In this case, if for instance $u_0 > 0$, then $v_0^{0,2} > 0$ and $v_0^{0,1} < 0$ and Eq. (6.3.28) takes the form

$$\begin{aligned} \tilde{\phi}(t; 0, v_0, 0, y_h, s_0; 0) = & \\ \left\{ \begin{array}{ll} (\phi_{\mathcal{U}}^+(t + s_0 - s_0^{2j,2}; 0, v_0^{2j,2}), \sigma^{\text{up}}(t), s_0 + t) & \text{if } s_0^{2j,2} \leq t + s_0 < s_0^{2j+1,2} \\ (\phi_{\mathcal{U}}^-(t + s_0 - s_0^{2j+1,2}; 0, v_0^{2j+1,2}), \sigma^{\text{up}}(t), s_0 + t) & \text{if } s_0^{2j+1,1} \leq t + s_0 < s_0^{2j+2} \\ (\phi_{\mathcal{U}}^+(t + s_0 - s_0^{0,2}; 0, v_0^{0,2}), \sigma^{\text{up}}(t), s_0 + t) & \\ = (\phi_{\mathcal{U}}^+(t; u_0, v_0), \sigma^{\text{up}}(t), s_0 + t) & \text{if } s_0^{0,2} \leq t + s_0 < s_0^{0,1} \\ (\phi_{\mathcal{U}}^-(t + s_0 - s_0^{2i,1}; 0, v_0^{2i,1}), \sigma^{\text{up}}(t), s_0 + t) & \text{if } s_0^{2i,1} \leq t + s_0 < s_0^{2i+1,1} \\ (\phi_{\mathcal{U}}^+(t + s_0 - s_0^{2i+1,1}; 0, v_0^{2i+1,1}), \sigma^{\text{up}}(t), s_0 + t) & \text{if } s_0^{2i+1,1} \leq t + s_0 < s_0^{2i+2}. \end{array} \right. \quad (6.3.29) \end{aligned}$$

with

$$\begin{aligned} 0 &\leq 2i, 2i + 1 < \infty \\ -\infty &< 2j, 2j + 1 \leq 0. \end{aligned}$$

Analogously if $u_0 < 0$.

6.3.5 Perturbative formulas

As we will see in §6.3.6, in the unperturbed case, the existence of heteroclinic manifolds in system (6.2.14) will be given by the heteroclinic manifold $W^u(Q^-) = W^s(Q^+)$. As this heteroclinic will intersect transversally the switching manifold given by $x = 0$, so will also

the stable and unstable manifolds that we will show that exist for $\varepsilon > 0$. Hence, in §6.4.1, in order to find suitable heteroclinic connections, we will be interested on measuring the distance between points belonging to stable and unstable manifolds at their intersection with the switching surface $x = 0$. As we will show in §6.4.1, the heteroclinic connections will be found by using Melnikov-like arguments, involving the integral of Poisson brackets between the unperturbed and perturbed Hamiltonians along trajectories to measure such distances.

Taking into account that these trajectories will be given by initial conditions at the switching manifold $x = 0$, and hence by points of the form (6.3.27),

$$\tilde{z}_0 = (u_0, v_0, 0, y_0, s_0), \quad U(u_0, v_0) < \bar{c}, \quad y_0 > 0,$$

the integrals

$$\int_{t_i}^{t_f} \{X, h\} \left(\tilde{\phi}(t; \tilde{z}_0; \varepsilon) \right) dt \quad (6.3.30)$$

$$\int_{\bar{t}_i}^{\bar{t}_f} \{U, h\} \left(\tilde{\phi}(t; \tilde{z}_0; \varepsilon) \right) dt, \quad (6.3.31)$$

for some suitable $t_i, t_f, \bar{t}_i, \bar{t}_f$, have to be considered as piecewise integrals regarding the expression of the flow given in (6.3.28). These pieces are separated by the intervals $[s_\varepsilon^{i,k}, s_\varepsilon^{i+1,k})$, $k = 1, 2$, given by the impact sequences associated with the points $\tilde{\omega}_1 = \kappa_\varepsilon(\tilde{z}_0)$ and $\tilde{\omega}_2 = \bar{\kappa}_\varepsilon(\tilde{z}_0)$. Note that, at each interval, one does not only have to distinguish between the flows $\phi^{\pm\pm}$, but also between the integrands $\{X^\pm, h\}$ and $\{U^\pm, h\}$.

For the case of the Poisson bracket $\{X, h\}$, by the definition of the impact sequence, the impact manifold $x = 0$ is only crossed for $t = 0$, and the integral (6.3.30) can be separated in two piecewise integrals of as follows

$$\begin{aligned} \int_{s_\varepsilon^{j,2}}^{s_\varepsilon^{i,1}} \{X, h\} (\phi(t; \tilde{z}_0; \varepsilon)) dt &= \int_{s_\varepsilon^{j,2}}^0 \{X^-, h\} (\phi(t; \tilde{z}_0; \varepsilon)) dt \\ &+ \int_0^{s_\varepsilon^{i,1}} \{X^+, h\} (\phi(t; \tilde{z}_0; \varepsilon)) dt. \end{aligned}$$

Let us emphasize that in both integrals the flow crosses the switching manifold given by $u = 0$ at every impact time $s_\varepsilon^{l,k}$. Therefore, both integrals consist on a sum of j integrals over $\tilde{\phi}^{-\pm}$ and i integrals over $\tilde{\phi}^{+\pm}$.

For the case of $\{U, h\}$, one has to consider that the switching manifold $u = 0$ is crossed at every impact. Hence, not only the flow but the integrand changes between $\{U^+, h\}$ and $\{U^-, h\}$ at each integrating interval.

The following lemma provides us formulas for the unperturbed Hamiltonian X evaluated at points at the switching manifold $\tilde{\Sigma}$. These will be used later on §6.4.1 to obtain

expressions for the distance between points in the switching manifold given by $x = 0$ through the projection by κ_ε and $\bar{\kappa}_\varepsilon$. As remarked below, in Remark 6.3.7, similar formulas can be obtained for the Hamiltonian U .

Lemma 6.3.1. *Let us consider a point*

$$\tilde{\omega} \in \tilde{\mathcal{O}}_{P_\varepsilon} \cap \tilde{\mathcal{O}}_{P_\varepsilon^{-1}}$$

and $\tilde{z} = (0, \tilde{\omega})$ in the extended phase space, and let $(v_\varepsilon^i, x_\varepsilon^i, y_\varepsilon^i, s_\varepsilon^i)$ ($n_2 \leq i \leq n_1$, $n_2 < 0$ and $n_1 > 0$) be it's (direct and inverse) impact sequence. Then, it holds that

$$\begin{aligned} X(\tilde{\omega}) &:= X(\Pi_x(\tilde{\omega}), \Pi_y(\tilde{\omega})) \\ &= \varepsilon \int_{s_\varepsilon^i - s_\varepsilon^0}^0 \{X, h\} \left(\tilde{\phi}(t; \tilde{z}; \varepsilon) \right) dt + X(x_0^i, y_0^i) \end{aligned}$$

for any $n_2 \leq i \leq n_1$.

Proof. By a very straightforward piecewise-application of the fundamental theorem of calculus. \square

Remark 6.3.6. *The integral given in Lemma 6.3.1 is a piecewise integral separated by the intervals given by the impact sequence of $\tilde{\omega}$ (or \tilde{z}) as in Eq. (6.3.21). However, the integrand $\{X, h\}$ is kept constant, and is set to $\{X^+, h\}$ or $\{X^-, h\}$ depending on which component of the sets $\tilde{\mathcal{O}}_{P_\varepsilon^{-1}}$ and $\tilde{\mathcal{O}}_{P_\varepsilon}$ the point $\tilde{\omega}$ belongs to. As an example, if $\tilde{\omega} \in [v_1, v_2] \times S^+ \times \mathbb{T}_T$ (and therefore $\tilde{z} \in \Sigma^+ \times S^+ \times \mathbb{T}_T$), the flow with initial condition $\tilde{\omega}$ is given in (6.3.21). Then the expression provided by Lemma 6.3.1 becomes*

$$\begin{aligned} X(\tilde{\omega}) &:= X^-(\tilde{\omega}) \\ &= \varepsilon \sum_{i \leq 2k-1}^{k=0} \int_{s_\varepsilon^{2k-1} - s_\varepsilon^0}^{s_\varepsilon^{2k} - s_\varepsilon^0} \{X^-, h\} \left(\tilde{\phi}^{-+}(t - s_\varepsilon^{2k-1} + s_\varepsilon^0; (0, \tilde{\omega}^{2k-1}); \varepsilon) \right) dt \\ &\quad + \varepsilon \sum_{i \leq 2k}^{k=-1} \int_{s_\varepsilon^{2k} - s_\varepsilon^0}^{s_\varepsilon^{2k+1} - s_\varepsilon^0} \{X^-, h\} \left(\tilde{\phi}^{++}(t - s_\varepsilon^{2k} + s_\varepsilon^0; (0, \tilde{\omega}^{2k}); \varepsilon) \right) dt + X(\tilde{\omega}^i), \end{aligned}$$

for $n_2 \leq i \leq n_1$.

Remark 6.3.7. *A similar expression can be derived for $U(\tilde{\omega})$, which will be used in §6.4.2 to derive properties of the scattering map. However, by contrast to the case of the Hamiltonian X , the integrand $\{U, h\}$ changes as the flow between $\{U^+, h\}$ and $\{U^-, h\}$ at every interval conforming the integral given in Lemma 6.3.1.*

6.3.6 Invariant manifolds and their persistence

6.3.6.1 Unperturbed case in the extended phase space

Let us first focus on the invariant objects of system (6.2.14), relevant for our study, when $\varepsilon = 0$. As we work in the extended phase space to deal with the non-autonomous perturbation, we first embed the invariant objects described in 6.2.1.

The cross products of the hyperbolic critical points Q^\pm and the periodic orbits Λ_c give place to two families of invariant 2-dimensional tori of the form

$$\begin{aligned}\tilde{\mathcal{T}}_c^+ &= \Lambda_c \times Q^+ \times \mathbb{T}_T = \\ &\quad \{(u, v, x, y, s) \mid U(u, v) = c, (x, y) = Q^+, s \in \mathbb{T}_T\} \\ \tilde{\mathcal{T}}_c^- &= \Lambda_c \times Q^- \times \mathbb{T}_T = \\ &\quad \{(u, v, x, y, s) \mid U(u, v) = c, (x, y) = Q^-, s \in \mathbb{T}_T\},\end{aligned}\tag{6.3.32}$$

with $0 < c \leq \bar{c}$. These tori are only continuous manifolds, because of the singularity of the Hamiltonian U at $u = 0$. See Fig. 6.4.

Let us parametrize $\tilde{\mathcal{T}}_c$ by

$$\tilde{\mathcal{T}}_c^\pm = \{(\phi_U(\theta\alpha(v); 0, v), Q^\pm, s), \theta \in \mathbb{T}, v \in \mathbb{R}, U(0, v) = c, s \in \mathbb{T}_T\},\tag{6.3.33}$$

where $\alpha(v)$ is the period of the periodic orbit Λ_c given in Eq. (6.3.15), $\mathbb{T} = \mathbb{R} \setminus \mathbb{Z}$ is the usual circle and ϕ_U is the flow associated with system (6.2.4). Then the flow $\tilde{\phi}$ restricted to these tori becomes

$$\begin{aligned}\tilde{\phi}(t; \phi_U(\theta\alpha(v); 0, v), Q^\pm, s; 0) \\ = \left(\phi_U \left(\left(\theta + \frac{t}{\alpha(v)} \right) \alpha(v); 0, v \right), Q^\pm, s + t; 0 \right), \forall t \in \mathbb{R},\end{aligned}$$

and $\tilde{\mathcal{T}}_c$ is hence invariant.

Note that these tori have two different frequencies, $\frac{1}{\alpha(v)}$ for θ and 1 for s . In order to normalize, one could also consider a new parameter, $r = \frac{1}{T}$, such that $(\theta, r) \in \mathbb{T}^2$ with $\mathbb{T} = \mathbb{R} \setminus \mathbb{Z}$ the usual circle, with frequencies $(\frac{1}{\alpha(v)}, \frac{1}{T})$. We use however the original coordinate s .

For each of these invariant tori there exist 3-dimensional continuous manifolds

$$\begin{aligned}W^s(\tilde{\mathcal{T}}_c^+) &= W^u(\tilde{\mathcal{T}}_c^-) \\ &= \Lambda_c \times W^s(Q^-) \times \mathbb{T}_T = \Lambda_c \times W^u(Q^+) \times \mathbb{T}_T \\ &= \{(\phi_U(\theta\alpha(v); 0, v), \sigma^{\text{up}}(\xi), s), \mid U(0, v) = c, \theta \in \mathbb{T}, \xi \in (-\infty, \infty), s \in \mathbb{T}_T\},\end{aligned}$$

where $\sigma^{\text{up}}(\xi)$, given in (6.2.10)-(6.2.11), parametrizes the upper heteroclinic orbit of system \mathcal{X} (see Fig. 6.4). These manifolds are invariant and the flow $\tilde{\phi}$ restricted to them can

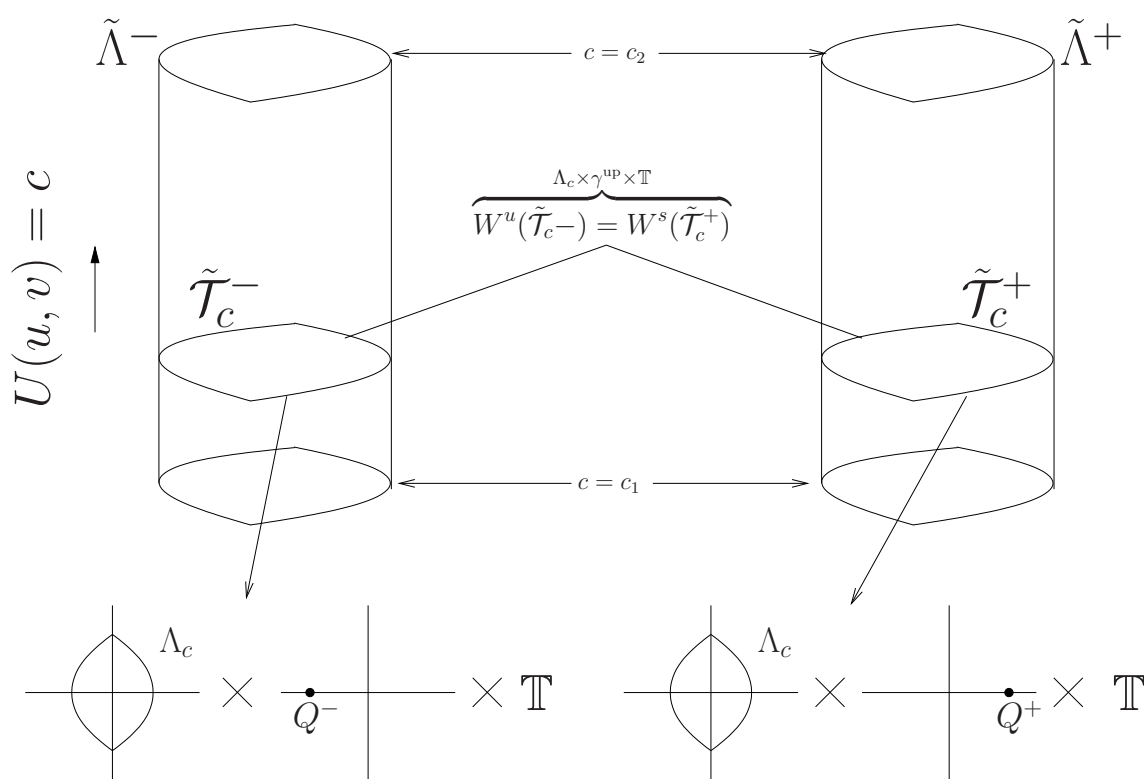


Figure 6.4: Scheme of the manifolds $\tilde{\Lambda}^\pm$, the tori $\tilde{\mathcal{T}}_c^\pm$ and their invariant manifolds.

be written as

$$\begin{aligned} & \tilde{\phi}(t; \phi_{\mathcal{U}}(\theta\alpha(v); 0, v), \sigma^{\text{up}}(\xi), s; 0) \\ &= \left(\phi_{\mathcal{U}} \left(\left(\theta + \frac{t}{\alpha(v)} \right) \alpha(v); 0, v \right), \sigma^{\text{up}}(\xi + t), s + t \right), \forall t \in \mathbb{R}, \end{aligned}$$

and they are hence invariant. Moreover, for any $\tilde{z} = (\phi_{\mathcal{U}}(\theta\alpha(v); 0, v), \sigma^{\text{up}}(\xi), s) \in W^s(\tilde{\mathcal{T}}_c^+) = W^u(\tilde{\mathcal{T}}_c^-)$, there exists two points

$$\tilde{z}^{\pm} = (\phi_{\mathcal{U}}(\theta\alpha(v); 0, v), Q^{\pm}, s) \in \tilde{\mathcal{T}}_c^{\pm}$$

such that

$$\lim_{t \rightarrow \pm\infty} \left| \tilde{\phi}(t; \tilde{z}; 0) - \tilde{\phi}(t; \tilde{z}^{\pm}; 0) \right| = \lim_{t \rightarrow \pm\infty} (0, 0, \sigma^{\text{up}}(\xi + t) - Q^{\pm}, 0) = 0.$$

In addition, as the points Q^{\pm} are hyperbolic for the flows $\phi_{\mathcal{X}}^{\pm}$, there exist then positive constants K^{\pm} and λ^{\pm} such that

$$\left| \phi(t; \tilde{z}; 0) - \phi(t; \tilde{z}^{\pm}; 0) \right| < K^{\pm} e^{-\lambda^{\pm}|t|}, \quad t \rightarrow \pm\infty. \quad (6.3.34)$$

Note that $\pm\lambda^+$ and $\pm\lambda^-$ are the eigenvalues of $D\mathcal{X}^+$ and $D\mathcal{X}^-$, respectively, which are opposite one to each other because $\phi_{\mathcal{X}}^{\pm}$ are Hamiltonian flows.

Although $W^{u,s}(\tilde{\mathcal{T}}_c^{\pm})$ are just continuous manifolds, we will call them the stable and unstable manifolds of $\tilde{\mathcal{T}}_c^{\pm}$. As they coincide, the 3-dimensional continuous manifold

$$\tilde{\gamma}_c^{\text{up}} = W^s(\tilde{\mathcal{T}}_c^+) = W^u(\tilde{\mathcal{T}}_c^-)$$

will be a 2-dimensional heteroclinic manifold between the tori $\tilde{\mathcal{T}}_c^-$ and $\tilde{\mathcal{T}}_c^+$.

Analogously, the lower heteroclinic connection mentioned in condition C.2 leads also to similar heteroclinic manifolds between the tori $\tilde{\mathcal{T}}_c^{\pm}$. However, as it is enough for our purposes, we will focus from now on only on the heteroclinic manifold $\tilde{\gamma}_c^{\text{up}}$.

Following [DdLS00], considering all the tori $\tilde{\mathcal{T}}_c^+$ and $\tilde{\mathcal{T}}_c^-$ together we end up with two 3-dimensional continuous manifolds

$$\begin{aligned} \tilde{\Lambda}^+ &= \bigcup_{c \in [c_1, c_2]} \tilde{\mathcal{T}}_c^+ = \bigcup_{c \in [c_1, c_2]} Q^+ \times \Lambda_c \times \mathbb{T}_T \\ &= \left\{ (u, v, x, y, s), c_1 \leq U(u, v) \leq c_2, (x, y) = Q^+, s \in \mathbb{T}_T \right\} \\ &= \left\{ (\phi_{\mathcal{U}}(\theta\alpha(v); 0, v), Q^+, s), \theta \in \mathbb{T}, c_1 \leq U(0, v) \leq c_2, s \in \mathbb{T}_T \right\} \\ \tilde{\Lambda}^- &= \bigcup_{c \in [c_1, c_2]} \tilde{\mathcal{T}}_c^- = \bigcup_{c \in [c_1, c_2]} Q^- \times \Lambda_c \times \mathbb{T}_T \\ &= \left\{ (u, v, x, y, s), c_1 \leq U(u, v) \leq c_2, (x, y) = Q^-, s \in \mathbb{T}_T \right\} \\ &= \left\{ (\phi_{\mathcal{U}}(\theta\alpha(v); 0, v), Q^-, s), \theta \in \mathbb{T}, c_1 \leq U(0, v) \leq c_2, s \in \mathbb{T}_T \right\} \end{aligned} \quad (6.3.35)$$

with $0 < c_1 < c_2 < \bar{c}$, schematically shown in Fig. 6.4.

These manifolds have also 4-dimensional stable and unstable continuous manifolds that will consist on

$$\begin{aligned} W^s(\tilde{\Lambda}^+) &= W^u(\tilde{\Lambda}^-) = \bigcup_{c \in [c_1, c_2]} W^s(\tilde{\mathcal{T}}_c^+) = \bigcup_{c \in [c_1, c_2]} W^u(\tilde{\mathcal{T}}_c^-) \\ &= \{(\phi_{\mathcal{U}}(\theta\alpha(v); 0, v), \sigma^{\text{up}}(\xi), s), \theta \in \mathbb{T}, c_1 \leq U(0, v) \leq c_2, \xi \in \mathbb{R}, s \in \mathbb{T}_T\} \end{aligned} \quad (6.3.36)$$

where $\sigma^{\text{up}}(\xi)$, given in (6.2.10)-(6.2.11), parametrizes the upper unperturbed heteroclinic connections of system (6.2.3).

As they coincide, this will define a 4-dimensional heteroclinic continuous manifold between the manifolds $\tilde{\Lambda}^\pm$, to which we will refer as

$$\tilde{\gamma}^{\text{up}} := W^s(\tilde{\Lambda}^+) = W^u(\tilde{\Lambda}^-).$$

It will be convenient to write the manifolds $\tilde{\Lambda}^\pm$ in terms of a *reference manifold* N (see [DdlLS08]) as follows. Let

$$N = \{(\theta, v, s) \in \mathbb{T} \times [v_1, v_2] \times \mathbb{T}_T\} \quad (6.3.37)$$

where $c_i = U(0, v_i)$, and consider two homeomorphisms

$$\begin{aligned} F_0^\pm : \quad N &\longrightarrow \tilde{\Lambda}^\pm \\ (\theta, v, s) &\longmapsto (\phi_{\mathcal{U}}(\theta\alpha(v); 0, v), Q^\pm, s). \end{aligned} \quad (6.3.38)$$

Note that F_0^\pm are in fact diffeomorphisms as long as $\theta \in \left(0, \frac{\alpha^+(v)}{\alpha(v)}\right) \cup \left(\frac{\alpha^+(v)}{\alpha(v)}, 1\right)$ as $\phi_{\mathcal{U}}(\theta\alpha(v); 0, v)$ hits the switching manifold given by $u = 0$ for $\theta = 0$, $\theta = \frac{\alpha^+(v)}{\alpha(v)}$ and $\theta = 1$.

Hence the continuous manifolds $\tilde{\Lambda}^\pm$ are given by $\tilde{\Lambda}^\pm = F_0^\pm(N)$. This will later allow us to identify points on the perturbed manifolds $\tilde{\Lambda}_\varepsilon^\pm$ in terms of the same coordinates (θ, v, s) if $\varepsilon > 0$ is small enough.

Due to the singularity given at $\theta = \frac{\alpha^+(v)}{\alpha(v)}$, these manifolds are only C^0 manifolds, and, hence, their tangent space is not defined at $u = 0$.

The homeomorphisms F_0^\pm induce flows on the manifold N which are topologically conjugated to $\tilde{\phi}$ restricted to the manifolds $\tilde{\Lambda}^\pm$. This induced flow is in fact the rotation

$$\begin{aligned} \dot{\theta} &= \frac{1}{\alpha(v)} \\ \dot{s} &= 1. \end{aligned}$$

6.3.6.2 Invariant manifolds for the unperturbed impact map

The fact that the manifolds $\tilde{\Lambda}^\pm$ are only continuous manifolds will prevent us to apply classical perturbation theory for hyperbolic manifolds ([Fen72, Fen74, Fen77, HPS77, DdILS00]) to study their persistence for $\varepsilon > 0$.

In the smooth case, the usual tool to proof such persistence after a non-autonomous periodic perturbation is the stroboscopic Poincaré map, which integrates the system during a certain time T , the period of the perturbation. However, in our case, such map becomes unwieldy because, for a given time, the number of times that the switching manifold can be crossed is unknown and can be even arbitrarily large. Instead, we will consider the Poincaré impact map defined in §6.3.1, which is a smooth map as regular as the flows $\tilde{\phi}^{\pm\pm}$ restricted to their respective domains.

We first describe the invariant objects introduced above for the impact map restricted to $\tilde{\Sigma}^+$ when $\varepsilon = 0$.

As we said in §6.3.1, we will identify the switching manifold $\tilde{\Sigma}^+$ with the set $\mathbb{R}^2 \times ([-v_2, -v_1] \cup [v_1, v_2]) \times \mathbb{T}_T$ and omit the repetition of the coordinate $u = 0$ for points in $\tilde{\Sigma}$. We then consider the impact map

$$P_0 : \tilde{\mathcal{O}}_{P_0} \cap \{(v, x, y, s), |v > 0\} \longrightarrow \mathbb{R}^3 \times \mathbb{T}_T.$$

Taking into account that

$$P_0(v, Q^\pm, s) = (v, Q^\pm, s + \alpha(v)), \quad (6.3.39)$$

$\alpha(v)$ defined in (6.3.15), and letting $U(0, v) = c$, the invariant tori (6.3.32) become smooth invariant curves, that is, $\tilde{\Lambda}_c^\pm \cap \tilde{\Sigma}$, become

$$\begin{aligned} \tilde{\mathcal{C}}_c^+ &= \{v\} \times Q^+ \times \mathbb{T}_T \\ &= \{(v, x, y, s) \in \mathbb{R}^3 \times \mathbb{T}_T \mid U(0, v) = c, (x, y) = Q^+\} \end{aligned} \quad (6.3.40)$$

$$\begin{aligned} \tilde{\mathcal{C}}_c^- &= \{v\} \times Q^- \times \mathbb{T}_T \\ &= \{(v, x, y, s) \in \mathbb{R}^3 \times \mathbb{T}_T \mid U(0, v) = c, (x, y) = Q^-\}, \end{aligned} \quad (6.3.41)$$

with $0 < c \leq \bar{c}$.

For those values of c such that $m\alpha(v) = nT$, for some natural numbers n and m , the curves $\tilde{\mathcal{C}}_c^\pm$ are filled by periodic points. The rest are formed by points whose trajectories are dense in $\tilde{\mathcal{C}}_c^\pm$.

For each of these curves there exist 2-dimensional smooth manifolds

$$\begin{aligned} W^s(\tilde{\mathcal{C}}_c^+) &= W^u(\tilde{\mathcal{C}}_c^-) \\ &= \{(v, \sigma^{\text{up}}(\xi), s), U(0, v) = c, \xi \in \mathbb{R}, s \in \mathbb{T}_T\} \end{aligned}$$

which are invariant by P_0 :

$$P_0(v, \sigma^{\text{up}}(\xi), s) = (v, \sigma^{\text{up}}(\xi + \alpha(v)), s + \alpha(v)) \in W^u(\tilde{\mathcal{C}}_c^-) = W^s(\tilde{\mathcal{C}}_c^+).$$

Moreover, due to the hyperbolicity of the points Q^\pm (see (6.3.34)), it comes that, for any $\tilde{\omega} = (v, \sigma^{\text{up}}(\xi), s) \in W^u(\tilde{\mathcal{C}}_-) = W^s(\tilde{\mathcal{C}}_+)$, there exist $\tilde{\omega}^\pm = (v, Q^\pm, s) \in \tilde{\mathcal{C}}_c^\pm$ such that

$$|P_0^n(\tilde{\omega}) - P_0^n(\tilde{\omega}^\pm)| = |(0, \sigma^{\text{up}}(\xi + n\alpha(v)) - Q^\pm, 0)| < \tilde{K}^\pm(\hat{\lambda}^\pm)^{|n|}, \quad n \rightarrow \pm\infty, \quad (6.3.42)$$

where $\tilde{K}^\pm = K^\pm e^{-\lambda^\pm \xi}$, $0 < \hat{\lambda}^\pm = e^{-\lambda^\pm \alpha(v)} < 1$ and λ^\pm, K^\pm are defined in (6.3.34).

Proceeding similarly as with the flow, we now consider the union by c of all the curves $\tilde{\mathcal{C}}_c^\pm$ which become the smooth cylinders

$$\begin{aligned} \tilde{\Gamma}^+ &= \bigcup_{c \in [c_1, c_2]} \tilde{\mathcal{C}}_c^+ = \{(v, Q^+, s) \mid v_1 < v < v_2, s \in \mathbb{T}_T\} \\ \tilde{\Gamma}^- &= \bigcup_{c \in [c_1, c_2]} \tilde{\mathcal{C}}_c^- = \{(v, Q^-, s) \mid v_1 < v < v_2, s \in \mathbb{T}_T\}, \end{aligned} \quad (6.3.43)$$

with $0 < c_i \leq \bar{c}$ and $c_i = U(0, v_i)$, $i = 1, 2$, which are invariant by P_0 . Let us note that the manifolds $\tilde{\Gamma}^\pm$ correspond to the intersection

$$\tilde{\Lambda}^\pm \cap \tilde{\Sigma}^+ = \{0\} \times \tilde{\Gamma}^\pm.$$

As we did before for the flow, it will be convenient to write the manifolds $\tilde{\Gamma}^\pm$ in terms of a reference manifold. Let

$$L = \{(v, s) \in \mathbb{R} \times \mathbb{T}_T, v_1 \leq v \leq v_2\} \quad (6.3.44)$$

and consider the two diffeomorphisms

$$\begin{aligned} G_0^\pm : \quad L &\longrightarrow \tilde{\Gamma}^\pm \\ (v, s) &\longmapsto (v, Q^\pm, s). \end{aligned}$$

Then, the smooth manifolds $\tilde{\Gamma}^\pm$ are given by $G_0^\pm(L)$. Moreover, for any $(v, s) \in L$

$$P_0(G_0^\pm(v, s)) = G_0^\pm(v, s + \alpha(v)).$$

This induces a map

$$\begin{aligned} p_0 : \quad L &\longrightarrow L \\ (v, s) &\longmapsto (v, s + \alpha(v)), \end{aligned} \quad (6.3.45)$$

which is a twist map on the manifolds $\tilde{\Gamma}^\pm$ and describes the dynamics of P_0^\pm restricted to both those:

$$\begin{aligned} P_0 \circ G_0^\pm(v, s) &= P_0(v, Q^\pm, s) = (v, Q^\pm, s + \alpha(v)) \\ &= G_0^\pm(v, s + \alpha(v)) = G_0^\pm \circ p_0(v, s). \end{aligned}$$

We now argue that $\tilde{\Gamma}^\pm$ are manifolds with boundaries which are normally hyperbolic and locally invariant for the unperturbed impact map P_0 . Provided that $\tilde{\Gamma}^\pm$ are smooth manifolds in $\mathbb{R}^3 \times \mathbb{T}_T$, as smooth as the flows $\tilde{\phi}^{\pm\pm}$ restricted to their respective domains, for every $\tilde{\omega} \in \tilde{\Gamma}^\pm$ we can consider the tangent spaces $T_{\tilde{\omega}}\tilde{\Gamma}^\pm$. From expressions (6.3.43), these become

$$T_{\tilde{\omega}}\tilde{\Gamma}^\pm = \{(1, 0, 0, 0), (0, 0, 0, 1)\}.$$

Let \mathcal{X}^\pm be the fields associated with the Hamiltonians X^\pm and given in (6.2.3). Let $w_s^\pm \in \mathbb{R}^2$ and $w_u^\pm \in \mathbb{R}^2$ be the eigenvectors of $D\mathcal{X}^\pm$ at Q^\pm , associated with the eigenvalues $-\lambda^\pm$ and λ^\pm , respectively.

Using expression (6.3.39) for the unperturbed impact map, the Jacobian matrix of $P_0(v, x, y, s)$ evaluated at $\tilde{\Gamma}_0^\pm$ becomes

$$DP_0(v, Q^\pm, s) = \begin{pmatrix} 1 & 0 & 0 & 0 \\ 0 & e^{D\mathcal{X}^\pm(Q^\pm)\alpha(v)} & 0 & 0 \\ 0 & 0 & 0 & 0 \\ \alpha'(v) & 0 & 0 & 1 \end{pmatrix}.$$

Given $\tilde{\omega} \in \tilde{\Gamma}^\pm$, we can consider the splitting for the tangent space $T_{\tilde{\omega}}(\mathbb{R}^3 \times \mathbb{T}_T)$

$$T_{\tilde{\omega}}(\mathbb{R}^3 \times \mathbb{T}_T) = E_{\tilde{\omega}}^s \oplus E_{\tilde{\omega}}^u \oplus T_{\tilde{\omega}}(\tilde{\Gamma}^\pm),$$

where

$$\begin{aligned} E_{\tilde{\omega}}^s &= \langle 0, w_s^\pm, 0 \rangle \\ E_{\tilde{\omega}}^u &= \langle 0, w_u^\pm, 0 \rangle \end{aligned}$$

are the eigenspaces generated by the vectors w_s^\pm and w_u^\pm .

Taking into account that $\tilde{\Gamma}^\pm$ are compact manifolds with boundaries given by $v = v_1$ and $v = v_2$, there exist constants $\bar{\mu} > 1$, $0 < \bar{\lambda}^\pm < 1$ such that, for all $\tilde{\omega} \in \tilde{\Gamma}^\pm$

$$\begin{aligned} w \in E_{\tilde{\omega}}^s &\iff |DP_0^n(\tilde{\omega})w| \leq K^\pm (\bar{\lambda}^\pm)^n |w|, & n \geq 0 \\ w \in E_{\tilde{\omega}}^u &\iff |DP_0^n(\tilde{\omega})w| \leq K^\pm (\bar{\lambda}^\pm)^{-n} |w|, & n \leq 0 \\ w \in T_{\tilde{\omega}}\tilde{\Gamma}^\pm &\iff |DP_0^n(\tilde{\omega})w| \leq K^\pm (\bar{\mu}^\pm)^{|n|} |w|, & n \in \mathbb{Z}. \end{aligned} \quad (6.3.46)$$

Assuming that $\alpha(v)$ is an increasing function of v , we can take

$$\bar{\lambda}^\pm = e^{-\alpha(v_1)\lambda^\pm}, \quad (6.3.47)$$

and $\bar{\mu}$ any constant satisfying $\bar{\mu} > 1$.

Hence, $\tilde{\Gamma}^\pm$ are C^∞ (as regular as the flows) normally hyperbolic manifolds for the unperturbed impact map P_0 , with stable and unstable invariant manifolds

$$\begin{aligned} W^u(\tilde{\Gamma}^-) &= W^s(\tilde{\Gamma}^+) = \bigcup_{c \in [c_1, c_2]} W^u(\tilde{\mathcal{C}}_c^-) = \bigcup_{c \in [c_1, c_2]} W^s(\tilde{\mathcal{C}}_c^+) \\ &= \{v, (\sigma^{\text{up}}(\xi), s), v_1 \leq v \leq v_2, \xi \in \mathbb{R}, s \in \mathbb{T}_T\}. \end{aligned}$$

It will also be convenient to introduce the following parametrization of the invariant manifolds $W^{s/u}(\tilde{\Gamma}^{+/-})$. Using σ^{down} , similar ones can be obtained for $W^{u/s}(\tilde{\Gamma}^{+/-})$. Let

$$E^{s,u} = \{(v, s, \eta) \in L \times [0, 1]\}$$

be a bundle on L . We then define

$$\begin{aligned} G_0^{s/u} : \quad E^{s/u} &\longrightarrow W^{s/u}(\tilde{\Gamma}^{+/-}) \\ (v, s, \eta) &\longmapsto (v, \sigma^{\text{up}}(-/ + \frac{\ln \eta}{\lambda^{+/-}}), s). \end{aligned} \quad (6.3.48)$$

As $\sigma^{\text{up}}(\xi) \rightarrow Q^\pm$ as $\xi \rightarrow \pm\infty$, we include $\eta = 0$ in the domains and define

$$G_0^{s/u}(v, s, 0) = G_0^{+/-}(v, s).$$

The diffeomorphisms $G_0^{s,u}$ induce dynamics on $W^{s/u}(\tilde{\Gamma}^{+/-})$ in terms of the parameters (v, s, η) . To simplify the notation, we proceed with $W^s(\tilde{\Gamma}^+)$. Let $\tilde{\omega}^s = G_0^s(v, s, \eta)$. Then,

$$\begin{aligned} P_0(G_0^s(v, s, \eta)) &= P_0(\tilde{\omega}^s) = (v, \sigma^{\text{up}}(-\frac{\ln \eta}{\lambda^+} + \alpha(v)), s + \alpha(v)) \\ &= (v, \sigma^{\text{up}}(-\frac{\ln(\eta \hat{\lambda}^+)}{\lambda^+}), s + \alpha(v)) = G_0^s(v, s + \alpha(v), \eta \hat{\lambda}^+), \end{aligned}$$

where $\hat{\lambda}^+ = e^{-\lambda^+ \alpha(v)}$ is defined in (6.3.42).

Hence, the dynamics induced in E^s is given by

$$\begin{aligned} p_0^s : \quad E^s &\longrightarrow E^s \\ (v, s, \eta) &\longmapsto (v, s + \alpha(v), \eta \hat{\lambda}^+), \end{aligned}$$

so that

$$P_0 \circ G_0^s = G_0^s \circ p_0^s,$$

and p_0^s also inherits the hyperbolic nature of the map P_0 ,

$$\begin{aligned} &\left| ((p_0^s)^n(v, s), 0) - (p_0^s)^n(v, s, \eta) \right| \\ &= \left| (0, 0, -\eta \hat{\lambda}^+) \right| < \eta (\bar{\lambda}^+)^n. \end{aligned}$$

6.3.6.3 Perturbed case

Let us now wonder about the persistence of the invariant manifolds introduced in the previous section when $\varepsilon > 0$ is small. We first focus on the normally hyperbolic manifolds, $\tilde{\Gamma}^\pm$, for the map P_0 .

As mentioned in Remark 6.3.2, the impact map P_ε is as regular as the flows $\tilde{\phi}^{\pm\pm}$ restricted to $S^\pm \times S^\pm \times \mathbb{T}_T$. Thus, the persistence of the normally hyperbolic manifolds $\tilde{\Gamma}^\pm$ for $\varepsilon > 0$ comes from the theory of normally hyperbolic manifolds ([HP70, Fen72, Fen74, HPS77, DdlLS08]). In particular, we apply the main result given in [HP70] and reformulated in [DdlLS08] which we repeat here for commodity in terms of our notation and needs.

Theorem 6.3.1. *Let $P_\varepsilon : \tilde{\mathcal{O}}_{P_\varepsilon} \subset \mathbb{R}^3 \times \mathbb{T}_T \rightarrow \mathbb{R}^3 \times \mathbb{T}_T$ be a C^∞ family of diffeomorphisms. Assume that $\tilde{\Gamma} \subset \mathbb{R}^3 \times \mathbb{T}_T$ is a normally hyperbolic invariant manifold for P_0 with rates $\hat{\lambda}$ and $\hat{\mu}$ as in (6.3.46). Then for any $l < \frac{|\log \hat{\lambda}|}{\log \hat{\mu}}$, there exists an $\varepsilon_0 > 0$ such that for $|\varepsilon| < \varepsilon_0$ there exist C^{l-1} families*

$$\begin{aligned} G_\varepsilon : L &\longrightarrow \mathbb{R}^3 \times \mathbb{T}_T \\ p_\varepsilon : L &\longrightarrow L \\ G_\varepsilon^{s,u} : E^{s,u} &\longrightarrow \mathbb{R}^3 \times \mathbb{T}_T \\ p_\varepsilon^{s,u} : E^{s,u} &\longrightarrow E^{s,u}, \end{aligned}$$

where $E^{s,u} = L \times [0, 1]$ are bundles over L , satisfying

$$P_\varepsilon \circ G_\varepsilon = G_\varepsilon \circ p_\varepsilon \tag{6.3.49}$$

$$P_\varepsilon \circ G_\varepsilon^{s,u} = G_\varepsilon^{s,u} \circ p_\varepsilon^{s,u} \tag{6.3.50}$$

and, for any $(v, s) \in L$,

$$G_\varepsilon^{s,u}((v, s), 0) = G_\varepsilon(v, s) \tag{6.3.51}$$

$$p_\varepsilon^{s,u}((v, s), 0) = p_\varepsilon(v, s) \tag{6.3.52}$$

$$D_2 G_\varepsilon^{s,u}((v, s), 0) E_{(v,s)}^{s,u} = E_{G_\varepsilon(v,s)}^{s,u}. \tag{6.3.53}$$

Moreover, there exists an open set $U \supset G_0(L) = \tilde{\Gamma}$ in such a way that the set $\tilde{\Gamma}_\varepsilon := G_\varepsilon(L)$ is a normally hyperbolic invariant manifold, verifies

$$\tilde{\Gamma}_\varepsilon = \bigcap_{n \in \mathbb{Z}} P_\varepsilon^n(U) \cap U,$$

and has stable and unstable manifolds given by

$$W^{s,u}(\tilde{\Gamma}_\varepsilon) = G_\varepsilon^{s,u}(E^{s,u}).$$

Moreover, if $\tilde{\omega} = G_\varepsilon(v, s) \in \tilde{\Gamma}_\varepsilon$, then

$$W^{s,u}(\tilde{\omega}) = \bigcup_{\eta \in [0,1]} G_\varepsilon^{s,u}(v, s, \eta).$$

Condition (6.3.49) gives us the persistence for $\varepsilon > 0$ small enough of the normally hyperbolic invariant manifolds $\tilde{\Gamma}^\pm$, which become $\tilde{\Gamma}_\varepsilon^\pm$, which are normally hyperbolic invariant manifolds for the impact map P_ε in (6.3.13).

In general, the Theorem of persistence of normally hyperbolic manifolds only gives locally invariance for the perturbed manifold. Nevertheless, as shown in (6.3.45), the unperturbed map is a twist map when restricted to $\tilde{\Gamma}^\pm$, some of the curves $v = ct$ which foliated it

(those such that $\alpha(v)$ is not congruent with the period T of the perturbation) are preserved by the classical twist theorem. These invariant curves provide invariant boundaries for the perturbed manifolds $\tilde{\Gamma}_\varepsilon^\pm$, and hence $\tilde{\Gamma}_\varepsilon^\pm$ are compact and invariant. In addition, this compactness makes the manifolds $\tilde{\Gamma}_\varepsilon^\pm$ given by the diffeomorphisms G_ε^\pm be unique.

The diffeomorphisms $G_\varepsilon^{s,u}$ provide formulas for the (local) stable and unstable manifolds of $\tilde{\Gamma}_\varepsilon^\pm$, $W_{\text{loc}}^{s,u}(\tilde{\Gamma}_\varepsilon^\pm)$, in terms of the bundle eigenspaces $E^{s,u}$. More precisely, the points of the stable and unstable manifolds of $\tilde{\Gamma}_\varepsilon^+$ (similarly for $\tilde{\Gamma}_\varepsilon^-$) are of the form

$$G_\varepsilon^{s,u}((v, s), \eta),$$

where $((v, s), \eta)$ is a point of the bundle

$$((v, s), \eta) \in E^{u,s} \subset L \times [0, 1] \subset \mathbb{R} \times \mathbb{T}_T \times \mathbb{R}.$$

Note that these maps $G_\varepsilon^{u,s}$ refer here to the invariant manifolds associated with $\tilde{\Gamma}_\varepsilon^+$. To avoid too lengthy notation, we have omitted the superscript $+$ in these maps. Similar ones would parametrize the stable and unstable manifolds of $\tilde{\Gamma}_\varepsilon^-$.

In addition, the regularity of the maps with respect to the perturbation parameter ε ensures that the perturbed objects are ε -close to the unperturbed ones.

Finally, conditions (6.3.51)-(6.3.53) relate points at the normally hyperbolic manifold $\tilde{\Gamma}_\varepsilon^+$ with points at its stable and unstable manifolds as follows.

Let $\tilde{\omega}^+ = G_\varepsilon^+(v, s)$ and $\tilde{\omega}^{s,u} = G_\varepsilon^{s,u}(v, s, \eta)$, with $(v, s) \in L$ and $\eta \in [0, 1]$; then,

$$\begin{aligned} |P_\varepsilon^n(\tilde{\omega}^{s/u}) - P_\varepsilon^n(\tilde{\omega}^+)| &= |P_\varepsilon^n \circ G_\varepsilon^{s,u}(v, s, \eta) - P_\varepsilon^n \circ G_\varepsilon^+(v, s)| \\ &= |G_\varepsilon^{s,u} \circ (p_\varepsilon^{s,u}(v, s, \eta))^n - G_\varepsilon^+(p_\varepsilon^n(v, s))| \\ &< K^+ (\bar{\lambda} + O(\varepsilon))^n \rightarrow 0, \quad n \rightarrow +/\infty, \end{aligned}$$

where $0 < \bar{\lambda}^+ < 1$ is the constant given in (6.3.46).

The parametrization of the normally hyperbolic manifolds $\tilde{\Gamma}_\varepsilon^\pm$ given by Theorem 6.3.1 are not unique. For our convenience, we choose from now the parametrizations G_ε^\pm to be the identity in the v and s coordinates,

$$\Pi_{v,s}(G_\varepsilon^\pm) = Id, \tag{6.3.54}$$

that is,

$$G_\varepsilon^\pm(v, s) = (v, g_\varepsilon^\pm(v, s), s).$$

Finally, note that, when $\varepsilon = 0$, these maps coincide with the ones defined in §6.3.6. Therefore,

$$g_0^\pm(v, s) = Q^\pm.$$

We now wonder about the existence of equivalent manifolds to $\tilde{\Gamma}_\varepsilon^\pm$ for the flow $\tilde{\phi}$. More precisely, we are interested in obtaining the perturbed version of the normally hyperbolic manifolds $\tilde{\Lambda}^\pm$ in terms of the reference manifold N given in (6.3.37).

Proposition 6.3.1. *Under the hypothesis of Theorem 6.3.1, there exist continuous maps*

$$F_\varepsilon^\pm : N \longrightarrow \mathbb{R}^4 \times \mathbb{T}_T,$$

that are Lipschitz in ε , such that the C^0 manifolds

$$\tilde{\Lambda}_\varepsilon^\pm = F_\varepsilon^\pm(N)$$

are invariant under $\tilde{\phi}$ and ε -close to $\tilde{\Lambda}_0^\pm$.

Moreover, there exist C^0 manifolds $W^{s,u}(\tilde{\Lambda}_\varepsilon^\pm)$, ε -close to $W^{s,u}(\tilde{\Lambda}_0^\pm)$, such that, for any $\tilde{z}^{s/u} = (z^{s/u}, s^{s,u}) \in W^{s/u}(\tilde{\Lambda}_\varepsilon^{+/-})$ there exists $\tilde{z}^{+/-} = (z^{+/-}, s^{+/-}) \in \tilde{\Lambda}_\varepsilon^{+/-}$ satisfying $s^{s/u} = s^{+/-}$ and

$$|\phi(t; \tilde{z}^{s/u}; \varepsilon) - \phi(t; \tilde{z}^{+/-}; \varepsilon)| < K^{+/-} e^{-\lambda^{+/-}|t|}, \quad t \rightarrow +/- \infty, \quad (6.3.55)$$

where $K^{+/-} > 0$ and $\lambda^{+/-} > 0$ are given in (6.3.34). Similarly for $\tilde{z}^{u/s} \in W^{u/s}(\tilde{\Lambda}_\varepsilon^{+/-})$.

Proof. We first obtain the maps

$$F_\varepsilon^\pm : N \longrightarrow \mathbb{R}^4 \times \mathbb{T}_T$$

which provide the invariant manifolds $\tilde{\Lambda}_\varepsilon^\pm$.

For each $(\theta, v, s) \in N$, we consider $G_\varepsilon^\pm(v, s) = \tilde{\omega}^\pm \in \tilde{\Gamma}_\varepsilon^\pm$ which, recalling the assumption stated in (6.3.54), are of the form

$$\tilde{\omega}^\pm = (v, g_\varepsilon^\pm(v, s), s).$$

Calling

$$\begin{aligned} \tilde{\omega}_1^\pm &= (\omega_1^\pm, s_1^\pm) = P_\varepsilon(\tilde{\omega}^\pm) \\ \tilde{z}^\pm &= (0, \tilde{\omega}^\pm) \in \{0\} \times \tilde{\Gamma}_\varepsilon^\pm \subset \tilde{\Sigma}, \end{aligned}$$

we then consider the maps

$$F_\varepsilon^\pm(\theta, v, s) = \tilde{\phi}((s_1^\pm - s)\theta; \tilde{z}^\pm; \varepsilon) \quad (6.3.56)$$

$$= \tilde{\phi}((s_1 - s)\theta; 0, v, g_\varepsilon^\pm(v, s), s), \quad \theta \in [0, 1], \quad (6.3.57)$$

which are a smooth maps as long as the flow does not hit $u = 0$, which occurs at

$$\theta = 0, \quad \theta = \frac{\Pi_s(P_\varepsilon^+(\tilde{\omega}^\pm)) - s}{s_1^\pm - s}, \quad \theta = 1.$$

The maps F_ε^\pm fulfill

$$F_\varepsilon^\pm(0, v, s) = \tilde{\phi}(0; \tilde{z}^\pm; \varepsilon) = (0, \tilde{\omega}^\pm) \in \{0\} \times \tilde{\Gamma}_\varepsilon^\pm$$

and

$$\begin{aligned} F_\varepsilon^\pm(1, v, s) &= \tilde{\phi}(s_1^\pm - s; \tilde{z}^\pm; \varepsilon) = (0, P_\varepsilon(\tilde{\omega}^\pm)) \\ &= (0, P_\varepsilon \circ G_\varepsilon^\pm(v, s)) = (0, G_\varepsilon^\pm(p_\varepsilon^\pm(v, s))) \in \{0\} \times \tilde{\Gamma}_\varepsilon^\pm. \end{aligned} \quad (6.3.58)$$

Note that, when $\varepsilon = 0$, $\tilde{z}^\pm = (0, \tilde{\omega}^\pm) = (0, G_0^\pm(v, s)) = (0, v, Q^\pm, s) \in \tilde{\Gamma}_0^\pm$ and $(s_1^\pm - s) = \alpha(v)$. Therefore,

$$F_0^\pm(\theta, v, s) = \tilde{\phi}(\alpha(v)\theta; \tilde{z}^\pm; 0) = (\phi_u(\theta\alpha(v); 0, v), Q^\pm, s)$$

and, in the unperturbed case, these parametrizations coincide with F_0^\pm defined in (6.3.38). This allows us to obtain the 3-dimensional continuous manifolds

$$\tilde{\Lambda}_\varepsilon^\pm = F_\varepsilon^\pm(N), \quad (6.3.59)$$

which, as we argue below, are invariant by the flow $\tilde{\phi}(t; \tilde{z}_0; \varepsilon)$.

We first see the invariance of $\tilde{\Lambda}_0^\pm$, for $\varepsilon = 0$. Let us consider $\tilde{z}^\pm = F_0^\pm(\theta, v, s)$ and the flow $\tilde{\phi}(t; \tilde{z}^\pm; 0)$. If $0 \leq t \leq (1 - \theta)\alpha(v)$ then

$$\tilde{\phi}(t; \tilde{z}^\pm; 0) = F_0^\pm\left(\theta + \frac{t}{\alpha(v)}, v, s\right) \in \tilde{\Lambda}_0^\pm$$

and it is hence invariant, as it is given by the image by F_0^\pm of a point in N . At $t = (1 - \theta)\alpha(v)$, the flow crosses the switching manifold $u = 0$ with positive v at the point which, using property (6.3.58), is given by $F_0^\pm(1, v, s) = (0, G_0^\pm(p_0^\pm(v, s))) = (0, v, Q^\pm, s + \alpha(v))$. Hence, if $(1 - \theta)\alpha(v) \leq t \leq (2 - \theta)\alpha(v)$, we can write

$$\begin{aligned} \tilde{\phi}(t; \tilde{z}^\pm; 0) &= \tilde{\phi}(t - (1 - \theta)\alpha(v); F_0^\pm(1, v, s); 0) \\ &= \tilde{\phi}(t - (1 - \theta)\alpha(v); 0, v, Q^\pm, s + \alpha(v)) \\ &= F_0^\pm\left(\frac{t}{\alpha(v)} - (1 - \theta), p_0^\pm(v, s)\right) \\ &= F_0^\pm\left(\frac{t}{\alpha(v)} - (1 - \theta), v, s + \alpha(v)\right), \end{aligned}$$

and hence is also invariant because it is given by the image of a point in N by F_0^\pm . In general, using that the impacts with the switching manifold $\tilde{\Sigma}^+$ ($v > 0$) are given at $t_n = (n - \theta)\alpha(v)$, we can write the flow for $(n - \theta)\alpha(v) \leq t \leq (n + 1 - \theta)\alpha(v)$ as

$$\begin{aligned} \tilde{\phi}(t; \tilde{z}^\pm; 0) &= \tilde{\phi}(t - (n - \theta)\alpha(v); F_0^\pm(1, (p_0^\pm)^{n-1}(v, s)); 0) \\ &= F_0^\pm\left(\frac{t}{\alpha(v)} - (n - \theta), (p_0^\pm)^n(v, s)\right) \\ &= F_0^\pm\left(\frac{t}{\alpha(v)} - (n - \theta), v, s + n\alpha(v)\right), \end{aligned}$$

providing us the invariance for all $t \geq 0$. Proceeding similarly for $t \leq 0$, we get the invariance of the manifolds $\tilde{\Lambda}_0^\pm = F_0^\pm(N)$ for the flow $\tilde{\phi}$ for all $t \in \mathbb{R}$.

Let us consider $\varepsilon > 0$ and $\tilde{z}^+ = F_\varepsilon^+(\theta, v, s)$ (analogously for $\tilde{z}^- = F_\varepsilon^-(\theta, v, s)$). We first find the first impact with the switching manifold $\tilde{\Sigma}^+$ with $v > 0$,

$$\tilde{z}_1 = (0, G_\varepsilon^+(p_\varepsilon^+(v, s))).$$

Calling $s_1 = \Pi_s(\tilde{z}_1)$, and $t_1 = s_1 - s$, this impact occurs for the flow $\tilde{\phi}(t; \tilde{z}^+; \varepsilon)$ at

$$t = (1 - \theta)t_1.$$

Then, for $0 \leq t \leq (1 - \theta)t_1$,

$$\tilde{\phi}(t; \tilde{z}^+; \varepsilon) = F_\varepsilon^+(\theta + \frac{t}{t_1}, v, s) \in \tilde{\Lambda}_\varepsilon^+,$$

and it is hence invariant because it is given by the image by F_ε^+ of a point in N . As for the unperturbed case, after the first impact we write the flow using the last impact as initial condition. In general, the flow $\tilde{\phi}(t; \tilde{z}^+; \varepsilon)$ impacts $\tilde{\Sigma}^+$ at points

$$\tilde{z}_n = (0, G_\varepsilon^+((p_0^+)^n(v, s))),$$

and occur at times given by

$$t = \underbrace{(s_n - s)}_{:=t_n} - \theta \underbrace{(s - s_1)}_{t_1}, \quad n \geq 1,$$

where

$$s_n = \Pi_s((p_\varepsilon^+)^n(v, s)).$$

Hence, if $t_n - \theta t_1 \leq t \leq t_{n+1} - \theta t_1$, we can write

$$\begin{aligned} \tilde{\phi}(t; \tilde{z}; \varepsilon) &= \tilde{\phi}(t - t_n + \theta t_1; (0, G_\varepsilon^+((p_\varepsilon^+)^n(v, s)))) ; \varepsilon) \\ &= F_\varepsilon^+ \left(\frac{t - t_n + \theta t_1}{s_{n+1} - s_n}, (p_0^+)^n(v, s) \right), \end{aligned}$$

and $\tilde{\Lambda}_\varepsilon^+$ is thus invariant for $\tilde{\phi}$ for $t \geq 0$. Arguing similarly for $t < 0$, we get that

$$\tilde{\phi}(t; \tilde{z}^+; \varepsilon) \in \tilde{\Lambda}_\varepsilon^+, \quad \forall t \in \mathbb{R}.$$

Analogous arguments hold for $\tilde{\phi}(t; \tilde{z}^-; \varepsilon)$ if $\tilde{z}^- = F_\varepsilon^-(\theta, v, s)$.

As $\phi(t; \tilde{z}; \varepsilon)$ and $\tilde{\Gamma}_\varepsilon^\pm$ are ε -close to $\phi(t; \tilde{z}; 0)$ and $\tilde{\Gamma}^\pm$, respectively, we have that

$$|F_\varepsilon^\pm(\theta, v, s) - F_0^\pm(\theta, v, s)| = O(\varepsilon),$$

which gives us the Lipschitz property. In addition, note that

$$\tilde{\Lambda}_\varepsilon^\pm \cap \tilde{\Sigma}^+ = \{0\} \times \tilde{\Gamma}_\varepsilon^\pm.$$

Let us now wonder about the stable and unstable manifolds $W^{s,u}(\tilde{\Lambda}_\varepsilon^\pm)$. For every $\tilde{z}^\pm \in \tilde{\Lambda}_\varepsilon^\pm$ we want to find points $\tilde{z}^{s,u}$ fulfilling (6.3.55) and hence defining $W^u(\tilde{\Lambda}_\varepsilon^-)$ and $W^s(\tilde{\Lambda}_\varepsilon^+)$ (similarly for $W^s(\tilde{\Lambda}_\varepsilon^-)$ and $W^u(\tilde{\Lambda}_\varepsilon^+)$). We proceed here with the manifold $W^s(\tilde{\Lambda}_\varepsilon^+)$; analogous arguments hold for the other manifolds.

Let

$$\tilde{z}^+ = F_\varepsilon^+(\theta, v, s) = \tilde{\phi}(\tau^+; (0, \tilde{\omega}^+); \varepsilon),$$

with

$$\begin{aligned} \tilde{\omega}^+ &= G_\varepsilon^+(v, s) = (v, g_\varepsilon(v, s), s) \in \tilde{\Gamma}_\varepsilon^+ \\ \tau^+ &= (\Pi_s(P_\varepsilon(\tilde{\omega}^+)) - s) \theta, \end{aligned}$$

be a point in $\tilde{\Lambda}_\varepsilon^+$.

From Theorem 6.3.1 we know that there exists

$$\tilde{\omega}^s = (\omega^s, s^s) = G_\varepsilon^s(v, s, \eta) \in W^s(\tilde{\Gamma}_\varepsilon^+)$$

such that

$$|P_\varepsilon^n(\tilde{\omega}^s) - P_\varepsilon^n(\tilde{\omega}^+)| < K^+(\bar{\lambda}^+)^n, \quad n \rightarrow \infty, \quad (6.3.60)$$

where $0 < \bar{\lambda}^+ < 1$ is given in (6.3.46).

Let us now consider the impact sequences associated with the points $\tilde{\omega}^+$ and $\tilde{\omega}^s$,

$$\begin{aligned} \tilde{\omega}_i^+ &= (v_\varepsilon^{i,+}, x_\varepsilon^{i,+}, y_\varepsilon^{i,+}, s_\varepsilon^{i,+}) \\ \tilde{\omega}_i^s &= (v_\varepsilon^{i,s}, x_\varepsilon^{i,s}, y_\varepsilon^{i,s}, s_\varepsilon^{i,s}). \end{aligned}$$

Using that

$$\begin{aligned} P_\varepsilon^n(\tilde{\omega}^+) &= \tilde{\omega}_{2n}^+ \\ P_\varepsilon^n(\tilde{\omega}^s) &= \tilde{\omega}_{2n}^s, \end{aligned}$$

and recalling that, using the auxiliary map P_ε^* defined in (6.3.7),

$$\begin{aligned} \tilde{\omega}_{2i+1}^+ &= P_\varepsilon^+(\tilde{\omega}_{2i}^+) \\ \tilde{\omega}_{2i+1}^s &= P_\varepsilon^+(\tilde{\omega}_{2i}^s) \end{aligned}$$

if $(0, \tilde{\omega}^+), (0, \tilde{\omega}^s) \in \Sigma^+ \times \mathbb{R}^2 \times \mathbb{T}_T$, as the map P_ε^+ defined in §6.3.1 is a smooth map, by property (6.3.60) we also have that

$$|\tilde{\omega}_i^s - \tilde{\omega}_i^+| < \tilde{K}^+(\bar{\lambda}^+)^i, \quad i \rightarrow \infty,$$

for some $\tilde{K}^+ > 0$.

Consequently, the sequences $s_i^s = s_\varepsilon^{i,s}$ and $s_i^+ = s_\varepsilon^{i,+}$ fulfill

$$|s_i^s - s_i^+| < \hat{K}^+(\bar{\lambda}^+)^i, \quad i \rightarrow \infty,$$

for some $\hat{K}^+ > 0$.

In other words, there exist two sequences of times, $t_i^s = s_i^s - s^s$ and $t_i^+ = s_i^+ - s$, where the impacts occur, such that

$$\left| \tilde{\phi}(t_i^s; (0, \tilde{\omega}^s); \varepsilon) - \tilde{\phi}(t_i^+; (0, \tilde{\omega}^+); \varepsilon) \right| < \tilde{K}^+ \bar{\lambda}^i, \quad i \rightarrow \infty \quad (6.3.61)$$

and

$$|t_i^s - t_i^+| < \underbrace{|s^+ - s^s|}_{s-s^s} + \tilde{K}^+(\hat{\lambda}^+)^i, \quad i \rightarrow \infty.$$

Let now τ' be

$$\tau' = s^+ - s^s = s - s^s$$

and define

$$\tilde{z}^s = \tilde{\phi}(\tau^+ + \tau'; (0, \tilde{\omega}^s); \varepsilon).$$

Let us now show that this is the point we are looking for.

We first note that

$$\begin{aligned} \Pi_s \left(\tilde{\phi}(t; \tilde{z}^+; \varepsilon) \right) &= s + \tau^+ + t \\ \Pi_s \left(\tilde{\phi}(t; \tilde{z}^s; \varepsilon) \right) &= s^s + \tau^+ + \tau' + t \\ &= s + \tau^+ + t, \end{aligned}$$

and the s coordinates of both trajectories are the same, which is a necessary condition. The fact that the perturbed manifold $\tilde{\Gamma}_\varepsilon^+$ is compact ensures us that the sequences $t_{i+1}^s - t_i^s$ and $t_{i+1}^+ - t_i^+$ are bounded (they are in fact $\alpha^+(v) + O(\varepsilon)$ or $\alpha^-(-v) + O(\varepsilon)$). Hence, if t is large enough, we can always find i such that

$$\begin{aligned} t_i^+ - \tau^+ &< t < t_{i+1}^+ - \tau^+ \\ t_i^s - \tau^+ - \tau' &< t < t_{i+1}^s - \tau^+ - \tau', \end{aligned}$$

and write the flows

$$\tilde{\phi}(t; \tilde{z}^+; \varepsilon) = \tilde{\phi}(t - t_i^+ + \tau^+; (0, \tilde{\omega}_i^+); \varepsilon) \quad (6.3.62)$$

$$\tilde{\phi}(t; \tilde{z}^s; \varepsilon) = \tilde{\phi}(t - t_i^s + \tau^+ + \tau'; (0, \tilde{\omega}_i^s); \varepsilon). \quad (6.3.63)$$

In particular, as

$$(t_i^+ - \tau^+) - (t_i^s - \tau^+ - \tau') \longrightarrow 0,$$

if t is large enough, we can always assume that

$$a_i := \max(t_i^+ - \tau^+, t_i^s - \tau^+ - \tau') < t < \min(t_{i+1}^+ - \tau^+, t_{i+1}^s - \tau^+ - \tau') =: b_{i+1}.$$

For $t \in (a_i, b_{i+1})$, both flows (6.3.62) and (6.3.63) are located at the same domain $S^\pm \times S^+ \times \mathbb{T}_T$ and hence, the derivative of the function

$$\mathbf{u}(t) = |\tilde{\phi}(t; \tilde{z}^+; \varepsilon) - \tilde{\phi}(t; \tilde{z}^s; \varepsilon)|$$

is a Lipschitz function because so are the fields associated with the flows $\tilde{\phi}^{\pm+}$. Note that no impacts occur in the interval (a_i, b_{i+1}) . Let $\mathfrak{K} > 0$ be the largest Lipschitz constant of these two fields; then, for $t \in (a_i, b_{i+1})$ we have

$$\mathbf{u}(t) \leq K^+(\bar{\lambda}^+)^i + \int_{a_i}^t \mathfrak{K} \mathbf{u}(t) dt.$$

Applying Gronwall's Lemma, we obtain

$$\mathbf{u}(t) \leq K^+(\bar{\lambda}^+)^i e^{\mathfrak{K}(b_{i+1}-a_i)}.$$

As the difference $b_{i+1} - a_i$ is bounded by $\max(\alpha^+(v), \alpha^-(-v)) + O(\varepsilon)$, it comes that there exist a positive constant K^+ such that

$$|\phi(t; \tilde{z}^s; \varepsilon) - \phi(t; \tilde{z}^+; \varepsilon)| < K^+ e^{-\lambda^+|t|}, \quad t \rightarrow \infty,$$

which is what we wanted to prove. This constant may be different from the one defined in (6.3.34) and used in (6.3.60). To simplify the notation, we take the maximum between both and use the same name.

In order to see that $W^{u,s}(\tilde{\Lambda}_\varepsilon^\pm)$ are ε -close to $W^{u,s}(\tilde{\Lambda}_0^\pm)$ we recall that so do the manifolds $\tilde{\Gamma}_\varepsilon^\pm$ and $\tilde{\Gamma}^\pm$. This implies that τ' given in (6.3.65) is of order ε . Now, using that, for $\varepsilon = 0$,

$$\begin{aligned} \tilde{\omega}^s &= (0, v, \sigma^{\text{up}}(\xi), s) \\ \tilde{\omega}^+ &= (0, v, Q^+, s) \\ \tilde{z}^s &= (\phi_{\mathcal{U}}(\tau^+; 0, v), \sigma^{\text{up}}(\xi + \tau^+), s + \tau^+) \\ \tilde{z}^+ &= (\phi_{\mathcal{U}}(\tau^+; 0, v), Q^+, s + \tau^+) \end{aligned}$$

for $\xi = -\frac{\log \eta}{\lambda^+}$, and that the flow $\tilde{\phi}(t; \tilde{z}; \varepsilon)$ is ε -close to $\tilde{\phi}(t; \tilde{z}; 0)$, it comes that, for $\varepsilon > 0$,

$$\begin{aligned} \tilde{z}^s &= (\phi_{\mathcal{U}}(\tau^+; 0, v), \sigma^{\text{up}}(\xi + \tau^+), s + \tau^+) + O(\varepsilon) \\ \tilde{z}^+ &= (\phi_{\mathcal{U}}(\tau^+; 0, v), Q^+, s + \tau^+) + O(\varepsilon). \end{aligned}$$

Hence, the manifolds $W^{u,s}(\tilde{\Lambda}_\varepsilon^\pm)$ are ε -close to the unperturbed manifolds $W^{u,s}(\tilde{\Lambda}^\pm)$. \square

Remark 6.3.8. *From the above construction, we can also provide maps equivalent to $G_\varepsilon^{s,u}$ to obtain the manifolds $W^{s,u}(\tilde{\Lambda}_\varepsilon^+)$,*

$$\begin{aligned} F_\varepsilon^{s,u} : \quad E^s &\longrightarrow W^{s,u}(\tilde{\Lambda}_\varepsilon^+) \\ ((\theta, v, s), \eta) &\longmapsto \tilde{z}^{s,u} \end{aligned} \quad (6.3.64)$$

Calling

$$\begin{aligned} \tilde{\omega}^s &= G_\varepsilon^s(v, s, \eta) = (\omega^s, s^s) \\ \tilde{\omega}^+ &= G_\varepsilon^+(v, s) = (\omega^+, s^+) = (v, g_\varepsilon^+(v, s), s^+) \\ \tau &= (\Pi_s(P_\varepsilon(\tilde{\omega}^s)) - s^s)\theta \\ \tau' &= s^+ - s^s, \end{aligned} \quad (6.3.65)$$

the map F_ε^s becomes

$$F_\varepsilon^s(\theta, v, s, \eta) = \tilde{\phi}(\tau + \tau'; (0, \tilde{\omega}^s); \varepsilon).$$

Similarly for $F_\varepsilon^u(\theta, v, s, \eta)$ and also for the manifolds $W^{s,u}(\tilde{\Lambda}_\varepsilon^-)$.

As shown in Proposition 6.3.1, if

$$\begin{aligned} \tilde{z}^+ &= F_\varepsilon^+(\theta, v, s) \in \tilde{\Lambda}_\varepsilon^+ \\ \tilde{z}^{s,u} &= F_\varepsilon^{s,u}(\theta, v, s, \eta) \in W^{s,u}(\tilde{\Lambda}_\varepsilon^+), \end{aligned}$$

then

$$\left| \tilde{\phi}(t; \tilde{z}^+; \varepsilon) - \tilde{\phi}(t; \tilde{z}^{s,u} < ++ >; \varepsilon) \right| < K^{+/-} e^{-\lambda^+ |t|}, \quad t \rightarrow +/- \infty.$$

Similarly for $\tilde{z}^- \in \tilde{\Lambda}_\varepsilon^-$ and $\tilde{z}^{s,u} \in W^{s,u}(\tilde{\Lambda}_\varepsilon^-)$.

Remark 6.3.9. *The delay τ' given in (6.3.65) has to be considered because the section $\tilde{\Sigma}$ does not necessary have to be an isochrone. Note that, when considering the delay τ' , we are in fact constructing such isochrone because we are finding for each η the point whose orbit goes through $(0, \tilde{\omega}^s)$ and takes the same time as $(0, \tilde{\omega}^+)$ to return to $\tilde{\Sigma}^+$.*

Remark 6.3.10. *In the previous arguments we have used that the direct impact sequences of the points $\tilde{\omega}^+$ and $\tilde{\omega}^s$ are infinite.*

The first fact comes from the fact that $\tilde{\omega}^+ \in \tilde{\Gamma}_\varepsilon^+$ and hence, as $\tilde{\Gamma}_\varepsilon^+$ is invariant and ε -close to $\tilde{\Gamma}_0^+$, it is contained in $\Sigma^+ \times S^+ \times \mathbb{T}_T$, the flow $\tilde{\phi}(t; (0, \tilde{\omega}^+); \varepsilon)$ never crosses the switching manifold associated with $x = 0$.

To see the second fact, if $\tilde{\omega}^s$ is chosen to be in $\Sigma^+ \times S^+ \times \mathbb{T}_T$, then the flow $\tilde{\phi}(t; (0, \tilde{\omega}^s); \varepsilon)$ approaches $\tilde{\Lambda}_\varepsilon^+$ for $t > 0$, and thus neither crosses the switching manifold $x = 0$. It may happen however that $W^s(\tilde{\Lambda}_\varepsilon^+)$ crosses $x = 0$ more than once backwards in time. In this case, $\tilde{\omega}^s$ has to be chosen in the piece of $W^s(\tilde{\Gamma}_\varepsilon^+)$ “closest to” $\tilde{\Gamma}_\varepsilon^+$.

Finally, property (6.3.55) allows us to refer to $W^{s,u}(\tilde{\Lambda}_\varepsilon^\pm)$ as invariant stable and unstable manifolds of $\tilde{\Lambda}_\varepsilon^\pm$ and hence, to refer to $\tilde{\Lambda}_\varepsilon^\pm$ as normally hyperbolic-like invariant manifolds.

6.4 Scattering map

6.4.1 Transverse intersection of the stable and unstable manifolds

In order to introduce the scattering map, we first wonder about sufficient conditions for the intersection of the stable and unstable manifolds of $\tilde{\Lambda}_\varepsilon^+$ and $\tilde{\Lambda}_\varepsilon^-$ when $\varepsilon > 0$. The following result, equivalent to Proposition 9.1 in [DdILS06], provides sufficient conditions for both manifolds to intersect transversally in a three-dimensional heteroclinic manifold which can be parametrized by the coordinates $(\theta, v, s) \in \mathbb{T} \times [v_1, v_2] \times \mathbb{T}_T$.

Proposition 6.4.1. *Let (6.3.36) be a parametrization of the unperturbed heteroclinic manifold $W^u(\tilde{\Lambda}_0^-) = W^s(\tilde{\Lambda}_0^+)$, and assume that there exists an open set $J \subset N$ such that, for all $(\theta_0, v_0, s_0) \in J$, the function*

$$\zeta \longmapsto M(\zeta, \theta_0, v_0, s_0), \quad (6.4.1)$$

with

$$M(\zeta, \theta_0, v_0, s_0) := \int_{-\infty}^{\infty} \{X, h\} (\phi_{\mathcal{U}}(\theta_0 \alpha(v_0) + \zeta + t; 0, v_0), \sigma^{up}(t), s_0 + \zeta + t) dt, \quad (6.4.2)$$

has a simple zero at $\zeta = \bar{\zeta}(\theta_0, v_0, s_0)$. Then, there exists locally unique points $\tilde{z}^*(\theta_0, v_0, s_0; \varepsilon) \in W^s(\tilde{\Lambda}_\varepsilon^+) \cap W^u(\tilde{\Lambda}_\varepsilon^-)$ and $\tilde{z}^\pm(\theta_0, v_0, s_0) \in \tilde{\Lambda}_\varepsilon^\pm$ such that

$$\lim_{t \rightarrow \pm\infty} \tilde{\phi}(t; \tilde{z}^*; \varepsilon) - \tilde{\phi}(t; \tilde{z}^\pm; \varepsilon) = 0.$$

Moreover, the heteroclinic trajectory $\tilde{\phi}(t; \tilde{z}^*; \varepsilon)$ intersects the switching manifold given by $x = 0$ at a point $\tilde{z}_0^*(\theta_0, v_0, s_0, \varepsilon) \in \mathbb{R}^2 \times \Sigma \times \mathbb{T}_T$ fulfilling

$$\begin{aligned} \Pi_y(\tilde{z}_0^*) &= y_h \\ &+ \frac{\varepsilon}{y_h} \int_{-\infty}^0 \{X^-, h\} (\phi_{\mathcal{U}}(\theta_0 \alpha(v_0) + \bar{\zeta} + t; 0, v_0), \sigma^{up}(t), s_0 + \bar{\zeta} + t) dt + O(\varepsilon^2), \end{aligned} \quad (6.4.3)$$

where y_h is the y coordinate of the unperturbed upper heteroclinic connection given in (6.2.10)-(6.2.11), $\sigma^{up}(0) = (0, y_h)$.

Proof. We first study the intersection of the $W^s(\tilde{\Lambda}_\varepsilon^+)$ and $W^u(\tilde{\Lambda}_\varepsilon^-)$ with the section given by $x = 0$, $\mathbb{R}^2 \times \Sigma \times \mathbb{T}_T$. To this end, we consider a point at the intersection between the unperturbed heteroclinic connection and this section. In terms of the parametrization provided in (6.3.64), such a point in this 3-dimensional manifold can be given in terms of the parameters (θ, v, s) as

$$\begin{aligned} \tilde{z}_0(\theta_0, v_0, s_0) &:= F_0^{s,u}(\theta_0, v_0, s_0, 1) = (\phi_{\mathcal{U}}(\theta_0 \alpha(v_0); 0, v_0), \sigma^{up}(0), s_0) \\ &= (\phi_{\mathcal{U}}(\theta_0 \alpha(v_0); 0, v_0), 0, y_h, s_0) \in \{x = 0\} \cap W^u(\tilde{\Lambda}^-) = \{x = 0\} \cap W^s(\tilde{\Lambda}^+), \end{aligned}$$

where $(0, y_h) = \sigma^{\text{up}}(0)$, $\tilde{\Sigma}$ is given in (6.3.1) and $\phi_{\mathcal{U}}(\theta_0\alpha(v_0); 0, v_0)$ is the solution of system (6.2.4) such that $\phi_{\mathcal{U}}(0; 0, v_0) = (0, v_0)$. However, in order to easily identify points in the perturbed heteroclinic manifold with points in the normally hyperbolic manifolds $\tilde{\Lambda}_\varepsilon^\pm$, we introduce a fourth parameter, $\zeta \in \mathbb{R}$, in the parametrization of \tilde{z}_0 as follows

$$\begin{aligned} \tilde{z}_0(\theta_0 + \frac{\zeta}{\alpha(v_0)}, v_0, s_0 + \zeta) &:= (\phi_{\mathcal{U}}(\theta_0\alpha(v_0) + \zeta; 0, v_0), 0, y_h, s_0 + \zeta) \\ &\in \{x = 0\} \cap W^u(\tilde{\Lambda}^-) = \{x = 0\} \cap W^s(\tilde{\Lambda}^+). \end{aligned} \quad (6.4.4)$$

Let us consider the line

$$\tilde{N} = \{\tilde{z}_0 + l(0, 0, 0, 1, 0), l \in \mathbb{R}\} \subset \mathbb{R}^2 \times \Sigma \times \mathbb{T}_T$$

and define the points

$$\begin{aligned} \tilde{z}^{s/u}(\zeta, \theta_0, v_0, s_0, \varepsilon) \\ = \left(0, y^{s/u}, \phi_{\mathcal{U}}\left(\left(\theta_0 + \frac{\zeta}{\alpha(v_0)}\right)\alpha(v_0) + \zeta; 0, v_0\right), s_0 + \zeta\right) = W^{s/u}(\tilde{\Lambda}_\varepsilon^{+/-}) \cap \tilde{N}. \end{aligned} \quad (6.4.5)$$

The existence of $\tilde{z}^{s/u}$ comes from the following argument.

On one hand, the 4-dimensional perturbed manifolds $W^{s/u}(\tilde{\Lambda}_\varepsilon^{+/-})$ exist and are ε -close to $W^{s/u}(\tilde{\Lambda}^{+/-})$ (see Proposition 6.3.1). On the other hand, due to the form of the Hamiltonians X^\pm given in (6.2.5), the intersection of \tilde{N} with the unperturbed manifold $W^u(\tilde{\Lambda}^-) = W^s(\tilde{\Lambda}^+)$ is transversal at \tilde{z}_0 . This permits us to ensure that these points exist and are unique for $\varepsilon > 0$ small enough. Moreover, they are of the form

$$\tilde{z}^{u/s} = \tilde{z}_0 + (0, O(\varepsilon), 0, 0, 0).$$

In order to see that the manifolds $W^u(\tilde{\Lambda}_\varepsilon^-)$ and $W^s(\tilde{\Lambda}_\varepsilon^+)$ intersect transversally at the section given by $x = 0$, $\mathbb{R}^2 \times \Sigma \times \mathbb{T}_T$, we study the distance between the points $\tilde{z}^{u,s}$ measured using the unperturbed Hamiltonian,

$$\Delta(\theta_0 + \frac{\zeta}{\alpha(v_0)}, v_0, s_0 + \zeta, \varepsilon) = H_0(\tilde{z}^u) - H_0(\tilde{z}^s) = X(\tilde{z}^u) - X(\tilde{z}^s), \quad (6.4.6)$$

where $X(x, y)$ is the piecewise-defined Hamiltonian associated with system (6.2.3) and $X(\tilde{z})$ is a shorthand for $X(\Pi_x(\tilde{z}), \Pi_y(\tilde{z}))$. Note that, as the Hamiltonian X is continuous at the switching surface $x = 0$ where the points $\tilde{z}^{s,u}$ belong to, it is not relevant which of the branches, X^\pm , is applied to evaluate (6.4.6). In fact we have $X(\tilde{z}^u) - X(\tilde{z}^s) = \frac{(y^u)^2}{2} - \frac{(y^s)^2}{2}$. We proceed now solving the equation

$$\Delta(\theta_0 + \frac{\zeta}{\alpha(v_0)}, v_0, s_0 + \zeta, \varepsilon) = 0, \quad (6.4.7)$$

which we choose to solve for ζ . That is, we want to find $\zeta^*(\theta_0, v_0, s_0, \varepsilon)$ such that

$$\Delta(\theta_0 + \frac{\zeta^*}{\alpha(v_0)}, v_0, s_0 + \zeta^*, \varepsilon) = 0.$$

In order to find ζ^* we proceed as usual in Melnikov-like methods. That is, we first obtain an explicit expression of the first order term of the expansion in powers of ε of Eq. (6.4.7). Then, assuming the existence of simple zeros for γ of this first order term, we apply the implicit function theorem to find ζ^* .

To find an expression for Δ we proceed as in the proof of Proposition 6.3.1 but making the reverse argument.

As \tilde{z}^s and \tilde{z}^u do not necessarily belong to $\tilde{\Sigma}$, we evolve with the flow $\tilde{\phi}$ with initial conditions \tilde{z}^s and \tilde{z}^u forwards and backwards in time, respectively, until the section $\tilde{\Sigma}^+$ is reached, so we obtain points in $\{0\} \times W^s(\tilde{\Gamma}_\varepsilon^+)$ and $\{0\} \times W^u(\tilde{\Gamma}_\varepsilon^-)$, respectively. That is, we use the maps κ_ε , $\bar{\kappa}_\varepsilon$, P_ε^- and P_ε^+ defined in section 6.3.1 to obtain the points

$$(0, \tilde{\omega}^s) = \begin{cases} \kappa_\varepsilon(\tilde{z}^s) & \text{if } \tilde{z}^s \in S^- \times \Sigma^+ \times \mathbb{T}_T \\ P_\varepsilon^-(\kappa_\varepsilon(\tilde{z}^s)) & \text{if } \tilde{z}^s \in S^+ \times \Sigma^+ \times \mathbb{T}_T \end{cases}$$

and

$$(0, \tilde{\omega}^u) = \begin{cases} \bar{\kappa}_\varepsilon(\tilde{z}^u) & \text{if } \tilde{z}^u \in S^+ \times \Sigma^+ \times \mathbb{T}_T \\ (P_\varepsilon^+)^{-1}(\bar{\kappa}_\varepsilon(\tilde{z}^u)) & \text{if } \tilde{z}^u \in S^- \times \Sigma^+ \times \mathbb{T}_T \end{cases}$$

Adding and subtracting $X(\tilde{\omega}^s) = X^+(\tilde{\omega}^s)$ and $X(\tilde{\omega}^u) = X^-(\tilde{\omega}^u)$ in Eq. (6.4.6), we write Δ as

$$\begin{aligned} \Delta(\theta_0 + \frac{\zeta}{\alpha(v_0)}, v_0, s_0 + \zeta, \varepsilon) = \\ \Delta^-(\theta_0 + \frac{\zeta}{\alpha(v_0)}, v_0, s_0 + \zeta, \varepsilon) - \Delta^+(\theta_0 + \frac{\zeta}{\alpha(v_0)}, v_0, s_0 + \zeta, \varepsilon) \end{aligned} \quad (6.4.8)$$

where

$$\Delta^-(\theta_0 + \frac{\zeta}{\alpha(v_0)}, v_0, s_0 + \zeta, \varepsilon) = X^-(\tilde{\omega}^u) - X^-(\tilde{\omega}^u) + X(\tilde{z}^u) \quad (6.4.9)$$

$$\Delta^+(\theta_0 + \frac{\zeta}{\alpha(v_0)}, v_0, s_0 + \zeta, \varepsilon) = X^+(\tilde{\omega}^s) - X^+(\tilde{\omega}^s) + X(\tilde{z}^s). \quad (6.4.10)$$

As the points $\tilde{z}^{s/u}$ belong to $W^{s/u}(\tilde{\Lambda}_\varepsilon^{+/-})$, the points $\tilde{\omega}^{s/u}$ belong to $W^{s/u}(\tilde{\Gamma}_\varepsilon^{+/-})$. From Theorem 6.3.1 it comes that there exist two points, $\tilde{\omega}^\pm \in \tilde{\Gamma}_\varepsilon^\pm$ such that

$$P^{-n}(\tilde{\omega}^u) - P^{-n}(\tilde{\omega}^-) < K^-(\bar{\lambda}^-)^{-n} \longrightarrow 0 \quad (6.4.11)$$

$$P^n(\tilde{\omega}^s) - P^n(\tilde{\omega}^+) < K^+(\bar{\lambda}^+)^n \longrightarrow 0 \quad (6.4.12)$$

as $n \rightarrow \infty$. We now obtain expressions for Δ^\pm . We write here the details for the derivations of these expressions for Δ^- ; proceeding similarly, one derives also equivalent formulas for Δ^+ .

Let us observe that, as $\tilde{z}^u \in W^u(\tilde{\Lambda}_\varepsilon^-)$, its backward flow never reaches $x = 0$ and therefore $\bar{\kappa}_\varepsilon(\tilde{z}^u)$ is well defined. Moreover, $(0, \tilde{\omega}^u) \in \Sigma \times \mathbb{R}^2 \times \mathbb{T}_T$. Analogously for \tilde{z}^s . Adding and subtracting $X^-(\tilde{\omega}^-)$ in (6.4.9) we write Δ^- as

$$\Delta^-(\theta_0 + \frac{\zeta}{\alpha(v_0)}, v_0, s_0 + \zeta, \varepsilon) = X^-(\tilde{\omega}^u) \tag{6.4.13}$$

$$- X^-(\tilde{\omega}^-) \tag{6.4.14}$$

$$- X^-(\tilde{\omega}^u) + X(\tilde{z}^u)$$

$$+ X^-(\tilde{\omega}^-),$$

where we have split the equation to make what follows more clear.

We now remark that, for all n , the points $P_\varepsilon^{-n}(\tilde{\omega}^u)$ and $P_\varepsilon^{-n}(\tilde{\omega}^-)$ belong to the (inverse) impact sequence of the points $\tilde{\omega}^u$ and $\tilde{\omega}^-$, respectively. Hence, we can apply Lemma 6.3.1 to Eqs. (6.4.13) and (6.4.14) to obtain

$$\begin{aligned} \Delta^-(\theta_0 + \frac{\zeta}{\alpha(v_0)}, v_0, s_0 + \zeta, \varepsilon) &= \varepsilon \int_{s_\varepsilon^{n,u} - \Pi_s(\tilde{\omega}^u)}^0 \{X^-, h\} \left(\tilde{\phi}(t; (0, \tilde{\omega}^u); \varepsilon) \right) dt + X^-(P_\varepsilon^{-n}(\tilde{\omega}^u)) \\ &- \varepsilon \int_{s_\varepsilon^{n,-} - \Pi_s(\tilde{\omega}^-)}^0 \{X^-, h\} \left(\tilde{\phi}(t; (0, \tilde{\omega}^-); \varepsilon) \right) dt - X^-(P_\varepsilon^{-n}(\tilde{\omega}^-)) \\ &- X^-(\tilde{\omega}^u) + X(\tilde{z}^u) \\ &+ X^-(\tilde{\omega}^-), \end{aligned}$$

where

$$\begin{aligned} s_\varepsilon^{i,u} &= \Pi_s(P_\varepsilon^{-i}(\tilde{\omega}^u)) \\ s_\varepsilon^{i,-} &= \Pi_s(P_\varepsilon^i(\tilde{\omega}^-)) \end{aligned}$$

are the s coordinate of the even terms of the (inverse) impact sequences of $\tilde{\omega}^u$ and $\tilde{\omega}^-$, respectively.

We now merge the two integrals and we write Δ^- as

$$\begin{aligned} \Delta^-(\theta_0 + \frac{\zeta}{\alpha(v_0)}, v_0, s_0 + \zeta, \varepsilon) \\ = \varepsilon \int_{s_\varepsilon^{-n,u} - \Pi_s(\tilde{\omega}^u)}^0 \left(\{X^-, h\} \left(\tilde{\phi}(t; (0, \tilde{\omega}^u); \varepsilon) \right) \right. \\ \left. - \{X^-, h\} \left(\tilde{\phi}(t; (0, \tilde{\omega}^-); \varepsilon) \right) \right) dt \end{aligned} \quad (6.4.15)$$

$$+ \varepsilon \int_{s_\varepsilon^{-n,u} - \Pi_s(\tilde{\omega}^u)}^{s_\varepsilon^{-n,-} - \Pi_s(\tilde{\omega}^-)} \{X^-, h\} \left(\tilde{\phi}(t; (0, \tilde{\omega}^-); \varepsilon) \right) dt \quad (6.4.16)$$

$$\begin{aligned} + X^-(P_\varepsilon^{-n}(\tilde{\omega}^u)) - X^-(P_\varepsilon^{-n}(\tilde{\omega}^-)) \\ - X^-(\tilde{\omega}^u) + X^-(\tilde{\omega}^-), \end{aligned} \quad (6.4.17)$$

where now the integral in (6.4.15) has to be split in $2n$ integrals delimited by consecutive values of t given by both impact sequences. The integral in (6.4.16) has to be added to compensate the change of the lower integration limit of the integrand

$$\{X^-, h\} \left(\tilde{\phi}(t; (0, \tilde{\omega}^-); \varepsilon) \right).$$

We now want to make $n \rightarrow \infty$.

On the one hand, property (6.4.11) tells us that expression (6.4.17) tends to zero when $n \rightarrow \infty$.

On the other hand, when $n \rightarrow \infty$, Eq. (6.4.16) is of order $O(\varepsilon^2)$. This comes from the following argument. We first recall that the points $\tilde{\omega}^-$ and $\tilde{\omega}^u$ are images of points in N and E^u by the maps G_ε^- and G_ε^u given in Theorem 6.3.1, respectively. As these maps are regular in ε , and $\Pi_s(G_0^-(v, s) = \Pi_s(G_0^u(v, s, \eta)))$, $\forall \eta \in [0, 1]$, we have that $\Pi_s(\tilde{\omega}^u) - \Pi_s(\tilde{\omega}^-) = O(\varepsilon)$. Hence, recalling that, by property (6.4.11), $s_\varepsilon^{-n,-} - s_\varepsilon^{-n,u}$ tends to zero exponentially, it comes that

$$\begin{aligned} s_\varepsilon^{-n,-} - \Pi_s(\tilde{\omega}^-) - (s_\varepsilon^{-n,u} - \Pi_s(\tilde{\omega}^u)) \\ < K^-(\bar{\lambda}^-)^{-n} + O(\varepsilon) \longrightarrow O(\varepsilon), n \longrightarrow \infty. \end{aligned}$$

As the integrand is continuous, expression (6.4.16) becomes of order $O(\varepsilon^2)$ when $n \rightarrow \infty$. We now focus on the integral given in (6.4.15). As noted in the proof of Proposition 6.3.1, this integral does not converge when $n \rightarrow \infty$. This is because, for $\varepsilon > 0$, the switching manifold $\tilde{\Sigma}$ is not an isochrone and hence $\tilde{\phi}(t; (0, \tilde{\omega}^u); \varepsilon) \notin W^u(\tilde{\phi}(t; (0, \tilde{\omega}^-); \varepsilon))$. As argued in the proof of Proposition 6.3.1, one has to consider the delay $\tau' = \Pi_s(\tilde{\omega}^-) - \Pi_s(\tilde{\omega}^u)$ to obtain $\tilde{\phi}(t + \tau'; (0, \tilde{\omega}^u); \varepsilon) \in W^u(\tilde{\phi}(t; (0, \tilde{\omega}^-); \varepsilon))$. Hence, due to the hyperbolicity property

$$\left| \tilde{\phi}(t; (0, \tilde{\omega}^-); \varepsilon) - \tilde{\phi}(t + \tau'; (0, \tilde{\omega}^u); \varepsilon) \right| < K^- e^{\lambda^- t} \longrightarrow 0, t \rightarrow -\infty$$

the integral becomes convergent.

Then, the error due to introducing the delay τ' becomes

$$\begin{aligned}
& \varepsilon \int_{s_\varepsilon^{-n,u} - \Pi_s(\tilde{\omega}^u)}^0 \left(\{X^-, h\} \left(\tilde{\phi}(t; (0, \tilde{\omega}^u); \varepsilon) \right) \right. \\
& \quad \left. - \{X^-, h\} \left(\tilde{\phi}(t + \tau'; (0, \tilde{\omega}^u); \varepsilon) \right) \right) dt \\
& = \varepsilon \left(X^-(\tilde{\omega}^u) - X^-(\tilde{\phi}(\tau'; (0, \tilde{\omega}^u); \varepsilon)) \right. \\
& \quad \left. - X^-(\tilde{\phi}(s_\varepsilon^{-n,u} - \Pi_s(\tilde{\omega}^u); (0, \tilde{\omega}^u); \varepsilon)) \right. \\
& \quad \left. + X^-(\tilde{\phi}(s_\varepsilon^{-n,u} - \Pi_s(\tilde{\omega}^u) + \tau'; (0, \tilde{\omega}^u); \varepsilon)) \right) \\
& = \varepsilon \int_{-\tau'}^0 \left(\{X^-, h\} \left(\tilde{\phi}(t; (0, \tilde{\omega}^u); \varepsilon) \right) \right) dt \tag{6.4.18}
\end{aligned}$$

$$\begin{aligned}
& - \varepsilon \int_{-\tau'}^0 \left(\{X^-, h\} \left(\tilde{\phi}(t + s_\varepsilon^{-n,u} - \Pi_s(\tilde{\omega}^u); (0, \tilde{\omega}^u); \varepsilon) \right) \right) dt \tag{6.4.19} \\
& = O(\varepsilon^2).
\end{aligned}$$

Recalling that $\tau = O(\varepsilon)$ and that the flows restricted to the unstable manifold are bounded backwards in time, the integrals in (6.4.18) and (6.4.19) are of order $O(\varepsilon)$, and hence the total error produced by introducing the delay τ' in $\tilde{\phi}(t; (0, \tilde{\omega}^u); \varepsilon)$ is of order $O(\varepsilon^2)$.

We then make $n \rightarrow \infty$, to obtain

$$\begin{aligned}
& \Delta^-(\theta_0 + \frac{\zeta}{\alpha(v_0)}, v_0, s_0 + \zeta, \varepsilon) \\
& = \varepsilon \int_{-\infty}^0 \left(\{X, h\} \left(\tilde{\phi}(t + \tau'; (0, \tilde{\omega}^u); \varepsilon) \right) \right. \\
& \quad \left. - \{X^-, h\} \left(\tilde{\phi}(t; (0, \tilde{\omega}^-); \varepsilon) \right) \right) dt + O(\varepsilon^2) \tag{6.4.20} \\
& + O(\varepsilon^2) \\
& - X^-(\tilde{\omega}^u) + X(\tilde{z}^u) \\
& + X^-(\tilde{\omega}^-).
\end{aligned}$$

We now expand this in powers of ε . On one hand, as Q^- is critical point of the system associated with the Hamiltonian X , using that

$$(\Pi_x(\tilde{\omega}^-), \Pi_y(\tilde{\omega}^-)) = Q^- + O(\varepsilon),$$

it comes that

$$\{X^-, h\} \left(\tilde{\phi}(t; \tilde{\omega}^-; \varepsilon) \right) = O(\varepsilon).$$

On the other hand, and for the same reason, we have that

$$X^-(\tilde{\omega}^-) = X^-(Q^-) + O(\varepsilon^2).$$

Hence, we can write Δ^- as

$$\begin{aligned} \Delta^-(\theta_0 + \frac{\zeta}{\alpha(v_0)}, v_0, s_0 + \gamma, \varepsilon) \\ = \varepsilon \int_{-\infty}^0 (\{X^-, h\} (\tilde{\phi}(t; (0, \tilde{\omega}_0^u); 0))) dt + O(\varepsilon^2) \end{aligned} \quad (6.4.21)$$

$$\begin{aligned} - X^-(\tilde{\omega}^u) + X(\tilde{z}^u) \\ + X^-(Q^-) + O(\varepsilon^2), \end{aligned} \quad (6.4.22)$$

where

$$(0, \tilde{\omega}_0^u) = \kappa_0^{-1}(\tilde{z}_0),$$

and \tilde{z}_0 is given in (6.4.4).

Let us now worry about the difference given in (6.4.22). As the flow ϕ is as smooth as the flows $\phi^{\pm\pm}$ between the points $\tilde{\omega}^u$ and \tilde{z}^u , we can apply the fundamental theorem of calculus to obtain

$$\begin{aligned} X^-(\tilde{z}^u) - X^-(\tilde{\omega}^u) &= \varepsilon \int_{s_\varepsilon - \Pi_s(\tilde{\omega}^u)}^0 \{X^-, h\} (\phi(t; \tilde{z}^u; \varepsilon)) dt \\ &= \varepsilon \int_{s_0 - \Pi_s(\tilde{\omega}_0^u)}^0 \{X^-, h\} (\phi(t; \tilde{z}_0; 0)) dt + O(\varepsilon^2). \end{aligned}$$

Taking into account that $\phi(t + s_0 - \Pi_s(\tilde{\omega}_0^u); \tilde{z}_0; 0) = \phi(t; \tilde{\omega}_0^u; 0)$, we can merge this last integral with the one given in (6.4.21) to finally obtain

$$\Delta^-(\theta_0 + \frac{\zeta}{\alpha(v_0)}, v_0, s_0 + \zeta, \varepsilon) = X^-(Q^-) + \varepsilon \int_{-\infty}^0 \{X^-, h\} (\phi(t; \tilde{z}_0; 0)) dt + O(\varepsilon^2). \quad (6.4.23)$$

Proceeding similarly for Δ^+ , we also get

$$\Delta^+(\theta_0 + \frac{\zeta}{\alpha(v_0)}, v_0, s_0 + \zeta, \varepsilon) = X^+(Q^+) - \varepsilon \int_0^\infty \{X^+, h\} (\phi(t; \tilde{z}_0; 0)) dt + O(\varepsilon^2).$$

Replacing these expressions in Eq. (6.4.8), we finally obtain an explicit expression for the first term of the expansions in powers of ε of the distance between the points \tilde{z}^u and \tilde{z}^s ,

$$\begin{aligned} \Delta(\theta_0 + \frac{\zeta}{\alpha(v_0)}, v_0, s_0 + \zeta, \varepsilon) &= \\ \varepsilon \int_{-\infty}^\infty \{X, h\} (\phi_U(\theta_0 \alpha(v_0) + \zeta + t; 0, v_0), \sigma^{\text{up}}(t), s_0 + \zeta + t) dt + O(\varepsilon^2) \\ &:= \varepsilon M(\zeta, \theta_0, v_0, s_0) + O(\varepsilon^2). \end{aligned} \quad (6.4.24)$$

On one hand, this integral has to be separated in two pieces from $-\infty$ to 0 and from 0 to $+\infty$ to distinguish between the integrands $\{X^-, h\}$ and $\{X^+, h\}$ respectively. On the other hand, as detailed in Remark 6.3.6, each of these integrals is compound by a sum of integrals given by the impact sequence associated with $u = 0$ of the point \tilde{z}_0 and whose integrands are smooth functions. Hence, the function

$$\zeta \longmapsto M(\zeta, \theta_0, v_0, s_0) \quad (6.4.25)$$

is a smooth function as regular as the flows $\tilde{\phi}^{\pm\pm}$ associated with system (6.2.14) restricted to their respective domains.

Taking $(\theta_0, v_0, s_0) \in J$ given in Proposition 6.4.1, let $\bar{\zeta}(\theta_0, v_0, s_0)$ be a simple zero of (6.4.25). Then, by applying the implicit function theorem to the equation

$$\frac{\Delta(\theta_0 + \frac{\zeta}{\alpha(v_0)}, v_0, s_0 + \zeta)}{\varepsilon} = M(\zeta, \theta_0, v_0, s_0) + O(\varepsilon) = 0$$

at the point $(\zeta, \theta_0, v_0, s_0, \varepsilon) = (\bar{\zeta}, \theta_0, v_0, s_0, 0)$, it comes that, if $\varepsilon > 0$ is small enough, there exists then

$$\zeta^*(\theta_0, v_0, s_0, \varepsilon) = \bar{\zeta} + O(\varepsilon) \quad (6.4.26)$$

which solves Eq. (6.4.7).

Thus, for every $(\theta_0, v_0, s_0) \in J$, there exists a locally unique point at the section $\mathbb{R}^2 \times \Sigma \times \mathbb{T}_T$ belonging to the heteroclinic manifold between the manifolds $\tilde{\Lambda}_\varepsilon^\pm$,

$$\begin{aligned} \tilde{z}_0^*(\theta_0 + \frac{\zeta^*}{\alpha(v_0)}, v_0, s_0 + \zeta^*; \varepsilon) &= \tilde{z}^u(\zeta^*, \theta_0, v_0, s_0, \varepsilon) \\ &= \tilde{z}^s(\zeta^*, \theta_0, v_0, s_0, \varepsilon) \\ &\in W^u(\tilde{\Lambda}_\varepsilon^-) \cap W^s(\tilde{\Lambda}_\varepsilon^+) \cap \Sigma \times \mathbb{R}^2 \times \mathbb{T}_T, \end{aligned} \quad (6.4.27)$$

which is of the form

$$\tilde{z}_0^*(\theta_0, v_0, s_0; \varepsilon) = (0, y_h^*, \phi_u(\theta_0 \alpha(v_0) + \zeta^*; 0, v_0), s_0 + \zeta^*).$$

Let us now obtain the explicit expression, given in (6.4.3), of the first order term of the expansion in powers of ε of y_h^* .

Recalling that $X^-(0, y) = \frac{y^2}{2}$, we expand in powers of ε the value $y_h^* = \sqrt{2X(\tilde{z}_0^*)}$. We first have, using $\tilde{z}_0^*(\theta_0, v_0, s_0; 0) = \tilde{z}_0$,

$$y_h^* = \underbrace{\sqrt{2X(\tilde{z}_0)}}_{y_h} + \varepsilon \underbrace{\frac{1}{\sqrt{2X(\tilde{z}_0)}}}_{y_h} \frac{d}{d\varepsilon} \left(X(\tilde{z}_0^*) \right)_{|\varepsilon=0}.$$

Using the definition of Δ^- given in (6.4.9) and using that $\tilde{z}_0^* = \tilde{z}^u$, it comes that

$$\frac{d}{d\varepsilon} X(\tilde{z}^u)_{|\varepsilon=0} = \frac{d}{d\varepsilon} \Delta^-_{|\varepsilon=0}.$$

Hence, from the expansion in powers of ε of Δ^- given in (6.4.23) we get

$$\begin{aligned} y_h^* &= y_h + \frac{\varepsilon}{y_h} \int_{-\infty}^0 \{X^-, h\} \left(\tilde{\phi}(t; \tilde{z}_0; \varepsilon) \right) dt + O(\varepsilon^2) = \\ & y_h + \frac{\varepsilon}{y_h} \int_{-\infty}^0 \{X^-, h\} \left(\phi_{\mathcal{U}}(\theta_0 \alpha(v_0) + \bar{\zeta} + t; 0, v_0), \sigma^{\text{up}}(t), s_0 + \bar{\zeta} + t \right) dt + O(\varepsilon^2), \end{aligned}$$

We finally consider the point

$$\tilde{z}^*(\theta_0, v_0, s_0; \varepsilon) = \phi_{-\zeta^*}(\tilde{z}_0^*; \varepsilon), \quad (6.4.28)$$

which belongs to $W^u(\Lambda_\varepsilon^-) \cap W^s(\Lambda_\varepsilon^+)$ but is not in $\tilde{\Sigma}$. Moreover, using that $\zeta^* = \bar{\zeta} + O(\varepsilon)$, as given in (6.4.26), \tilde{z}^* is of the form

$$\tilde{z}^*(\theta_0, v_0, s_0; \varepsilon) = \left(\phi_{\mathcal{U}}(\theta_0 \alpha(v_0); 0, v_0), \sigma(-\bar{\zeta}), s_0 \right) + O(\varepsilon),$$

where $(\phi_{\mathcal{U}}(\theta_0 \alpha(v); 0, v), \sigma(\xi), s)$ is the parametrization of the unperturbed heteroclinic connection introduced in (6.3.36). As \tilde{z}^* depends on $(\theta_0, v_0, s_0) \in N$, this permits us to consider two points

$$\tilde{z}^\pm(\theta_0, v_0, s_0; \varepsilon) = F_\varepsilon^\pm(\theta_0^\pm, v_0^\pm, s_0^\pm) = F_\varepsilon^\pm(\theta_0, v_0, s_0) + O(\varepsilon) \in \tilde{\Lambda}_\varepsilon^\pm, \quad (6.4.29)$$

such that

$$\lim_{t \rightarrow \pm\infty} \phi(t; \tilde{z}^*; \varepsilon) - \phi(t; \tilde{z}^\pm; \varepsilon) = 0,$$

where F_ε^\pm are the parametrizations of $\tilde{\Lambda}_\varepsilon^\pm$ defined in (6.3.59) and $(\theta_0^\pm, v_0^\pm, s_0^\pm) \in N$, with N the reference manifold given in (6.3.37). \square

Note that, as $\tilde{\Lambda}_\varepsilon^\pm$ are invariant manifolds, the flows $\tilde{\phi}(t; \tilde{z}^\pm; \varepsilon)$ do not cross the switching manifold given by $x = 0$ for any $t \in (-\infty, \infty)$. As a consequence of that, the direct and inverse impact sequences introduced in (6.3.17)-(6.3.18) associated with the points \tilde{z}^\pm are defined for all their iterates. Hence, the flows $\tilde{\phi}(t; \tilde{z}^\pm; \varepsilon)$ can be written of the form given in (6.3.28) for $t \in (-\infty, \infty)$.

Regarding the flow $\tilde{\phi}(t; \tilde{z}^*; \varepsilon)$, as it is restricted to the heteroclinic manifold between $\tilde{\Lambda}_\varepsilon^-$ and $\tilde{\Lambda}_\varepsilon^+$, it crosses the switching manifold given by $x = 0$ only once. This crossing occurs for $t = \zeta^*$ at \tilde{z}_0^* given in (6.4.27), and all the iterates for the direct and inverse impact sequence associated with \tilde{z}_0^* are defined. Hence, using that

$$\tilde{\phi}(t; \tilde{z}^*; \varepsilon) = \tilde{\phi}(t - \zeta^*; \tilde{z}_0^*; \varepsilon), \quad (6.4.30)$$

the flow $\tilde{\phi}(t; \tilde{z}^*; \varepsilon)$ can also be written as in (6.3.28) for $t \in (-\infty, \infty)$.

Remark 6.4.1. *We remind that, from the beginning of this work, we have focused on the heteroclinic manifold close to $W^u(\tilde{\Lambda}_0^-) = W^s(\tilde{\Lambda}_0^+)$, which is given by the “upper” heteroclinic connection of system \mathcal{X} . Obviously, one can derive equivalent conditions to Proposition 6.4.1 for the intersection between the manifolds $W^s(\tilde{\Lambda}_\varepsilon^-)$ and $W^u(\tilde{\Lambda}_\varepsilon^+)$.*

6.4.2 First order properties of the scattering map

Let $\bar{\zeta}$ be a simple zero of the function (6.4.1) for any $(\theta, v, s) \in J \subset N$. Then, for any $(\theta, v, s) \in J$ we can define the scattering map

$$S_\varepsilon^{\text{up}} : \begin{array}{ccc} \tilde{\Lambda}_\varepsilon^- & \longrightarrow & \tilde{\Lambda}_\varepsilon^+ \\ \tilde{z}^-(\theta, v, s; \varepsilon) & \longmapsto & \tilde{z}^+(\theta, v, s; \varepsilon) \end{array} \quad (6.4.31)$$

which identifies the points in (6.4.29) connected by the orbit of the heteroclinic point $\tilde{z}^*(\theta, v, s; \varepsilon) \in W^u(\tilde{z}^-) \cap W^s(\tilde{z}^+)$, which is of the form

$$\tilde{z}^*(\theta, v, s; \varepsilon) = (\phi_U(\theta\alpha(v); 0, v), \sigma^{\text{up}}(-\bar{\zeta}), s) + O(\varepsilon).$$

Following Remark 6.4.1, it is of course also possible to define another scattering map, $S_\varepsilon^{\text{down}}$, by identifying points in the manifolds $\tilde{\Lambda}_\varepsilon^\pm$ connected by the orbit of a point at the intersection of the manifolds $W^s(\tilde{\Lambda}_\varepsilon^-)$ and $W^u(\tilde{\Lambda}_\varepsilon^+)$.

Note that, by contrast to [DdlLS06], we deal here with heteroclinic manifolds and not homoclinic. In the homoclinic case, the scattering map is understood as a map from a normally hyperbolic manifold onto itself. We could also have such a situation here by considering the composition of the two scattering maps mentioned above,

$$\begin{array}{ccc} S_\varepsilon^{\text{down}} \circ S_\varepsilon^{\text{up}} & : & \tilde{\Lambda}_\varepsilon^- \longrightarrow \tilde{\Lambda}_\varepsilon^- \\ S_\varepsilon^{\text{up}} \circ S_\varepsilon^{\text{down}} & : & \tilde{\Lambda}_\varepsilon^+ \longrightarrow \tilde{\Lambda}_\varepsilon^+ \end{array}$$

However, for this purpose one first needs to understand the dynamics inside the manifolds and this is left for future work.

In this section, we focus on the scattering map $S_\varepsilon^{\text{up}}$ defined by identifying points in the manifolds $\tilde{\Lambda}_\varepsilon^-$ and $\tilde{\Lambda}_\varepsilon^+$, as written in (6.4.31). Obviously, everything that we derive in this section can also be stated for the scattering map $S_\varepsilon^{\text{down}}$, from $\tilde{\Lambda}_\varepsilon^+$ to $\tilde{\Lambda}_\varepsilon^-$ determined by the orbits of heteroclinic points in the intersection of $W^s(\tilde{\Lambda}_\varepsilon^-)$ and $W^u(\tilde{\Lambda}_\varepsilon^+)$.

As it comes from Proposition 6.3.1 and has been shown in Eq. (6.4.29), the points $\tilde{z}^\pm(\theta, v, s)$ can be written in terms of the reference manifold N defined in (6.3.37) as

$$\begin{aligned} \tilde{z}^\pm(\theta, v, s; \varepsilon) &= F_\varepsilon^\pm(\theta^\pm, v^\pm, s^\pm) \\ &= F_0^\pm(\theta, v, s) + O(\varepsilon) \\ &= (\phi_U(\theta\alpha(v); 0, v), Q^\pm, s) + O(\varepsilon). \end{aligned}$$

This induces a map

$$\mathfrak{s}_\varepsilon^{\text{up}} : \begin{array}{ccc} N & \longrightarrow & N \\ (\theta^-, v^-, s^-) & \longmapsto & (\theta^+, v^+, s^+) \end{array}$$

fulfilling

$$S_\varepsilon^{\text{up}}(F_\varepsilon^-(\theta^-, v^-, s^-)) = F_\varepsilon^+(\mathfrak{s}_\varepsilon^{\text{up}}(\theta^-, v^-, s^-)).$$

For $\varepsilon = 0$, $\tilde{z}^- = F_0^-(\theta, v, s)$ and $\tilde{z}^+ = F_0^+(\theta, v, s)$, and the map S_0^{up} sends a point $(\phi_{\mathcal{U}}(\theta\alpha(v); 0, v), Q^-, s) \in \tilde{\Lambda}_0^-$ to $(\phi_{\mathcal{U}}(\theta\alpha(v); 0, v), Q^+, s) \in \tilde{\Lambda}_0^+$. Hence, in this case,

$$S_0^{\text{up}} \circ F_0^-(\theta, v, s) = F_0^+(\theta, v, s), \forall (\theta, v, s) \in N,$$

and $\mathfrak{s}_0^{\text{up}}$ becomes the identity.

If $\varepsilon > 0$, $\mathfrak{s}_\varepsilon^{\text{up}}(\theta^-, v^-, s^-)$ and (θ^-, v^-, s^-) become ε -close.

Using the maps given in Remark 6.3.8 that parametrize the stable and unstable manifolds $W^{s,u}(\tilde{\Lambda}_\varepsilon^{\pm})$, the points $\tilde{z}^*(\theta, v, s) \in W^s(\tilde{\Lambda}_\varepsilon^+) \cap W^u(\tilde{\Lambda}_\varepsilon^-)$ can be also written as

$$\begin{aligned} \tilde{z}^*(\theta, v, s; \varepsilon) &= (\phi_{\mathcal{U}}(\theta\alpha(v); 0, v), \sigma^{\text{up}}(-\bar{\zeta}), s) + O(\varepsilon) \\ &= F_0^s(\theta, v, s, \eta_0^+) + O(\varepsilon), \end{aligned}$$

or also in terms of F_ε^u as

$$\begin{aligned} \tilde{z}^*(\theta, v, s; \varepsilon) &= (\phi_{\mathcal{U}}(\theta\alpha(v); 0, v), \sigma^{\text{up}}(-\bar{\zeta}), s) + O(\varepsilon) \\ &= F_0^u(\theta, v, s, \eta_0^-) + O(\varepsilon). \end{aligned}$$

where, using (6.3.48), η_0^\pm become

$$\eta_0^\pm = e^{\pm\bar{\zeta}\lambda^\pm}. \quad (6.4.32)$$

We now want to derive properties of the image of the Scattering map (6.4.31). More precisely, we want to measure the difference of the energy levels of the points \tilde{z}^\pm . This is equivalent to measure the difference between energy levels of points in N and their image by $\mathfrak{s}_\varepsilon^{\text{up}}$. To this end, as it is usual in Melnikov-like theory, we use the Hamiltonian U which, recalling that $U(0, v) = \frac{v^2}{2}$, is equivalent to measure the distance in the coordinate v . That is, we wonder about

$$\Delta U = U(\tilde{z}^+) - U(\tilde{z}^-), \quad (6.4.33)$$

where $U(\tilde{z})$ is a shorthand for $U(\Pi_u(\tilde{z}), \Pi_v(\tilde{z}))$. Note that this difference is 0 for $\varepsilon = 0$, and therefore $\Delta U = O(\varepsilon)$.

The following Proposition provides an expression for the first order term in ε of ΔU .

Proposition 6.4.2. *Let $(\theta, v, s) \in J \subset N$ given in Proposition 6.4.1, and let $\bar{\zeta} = \bar{\zeta}(\theta, v, s)$ be a simple zero of the function*

$$\zeta \longrightarrow M(\zeta, \theta, v, s),$$

where M is defined in (6.4.2). Let also $\tilde{z}^\pm \in \tilde{\Lambda}_\varepsilon^\pm$ be points such that

$$\tilde{z}^+ = S_\varepsilon^{\text{up}}(\tilde{z}^-).$$

Then,

$$\begin{aligned}
U(\tilde{z}^+) - U(\tilde{z}^-) &= \varepsilon \int_{-\infty}^0 \left(\{U, h\} ((\phi_U(\theta\alpha(v) + t; 0, v), \sigma^{up}(t - \bar{\zeta}), s + t)) \right. \\
&\quad \left. - \{U, h\} (\phi_U(\theta\alpha(v) + t; 0, v), Q^-, s + t) \right) dt \\
&\quad + \varepsilon \int_0^{+\infty} \left(\{U, h\} ((\phi_U(\theta\alpha(v) + t; 0, v), \sigma^{up}(t - \bar{\zeta}), s + t)) \right. \\
&\quad \left. - \{U, h\} (\phi_U(\theta\alpha(v) + t; 0, v), Q^+, s + t) \right) dt \\
&\quad + O(\varepsilon^{1+\rho_2}),
\end{aligned} \tag{6.4.34}$$

for some $\rho_2 > 0$.

In order to prove this, we will use the following Lemma, whose proof is given after proving Proposition 6.4.2.

Lemma 6.4.1. *Let*

$$\begin{aligned}
(0, \tilde{\omega}^+) &= (0, G_\varepsilon^+(v, s)) \in \tilde{\Lambda}_\varepsilon^+ \\
(0, \tilde{\omega}_0^+) &= (0, G_0^+(v, s)) \in \tilde{\Lambda}_0^+.
\end{aligned}$$

Then, there exists $\rho > 0$ and $c > 0$ independent of ε such that, if $\varepsilon > 0$ is small enough,

$$\left| \tilde{\phi}(t; (0, \tilde{\omega}^+); \varepsilon) - \tilde{\phi}(t; (0, \tilde{\omega}_0^+); 0) \right| = O(\varepsilon^\rho)$$

for $0 \leq t \leq c \ln \frac{1}{\varepsilon}$.

Proof. Of Proposition 6.4.2

Let $(\theta, v, s) \in J$ and let $\bar{\zeta}$ be a simple zero of the function

$$\zeta \longrightarrow M(\zeta, \theta, v, s),$$

where M is defined in (6.4.2). Let also $\zeta^*(\theta, v, s, \varepsilon)$ be the solution of Eq. (6.4.7) given by the implicit function theorem near $\bar{\zeta}$, and $\tilde{z}^*(\theta, v, s; \varepsilon)$ the point defined in (6.4.28).

We now want to derive an expression for the first order term of the expansion in powers of ε of expression (6.4.33). Let us write ΔU as

$$\Delta U = \Delta U_+ + \Delta U_-, \tag{6.4.35}$$

where

$$\begin{aligned}
\Delta U_+ &= U(\tilde{z}^+) - U(\tilde{z}^*) \\
\Delta U_- &= U(\tilde{z}^*) - U(\tilde{z}^-).
\end{aligned}$$

We first proceed providing an expression for the difference ΔU_+ ; an analogous one can be obtained for ΔU_- .

Let us now consider the points $\tilde{\omega}^+ \in \tilde{\Gamma}_\varepsilon^+$ and $\tilde{\omega}^* \in W^s(\tilde{\omega}^+)$ given by

$$\begin{aligned}\tilde{\omega}^+ &= G_\varepsilon^+(v^+, s^+) = (\omega^+, s^+) \\ \tilde{\omega}^* &= G_\varepsilon^s(v^+, s^+, \eta^+) = (\omega^*, s^*),\end{aligned}$$

and hence

$$\begin{aligned}(0, \tilde{\omega}^+) &= F_\varepsilon^+(0, v^+, s^+) = (0, \omega^+, s^+) \\ (0, \tilde{\omega}^*) &= F_\varepsilon^s(0, v^+, s^+, \eta^+) = (0, \omega^*, s^*).\end{aligned}$$

We now add and subtract $U(\tilde{\omega}^+)$ and $U(\tilde{\omega}^*)$ in the expression of ΔU_+ , so that it becomes

$$\begin{aligned}\Delta U_+ &= U(\tilde{\omega}^+) \\ &\quad - U(\tilde{\omega}^*) \\ &\quad - U(\tilde{\omega}^+) + U(\tilde{z}^+) \\ &\quad + U(\tilde{\omega}^*) - U(\tilde{z}^*).\end{aligned}$$

As $(0, \tilde{\omega}^+)$ and $(0, \tilde{\omega}^*)$ belong to the switching manifold given by $u = 0$, we can apply Lemma 6.3.1 (Remark 6.3.7) to obtain expressions for $U(\tilde{\omega}^+)$ and $U(\tilde{\omega}^*)$ and write ΔU_+ as

$$\begin{aligned}\Delta U_+ &= -\varepsilon \int_0^{s_\varepsilon^{2n, +} - s^+} \{U, h\} \left(\tilde{\phi}(t; (0, \tilde{\omega}^+); \varepsilon) \right) dt + U(P_\varepsilon^n(\tilde{\omega}^+)) \\ &\quad + \varepsilon \int_0^{s_\varepsilon^{2n, *} - s^*} \{U, h\} \left(\tilde{\phi}(t; (0, \tilde{\omega}^*); \varepsilon) \right) dt - U(P_\varepsilon^n(\tilde{\omega}^*)) \\ &\quad - U(\tilde{\omega}^+) + U(\tilde{z}^+) \\ &\quad + U(\tilde{\omega}^*) - U(\tilde{z}^*),\end{aligned}$$

where $s_\varepsilon^{i, +}$ and $s_\varepsilon^{i, *}$ are the s coordinates of the impact sequences associated with the points $\tilde{\omega}^+$ and $\tilde{\omega}^*$, respectively.

We now proceed as in the proof of Proposition 6.4.1 to merge these two integrals and obtain

$$\Delta U_+ = \varepsilon \int_0^{s_\varepsilon^{2n, +} - s^+} \left(\{U, h\} \left(\tilde{\phi}(t; (0, \tilde{\omega}^*); \varepsilon) \right) - \{U, h\} \left(\tilde{\phi}(t; (0, \tilde{\omega}^+); \varepsilon) \right) \right) dt \quad (6.4.36)$$

$$- \varepsilon \int_{s_\varepsilon^{n, *} - s^*}^{s_\varepsilon^{2n, +} - s^+} \{U, h\} \left(\tilde{\phi}(t; (0, \tilde{\omega}^*); \varepsilon) \right) dt \quad (6.4.37)$$

$$+ U(P_\varepsilon^n(\tilde{\omega}^+)) - U(P_\varepsilon^n(\tilde{\omega}^*)) \quad (6.4.38)$$

$$- U(\tilde{\omega}^+) + U(\tilde{z}^+)$$

$$+ U(\tilde{\omega}^*) - U(\tilde{z}^*),$$

where the integral in (6.4.37) compensates the change of the integrals limits regarding the integrand $\{U, h\} \tilde{\phi}(t; (0, \tilde{\omega}^*); \varepsilon)$. Note that the integral in (6.4.36) has to be split in several integrals delimited by consecutive values of t given by both impact sequences associated with $\tilde{\omega}^+$ and $\tilde{\omega}^*$.

We now want to make $n \rightarrow \infty$.

First of all, we note that the impact sequence associated with the point $\tilde{\omega}^*$ may be finite because the flow may eventually cross the switching manifold given by $x = 0$. However, using the expression in (6.4.28) we can always relate the impact sequences associated with the points \tilde{z}^* and \tilde{z}_0^* , and hence extend the impact sequence associated with $\tilde{\omega}^*$ after crossing $x = 0$. As \tilde{z}_0^* belongs to the heteroclinic manifold and is located at $x = 0$, its impact sequence is defined for all n , and thus we can assume that so it is for $\tilde{\omega}^*$.

Arguing as for Proposition 6.4.1, when $n \rightarrow \infty$, the expression (6.4.37) tends to be of order $O(\varepsilon^2)$. This is due to the fact that

$$s_\varepsilon^{2n,+} - s^+ - (s_\varepsilon^{2n,*} - s^*) \rightarrow O(\varepsilon),$$

and that integrand is bounded.

Moreover, the term in (6.4.38) vanishes when $n \rightarrow \infty$.

As happened for Proposition 6.4.1, the integrand in (6.4.36) does not converge when $n \rightarrow \infty$. In order to have convergence, we first have to delay the flow $\tilde{\phi}(t; (0, \tilde{\omega}^*); \varepsilon)$ by

$$\tau' = \Pi_s(\tilde{\omega}^+) - \Pi_s(\tilde{\omega}^*) = s^+ - s^*.$$

As shown in Proposition 6.3.1, this gives us convergence for the flows

$$\left| \tilde{\phi}(t + \tau'; (0, \tilde{\omega}^*); \varepsilon) - \tilde{\phi}(t; (0, \tilde{\omega}^+); \varepsilon) \right| < K^+ e^{-\lambda^+ t}, \quad t \rightarrow \infty. \quad (6.4.39)$$

We then write the integral in (6.4.36) as

$$\begin{aligned} & \varepsilon \int_0^{s_\varepsilon^{2n,+} - s^+} \left(\{U, h\} \left(\tilde{\phi}(t; (0, \tilde{\omega}^*); \varepsilon) \right) - \{U, h\} \left(\tilde{\phi}(t; (0, \tilde{\omega}^+); \varepsilon) \right) \right) dt \\ &= \varepsilon \int_0^{s_\varepsilon^{2n,+} - s^+} \left(\{U, h\} \left(\tilde{\phi}(t + \tau'; (0, \tilde{\omega}^*); \varepsilon) \right) - \{U, h\} \left(\tilde{\phi}(t; (0, \tilde{\omega}^+); \varepsilon) \right) \right) dt \end{aligned} \quad (6.4.40)$$

$$+ \varepsilon \int_0^{\tau'} \{U, h\} \left(\tilde{\phi}(t; (0, \tilde{\omega}^*); \varepsilon) \right) dt \quad (6.4.41)$$

$$- \varepsilon \int_0^{\tau'} \{U, h\} \left(\tilde{\phi}(t + s_\varepsilon^{2n,+} - s^+; (0, \tilde{\omega}^*); \varepsilon) \right) dt, \quad (6.4.42)$$

where, as in the proof of Proposition 6.4.1 (Eqs. (6.4.18)-(6.4.19)) the integrals (6.4.41) and (6.4.42) compensate the addition of the delay τ' in $\tilde{\phi}(t; (0, \tilde{\omega}^*); \varepsilon)$. Arguing similarly the total error caused by introducing the delay τ' is of order $O(\varepsilon^2)$.

We now show that the integral in (6.4.40) converges when $n \rightarrow \infty$. We proceed similarly as in the proof of Proposition 6.3.1. As mentioned above, the integral in (6.4.40) has to be split in the sum of several integrals given by the impacts with the switching manifold $\tilde{\Sigma}$, which occur at the times

$$\begin{aligned} t_i^+ &= s_\varepsilon^{i,+} - s^+ \\ t_i^* &= s_\varepsilon^{i,*} - s^* - \tau'. \end{aligned}$$

Calling

$$\begin{aligned} a_i &= \min(t_i^+, t_i^*) \\ b_i &= \max(t_i^+, t_i^*), \end{aligned}$$

each of these integrals are of the form

$$\int_{a_i}^{b_{i+1}} \left(\{U, h\} \left(\tilde{\phi}(t + \tau'; (0, \tilde{\omega}^*); \varepsilon) \right) - \{U, h\} \left(\tilde{\phi}(t; (0, \tilde{\omega}^+); \varepsilon) \right) \right) dt. \quad (6.4.43)$$

At the same time, each of these integrals has to be split in three integrals in the intervals

$$\begin{aligned} \mathfrak{J}_1 &= [a_i, b_i] \\ \mathfrak{J}_2 &= [b_i, a_{i+1}] \\ \mathfrak{J}_3 &= [a_{i+1}, b_{i+1}]. \end{aligned}$$

If $t \in \mathfrak{J}_1 \cup \mathfrak{J}_3$, the two Poisson brackets in (6.4.43) differ because the flows belong to different domains,

$$\begin{aligned} \tilde{\phi}(t + \tau'; (0, \tilde{\omega}^*); \varepsilon) &\in S^\pm \times S^\pm \times \mathbb{T}_T \\ \tilde{\phi}(t; (0, \tilde{\omega}^+); \varepsilon) &\in S^\mp \times S^\pm \times \mathbb{T}_T. \end{aligned}$$

However, both flows are bounded and therefore so is the integrand when $t \in \mathfrak{J}_1 \cup \mathfrak{J}_3$. Using that $|t_i^+ - t_i^*| < K^+(\bar{\lambda}^+)^i$, which comes from the hyperbolicity given by Theorem 6.3.1, the length of the intervals \mathfrak{J}_1 and \mathfrak{J}_3 tends exponentially to zero. Thus, the sum of integrals in the intervals \mathfrak{J}_1 and \mathfrak{J}_3 converges.

If $t \in \mathfrak{J}_2$, the hyperbolicity condition (6.4.39) holds which finally gives us the convergence of the integral (6.4.40) when $n \rightarrow \infty$. As a consequence of all this, the integral in (6.4.36) is convergent when $n \rightarrow \infty$. Hence, we can write ΔU_+ as

$$\begin{aligned} \Delta U_+ &= \varepsilon \int_0^\infty \left(\{U, h\} \left(\tilde{\phi}(t + \tau'; (0, \tilde{\omega}^*); \varepsilon) \right) \right. \\ &\quad \left. - \{U, h\} \left(\tilde{\phi}(t; (0, \tilde{\omega}^+); \varepsilon) \right) \right) dt + O(\varepsilon^2) \end{aligned} \quad (6.4.44)$$

$$\begin{aligned} &+ O(\varepsilon^2) \\ &- U(\tilde{\omega}^+) + U(\tilde{z}^+) \\ &+ U(\tilde{\omega}^*) - U(\tilde{z}^*), \end{aligned} \quad (6.4.45)$$

where now the integral (6.4.44) is convergent due to the hyperbolicity condition (6.3.55).

We now want to expand (6.4.44) in powers of ε . Unlike in the proof of Proposition 6.4.1, when using the Hamiltonian U instead of X (compare expressions (6.4.20) and (6.4.44)), the first order term in ε of the Poisson bracket $\{U, h\}$ restricted to the manifold $\tilde{\Lambda}_\varepsilon^+$ does not vanish. For finite fixed times, the difference between the perturbed and unperturbed flows restricted to $\tilde{\Lambda}_\varepsilon^+$ is of order $O(\varepsilon)$. However, as the integral is performed from 0 to ∞ , one has to proceed carefully.

Recalling that $\tau' = O(\varepsilon)$ and using Lemma 6.4.1, we can expand the integral in (6.4.44) to obtain

$$\begin{aligned}
& \int_0^\infty \left(\{U, h\} \left(\tilde{\phi}(t + \tau'; (0, \tilde{\omega}^*); \varepsilon) \right) - \{U, h\} \left(\tilde{\phi}(t + \tau'; (0, \tilde{\omega}^+); \varepsilon) \right) \right) dt \\
&= \int_0^{c \ln \frac{1}{\varepsilon}} \left(\{U, h\} \left(\tilde{\phi}(t; (0, \tilde{\omega}^*); \varepsilon) \right) - \{U, h\} \left(\tilde{\phi}(t; (0, \tilde{\omega}^+); \varepsilon) \right) \right) dt \\
&+ \int_{c \ln(\frac{1}{\varepsilon})}^\infty \left(\{U, h\} \left(\tilde{\phi}(t + \tau'; (0, \tilde{\omega}^*); \varepsilon) \right) - \{U, h\} \left(\tilde{\phi}(t; (0, \tilde{\omega}^+); \varepsilon) \right) \right) dt \\
&= \int_0^{c \ln \frac{1}{\varepsilon}} \left(\{U, h\} \left(\tilde{\phi}(t; (0, \tilde{\omega}_0^*); 0) \right) - \{U, h\} \left(\tilde{\phi}(t; (0, \tilde{\omega}_0^+); 0) \right) \right) dt + O(\varepsilon^\rho \ln \frac{1}{\varepsilon}) \\
&+ \int_{c \ln \frac{1}{\varepsilon}}^\infty \left(\{U, h\} \left(\tilde{\phi}(t; (0, \tilde{\omega}^*); \varepsilon) \right) - \{U, h\} \left(\tilde{\phi}(t; (0, \tilde{\omega}^+); \varepsilon) \right) \right) dt, \tag{6.4.46}
\end{aligned}$$

where¹

$$\begin{aligned}
\tilde{\omega}_0^+ &= G_0^+(v, s) = (\omega_0^+, s) \\
\tilde{\omega}_0^* &= G_0^s(v, s, \eta_0^+) = (\omega_0^*, s),
\end{aligned}$$

and η_0^+ is given in (6.4.32).

We now wonder about the integral (6.4.46). Using the hyperbolicity property of the flow, given by Proposition 6.3.1, we have that

$$\begin{aligned}
& \int_{c \ln \frac{1}{\varepsilon}}^\infty \left(\{U, h\} \left(\tilde{\phi}(t; (0, \tilde{\omega}^*); \varepsilon) \right) - \{U, h\} \left(\tilde{\phi}(t; (0, \tilde{\omega}^+); \varepsilon) \right) \right) dt \\
&< \int_{c \ln \frac{1}{\varepsilon}}^\infty K^+ e^{-\lambda^+ t} = \frac{K^+}{\lambda^+} e^{-\lambda^+ c \ln \frac{1}{\varepsilon}} = \frac{K^+}{\lambda^+} \varepsilon^{c\lambda^+} = \frac{K^+}{\lambda^+} \varepsilon^{\bar{\rho}},
\end{aligned}$$

¹Let us remind that, when $\varepsilon = 0$, $(v^+, s^+) = (v, s)$

with $\bar{\rho} = c\lambda^+ > 0$. This allows us to write the integral (6.4.44) as

$$\begin{aligned} & \int_0^\infty \left(\{U, h\} \left(\tilde{\phi}(t + \tau'; (0, \tilde{\omega}^*); \varepsilon) \right) - \{U, h\} \left(\tilde{\phi}(t + \tau'; (0, \tilde{\omega}^+); \varepsilon) \right) \right) dt \\ &= \int_0^{c \ln \frac{1}{\varepsilon}} \left(\{U, h\} \left(\tilde{\phi}(t; (0, \tilde{\omega}_0^*); 0) \right) - \{U, h\} \left(\tilde{\phi}(t; (0, \tilde{\omega}_0^+); 0) \right) \right) dt \\ &+ O(\varepsilon^\rho \ln \frac{1}{\varepsilon}) + O(\varepsilon^{\bar{\rho}}). \end{aligned}$$

By reverting the last argument, we can complete this integral from $c \ln \frac{1}{\varepsilon}$ to ∞ to finally obtain

$$\begin{aligned} \Delta U_+ &= \varepsilon \int_0^\infty \left(\{U, h\} \left(\tilde{\phi}(t; (0, \tilde{\omega}_0^*); 0) \right) \right. \\ &\quad \left. - \{U, h\} \left(\tilde{\phi}(t; (0, \tilde{\omega}_0^+); 0) \right) \right) dt + O(\varepsilon^{\rho_1}) \end{aligned} \quad (6.4.47)$$

$$- U(\tilde{\omega}^+) + U(\tilde{z}^+) \quad (6.4.48)$$

$$+ U(\tilde{\omega}^*) - U(\tilde{z}^*) \quad (6.4.49)$$

for some $\rho_1 > 0$.

As we did for Proposition 6.4.1, we now apply the fundamental theorem of calculus between the points $\tilde{\omega}^+$ and \tilde{z}^+ and $\tilde{\omega}^*$ and \tilde{z}^* to obtain expressions for (6.4.48) and (6.4.49). Denoting $\tilde{z}^+(0) = \tilde{z}^+(\theta, v, s; 0)$ and $\tilde{z}^*(0) = \tilde{z}^*(\theta, v, s; 0)$ we have that

$$\begin{aligned} U(\tilde{\omega}^+) - U(\tilde{z}^+) &= \varepsilon \int_0^{\Pi_s(\tilde{z}^+) - \Pi_s(\tilde{\omega}^+) = \theta^+ t_1^+} \{U, h\} \left(\tilde{\phi}(t; (0, \tilde{\omega}^+); \varepsilon) \right) dt \\ &= \varepsilon \int_0^{\theta\alpha(v)} \{U, h\} \left(\tilde{\phi}(t; (0, \tilde{\omega}_0^+)) \right) dt + O(\varepsilon^2) \\ U(\tilde{\omega}^*) - U(\tilde{z}^*) &= -\varepsilon \int_0^{\Pi_s(\tilde{z}^*) - \Pi_s(\tilde{\omega}^*) = \theta^+ t_1^+ + \tau'} \{U, h\} \left(\tilde{\phi}(t; (0, \tilde{\omega}^*); \varepsilon) \right) dt \\ &= -\varepsilon \int_0^{\theta\alpha(v)} \{U, h\} \left(\tilde{\phi}(t; (0, \tilde{\omega}_0^*); 0) \right) dt + O(\varepsilon^2). \end{aligned}$$

Then, using that

$$\begin{aligned} \tilde{\phi}(t + \theta\alpha(v); (0, \tilde{\omega}_0^+); 0) &= \tilde{\phi}(t; \tilde{z}^+(\theta, v, s; 0); 0) \\ \tilde{\phi}(t + \theta\alpha(v); (0, \tilde{\omega}_0^*); 0) &= \tilde{\phi}(t; \tilde{z}^*(\theta, v, s; 0); 0), \end{aligned}$$

we can concatenate all integrals to obtain

$$\begin{aligned}
\Delta U_+ &= \varepsilon \int_{-\theta\alpha(v)}^{\infty} \left(\{U, h\} \left(\tilde{\phi}(t; \tilde{z}^*(\theta, v, s; 0); 0) \right) \right. \\
&\quad \left. - \{U, h\} \left(\tilde{\phi}(t; \tilde{z}^+(\theta, v, s; 0); 0) \right) \right) dt + O(\varepsilon^{\rho_1}) \\
&+ \varepsilon \int_0^{-\theta\alpha(v)} \{U, h\} \left(\tilde{\phi}(t; \tilde{z}^+(\theta, v, s; 0)) \right) dt + O(\varepsilon^2) \\
&- \varepsilon \int_{-\theta\alpha(v)}^0 \{U, h\} \left(\tilde{\phi}(t; \tilde{z}^*(\theta, v, s; 0); 0) \right) dt + O(\varepsilon^2) \\
&= \varepsilon \int_0^{+\infty} \left(\{U, h\} \left(\tilde{\phi}(t; \tilde{z}^*(\theta, v, s; 0); 0) \right) \right. \\
&\quad \left. - \{U, h\} \left(\tilde{\phi}(t; \tilde{z}^+(\theta, v, s; 0); 0) \right) \right) dt + O(\varepsilon^{\rho_1} \ln \frac{1}{\varepsilon}) \\
&= \varepsilon \int_0^{+\infty} \left(\{U, h\} \left((\phi_{\mathcal{U}}(\theta\alpha(v) + t; 0, v), \sigma^{\text{up}}(t - \bar{\zeta}), s + t) \right) \right. \\
&\quad \left. - \{U, h\} \left(\phi_{\mathcal{U}}(\theta\alpha(v) + t; 0, v), Q^+, s + t \right) \right) dt + O(\varepsilon^{1+\rho_1}).
\end{aligned}$$

Finally, proceeding similarly for Δ^- , expression (6.4.35) becomes

$$\begin{aligned}
U(\tilde{z}^+) - U(\tilde{z}^-) &= \varepsilon \int_{-\infty}^0 \left(\{U, h\} \left((\phi_{\mathcal{U}}(\theta\alpha(v) + t; 0, v), \sigma^{\text{up}}(t - \bar{\zeta}), s + t) \right) \right. \\
&\quad \left. - \{U, h\} \left(\phi_{\mathcal{U}}(\theta\alpha(v) + t; 0, v), Q^-, s + t \right) \right) dt \\
&+ \varepsilon \int_0^{+\infty} \left(\{U, h\} \left((\phi_{\mathcal{U}}(\theta\alpha(v) + t; 0, v), \sigma^{\text{up}}(t - \bar{\zeta}), s + t) \right) \right. \\
&\quad \left. - \{U, h\} \left(\phi_{\mathcal{U}}(\theta\alpha(v) + t; 0, v), Q^+, s + t \right) \right) dt \\
&+ O(\varepsilon^{1+\rho_2}),
\end{aligned}$$

for some $\rho_2 > 0$. □

Proof. Of Lemma 6.4.1

Let

$$\begin{aligned}
\tilde{z}^{n,+} &= (0, \tilde{\omega}^{n,+}) = (0, v_{\varepsilon}^{n,+}, x_{\varepsilon}^{n,+}, y_{\varepsilon}^{n,+}, s_{\varepsilon}^{n,+}) \\
\tilde{z}_0^{n,+} &= (0, \tilde{\omega}_0^{n,+}) = (0, v_0^{n,+}, x_0^{n,+}, y_0^{n,+}, s_0^{n,+})
\end{aligned}$$

be the impact sequences associated with the points

$$\begin{aligned}
\tilde{\omega}^+ &= G_{\varepsilon}^+(v, s) \in \tilde{\Gamma}_{\varepsilon}^+ \\
\tilde{\omega}_0^+ &= G_0^+(v, s) \in \tilde{\Gamma}_0^+.
\end{aligned}$$

We first write

$$\begin{aligned}\Delta(t) &:= \left| \tilde{\phi}(t; (0, \tilde{\omega}^+); \varepsilon) - \tilde{\phi}(t; (0, \tilde{\omega}_0^+); 0) \right| \\ &= \left| \tilde{\phi}(t - s_\varepsilon^{n,+} + s^+; \tilde{z}^{n,+}; \varepsilon) - \tilde{\phi}(t - s_0^{n,+} + s_0^+; \tilde{z}_0^{n,+}; 0) \right|.\end{aligned}$$

Proceeding as in the proof of Proposition 6.4.2, we define

$$\begin{aligned}a_n &= \min(s_\varepsilon^{n,+} - s^+, s_0^{n,+} - s_0^+) \\ b_n &= \max(s_\varepsilon^{n,+} - s^+, s_0^{n,+} - s_0^+).\end{aligned}$$

Letting \mathcal{F}_ε be the piecewise defined field associated with the perturbed system (6.2.14), and applying the fundamental theorem of calculus and we get

$$\begin{aligned}\Delta(t) &\leq |\tilde{z}^{n,+} - \tilde{\omega}_0^{n,+}| \\ &+ \int_{a_n}^{b_n} \left| \mathcal{F}_\varepsilon \left(\tilde{\phi}(t - s_\varepsilon^{n,+}; \tilde{z}^{n,+}; \varepsilon) \right) - \mathcal{F}_0 \left(\tilde{\phi}(t - s_0^{n,+} + s_0^+; \tilde{z}_0^{n,+}; 0) \right) \right| dt \\ &+ \int_{b_n}^{a_{n+1}} \left| \mathcal{F}_\varepsilon \left(\tilde{\phi}(t - s_\varepsilon^{n,+}; \tilde{z}^{n,+}; \varepsilon) \right) - \mathcal{F}_0 \left(\tilde{\phi}(t - s_0^{n,+} + s_0^+; \tilde{z}_0^{n,+}; 0) \right) \right| dt \\ &+ \int_{a_{n+1}}^{b_{n+1}} \left| \mathcal{F}_\varepsilon \left(\tilde{\phi}(t - s_\varepsilon^{n,+}; \tilde{z}^{n,+}; \varepsilon) \right) - \mathcal{F}_0 \left(\tilde{\phi}(t - s_0^{n,+} + s_0^+; \tilde{z}_0^{n,+}; 0) \right) \right| dt,\end{aligned}$$

For the first and third integral, as both flows do not belong to the same domain $S^\pm \times S^\pm \times \mathbb{T}_T$, the fields do not fulfill that $\mathcal{F}_\varepsilon \rightarrow \mathcal{F}_0$ as $\varepsilon \rightarrow 0$. However, their difference is bounded by some $K_1 > 0$ and we can hence bound the integrands by this constant.

For the middle integral, both flows are located at the same domains and the fields \mathcal{F}_ε and \mathcal{F}_0 are ε -close. Hence, there exists a constant $K > 0$ such that

$$\begin{aligned}\Delta(t) &\leq |\tilde{z}^{n,+} - \tilde{z}_0^{n,+}| \\ &+ K_1(b_n - a_n) \\ &+ \int_{b_n}^{a_{n+1}} K \left| \tilde{\phi}(t; \tilde{z}^{n,+}; \varepsilon) - \tilde{\phi}(t; \tilde{z}_0^{n,+}; 0) \right| dt \\ &+ K_1(a_{n+1} - b_{n+1}).\end{aligned}$$

Using that

$$P_\varepsilon^\pm(\tilde{\omega}^{n-1,+}) - P_0^\pm(\tilde{\omega}_0^{n-1,+}) = O(\varepsilon),$$

and therefore

$$s_\varepsilon^{n,+} - s_0^{n,+} = O(\varepsilon),$$

we have that there exists $K_2 > 0$ such that

$$K_1(b_n - a_n) + K_1(a_{n+1} - b_{n+1}) = K_2 n \varepsilon.$$

Hence, if $t \in [a_n, b_{n+1}]$, we have

$$\Delta(t) \leq |\tilde{z}^{n,+} - \tilde{z}_0^{n,+}| + K_2 n \varepsilon + \int_{b_n}^{a_{n+1}} K \Delta(r) dr.$$

We now want to bound $|\tilde{z}^{n,+} - \tilde{z}_0^{n,+}|$. Hence, we write

$$\begin{aligned} |\tilde{z}^{n,+} - \tilde{z}_0^{n,+}| &= |\tilde{\omega}^{n,+} - \tilde{\omega}_0^{n,+}| \\ &= |P_\varepsilon^\pm(\tilde{\omega}^{n-1,+}) - P_0^\pm(\tilde{\omega}_0^{n-1,+})| \\ &= \left| P_\varepsilon^\pm(\tilde{\omega}^{n-1,+}) - P_0^\pm(\tilde{\omega}^{n-1,+}) \right. \\ &\quad \left. + P_0^\pm(\tilde{\omega}^{n-1,+}) - P_0^\pm(\tilde{\omega}_0^{n-1,+}) \right|, \end{aligned}$$

where we apply P_ε^+ or P_ε^- and P_0^+ or P_0^- depending on the sign of $\Pi_v(\tilde{\omega}^{n-1,+})$ and $\Pi_v(\tilde{\omega}_0^{n-1,+})$, respectively.

Using that P_ε^\pm and P_0^\pm are ε -close and that P_0^\pm are Lipschitz maps, it comes that there exists positive constants c , K_{P_0} and c_0 such that, for $n = 1$,

$$\begin{aligned} &\left| P_\varepsilon^\pm(\tilde{\omega}^{0,+}) - P_0^\pm(\tilde{\omega}^{0,+}) + P_0^\pm(\tilde{\omega}^{0,+}) - P_0^\pm(\tilde{\omega}_0^{0,+}) \right| \\ &\leq c\varepsilon + K_{P_0} |\tilde{\omega}^{0,+} - \tilde{\omega}_0^{0,+}| = c\varepsilon + K_{P_0} c_0 \varepsilon. \end{aligned}$$

By induction we obtain

$$\begin{aligned} |\tilde{z}^{n,+} - \tilde{z}_0^{n,+}| &= c\varepsilon + K_{P_0} |\tilde{\omega}^{n-1,+} - \tilde{\omega}_0^{n-1,+}| \\ &\leq c\varepsilon + K_{P_0} (c\varepsilon + K_{P_0} |\tilde{\omega}^{n-2,+} - \tilde{\omega}_0^{n-2,+}|) \\ &\leq c\varepsilon \sum_{i=0}^{n-1} (K_{P_0})^i + (K_{P_0})^n c_0 \varepsilon \\ &= c\varepsilon \frac{1 - (K_{P_0})^{n-1}}{1 - K_{P_0}} + (K_{P_0})^n c_0 \varepsilon \\ &\leq M (K_{P_0})^n \varepsilon, \end{aligned}$$

for some $M > 0$. Note that we do not necessary have that $|K_{P_0}| < 1$.

We now apply the Gronwall's inequality to the expression

$$\Delta(t) \leq M (K_{P_0})^n \varepsilon + K_2 n \varepsilon + \int_{b_n}^{a_{n+1}} K \Delta(r) dr.$$

Noting that

$$a_{n+1} - b_n = K_3 + nK_4\varepsilon,$$

with $K_3 = \max(\alpha^+(v), \alpha^-(-v))$ and $K_4 > 0$, this finally gives us

$$\begin{aligned} \Delta(t) &\leq (M (K_{P_0})^n \varepsilon + K_2 n \varepsilon) e^{K_3 + n K_4 \varepsilon} \\ &\leq M_2 (K_{P_0})^n \varepsilon e^{K_3 + n K_4 \varepsilon} \\ &= M_2 \varepsilon e^{K_3 + n(K_4 \varepsilon + \ln K_{P_0})} \\ &< M_2 \varepsilon e^{K_3 + n \ln K_5}, \end{aligned}$$

for some positive K_5 and M_2 .

Taking $n = c_2 \ln \frac{1}{\varepsilon}$ and making c_2 small enough such that $c_2 \ln K_5 < 1$, which is independent from ε , we finally have

$$\begin{aligned} \left| \tilde{\phi}(t; (0, \tilde{\omega}^+); \varepsilon) - \tilde{\phi}(t; (0, \tilde{\omega}_0^+); 0) \right| &\leq M_2 e^{K_3} \varepsilon \left(\frac{1}{\varepsilon} \right)^{c_2 (\ln K_5)} \\ &\leq M_2 e^{K_3} \varepsilon^\rho, \end{aligned}$$

for some $\rho > 0$, which is what we wanted to prove. \square

6.5 Example: two linked rocking blocks

In this section we apply some of the results presented in this chapter to a mechanical example consisting of the coupling of two rocking blocks by means of a spring (see Fig.6.5). Following §5.5, we call α_i the angle formed by the lateral side and the diagonal of each block. We then take as state variables u and x such that $\alpha_1 u$ and $\alpha_2 x$ are the angles formed by the vertical line and the lateral side of each block. As shown in §5.5, when assuming that both blocks are slender ($\alpha_i \ll 1$), the dynamics of each are modeled by the piecewise Hamiltonian systems

$$U(u, v) = \begin{cases} \frac{v^2}{2} - \frac{u^2}{2} + u, & \text{if } u \geq 0 \\ \frac{v^2}{2} - \frac{u^2}{2} - u, & \text{if } u < 0 \end{cases}$$

and

$$X(x, y) = \begin{cases} \frac{y^2}{2} - \frac{x^2}{2} + x, & \text{if } x \geq 0 \\ \frac{y^2}{2} - \frac{x^2}{2} - x, & \text{if } x < 0 \end{cases}$$

Recalling that both Hamiltonians U and X have the same phase portrait explained in §5.2, we note that both Hamiltonians satisfy the conditions, C.1–C.4, stated in §6.2. That is, each system has two critical points at $(\pm 1, 0)$, and there exist two heteroclinic connections

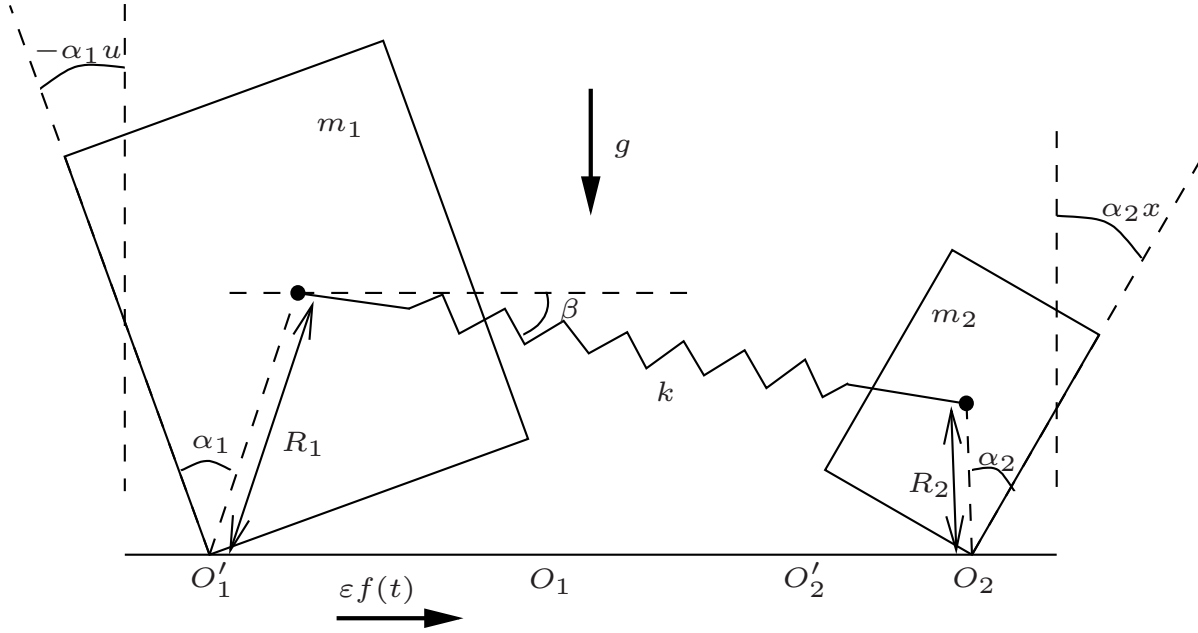


Figure 6.5: Two rocking blocks linked by a spring.

connecting them, which are given by the level of energy $U(u, v) = \frac{1}{2}$ and $X(x, y) = \frac{1}{2}$. Moreover, these heteroclinic connections surround a region filled with a continuum of period orbits, which are given by $U(u, v) = c$ and $X(x, y) = c$, with $0 < c < \frac{1}{2}$.

We now assume that both blocks have the same dimensions ($\alpha_1 = \alpha_2$ and $R_1 = R_2$). This allows us to assume that the angle formed by the spring and the horizontal line is small, and hence to linearize the coupling around $\beta = 0$. Taking into account the external small T -periodic forcing given by $\delta f(t)$, the (linearized) equations that govern the system in the extended phase space are

$$\begin{aligned}
 \dot{u} &= v \\
 \dot{v} &= u - \operatorname{sgn}(u) \\
 &\quad + k(u - x) - \delta f(t) \\
 \dot{x} &= y \\
 \dot{y} &= x - \operatorname{sgn}(x) \\
 &\quad + k(u - x) \\
 \dot{s} &= 1,
 \end{aligned} \tag{6.5.1}$$

This provides in fact a “Hamiltonian” system through the piecewise-defined Hamiltonian

$$\begin{aligned} H(u, v, x, y, s) = & \frac{v^2}{2} - \frac{u}{2} + |u| + \frac{y^2}{2} - \frac{x}{2} + |x| + \delta x f(t) \\ & + k \left(\frac{u^2}{2} + \frac{x^2}{2} - ux \right), \end{aligned} \quad (6.5.2)$$

with $u = 0$ and $x = 0$ as switching manifolds.

In order to apply the methods presented in this chapter, we need to obtain the coupled and perturbed systems as a perturbation of the uncoupled one. Hence, we assume that the constant of the spring is small and introduce the reparametrization

$$\delta = \tilde{\delta}\varepsilon, \quad k = \tilde{k}\varepsilon.$$

This allows us to rewrite the Hamiltonian (6.5.2) in the form given in (6.2.13) as

$$H_\varepsilon(u, v, x, y, s) = U(u, v) + X(x, y) + \varepsilon h(u, x, s) \quad (6.5.3)$$

where h is the Hamiltonian perturbation

$$h(u, x, s) = \tilde{\delta} u f(t) + \tilde{k} \left(\frac{u^2}{2} + \frac{x^2}{2} - ux \right). \quad (6.5.4)$$

We now focus on the periodic orbits of the block 1 ($\Lambda_c = \{U(u, v) = c\}$) and the heteroclinic connection for the second block (γ) when $\varepsilon = 0$. This exactly reproduces the situation described in this chapter, and hence we can apply the results provided so far.

On one hand, for $\varepsilon = 0$, the cross product of the critical points $Q^\pm = (\pm 1, 0)$ and the periodic orbits Λ_c gives rise to two 3-dimensional invariant manifolds in the extended phase space²,

$$\tilde{\Lambda}_0^\pm = \{(\phi_{\mathcal{U}}(\tau; 0, v), \pm 1, 0, s) \in \mathbb{R}^4 \times \mathbb{T}_T, \sqrt{2c_1} \leq v \leq \sqrt{2c_2}, 0 \leq \tau \leq \alpha(v)\},$$

where $\mathbb{T}_T = \mathbb{R} \setminus T$ and $\phi_{\mathcal{U}}(\tau; 0, v)$ is the (piecewise-defined) solution of the system associated with the Hamiltonian $U(u, v)$ fulfilling $\phi_{\mathcal{U}}(0; 0, v) = (0, v)$,

$$\phi_{\mathcal{U}}(\tau; 0, v) = \begin{cases} \left(\begin{array}{l} \frac{v-1}{2}e^\tau - \frac{v+1}{2}e^{-\tau} + 1, \\ \frac{v-1}{2}e^\tau + \frac{v+1}{2}e^{-\tau} \end{array} \right) & \text{if } 0 \leq \tau \leq \alpha^+(v) \\ \left(\begin{array}{l} -\frac{v-1}{2}e^{\tau-\alpha^+(v)} + \frac{v+1}{2}e^{-\tau+\alpha^+(v)} - 1, \\ -\frac{v-1}{2}e^{\tau-\alpha^+(v)} - \frac{v+1}{2}e^{-\tau+\alpha^+(v)} \end{array} \right) & \text{if } \tau\alpha^+(v) \leq \tau \leq \alpha(v), \end{cases}$$

²To simplify the notation, we will use in this section the parameter $\tau \in [0, \alpha(v)]$ instead of the parameter $\theta \in [0, 1]$, which was used in the previous sections to parametrize the manifolds $\tilde{\Lambda}_\varepsilon^\pm$. Both are related by $\tau = \theta\alpha(v)$.

and $\alpha^+(v)$ and $\alpha(v)$ are given in Eq. (5.5.11),

$$\begin{aligned}\alpha^+(v) &= 2 \int_0^{1-\sqrt{1-v^2}} \frac{1}{\sqrt{v^2 + u^2 - 2u}} du = \\ &= 2 \ln \left(\frac{1+u}{1-u} \right) \\ \alpha(v) &= 2\alpha^+(v).\end{aligned}$$

Both manifolds $\tilde{\Lambda}_0^\pm$ are connected by two heteroclinic invariant manifolds, an “upper” one, $W^s(\tilde{\Lambda}_0^+) = W^u(\tilde{\Lambda}_0^-)$, and a “lower” one, $W^u(\tilde{\Lambda}_0^+) = W^s(\tilde{\Lambda}_0^-)$. The “upper” heteroclinic connection of the system associated with the Hamiltonian $X(x, y)$ is given by,

$$\gamma^{\text{up}} = \{(x, y)\sigma^{\text{up}}(\xi), \xi \in \mathbb{R}\},$$

with

$$\sigma^{\text{up}}(\xi) = \begin{cases} (1 - e^{-\xi}, e^{-\xi}) & \text{if } \xi \geq 0 \\ (e^\xi - 1, e^\xi) & \text{if } \xi < 0. \end{cases}$$

Hence, the “upper” heteroclinic manifold $W^s(\tilde{\Lambda}_0^+) = W^u(\tilde{\Lambda}_0^-)$ becomes

$$\begin{aligned}\tilde{\gamma}^{\text{up}} &= \left\{ (u, v, x, y, s) \in \mathbb{R}^4 \times \mathbb{T}_T \mid c_1 \leq U(u, v) \leq c_2, \right. \\ &\quad \left. (x, y) = \sigma^{\text{up}}(\xi), \xi \in \mathbb{R} \right\}.\end{aligned}$$

From Proposition 6.3.1 we know that the manifolds $\tilde{\Lambda}_0^\pm$ persist for $\varepsilon > 0$ small enough, and become some 3-dimensional manifolds, $\tilde{\Lambda}_\varepsilon^\pm$, ε -close to $\tilde{\Lambda}_0^\pm$. We now study the persistence of heteroclinic connections between these manifolds. This is given in Proposition 6.4.1 by means of the existence of simple zeros of the Melnikov-like function defined in (6.4.2), which depends on the Poisson bracket between the Hamiltonian X and the Hamiltonian perturbation, h . As an example, we take the periodic forcing

$$f(t) = \cos(\omega t),$$

with $\omega = \frac{2\pi}{T}$. With this perturbation, the Melnikov function defined in (6.4.2) becomes

$$\zeta \longmapsto M(\zeta, \tau, v, s),$$

with

$$M(\zeta, \tau, v, s) := \int_{-\infty}^{\infty} \left(-y(t)(\tilde{\delta} \cos(\omega s) + \tilde{k}(x(t) - u(t))) \right) dt, \quad (6.5.5)$$

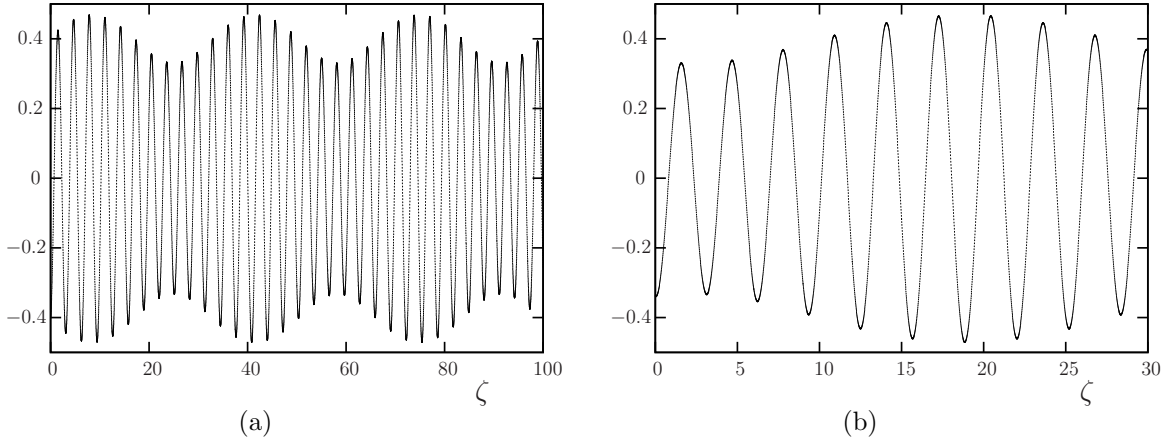


Figure 6.6: Melnikov-like function given in (6.5.5) for $v = 0.7$. (a) $\tau = s = 0$ and (b) $\tau = 1.1$.

$$(x(t), y(t)) = \sigma(t) \text{ and } u(t) = \Pi_u(\phi_u(\tau + t; 0, v)).$$

In Fig. 6.6(a) we show the result of numerically computing this integral for $v = 0.7$, $\tau = s = 0$. Note that it possesses simple zeros and hence, from Proposition 6.4.1, we have that, if $\varepsilon > 0$ is small enough, there exist heteroclinic points of the form

$$\tilde{z}_0^*(\tau, v, s) = (\phi_u(\tau + \bar{\zeta} + O(\varepsilon); 0, v), 0, 1 + O(\varepsilon), s + \bar{\zeta} + O(\varepsilon)),$$

where $\bar{\zeta}$ is a simple zero of (6.5.5).

As explained in §6.4.2, the points, $\tilde{z}^\pm \in \tilde{\Lambda}_\varepsilon^\pm$ associated by the heteroclinic connections going through \tilde{z}_0^* define the scattering map. Moreover, these two points may belong to tori in the manifolds $\tilde{\Lambda}_\varepsilon^\pm$ with different associated level of energy. This is determined by the difference ΔU given in (6.4.35), whose first order term in ε is given by the Melnikov-like function defined in (6.4.34).

As an example, suppose that we are interested on finding trajectories with increasing energy. Hence, we want to find proper values of (τ, v, s) such that some zero of the associated Melnikov-like function (6.5.5) leads to a heteroclinic connections with such property. In order to find such values, we consider the function

$$\tau \mapsto \Delta U_1(\tau, v, s),$$

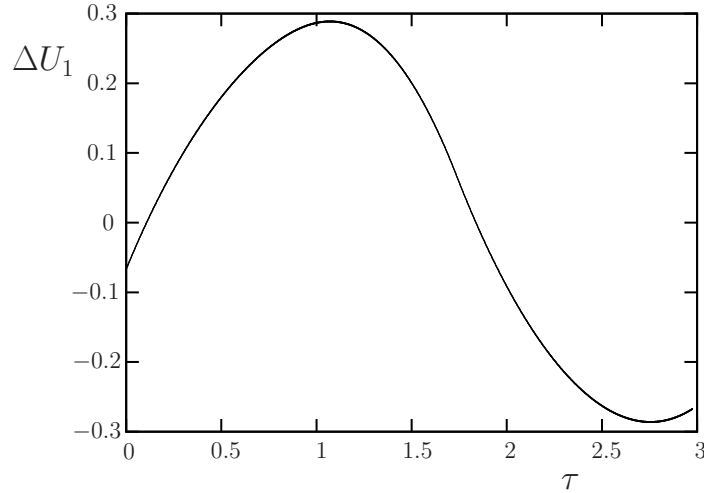


Figure 6.7: Function ΔU_1 for $v = 0.7$ and $s = 0$. $\bar{\zeta}$ has been set to the first positive zero of the respective Melnikov function (6.5.5).

where ΔU_1 is the first order term of ΔU and is given in (6.4.34), which we recall here

$$\begin{aligned} \Delta U_1 = & \int_{-\infty}^0 \left(\{U, h\} ((\phi_u(\tau + t; 0, v), \sigma^{\text{up}}(t - \bar{\zeta}), s + t)) \right. \\ & \left. - \{U, h\} (\phi_u(\tau + t; 0, v), Q^-, s + t) \right) dt \\ & + \int_0^{+\infty} \left(\{U, h\} ((\phi_u(\tau + t; 0, v), \sigma^{\text{up}}(t - \bar{\zeta}), s + t)) \right. \\ & \left. - \{U, h\} (\phi_u(\tau + t; 0, v), Q^+, s + t) \right) dt. \end{aligned}$$

Note that, in order to compute this function, we have to fix a zero of the Melnikov function which, at the same time, also depends on (τ, v, s) .

In Fig. 6.7 we show the function ΔU_1 for $v = 0.7$ and $s = 0$, varying τ and numerically finding the first positive zero of the Melnikov function. Note that it has a (positive) maximum around $\tau = 1.1$. This means that the first simple zero of the Melnikov function (6.5.5) with $\tau = 1.1$, $v = 0.7$ and $s = 0$ leads to a heteroclinic trajectory with increasing energy in the coordinates (u, v) . For $\tau = 1.1$, $v = 0.7$ and $s = 0$, the Melnikov function (6.5.5) possesses a simple zero around $\zeta = 0.7$ (see Fig. 6.6(b)).

Let us hence focus on the first positive zero, around $\zeta = 0.7$ for $\tau = 1.1$, $v = 0.7$ and $s = 0$. We then apply a numerical method to find the heteroclinic point \tilde{z}_0^* . It basically consists of, for a fixed $\varepsilon > 0$ small, applying a Bolzano's method to find a zero of the function

$$\zeta \longmapsto \tilde{z}^u(\zeta, \tau, v, s) - \tilde{z}^s(\zeta, \tau, v, s), \quad (6.5.6)$$

where

$$\begin{aligned}\tilde{z}^u &= (\phi_{\mathcal{U}}(\tau + \zeta; 0, v), 0, y^u, s + \zeta) \\ \tilde{z}^s &= (\phi_{\mathcal{U}}(\tau + \zeta; 0, v), 0, y^s, s + \zeta)\end{aligned}$$

are the intersection of the unstable and stable manifolds $W^u(\tilde{\Lambda}_\varepsilon^-)$ and $W^s(\tilde{\Lambda}_\varepsilon^+)$ with the line

$$\tilde{N} = \{\tilde{z}_0 + l(0, 1, 0, 0, 0), l \in \mathbb{R}\} \subset \mathbb{R}^2 \times \Sigma \times \mathbb{T}_T,$$

with

$$\tilde{z}_0 = (\phi_{\mathcal{U}}(\tau + \zeta; 0, v), 0, 1, s + \zeta).$$

Hence, the main difficulty remains on finding the values y^u and y^s for each ζ . To find y^s , we numerically integrate the system for a set of initial conditions of the form $(\phi_{\mathcal{U}}(\tau + \zeta; 0, v), 0, y_i, s + \zeta)$, where y_i surround a ε -neighbourhood of the unperturbed heteroclinic intersection $(1 \pm O(\varepsilon))$. As the heteroclinic manifold splits the space, we distinguish between values of y_i which lead to trajectories located “outside” and “inside” the heteroclinic manifold. We then identify the closest values to the heteroclinic manifold of these two types of points and repeat the process reducing the initial neighbourhood to the one given by these two values. This is repeated until this distance reaches a certain tolerance, and we identify y^s with the most inner value. We proceed similarly integrating backwards to obtain y^u .

To compensate the numerical error produced by expansion given by the unstable manifold when integrating forwards (by the stable one when backwards), we have used a multiple precision library (*arprec*) allowing us to obtain the points $y^{s,u}$ with high precision. This has allowed us to use tolerance for the points $y^{s,u}$ of 10^{-21} . Moreover, in order to reduce the calculation time, the processes to integrate the system for each set of initial conditions have been launched in parallel. This has been done in a heterogeneous network, using a total of 108 parallel processes (54 for each y^s and y^u).

Choosing $\varepsilon = 0.1$, after performing the Bolzano’s method to find a zero of the function (6.5.6) using a tolerance of 10^{-20} we obtain

$$\zeta^* = .7683636328526994941193923,$$

which leads to

$$\begin{aligned}\tilde{z}_0^* &= (\phi_{\mathcal{U}}(1.1 + \zeta^*; 0, 0.7), 0, y^s \simeq y^u, 0 + \zeta^*) \\ &= (-0.0849537161540264040157446, -0.5721098684521409990382415, \\ &\quad 0, 0.9780675560897323276693921, 0.7683636328526994941193923).\end{aligned}\tag{6.5.7}$$

The condition $y^s \simeq y^u$ comes from the fact that ζ^* is a zero of the function (6.5.6), which precisely makes \tilde{z}_0^* a heteroclinic point.

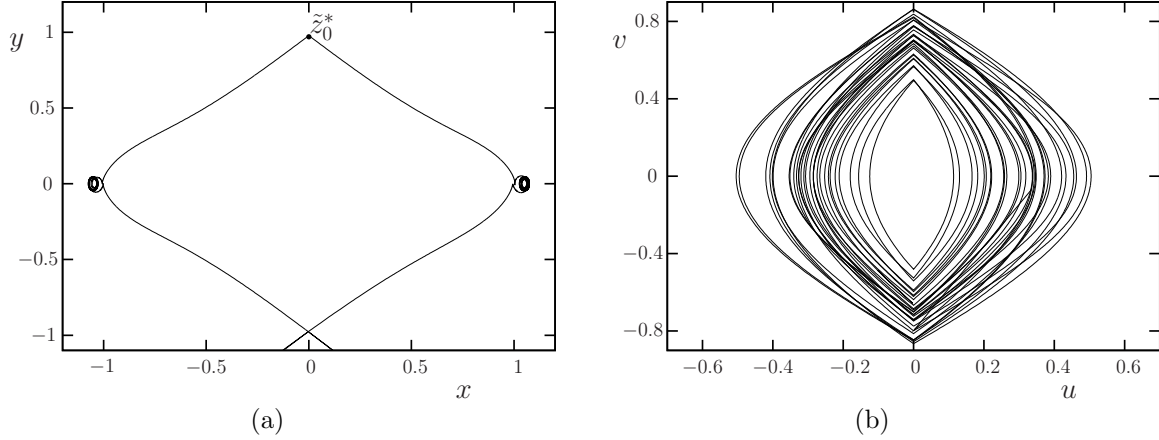


Figure 6.8: Heteroclinic trajectory with initial condition \tilde{z}_0^* given in (6.5.7) for $\varepsilon = 0.1$, integrating backwards and forwards in time. In (a) the $x - y$ coordinates, in (b) the $u - v$ ones.

In Fig. 6.8 we show the projections to the $x - y$ and $u - v$ planes of the heteroclinic trajectory obtained when integrating backwards and forwards in time the flow with the initial condition given in (6.5.7). In Fig. 6.8(a) note that, when integrating for $t \geq 0$ and $t < 0$, the trajectory rolls about $\tilde{\Lambda}_\varepsilon^+$ and $\tilde{\Lambda}_\varepsilon^-$, respectively, during a certain time until they escape. In Fig. 6.9 we show the result of evaluating the Hamiltonian U along the trajectory $\phi(t; \tilde{z}_0^*; \varepsilon)$. Approximately, the trajectory no longer rolls about the manifolds $\tilde{\Lambda}_\varepsilon^\pm$ at the times given by the vertical dashed lines. As one can see, the energy evaluated with the Hamiltonian U when the trajectory rolls about $\tilde{\Lambda}_\varepsilon^+$ is large than when it does about $\tilde{\Lambda}_\varepsilon^-$, as we wanted to show.

6.6 Conclusions

In this chapter we have considered the coupling of two of the systems obtained by a generalization of the model of the rocking block, presented in Chapter 5, under a small non-autonomous periodic forcing. This leads to a two and a half degrees of freedom piecewise-defined Hamiltonian system with two switching manifolds.

We have focused on the mode of movement given by small amplitude rocking for one block while the other one follows large oscillations of small frequency. This mode is captured

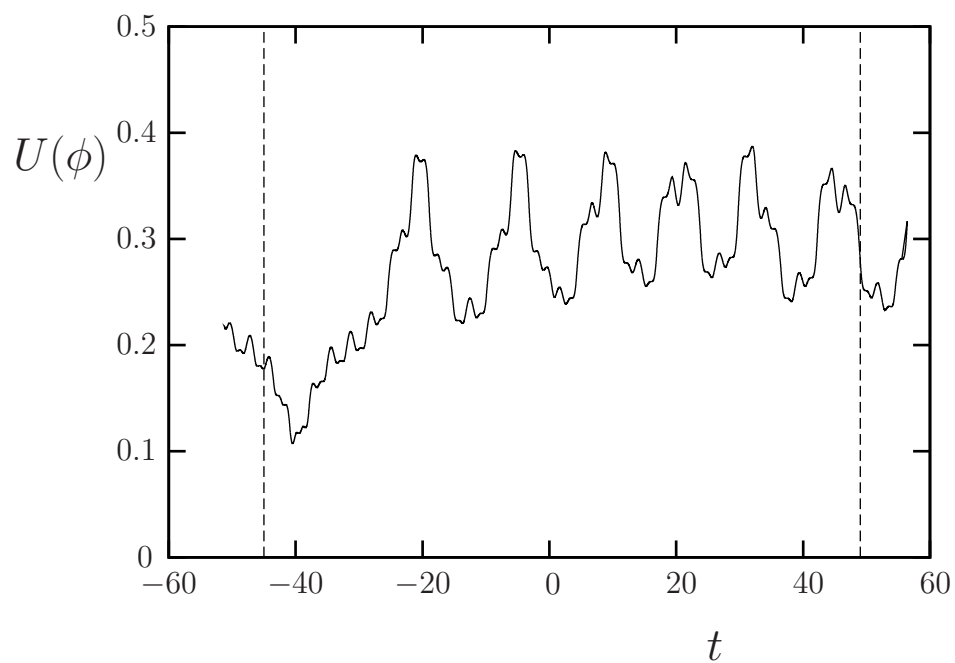


Figure 6.9: $U(\phi(t; \tilde{z}_0^*; \varepsilon))$ with $\varepsilon = 0.1$. The vertical dashed lines approximately correspond to the times where the trajectory no longer rolls about the manifolds $\tilde{\Lambda}_\varepsilon^\pm$ and escapes.

by 3-dimensional invariant manifolds with stable and unstable manifolds. In the unperturbed case, these stable and unstable manifolds coincide, hence leading to the existence of two 4-dimensional heteroclinic manifolds connecting the two invariant manifolds. This heteroclinic manifold is foliated by heteroclinic connections between C^0 tori located at same levels of energy in both invariant manifolds.

By means of an extension of the impact map presented in Chapter 5, we have proved the persistence of these objects when considering the perturbation. In addition, we have provided sufficient conditions of the existence of transversal heteroclinic intersections through the existence of simple zeros of Melnikov-like functions. This becomes thus an extension of some of the results given in [DdlLS06].

These heteroclinic manifolds allow us to define the so-called scattering map, which links asymptotic dynamics in the invariant manifolds through heteroclinic connections. First order properties of this map provide sufficient conditions to show that these asymptotic dynamics are located in different energy levels in the perturbed invariant manifolds. This is hence an essential tool in order to construct a heteroclinic skeleton which, when followed, can lead to the existence of Arnold diffusion: trajectories that, in large time scale destabilize the system by further accumulating energy.

Future work should be done to study the viability of a shadowing lemma in order to show the existence of trajectories following the heteroclinic skeleton.

Bibliography

- [AF03] Ll. Alsedà and A. Falcó. On the topological dynamics and phase-locking renormalization of lorenz-like maps. *Ann. Inst. Fourier*, 53:859–883, 2003.
- [AGS11] V. Avrutin, A. Granados, and M. Schanz. Sufficient conditions for a period increment big bang bifurcation in one-dimensional maps. *Nonlinearity*, 24(9):2575, 2011.
- [AL89] Ll. Alsedà and J. Llibre. Kneading theory of lorenz maps. *Dynamical systems and ergodic theory*, 23:83–89, 1989.
- [ALMS85] Ll. Alsedà, J. Llibre, M. Misiurewicz, and C. Simó. Twist periodic orbits and topological entropy for continuous maps of the circle of degree one which have a fixed point. *Ergod. Th. & Dynam. Sys.*, 5:501–517, 1985.
- [ALMT89] Ll. Alsedà, J. Llibre, M. Misiurewicz, and C. Tresser. Periods and entropy for lorenz-like maps. *Ann. Inst. Fourier (Grenoble)*, 39:929–952, 1989.
- [AM90] Ll. Alsedà and F. Mañosas. Kneading theory and rotation intervals for a class of circle maps of degree one. *Nonlinearity*, 3:413–452, 1990.
- [AS06a] V. Avrutin and M. Schanz. On multi-parametric bifurcations in a scalar piecewise-linear map. *Nonlinearity*, 19:531–552, 2006.
- [AS06b] V. Avrutin and M. Schanz. On multi-parametric bifurcations in a scalar piecewise-linear map. *Nonlinearity*, 19:531–552, 2006.
- [ASB06] V. Avrutin, M. Schanz, and S. Banerjee. Multi-parametric bifurcations in a piecewise-linear discontinuous map. *Nonlinearity*, 19:1875–1906, 2006.
- [ASB07] V. Avrutin, M. Schanz, and S. Banerjee. Codimension-3 bifurcations: Explanation of the complex 1-, 2- and 3D bifurcation structures in nonsmooth maps. *Phys. Rev. E*, 75:066205/1–7, 2007.

- [BF08] F. Battelli and M. Fečkan. Homoclinic trajectories in discontinuous systems. *J. Dynamics and Differential Equations*, 20:337–376, 2008. 10.1007/s10884-007-9087-9.
- [BF11] F. Battelli and M. Fečkan. Nonsmooth homoclinic orbits, Melnikov functions and chaos in discontinuous systems. *Physica D: Nonlinear Phenomena*, 2011.
- [BK91] B. Bruhn and B. P. Koch. Heteroclinic bifurcations and invariant manifolds in rocking block dynamics. *Z. Naturforsch.*, 46a:481–490, 1991.
- [CFGF11] V. Carmona, S. Fernández-García, and E. Freire. Periodic orbits for perturbations of piecewise linear systems. *J. Differential Equations*, 250:2244–2266, 2011.
- [CGT84] P. C. Coullet, J. M. Gambaudo, and C. Tresser. Une nouvelle bifurcation de codimension 2: le colage de cycles. *C. R. Acad. Sc. Paris, série I*, 299:253–256, 1984.
- [dBBCK08] M. di Bernardo, C. J. Budd, A. R. Champneys, and P. Kowalczyk. *Piecewise-smooth Dynamical Systems: Theory and Applications*, volume 163 of *Applied Mathematical Sciences*. Springer, 2008.
- [DdlLS00] A. Delshams, R. de la Llave, and T.M. Seara. A geometric approach to the existence of orbits with unbounded energy in generic periodic perturbations by a potential of generic geodesic flows of T^2 . *Comm. Math. Phys.*, 209:353–392, 2000.
- [DdlLS06] A. Delshams, R. de la Llave, and T.M. Seara. A geometric mechanism for diffusion in hamiltonian systems overcoming the large gap problem: Heuristics and rigorous verification on a model. *Memoirs of the American Mathematical Society*, 179, 2006.
- [DdlLS08] A. Delshams, R. de la Llave, and T.M. Seara. Geometric properties of the scattering map of a normally hyperbolic invariant manifold. *Advances in Mathematics*, 217(3):1096–1153, February 2008.
- [DL12] Z. Du and Y. Li. Bifurcation of periodic orbits with multiple crossings in a class of planar Filippov systems. *Math. Comp. Modelling*, 55:1072–1082, 2012.
- [DLZ08] Z. Du, Y. Li, and W. Zhang. Bifurcation of periodic orbits in a class of planar Filippov systems. *Nonlinear Analysis*, 69:3610–3628, 2008.
- [DZ05] Z. Du and W. Zhang. Melnikov method for homoclinic bifurcation in nonlinear impact oscillators. *Comput. Math. Appl.*, 50:445–458, 2005.

- [Fen72] N. Fenichel. Persistence and smoothness of invariant manifolds for flows. *Indiana Univ. Math. J.*, 21:193–226, 1971/1972.
- [Fen77] N. Fenichel. Asymptotic stability with rate conditions. II. *Indiana Univ. Math. J.*, 26(1):81–93, 1977.
- [Fen74] N. Fenichel. Asymptotic stability with rate conditions. *Indiana Univ. Math. J.*, 23:1109–1137, 1973/74.
- [FG11] E. Fossas and A. Granados. Big bang bifurcations in a first order systems with a relay. In *Proc. of Dynamical Systems Theory and Applications*, 2011.
- [FG12] E. Fossas and A. Granados. Occurrence of big bang bifurcations in discretized sliding-mode control systems. *Diff. Eqs. Dyn. Syst.* DOI 10.1007/s12591-012-0121-y, 2012.
- [Gal10] Z. Galias. Basins of attraction for periodic solutions of discretized sliding mode control systems. In *Circuits and Systems (ISCAS), Proceedings of 2010 IEEE International Symposium on*, 2010.
- [GGT84] J. M. Gambaudo, P. Glendinning, and C. Tresser. Collage de cycles et suites de Farey. *C. R. Acad. Sc. Paris, série I*, 299:711–714, 1984.
- [GGT88] J. M. Gambaudo, P. Glendinning, and T. Tresser. The gluing bifurcation: symbolic dynamics of the closed curves. *Nonlinearity*, 1:203–14, 1988.
- [GH83] J. Guckenheimer and P. J. Holmes. *Nonlinear Oscillations, Dynamical Systems and Bifurcations of Vector Fields*. Applied Mathematical Sciences. Springer, 4th edition, 1983.
- [GH94] R. Ghrist and P. J. Holmes. Knotting within the gluing bifurcation. In J. Thompson and S. Bishop, editors, *IUTAM Symposium on Nonlinearity and Chaos in the Engineering Dynamics*, pages 299–315. John Wiley Press, 1994.
- [GHS12] A. Granados, S.J. Hogan, and T.M. Seara. The Melnikov method and subharmonic orbits in a piecewise smooth system. *SIAM J. Appl. Dyn. Syst. (SIADS)*, *Accepted for publication*, 2012.
- [GIT84] J.M. Gambaudo, O.Lanford III, and C. Tresser. Dynamique symbolique des rotations. *C. R. Acad. Sc. Paris, série I*, 299:823–826, 1984.
- [Gle90] P. Glendinning. Topological conjugation of lorenz maps to β -transformations. *Math. Proc. Camb. Phil. Soc.*, 107:401–413, 1990.

- [GPTT86] J. M. Gambaudo, I. Procaccia, S. Thomae, and C. Tresser. New Universal Scenarios for the Onset of Chaos in Lorenz-Type Flows. *Phys. Rev. Lett.*, 57:925–928, 1986.
- [GST11] M. Guardia, T. M. Seara, and M. A. Teixeira. Generic bifurcations of low codimension of planar Filippov systems. *J. Differential Equations*, 250:1967–2023, 2011.
- [GT88] J. Gambaudo and C. Tresser. On the dynamics of quasi-contractions. *BOL. SOC. BRAS. MAT.*, 19:61–114, 1988.
- [GY08] Z. Galias and X. Yu. Analysis of zero-order holder discretization of two-dimensional sliding mode control systems. *IEEE Transactions on circuits and systems-II: express briefs*, 55(12):1269–1273, December 2008.
- [GY11] Z. Galias and X. Yu. Study of periodic solutions of discretized two-dimensional sliding mode control systems. *IEEE Transactions on circuits and systems-II: express briefs*, 58(6):381–385, June 2011.
- [Hog89] S. J. Hogan. On the dynamics of rigid block motion under harmonic forcing. *Proc. Roy. Soc. Lond. A*, 425:441–476, 1989.
- [Hog92] S. J. Hogan. Heteroclinic bifurcations in damped rigid block motion. *Proc. Roy. Soc. Lond. A*, 439:155–162, 1992.
- [Hom96] A. J. Homburg. Global aspects of homoclinic bifurcations of vector fields. *Memories of the American Math. Soc.*, 578, 1996.
- [Hou63] G.W. Housner. The behaviour of inverted pendulum structures during earthquakes. *Bull. Seism. Soc. Am.*, 53:403–417, 1963.
- [HP70] M.W. Hirsch and C.C. Pugh. Stable manifolds and hyperbolic sets. In S. Chern and S. Smale, editors, *Global Analysis (Proc. Sympos. Pure Math., Vol. XIV, Berkeley, Calif., 1968)*, pages 133–163, Providence, R.I., 1970. Amer. Math. Soc.
- [HPS77] M.W. Hirsch, C.C. Pugh, and M. Shub. *Invariant Manifolds*, volume 583 of *Lecture notes in mathematics*. Springer-Verlag, 1977.
- [HS90] J. H. Hubbard and C. T. Sparrow. The Classification of Topologically Expansive Lorenz Maps. *Communications of Pure and Applied Mathematics*, XLIII:431–443, 1990.
- [KKY97] M. Kunze, T. Küpper, and J. You. On the application of KAM theory to discontinuous dynamical systems. *J. Differential Equations*, 139:1–21, 1997.

- [KST04] T. Kabe, T. Saito, and H. Torikai. Analysis of piecewise constant models of power converters. In *NOLTA*, pages 71–74, 2004.
- [Kuk07] P. Kukučka. Melnikov method for discontinuous planar systems. *Nonlinear Analysis*, 66:2698–2719, 2007.
- [Kun00] M. Kunze. *Non-Smooth Dynamical Systems*. Springer-Verlag, 2000.
- [Kuz04] Y. Kuznetsov. *Elements of Applied Bifurcation Theory*. Springer, 2004. third edition.
- [Leo59] N. N. Leonov. On a pointwise mapping of a line into itself. *Radiofizika*, 2(6):942–956, 1959. (in Russian).
- [LH10] X. Liu and M. Han. Bifurcation of limit cycles by perturbing piecewise Hamiltonian systems. *Int. J. Bif. Chaos*, 20:1379–1390, 2010.
- [LM01] R. Labarca and C. Moreira. Bifurcation on the essential dynamics of lorenz maps and applications to lorenz-like flows: contributions to study of expanding case. *Bol. Soc. Bras. Mat.*, 32:107–44, 2001.
- [LM06] R. Labarca and C. Moreira. Essential dynamics for lorenz maps on the real line and the lexicographical world. *Ann. I.H. Poincaré*, AN 23, 2006.
- [LPZ89] D. V. Lyubimov, A. S. Pikovsky, and M. A. Zaks. *Universal Scenarios of Transitions to Chaos via Homoclinic Bifurcations*, volume 8 of *Math. Phys. Rev.* Harwood Academic, London, 1989. Russian version 1986 as a Preprint (192) of Russian Academy of Science, Institute of mechanics of solid matter, Sverdlovsk.
- [Mir87] C. Mira. *Chaotic Dynamics: From The One-Dimensional Endomorphism To The Two-Dimensional Diffeomorphism*. World Scientific, 1987.
- [MS89] K. Meyer and G. Sell. Melnikov transforms, Bernoulli bundles and almost periodic perturbations. *Trans. Am. Math. Soc.*, 314:63–105, 1989.
- [NOY94] H. E. Nusse, E. Ott, and J. A. Yorke. Border-collision bifurcations: An explanation for observed bifurcation phenomena. *Phys. Rev. E*, 49:1073–1076, 1994.
- [PTT87] I. Procaccia, S. Thomae, and C. Tresser. First-return maps as a unified renormalization scheme for dynamical systems. *Phys. Rev. A*, 35:1884–1900, 1987.

- [SK84] P. D. Spanos and A.-S. Koh. Rocking of rigid blocks due to harmonic shaking. *J. Eng. Mech. ASCE*, 110:1627–1642, 1984.
- [Spa82] C. Sparrow. *The Lorenz Equations: Bifurcations, Chaos, and Strange Attractors*. Springer-Verlag, 1982.
- [TA07] G. Tigan and A. Astolfi. A note on a piecewise-linear Duffing-type system. *Int. J. Bif. Chaos*, 17:4425–4429, 2007.
- [TS86] D. V. Turaev and L. P. Shil’nikov. On bifurcations of a homoclinic “Figure of Eight” for a saddle with a negative saddle value. *Soviet Math. Dokl.*, 34:397–401, 1987 (Russian version 1986).
- [Utk77] Vadim I. Utkin. Variable structure systems with sliding modes. *IEEE Transactions on automatic control*, ac-22(2):212–222, April 1977.
- [Vee86] P. Veerman. Symbolic dynamics and rotation numbers. *Physica A*, 134:543–576, 1986.
- [Vee87] P. Veerman. Symbolic dynamics of order-preserving orbits. *Physica D*, 29:191–201, 1987.
- [WYL08] B. Wang, X. Yu, and X. Li. ZOH discretization effect on high-order sliding mode control systems. *IEEE Transactions on Industrial Electronics*, 55(11):4055–4064, November 2008.
- [XFR09] W. Xu, J. Feng, and H. Rong. Melnikov’s method for a general nonlinear vibro-impact oscillator. *Nonlinear Analysis*, 71:418–426, 2009.
- [Yag] K. Yagasaki. Application of the subharmonic Melnikov method to piecewise-smooth systems. Submitted for publication. Preprint available at <http://www.eng.niigatau.ac.jp/~yagasaki/preprints/p09h.pdf>.
- [YC03] X. Yu and G. Chen. Discretization behaviors of equivalent control based sliding mode control systems. *IEEE Transactions on automatic control*, 48(9):1641–1646, September 2003.
- [YCP80] C.-S. Yim, A. K. Chopra, and J. Penzien. Rocking response of rigid blocks to earthquakes. *Earthquake Engng. Struct. Dyn.*, 8:565–587, 1980.